UNIVERSITÉ DU QUÉBEC À MONTRÉAL

ÉCOLOGIE FONCTIONNELLE DU PHYTOPLANCTON DES LACS TEMPÉRÉS ET BORÉAUX: LE RÔLE DES FACTEURS ENVIRONNEMENTAUX SUR LES COMMUNAUTÉS NANOPHYTOPLANCTONIQUES ET LA PRÉVALENCE DES STRATÉGIES D'ACQUISITION DE RESSOURCES ALTERNATIVES

THÈSE

PRÉSENTÉE

COMME EXIGENCE PARTIELLE

DU DOCTORAT EN BIOLOGIE

PAR

PHILIPPE LE NOAC'H

MAI 2023

REMERCIEMENTS

En avril 2019, j'ai embarqué pour Montréal avec quelques idées et beaucoup de doutes. Presque quatre ans et une pandémie plus tard, la plupart de mes idées sont tombées à plat et les doutes sont toujours là, mais j'ai tout de même achevé d'écrire un manuscrit de thèse. Ces quatre années furent mémorables, et il me parait important de remercier les personnes qui ont croisé ma route. Merci à Emilien, Cindy, Marie-Pier, Thomas, Vincent, Marine, Jade, Gillian, Fred, Riley, Dario et Samuel: le labo Beisner est une joyeuse galerie de personnalités sur lesquelles j'ai pu compter dans les moments forts comme dans les moments plus compliqués. Merci à Katherine, Alice et Sara pour toutes les discussions à l'heure du lunch et surtout pour m'avoir écouté me plaindre, en bon Français, de la météo Québecquoise. Merci à tous les étudiants et post-doctorants du GRIL avec qui j'ai partagé un café, une randonnée, une pinte, un moment de vie: mes années montréalaises auraient été bien moins intéressantes sans vous. Je mesure la chance que j'ai eu de faire partie du GRIL (et plus particulièrement du GRIL-UQAM), un environnement privilégié pour un doctorant fraîchement débarqué de France. Vous allez me manquer.

Merci à Sebastian Diehl pour sa bonne humeur et son expertise en modélisation, indispensable pour mener à bien le deuxième chapitre de cette thèse. Merci aux membres de mon comité de proposé et d'examen de synthèse, Yves Prairie et Gregor Fussman: leurs conseils et suggestions ont grandement contribué à améliorer la qualité de ce travail de thèse.

Et surtout, merci du fond du cœur à Beatrix. Merci pour ta confiance, tes conseils et ta patience: j'aurais difficilement pu imaginer meilleure mentore pour un doctorat. Je ne regrette pas d'avoir tenté ma chance et de t'avoir contacté en cette fin d'année 2018, j'espère que je me suis montré à la hauteur de tes attentes.

Finalement merci à ma famille et mes amis de l'autre côté de l'Atlantique. Je reviens bientôt, c'est promis.

AVANT-PROPOS

Une version préliminaire Chapitre I de ce manuscrit a été publiée sous forme d'article scientifique révisé par les pairs:

Le Noac'h, P., Ouellet Jobin, V. et Beisner, B. E. (2021). Effects of Vertical Spatial Overlap on Phytoplankton Diversity under Experimentally Altered Lake Stratification Regimes. *Microorganisms*, *9*(12), 2447. https://doi.org/10.3390/microorganisms9122447

Depuis la publication de cet article, le travail effectué pour les autres chapitres de cette thèse nous a poussés à retravailler sur les données de cette étude. En particulier, l'étude présentée dans le Chapitre III nous a permis de mettre à jour les stratégies de nutrition (autotrophie ou mixotrophie) des taxons identifiés dans l'expérience TIMEX. Pour une partie des analyses effectuées sur les données de l'expérience TIMEX, les résultats obtenus changent après correction de la matrice des traits fonctionnels. La version de l'étude présentée dans le Chapitre I de ce manuscrit de thèse prend en compte ces corrections et présente les résultats et conclusions les plus à jour. Nous allons prochainement proposer une correction de l'article publié.

Les Chapitres II et III de cette thèse, ainsi que la base de données des stratégies de nutrition nanophytoplanctoniques créée pour le Chapitre III (Annnexe M), seront à terme soumis pour publication dans des journaux scientifiques à comité de lecture.

TABLE DES MATIÈRES

LISTE DES FIGURES

LISTE DES TABLEAUX

LISTE DES ABRÉVIATIONS, DES SIGLES ET DES ACRONYMES

$\boldsymbol{\alpha}$	Functional mixotrophic investment in autotrophy (modèle Chapitre II)
A	Photo-autotroph nanoplankton strategist (modèle Chapitre II)
ANOVA	Analysis of variance
B	Bacteria (modèle Chapitre II)
Ca	Calcium
CFR	Competitor Favorable Range
CH_4	Methane
Chl*a*	chlorophyll-*a*
CO2	Carbon dioxide
$Cladocera_{Biom}$	Cladoceran biomass
df	Degree of freedom
DIC	Dissolved inorganic carbon
DO	Dissolved oxygen
DOC	Dissolved organic carbon
F_{Dis}	Functional dispersion
GAMM	Generalized additive mixed model
GFI	Goodness-of-Fit Index
H	Phago-heterotroph nanoplankton strategist (modèle Chapitre II)
H'	Shannon diversity index
K	Potassium
$\boldsymbol{k_{bg}}$	Water light attenuation coefficient
LakePulse	NSERC Canadian Lake Pulse Network survey
M	Phago-mixotroph nanoplankton strategist (modèle Chapitre II)
$Meta_{Width}$	Metalimnetic width
MLD	Maximum Length Diameter
NLA	Environmental Protection Agency's National Lake Assessment
pH	Potential of hydrogen
pfd	Mean photon flux density estimated within the mixed layer
ppm	Part per million
$prev_{mixo}$	Prevalence of mixotrophy

$\mathbf{prev_{cyano}}$	Prevalence of cyanobacteria
$\boldsymbol{R_{in}}$	Concentration of mineral nutrient in influx (modèle Chapitre II)
R	Dissolved mineral nutrient (modèle Chapitre II)
R	Genera richness
$\mathbf{R^2}$	R-Squared: coefficient of determination
$\mathbf{R^2_{adj}}$	Adjusted R-Squared
RDA	Redundancy analyses
RF	Random Forests
meanRTR	Mean Relative Thermal Resistance
SEM	Structural Equation Model
SO	Spatial Overlap
$\mathbf{Thermo_{Depth}}$	Thermocline depth
TN	Total nitrogen
TP	Total phosphorus
VIF	Variation inflation factor

LISTE DES SYMBOLES ET DES UNITÉS

< - Strictement inférieur à

≤ - Inférieur ou égal à

> - Strictement supérieur à

≥ - Supérieur ou égal à

= - Egal à

km² - Kilomètre carré

km - Kilomètre

m – Mètre

cm - Centimètre

mm - Millimètre

l - Litre

ml - Millilitre

m³ - Mètre cube

mS - Millisiemens

g - Gramme

g P - Gramme de Phosphore

g C - Gramme de Carbone

µg - Microgramme

J - Joule

µmol photon – Micromol de photon

p - p-value

˚**C** - Degré Celsius

d - Jour (day)

s - Seconde

% - Pourcentage

RÉSUMÉ

La diversité des communautés nanoplanctoniques des lacs est contrôlée par une variété de facteurs biotiques et biotiques, y compris la compétition interspécifique pour les ressources. La diversité des communautés se maintient lorsque les taxons peuvent éviter l'exclusion compétitive, les taxons évitent l'exclusion compétitive s'ils peuvent atténuer la compétition interspécifique au sein de la communauté. En théorie, les taxons peuvent réduire la compétition en se séparant spatialement le long des gradients de ressources verticaux généralement présents dans les systèmes stratifiés. Certains taxons utilisent également des stratégies alternatives d'acquisition des ressources, en particulier la phago-mixotrophie, pour compléter leurs apports en carbone et en nutriments. Cependant, ces deux mécanismes ne sont pas bien étudiés dans les lacs. La structure physique des lacs contrôle la répartition spatiale du nanophytoplancton, et la diversité des communautés est déterminée par une variété de facteurs biotiques et abiotiques en plus de la compétition pour les ressources. Cela limite notre capacité à déterminer si la répartition verticale de la communauté affecte réellement la diversité dans les systèmes naturels. Notre compréhension de la phago-mixotrophie nanophytoplanctonique est également incomplète. D'un point de vue théorique, il n'est pas si évident qu'une stratégie généraliste comme la mixotrophie puisse être viable face à des phago-hétérotrophes et des photo-autotrophes spécialisés. Nous savons également peu de choses sur les facteurs biotiques et abiotiques qui façonnent les assemblages de stratégie de nutrition nanoplanctoniques dans les systèmes d'eau douce. L'objectif de cette thèse est donc d'approfondir notre compréhension des effets de ces processus sur l'assemblage des communautés.

Dans le premier chapitre de cette thèse, nous avons étudié comment la répartition spatiale du nanophytoplancton contrôle la diversité taxonomique et fonctionnelle des communautés en conjonction avec la structure de stratification de la colonne d'eau et les interactions de prédations (c.a.d. le broutage par le zooplancton). Le niveau d'agrégation spatiale au sein de la communauté nanophytoplanctonique d'un lac stratifié a été modifié en perturbant sélectivement la structure thermique du lac. Des modèles en équations structurelles ont révélé que des niveaux accrus d'agrégation spatiale n'avaient pas d'effet détectable sur la diversité taxonomique et fonctionnelle de la communauté. L'effet de la compétition interspécifique induite par l'augmentation de

l'agrégation spatiale sur la diversité de la communauté était marginal comparé à l'effet de la composition de la communauté zooplanctonique et à la stratification de la colonne d'eau.

Dans une deuxième étude, nous avons testé la viabilité de la phago-mixotrophie nanoplanctonique en tant que stratégie d'acquisition des ressources du point de vue de la compétition pure pour les ressources. Nous avons développé un modèle mathématique de compétition spatiale entre trois stratégies nanoplanctoniques d'acquisition de ressources (phagotrophie pure, mixotrophie et phototrophie pure) et avons étudié les assemblages trophiques prédits par le modèle pour une variabilité des conditions de disponibilité en lumière et en nutriments. Nos résultats montrent qu'une stratégie de nutrition mixotrophique généraliste est viable face aux stratégies spécialisées et que le mixotrophe peut dominer la communauté s'il présente un équilibre fonctionnel mixotrophique adéquat. La position verticale des compétiteurs était également contrastée dans l'espace, et le mixotrophe peut se développer sur une plus grande partie de la colonne d'eau par rapport aux spécialistes. La variabilité fonctionnelle au sein du trait mixotrophe pourrait expliquer pourquoi les stratégies de nutrition alternatives sont omniprésentes dans les environnements aquatiques.

Dans le dernier chapitre de cette thèse, nous avons analysé des données de composition de communautés nanophytoplanctoniques provenant de deux campagnes d'échantillonnage de lacs à grande échelle, l'EPA National Lake Assessment aux États-Unis et le projet du NSERC Canadian Lake Pulse Network au Canada. Après avoir évalué le potentiel de mixotrophie des divers genres de nanophytoplancton identifiés dans les deux enquêtes, nous avons estimé la prévalence de la mixotrophie dans des centaines de lacs grâce à des relevés de composition taxonomique. Les mixotrophes se sont avérés omniprésents dans les lacs d'Amérique du Nord, bien qu'ils ne soient pas distribués uniformément dans les écorégions échantillonnées. La disponibilité des nutriments est le principal moteur des assemblages de stratégies de nutrition nanophytoplanctoniques dans les eaux de surface, avec une prévalence plus élevée de mixotrophie dans les lacs plus oligotrophes. L'état trophique du lac contrôle également la composition et la diversité de la partie mixotrophe de la communauté. L'effet de la disponibilité de la lumière sur la prévalence de la mixotrophie est marginal comparé à l'effet de la disponibilité des nutriments.

La répartition verticale des taxons et la mixotrophie sont des caractéristiques peu étudiées des communautés de nanophytoplancton dans les lacs, ces résultats sont donc des contributions importantes pour comprendre les mécanismes contrôlant l'assemblage de ces communautés dans les lacs. Ce travail a été conduit à l’aide d’une variété de méthodes numériques, de la modélisation mathématique mécaniste aux analyses multivariées approfondies de grands ensembles de données écologiques, soulignant l'importance des outils numériques pour les études écologiques.

Mots clés: écologie des communautés, nanoplancton, diversité, traits fonctionnels, phago-mixotrophie, gradients environnementaux

ABSTRACT

The diversity of lake nanoplankton communities is controlled by a variety of biotic and biotic factors, including interspecific resource competition. Community diversity is maintained when taxa can avoid competitive exclusion, which can be accomplished by alleviating interspecific competition within the community. In theory, taxa can reduce competition by occupying different spatial niches, i.e., by segregating over the vertical resource gradients usually present in stratified systems. Some taxa also use alternative resource acquisition strategies, in particular phago-mixotrophy, to complement their intake of carbon and nutrients. However, those two mechanisms are not well studied in lakes. Lake physical structure controls nanophytoplankton spatial repartition, and community diversity is driven by a variety of biotic and abiotic factors in addition to resource competition. This limits our ability to investigate whether the vertical distribution of the community truly affects diversity in natural systems without dedicated whole-lake experiments. Our understanding of nanophytoplankton phago-mixotrophy is also incomplete. At a basic theoretical level, it is still unclear how a generalist nutrition strategy like mixotrophy can be viable against specialist phago-heterotrophs and photo-autotrophs. We also know little of the biotic and abiotic drivers that shape nanoplankton assemblages of resource acquisition strategies in freshwater systems. The goal of this thesis work is thus to further our understanding of the effects of those processes for community assembly.

In the first chapter of this thesis, we investigated how nanophytoplankton spatial overlap shapes taxonomic and functional community diversity in conjunction with the stratification structure of the water column and top-down interactions (i.e., zooplankton grazing). The degree of spatial overlap within the nanophytoplankton community of a stratified lake was altered by disrupting the thermal structure of the lake. Structural equation models did not reveal an effect of increased levels of spatial overlap h on taxonomic and functional diversity within the community. Overall, the effect interspecific competition induced by increased spatial aggregation on community diversity was marginal compared to the effect of the zooplankton community composition and to water column stratification.

In a second study, we tested the viability of nanoplankton phago-mixotrophy as a resource acquisition strategy from a pure resource competition standpoint. We developed a mathematical model of spatial resource competition between three nanoplankton strategies of resource acquisition (pure phagotrophy, mixotrophy and pure phototrophy) and investigated the trophic assemblages predicted by the model for a variability of conditions of light and nutrient availability. Our results show that a generalist mixotrophic trophic strategy is viable against specialist trophic strategies and that a mixotrophs can dominate the community if it displays the adequate mixotrophic functional balance. The vertical position of the competitors was also spatially contrasted, and the mixotroph can grow over a larger portion of the water column relative to specialists. Functional variability within the mixotrophic trait could explain why alternative trophic strategies are ubiquitous in aquatic environments.

In the final chapter of this dissertation, we will present an analyse of nanophytoplankton community data from two large scale lake surveys, the EPA National Lake Assessment in the continental US and the NSERC Canadian Lake Pulse Network project in Canada. After assessing the potential for mixotrophy of the various nanophytoplankton genera identified in the two surveys, we assessed the prevalence of mixotrophy in hundreds of lakes using microscopic taxonomic assessment. Mixotrophs were found to ubiquitous across North American temperate and boreal lakes, although it was not uniformly distributed across the sampled ecoregions. Nutrient availability was identified as the main driver of nanophytoplankton trophic assemblages in surface waters, with higher prevalence of mixotrophy in more oligotrophic lakes. Lake trophic state also the controlled the composition and diversity of the mixotrophic portion of the composition. The effect of light availability on resource acquisition strategy assemblages appears to be marginal compared to the effect of nutrient availability.

The vertical distribution of taxa and mixotrophy are understudied feature of nanoplankton communities in lakes, those results are thus important contributions to understand the mechanisms controlling the assembly of those communities in lakes. This work made use of a variety of numerical methods, from mechanistic mathematical modelling to in-depth multivariate analyses of large ecological datasets, highlighting the importance of numerical tools for ecological studies.

Keywords: community ecology, nanoplankton, diversity, functional traits, phago-mixotrophy, environmental gradients

INTRODUCTION

0.1 Communautés planctoniques

Le plancton regroupe un large éventail d'organismes aquatiques vivant en suspension dans la colonne d'eau des océans, des cours d'eau et des lacs de la planète. Le terme phytoplancton désigne traditionnellement les protistes photo-autotrophes qui contribuent à la production primaire et qui constituent la base des réseaux trophiques aquatiques. Le phytoplancton couvre une variété de groupes taxonomiques, dont les cyanobactéries (algues bleues), les chlorophyceae (algues vertes), les chrysophyceae (algues dorées), les cryptophyceae, les dinophyceae et les bacillariophyceae (diatomées). Ces organismes généralement unicellulaires utilisent les nutriments (notamment l'azote, le phosphore et la silice) dissous dans l'eau et l'énergie lumineuse pour se développer via la photosynthèse. Les écosystèmes aquatiques abritent une multitude d'espèces de phytoplancton qui, bien qu'elles soient très diverses en matière de taille et de forme, partagent des exigences physiologiques similaires et occupent, à première vue, la même niche écologique. Autrement dit, ces espèces sont en compétition pour les mêmes ressources. Les espèces planctoniques dont la dimension linéaire maximale est comprise entre 2 et 20 µm sont appelées nanoplanctons. Ce terme regroupe non seulement des taxons phytoplanctoniques dotés de structures photosynthétiques (nanophytoplancton), mais aussi des micro-organismes purement hétérotrophes qui ne possèdent pas de pigment et qui obtiennent le carbone et les nutriments nécessaires à leur croissance en ingérant des bactéries via la phagotrophie. Le nanoplancton phagotrophe comme les nanoflagellés hétérotrophes (HNF) constitue un élément clé de boucle microbienne des lacs (Gasol *et al.*, 1995). Il est important de noter cette distinction entre nanoplancton et nanophytoplancton. Bien souvent dans le cas d'études basées sur des données de terrain, seuls les organismes photosynthétiques sont identifiés et énumérés avec précision: c'est donc uniquement le nanophytoplancton qui est considéré. Les organismes phagotrophes non photosynthétiques ne sont au contraire que rarement pris en compte. Les organismes nanoplanctoniques sont des proies pour le zooplancton, généralement considéré comme le second niveau trophique des écosystèmes aquatiques multicellulaires et qui contribuent à la production secondaire. Les groupes taxonomiques typiques du zooplancton lacustre sont les rotifères, les cladocères et les copépodes (calanoïdes et cyclopoïdes).

Un trait fonctionnel est une caractéristique physiologique, morphologique ou comportementale qui affecte la viabilité (*fitness*) d'un individu par sa croissance, son succès reproductif ou sa survie (Violle *et al.*, 2007). Depuis les années 2000, l'étude des communautés écologiques est passée d'une approche taxonomique classique, où chaque taxon est traité comme une entité individuelle au sein de la communauté, à une approche davantage axée sur les traits fonctionnels (McGill *et al.*, 2006). Les communautés nanoplanctoniques ne font pas exception (Litchman *et al.*, 2007, 2010; Weithoff, 2003) et sont maintenant couramment étudiées à travers le prisme des traits fonctionnels qui comprennent, entre autres, la taille des cellules, les types de pigments, les taux d'absorption des nutriments, la motilité et la capacité à effectuer de la phago-mixotrophie (Fig. 0.1; Litchman et Klausmeier, 2008). Des espèces ayant des origines phylogénétiques différentes peuvent jouer des rôles similaires dans la communauté lorsqu'elles présentent des traits similaires. Pour identifier les facteurs influençant la composition des communautés, les traits constituent un meilleur cadre que la classification taxonomique traditionnelle, car ils caractérisent directement la capacité des espèces à répondre aux conditions biotiques et abiotiques. *In fine*, les traits fonctionnels peuvent être utilisés pour prédire les changements dans la composition des communautés planctoniques le long de gradients environnementaux (Edwards *et al.*, 2013b; Margalef, 1978; Reynolds *et al.*, 2002) ainsi que leurs influences potentielles sur les processus écosystémiques tels que le cycle des nutriments (Hébert *et al.*, 2017; Litchman *et al.*, 2015).

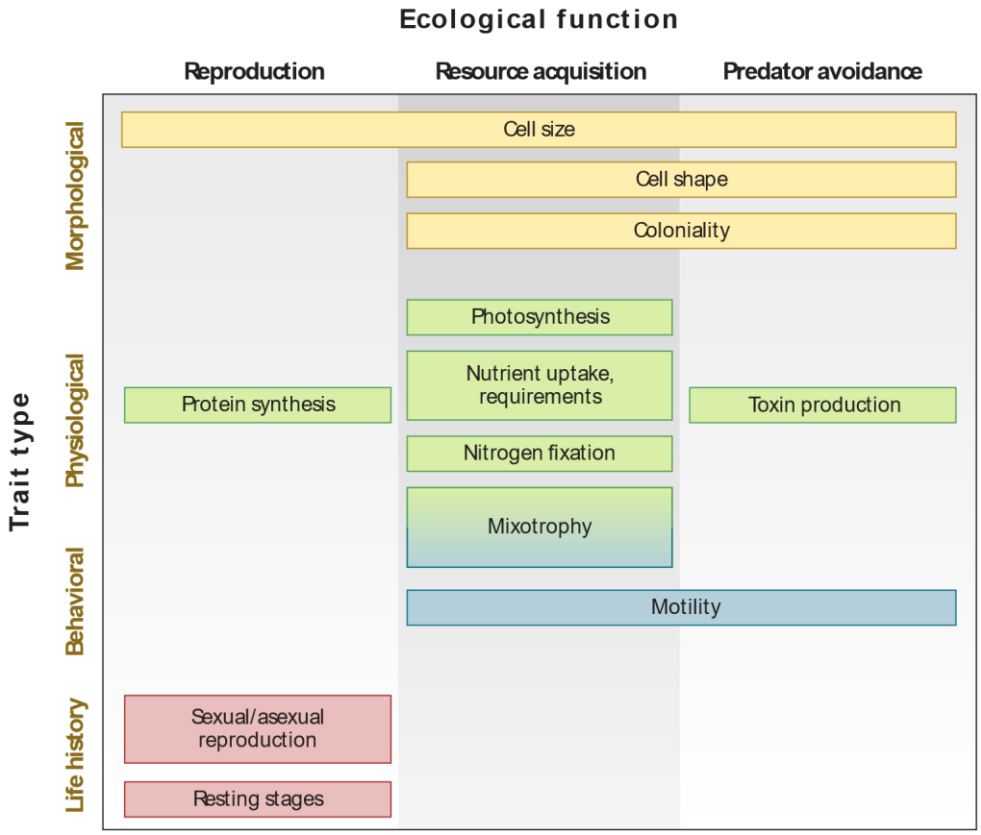

Figure 0.1. Typologie des différents traits fonctionnels nanophytolanconiques et de leurs fonctions écologiques. Repris de Litchman & Klausmeier (2008).

0.2 Diversité du nanophytoplancton

Une mesure clé pour caractériser une communauté est sa diversité. Celle-ci peut être grossièrement définie comme le nombre d'espèces ou de traits fonctionnels présents dans la communauté. La diversité d'une communauté (et de manière plus générale la composition de la communauté) dépend d'une variété de facteurs agissant de façon conjointe: localement, ces facteurs sont le filtrage environnemental et la compétition interspécifique (Borics *et al.*, 2021). La diversité d'une communauté est aussi un indicateur du fonctionnement et de la dynamique de l'écosystème (Tilman *et al.*, 2014). Par exemple, une communauté comportant plus d'espèces distinctes est comparativement plus stable dans le temps qu'une communauté plus pauvre (Tilman *et al.*, 2006). L'étude des patrons de diversité dans le temps ou le long de gradients environnementaux constitue ainsi une façon de comprendre et d'anticiper les changements dans le fonctionnement d'un écosystème, en particulier dans un contexte de changements globaux (Bulling *et al.*, 2010). Comme pour la composition, la diversité peut être définie de manière taxonomique ou fonctionnelle, et de nombreuses méthodes numériques ont été proposées pour

l’estimer (Daly *et al.*, 2018). La diversité taxonomique peut être évaluée en calculant le nombre de taxons distincts (espèces ou genres) dans la communauté (richesse taxonomique R), ou en calculant des indices plus complexes qui prennent en compte l'abondance relative des espèces, comme la régularité J de Pielou (Pielou, 1975) ou l'indice d'entropie H’ de Shannon (Shannon, 1948). De la même façon, de nombreuses métriques ont été proposées pour estimer la diversité fonctionnelle. Par exemple, la dispersion fonctionnelle F_{Dis} mesure la distance moyenne entre les taxons dans l'espace multidimensionnel formé par les modalités des traits fonctionnels présents dans une communauté (Laliberté et Legendre, 2010). Elle peut être calculée en combinant une matrice d'abondance ou de biomasse à une matrice de traits contenant les valeurs (quantitatives ou qualitatives) des traits pour chacun des taxons de la communauté.

Les assemblages nanoplanctoniques constituent un modèle unique en écologie des communautés et ont historiquement été essentiels pour comprendre comment les interactions interspécifiques agissent sur la composition des communautés. Par exemple, les travaux de Gause (1934) sur la coexistence in situ de paramécies hétérotrophes ont conduit Hardin (1960) à énoncer le principe d'exclusion compétitive, un principe écologique fondamentale. Par la suite, à l'aide d'expériences en microcosme sur deux espèces de diatomées, Tilman (1981) a également montré que pour que deux espèces coexistent, elles doivent être en compétition pour au moins deux ressources distinctes, et que le nombre d'espèces dans une communauté ne peut être supérieur au nombre de ressources limitantes. Il est intéressant de noter que les observations *in situ* ont montré que les communautés de phytoplancton dans les écosystèmes naturels sont très diversifiées et qu'elles abritent plus d'espèces que ne le prévoit la théorie pour des assemblages d’espèces en compétition pour un nombre relativement faible de ressources. Cette divergence entre la théorie et les observations sur le terrain est appelée le Paradoxe du plancton et a été notamment été décrite par Hutchinson (1961). Cette apparente contradiction intéresse les écologistes depuis lors, et de nombreux mécanismes ont été proposés pour y répondre (Bracco *et al.*, 2000; Li et Chesson, 2016; Roy et Chattopadhyay, 2007). L'hétérogénéité temporelle et spatiale de la distribution des ressources est l'un des mécanismes les plus couramment proposés pour résoudre le paradoxe (Anderies et Beisner, 2000; Roy et Chattopadhyay, 2007). Au-delà d’un intérêt purement théorique, étudier la diversité des communautés nanophytoplanctoniques est nécessaire parce que ces communautés jouent un rôle écosystémique essentiel. La diversité des communautés

nanophytoplanctonique est un paramètre clé du fonctionnement des écosystèmes aquatiques et peut affecter des fonctions écosystémiques aussi variées que la productivité des étages trophiques supérieurs ou que les cycles biogéochimiques globaux (Bonachela *et al.*, 2016; Striebel *et al.*, 2012). Il est donc essentiel de caractériser les mécanismes qui contrôlent la composition et la diversité de ces communautés.

Du fait de la proximité physiologique de nombreuses espèces nanophytoplanctoniques et du nombre relativement limité de ressources nécessaires à leur croissance, la compétition interspécifique pour les ressources apparait comme un facteur majeur affectant la diversité du nanophytoplancton (Borics *et al.*, 2021; Burson *et al.*, 2018; Interlandi et Kilham, 2001). Certains mécanismes à travers lesquels la compétition agit sur la diversité restent mal compris et méritent d'être étudiés plus en détail. Par exemple, dans un lac stratifié où la répartition des ressources est spatialement hétérogène, la structuration verticale des compétiteurs dans la colonne d'eau, et plus particulièrement le degré d'agrégation spatiale au sein de la communauté, devrait affecter l'intensité de la compétition pour la ressource. Bien qu'il y ait eu des tentatives pour identifier les facteurs environnementaux affectant la structure verticale des communautés nanophytoplanctoniques (Beisner et Longhi, 2013; Longhi et Beisner, 2009), notre compréhension de l'effet de l'agrégation spatiale sur la diversité reste limitée. Certains taxons nanophytoplanctoniques sont aussi capables de se différencier sur de nouveaux axes de niche en utilisant des stratégies de nutrition alternatives phago-mixotrophiques (Flynn *et al.*, 2013; Glibert, 2016). La mixotrophie est très répandue dans les communautés, mais notre compréhension des facteurs environnementaux affectant les assemblages de stratégies d'acquisition de ressources nanophytoplanctoniques dans les systèmes aquatiques d'eau douce mérite d'être approfondie.

0.3 Agrégation spatiale et diversité

La ségrégation spatiale le long de gradients de ressources opposés constitue l'un des mécanismes permettant à de multiples espèces de coexister sur un nombre limité de ressources (Connell, 1978; Hassell *et al.*, 1994). Dans les lacs stratifiés thermiquement, deux gradients importants pour la croissance du phytoplancton sont représentés par la lumière et les concentrations de nutriments. La lumière diminue à partir de la surface du lac, et les concentrations en nutriments augmentent en profondeur, formant ainsi des gradients opposés de ressources essentielles (Fig.

0.2). Dans ce contexte, la ségrégation active du phytoplancton dans la colonne d'eau est un mécanisme potentiellement important pour atténuer la compétition interspécifique (Huisman et Weissing, 1995). Dans un lac stratifié, les espèces capables de réguler leur position verticale peuvent s'établir à différentes profondeurs sur ces gradients opposés afin de maximiser l'acquisition de ressources, tout en évitant l'exclusion compétitive (Elliott *et al.*, 2002; Jäger *et al.*, 2008; Olli et Seppälä, 2001). Une réduction de l'agrégation spatiale (*Spatial Overlap*) entre les taxons devrait donc se produire, les espèces étant plus séparées verticalement lorsqu'elles se différencient le long de ces niches d'habitat de lumière et de nutriments.

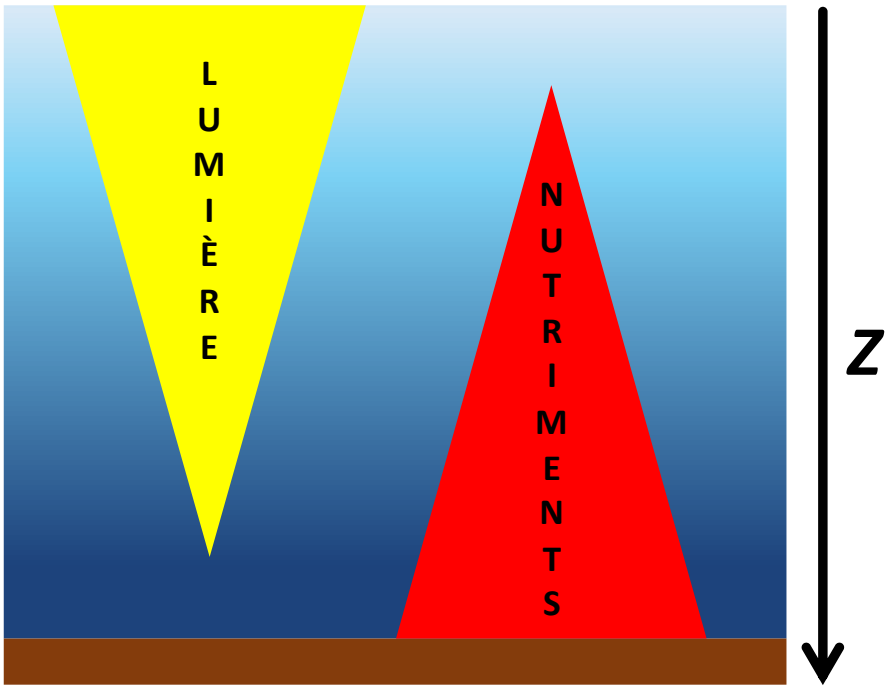

Figure 0.2. Représentantation schématique des gradients opposés des ressources nécessaires à la croissance du nanophytoplankton le long de la dimension verticale (*z*) dans les milieux aquatiques stratifiés. La lumière pénètre le système depuis la surface et le flux de nutriment provient principalement des sédiments.

Alors que les études de modélisation prédisent que l'hétérogénéité verticale des ressources affecte la composition des communautés phytoplanctoniques et favorise la diversité dans les environnements limités en nutriments (Weissing et Huisman, 1994; Yoshiyama *et al.*, 2009), plusieurs études ont également lié le niveau de ségrégation dans les communautés à la distribution hétérogène des ressources (Clegg *et al.*, 2007; Olli et Seppälä, 2001; Wall et Briand, 1980). En combinant l'observation sur le terrain et la modélisation prédictive, Clegg *et al.* (2007) ont observé une augmentation de la diversité des flagellés avec le degré de stratification du

milieu, qu'ils ont liée à une ségrégation des espèces le long de gradients de ressources opposés. Dans une étude portant sur plusieurs lacs tempérés nordiques, Beisner et Longhi (2013) ont examiné l'effet de la disponibilité des ressources sur l'agrégation spatiale verticale. En particulier, cette étude a révélé que les lacs fortement stratifiés présentaient un niveau d'agrégation spatiale plus faible parmi les principaux groupes nanophytoplanctoniques que les lacs moins stables thermiquement. En effet, l'environnement physique est probablement l'un des principaux moteurs de la distribution spatiale du plancton (George et Heaney, 1978; Margalef, 1978). Des niveaux élevés de mélange homogénéisent les concentrations de nutriments dans la colonne d'eau, ce qui entraîne une perturbation du double gradient opposé de ressources sur lequel les espèces peuvent se séparer, et empêche également les taxons de réguler leur position, augmentant ainsi le niveau d'agrégation verticale de la communauté.

Une réduction de l'agrégation de la communauté devrait être associée à des niveaux plus faibles de compétition interspécifique et, par conséquent, à une plus grande diversité taxonomique. Si la diversité taxonomique diminue lorsque l'agrégation augmente (plus d'exclusion compétitive), les espèces qui persistent devraient en revanche être plus diversifiées sur le plan fonctionnel car elles se séparent sur des axes de niche supplémentaires (par exemple au niveau de leurs stratégies de nutrition) plutôt que dans l'espace. Par exemple, Stomp *et al.* (2004) ont démontré expérimentalement que la coexistence dans un système mixte est possible entre des taxons de cyanobactéries dont la répartition spatiale se chevauche dans l'espace et ayant des types de pigments photosynthétiques différents, c'est-à-dire des exigences lumineuses différentes. Beisner et Longhi (2013) ont observé une augmentation de la diversité taxonomique du phytoplancton et de la richesse fonctionnelle (dans les traits de motilité et d'acquisition des ressources) dans les lacs clairs stratifiés profonds, où la communauté nanophytoplancton peut réduire son agrégation, par rapport aux lacs peu profonds et polymictiques.

Etablir un lien entre l'agrégation verticale du nanophytoplancton et la diversité des communautés dans les milieux naturels est difficile: d'autres facteurs biotiques et abiotiques peuvent contrôler la diversité. Par exemple, la diversité des communautés nanophytoplanctonique peut aussi être affectée par les relations proies-prédateurs (c.a.d. la prédation par le zooplancton) (McCauley et Briand, 1979; Menge et Sutherland, 1976). La structure physique du milieu contrôle non seulement l'agrégation de la communauté, mais peut aussi influencer directement la composition

de la communauté: par exemple, le phytoplancton non mobile comme les diatomées nécessite un certain niveau de mélange pour rester en suspension dans la zone photique (Bella, 1970). Isoler l'effet de l'agrégation spatiale sur la diversité de ces autres mécanismes environnementaux nécessite un système expérimental approprié, et des méthodes d'analyses statistiques adaptées.

0.4 Mixotrophie nanoplanctonique

0.4.1 Une stratégie alternative d'acquisition des ressources

Historiquement, la plupart des études portant sur les écosystèmes aquatiques ont tendance à considérer les stratégies de nutrition nanoplanctoniques de façon binaire: un taxon nanoplanctonique est considéré comme purement photo-autotrophe ou strictement phago-hétérotrophe. Ce postulat se reflète dans les hypothèses explorées et les méthodes utilisées dans les études des communautés planctoniques et de la productivité des écosystèmes aquatiques, et notamment dans les approches de modélisation. Les assemblages de stratégies d'acquisition de ressources nanoplanctoniques sont en réalité plus complexes: de nombreuses espèces nanoplanctoniques peuvent avoir des habitudes alimentaires à la fois autotrophes et hétérotrophes et peuvent réaliser à la fois la photosynthèse et la phagotrophie (Fig. 0.3). Dans un article de synthèse, Flynn *et al.* (2019) ont conçu un cadre précis pour classer les différentes stratégies de nutrition que les protistes planctoniques peuvent utiliser. Cette étude introduit le terme de *mixoplancton*, qui regroupe les protistes phagotrophes capables d'effectuer la photosynthèse de manière constitutive (grâce à des structures photosynthétiques qu'ils produisent eux-mêmes) ou non constitutive (grâce aux structures photosynthétiques des proies qu'ils consomment). Les communautés nanophytoplanctoniques abritent de nombreuses espèces mixotrophes constitutives: ces espèces utilisent non seulement la lumière et les nutriments inorganiques pour leur croissance, mais sont aussi capables de se comporter en prédateur (notamment via la bactérivorie) pour compléter leurs apports de nutriments et de carbone. Du fait de l'importance de la compétition pour les ressources pour l'assemblage des communautés nanoplanctoniques, la phago-mixotrophie est un trait fonctionnel qu'il est essentiel de mieux caractériser dans les assemblages nanoplanctoniques.

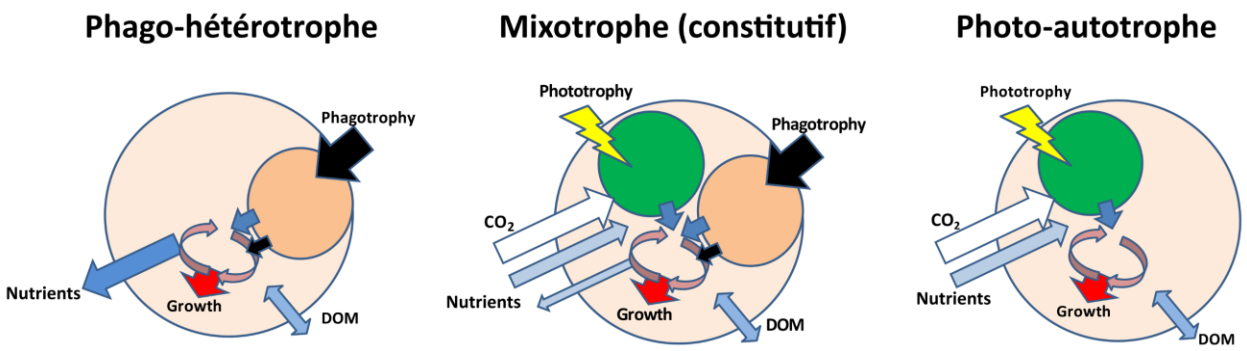

Figure 0.3. Représentation shcématique de trois stratégies de nutrition nanoplanctoniques: phago-hétérotrophie (gauche), phago-mixotrophie (centre) et photo-autotrophie (droite). DOM: matière organique dissoute. Repris et adapté de Mitra *et al.* (2016).

La mixotrophie n'est pas un trait fonctionnel binaire (présence vs. absence chez un taxon): il existe un degré de variabilité important dans la façon dont cette stratégie d'acquisition des ressources se manifeste dans les communautés. De nombreuses études montrent que le degré de mixotrophie peut varier fortement entre deux taxons mixotrophes. Le comportement de nutrition du plancton semble former un gradient, allant de l'autotrophie pure à l'hétérotrophie pure (Flynn *et al.*, 2013; Jones, 1997; Stoecker, 1998). Certains groupes taxonomiques du nanophytoplancton comme les cyanobactéries et les diatomées ne possèdent pas les structures physiologiques requises pour réaliser la phagotrophie. Parmi les groupes taxonomiques capables de réaliser la mixotrophie, certaines espèces sont principalement autotrophes et deviennent bactérivores lorsque la quantité de lumière diminue dans l'environnement. D'autres espèces de mixoplancton sont principalement hétérotrophes et n'utilisent la photosynthèse que comme source d'énergie complémentaire lorsque la densité des proies est faible. Un mixotrophe doit allouer ses ressources à la production de structures physiologiques pour la phototrophie (plastes) et pour la phagotrophie (vacuole pour la digestion des proies). L'investissement relatif dans ces deux voies d'acquisition des ressources détermine alors la place sur ce gradient fonctionnel allant de la phototrophie pure à la phagotrophie pure. Cela implique aussi qu'un compromis doit donc être fait: un mixotrophe ne peut investir autant dans la phototrophie (ou dans la phagotrophie) qu'un compétiteur purement phototrophe (ou purement phagotrophe). Par conséquent, il est généralement admis que les mixotrophes, qui peuvent être qualifiés de compétiteurs généralistes, ont des taux de croissance plus faibles que les spécialistes phototrophes ou phago-hétérotrophes lorsqu'un seul type de ressource est disponible (Dolan et Pérez, 2000; Raven, 1997). Par exemple, des expériences en laboratoire ont montré que des hétérotrophes phagotrophes purs étaient de

meilleurs compétiteurs que des flagellés mixotrophes *Ochromonas sp.* dans des cultures en batch maintenues dans l'obscurité, où seule la croissance phagotrophique était possible (Rothhaupt, 1996). Il est crucial de comprendre, dans un contexte de compétition pour les ressources, comment la mixotrophie peut être viable face à des compétiteurs phototrophes et phagotrophes spécialisés, et comment les assemblages de stratégies de nutrition varient dans les communautés nanoplanctoniques selon les conditions environnementales, en particulier selon la disponibilité des ressources.

La nécessité de prendre correctement en compte la mixotrophie dans les modèles conceptuels est régulièrement soulignée (Flynn *et al.*, 2013, 2019), par exemple pour évaluer avec précision les niveaux de production primaire et secondaire d'un écosystème donné, ou encore pour prédire l'apparition d'efflorescences planctoniques nuisibles causées par des taxons mixotrophes (Burkholder *et al.*, 2008; Mitra et Flynn, 2010). Pour mieux comprendre les mécanismes qui contrôlent la dynamique des communautés planctoniques et des réseaux trophiques aquatiques, les mixotrophes doivent être correctement identifiés et pris en compte lors de l'étude des communautés planctoniques, faute de quoi nous ne pouvons espérer prédire de manière fiable les trajectoires futures des écosystèmes aquatiques.

0.4.2 Assemblages de stratégies d'acquisition nanophytoplanctoniques dans les lacs

La mixotrophie nanoplanctonique constitutive est omniprésente dans les systèmes marins, comme le montrent des études biogéographiques océaniques à grande échelle (Faure *et al.*, 2019; Leles *et al.*, 2019). Nous ne disposons pas d'une connaissance similaire de la place de la phago-mixotrophie dans les lacs: les quelques études étudiant la prévalence des stratégies de nutrition alternatives dans les écosystèmes d'eau douce sont peu nombreuses et se concentrent sur des zones géographiques restreintes (Hansson *et al.*, 2019; Saad *et al.*, 2013, 2016). Il est pourtant crucial d'identifier quels facteurs environnementaux contrôlent les assemblages de stratégies d'acquisition des ressources dans les lacs du fait de l'importance de la communauté nanophytoplanctonique pour le fonctionnement de ces écosystèmes.

La phago-mixotrophie est une stratégie alternative d'acquisition des nutriments et du carbone, la disponibilité des ressources devrait donc en théorie contrôler les assemblages de stratégie de

nutrition. Des études ont montré à l'aide de modèles mathématiques que les taxons phago-mixotrophes devraient être compétitifs face à des phototrophes spécialisés lorsque la disponibilité des nutriments est faible (Crane et Grover, 2010). Sur le terrain, il semble en effet que les mixotrophes dominent les communautés nanophytoplanctoniques dans les lacs oligotrophes (Saad *et al.*, 2013). Il convient cependant de noter que les mixotrophes sont aussi présents dans les systèmes eutrophes et peuvent même y dominer la communauté nanoplanctonique (Burkholder *et al.*, 2008; Sanders *et al.*, 1990). L'effet de la disponibilité de la lumière sur les assemblages de stratégies de nutrition est moins évident à anticiper. Certains taxons mixotrophes peuvent dominer la communauté nanoplanctonique dans des environnements peu lumineux et riches en carbone organique dissous coloré (COD), car ils peuvent compenser la réduction de l'activité photosynthétique en ingérant les bactéries dont la croissance est favorisée par la disponibilité en matière organique (Bergström, 2009). À l'inverse, d'autres études ont montré que certains taxons mixotrophes ont besoin de niveaux élevés de lumière pour dominer la communauté, car ils obtiennent la majeure partie de leur carbone par photosynthèse et utilisent principalement la phagotrophie pour compléter leurs apports en nutriments (Calbet *et al.*, 2012). Dans les environnements marins, la biomasse mixotrophe semble augmenter avec le niveau d'irradiances (Edwards, 2019). L'effet de la lumière sur les assemblages des stratégies de nutrition nanoplanctoniques dans les lacs pourrait donc dépendre de la physiologie individuelle des mixotrophes, et par conséquent de la composition des communautés mixotrophes. La disponibilité des nutriments et de la lumière dans un lac est contrôlée par divers facteurs environnementaux, notamment le climat, l'utilisation du bassin versant et la morphométrie du site. La composition de la communauté est contrôlée non seulement par la disponibilité globale de la lumière et des nutriments dans l'environnement, mais aussi par la répartition spatiale, en particulier verticale, de ces ressources dans le système. Les mixotrophes bénéficient probablement de gradients de ressources clairement définis qui créent des conditions locales de disponibilité de la lumière et des nutriments favorables aux taxons qui peuvent compléter leur croissance par la phagotrophie. Il a été démontré que la répartition de certains mixotrophes est structurée verticalement dans les lacs stratifiés (Bird et Kalff, 1987; Clegg *et al.*, 2007). La structure de mélange des lacs est donc susceptible d'affecter le succès des mixotrophes, car l'état de stratification de la colonne d'eau détermine l'hétérogénéité de la disponibilité des nutriments en profondeur. Ainsi, les lacs stratifiés plus profonds avec une grande différence de température

entre le haut et le bas de la colonne d'eau pourraient potentiellement être des environnements plus favorables aux mixotrophes. La température de l'eau pourrait en soi affecter les assemblages de stratégies de nutrition, car l'augmentation de la température de l'eau est susceptible de favoriser la phagotrophie chez les mixotrophes (Lepori-Bui *et al.*, 2022). La prévalence des phagotrophes par rapport aux autotrophes pourrait donc potentiellement augmenter avec la température de l'eau. Les interactions proies-prédateurs pourraient également moduler les assemblages de stratégie d'acquisition des ressources. Hansson *et al.* (2019) ont montré que des abondances élevées de prédateurs zooplanctoniques sélectifs comme les copépodes étaient associées à une contribution globalement plus faible des mixotrophes aux communautés nanophytoplanctoniques dans les lacs boréaux. Ils ont attribué ce résultat aux différences potentielles de stœchiométrie entre les proies autotrophes et mixotrophes: les rapports stœchiométriques des photo-autotrophes purs dépendent entièrement des conditions de lumière et de disponibilité des nutriments et sont donc très variables, plus variables que les ratios élémentaires des phago-mixotrophes. Les photo-autotrophes seraient donc, comparés aux phago-mixotrophes, une source de nourriture sous-optimale pour le zooplancton dans certains systèmes. De l'autre côté de la chaîne trophique, l'abondance des bactéries est également un facteur potentiel qui contrôle la prévalence de la mixotrophie.

Un obstacle majeur à l'étude de la mixotrophie est la difficulté d'évaluer son occurrence dans les systèmes naturels. L'estimation des taux de mixotrophie *in situ* est difficile et nécessite des expériences dédiées (Beisner *et al.*, 2019). Simplement savoir si une espèce est fonctionnellement mixotrophique est difficile, et il y a un manque évident d'informations sur les stratégies de nutrition des taxons disponibles dans la littérature. Régulièrement, de nouvelles études montrent que des taxons précédemment considérés comme purement autotrophes sont capables d'ingérer des bactéries, même parmi des groupes traditionnellement considérés comme purement autotrophes comme les algues vertes (Bock *et al.*, 2021). Il existe des bases de données de traits publiées qui incluent la stratégie de nutrition des taxons (Laplace-Treyture *et al.*, 2021; Rimet et Druart, 2018) mais elles sont souvent en désaccord et ont tendance à fournir peu ou pas de sources pour les informations qu'elles rapportent. Un autre point de discorde est la confusion sémantique entre la phago-mixotrophie, c'est-à-dire l'ingestion d'autres organismes (plus particulièrement des bactéries) et l'osmo-mixotrophie, c'est-à-dire l'absorption de composés

organiques dissous présents dans l'environnement (Flynn *et al.*, 2019). Correctement identifier les taxons phago-mixotrophes est une étape préalable cruciale à toute étude des assemblages de stratégie de nutrition nanoplanctoniques. Construire une base de données fiable recensant les stratégies de nutrition des taxons nanoplanctoniques d'eau douce, bien que cela implique un travail de recherche bibliographique conséquent, serait une plus-value conséquente pour toute étude de la mixotrophie dans les lacs. Plus spécifiquement, une telle base de données de trait pourrait être combinée avec les données issues de campagnes d'échantillonnage de lacs à grande échelle, comme le National Lake Assessment (NLA) par l'EPA aux États-Unis (EPA NLA, 2009) et la campagne NERSC-Lake Pulse (LakePulse) au Canada (Huot *et al.*, 2019), deux projets utilisant globalement les mêmes méthodes d'acquisition des données. Ces enquêtes ont été conçues pour surveiller l'état de santé et la qualité de l'eau des lacs à travers l'Amérique du Nord et ont permis de collecter diverses mesures biotiques et abiotiques (morphologie des lacs, physico-chimie de l'eau, utilisation du bassin versant, composition de la communauté zooplanctonique…). Et surtout pour ce travail de thèse, ces études comprennent des données d'identification microscopique des taxons nanophytoplanctoniques, ce qui rend envisageable l'estimation de la prévalence de la mixotrophie dans les communautés nanophytoplanctoniques de ces lacs (sous réserve de disposer d'une base de données de traits de nutrition fiable).

0.5 Cadre du travail de thèse

Le but de ce travail de thèse est de mieux caractériser les mécanismes biotiques et abiotiques qui contrôlent la diversité et la composition des communautés nanoplanctoniques via la compétition interspécifique. Nous nous sommes intéressés plus particulièrement à deux axes de recherche: le lien entre la répartition verticale de la communauté et sa diversité, et la réponse des assemblages de stratégies d'acquisition des ressources aux conditions environnementales.

Dans le premier chapitre, nous avons étudié l'effet de la compétition interspécifique sur la diversité du nanophytoplancton via la répartition verticale de la communauté. Pour cela, nous avons analysé les données issues d'une expérience à l'échelle d'un lac entier dont la structure de stratification a été perturbée de manière sélective, l'expérience TIMEX (Cantin *et al.*, 2011; Gauthier *et al.*, 2014; Ouellet Jobin et Beisner, 2014). La modification de la structure de mélange de ce lac oligotrophe stratifié a affecté la capacité des taxons nanophytoplanctoniques à réguler

leurs positions verticales, nous permettant d'examiner si le degré de chevauchement spatial (*Spatial Overlap*) des principaux groupes nanophytoplanctoniques influence la diversité taxonomique et fonctionnelle de la communauté, tout en contrôlant le contexte abiotique (morphométrie du site, stratification thermique, chimie de l'eau) et biotique (composition de la communauté zooplanctonique).

Les chapitres suivants ont pour but de mieux comprendre la phago-mixotrophie nanoplanctonique lacustre. Dans le deuxième chapitre, nous avons exploré la viabilité de la phago-mixotrophie comme stratégie d'acquisition des ressources face à des stratégistes nanoplanctoniques spécialisés dans un contexte de compétition pour les nutriments et la lumière. Pour cela, nous avons développé un modèle mathématique simulant la compétition dans le temps et dans l'espace (dimension verticale) entre un compétiteur généraliste phago-mixotrophe, un photo-autotrophe spécialisé et un phagotrophe spécialisé. Nous avons utilisé ce modèle pour étudier l'assemblage de cette communauté nanoplanctonique théorique sous différentes conditions de disponibilité des ressources dans une colonne d'eau stratifiée caractérisée par des gradients de lumière et de nutriments opposés verticalement, et pour différentes stratégies mixotrophes. Nous avons aussi cherché à caractériser la répartition verticale et la niche spatiale des trois stratégistes.

Finalement, l'objectif du troisième chapitre est de caractériser la prévalence de la phago-mixotrophie dans les eaux de surface des lacs d'Amérique du Nord. Grâce à des données issues de deux campagnes d'échantillonnages de lacs à grande échelle, nous avons identifié les stratégies de nutrition (phototrophie ou phago-mixotrophie) de tous les genres nanophytoplanctoniques identifiés dans plusieurs centaines de lacs aux États-Unis et au Canada et nous avons estimé la prévalence du trait de phago-mixotrophie dans les communautés nanophytoplanctoniques de ces lacs. Nous avons combiné cette mesure de la prévalence de la mixotrophie, ainsi que la composition de la communauté mixotrophe, avec des mesures de variables environnementales collectées à chaque site afin d'identifier à une échelle continentale les facteurs biotiques et abiotiques qui contrôlent les assemblages de stratégies nanophytoplanctoniques d'acquisition des ressources dans les lacs.

Tous les aspects de ce travail de thèse ont été menés à l'aide de divers outils numériques: les chapitres II et III reposent sur de l'analyse de données multivariées, tandis que le chapitre II est une approche de modélisation mathématique.

0.6 Approches méthodologiques

0.6.1 Analyse statistique de données multivariées en écologie

La complexité des écosystèmes et la multitude de variables mesurées dans le cadre de campagne d'échantillonnage font de l'analyse de ces données une étape centrale de la méthode scientifique en écologie et en science de l'environnement. Bien choisir les analyses statistiques à mettre en œuvre pour confirmer ou infirmer une hypothèse de recherche est crucial, et découle directement du processus de collecte des données et de la nature des variables mesurées. Les jeux de données générés dans le cadre de l'étude d'écosystèmes sont par nature multivariés et nécessitent donc d'être exploré à l'aide d'analyses statistiques adaptées pour exploiter leur plein potentiel. L'étude des communautés nanoplanctoniques ne fait pas exception puisque les hypothèses de recherche considérées font intervenir une variété de compartiments biotiques et abiotiques. L'exploration de ces questions de recherche conduit à la collecte de grandes quantités de données sur le terrain, généralement des mesures de variables environnementales liées par exemple à la chimie de l'eau, à la morphologie du lac ou à la météorologie, et des évaluations de la biomasse biologique telles que des comptages de cellules nanoplanctoniques. Ces informations doivent être correctement analysées en utilisant un cadre multivarié, par de procédures exploratoires relativement simples ou bien à l'aide d'analyses plus complexes pour identifier les facteurs environnementaux contrôlant une variable réponse, ou même pour prédire la valeur de cette variable d'intérêt. Par exemple, les analyses canoniques comme l'analyse de redondance (RDA) sont des outils adaptés pour explorer comment l'assemblage d'une communauté varie le long de gradients environnementaux. Cette analyse produit une ordination contrainte d'une matrice d'abondance de taxons d'une communauté d'intérêt (par exemple des biovolumes nanophytoplanctoniques) par une matrice de variables biotiques et abiotiques, et permet de visualiser et d'identifier des prédicteurs environnementaux potentiellement importants pour expliquer la distribution des taxons et les changements dans la composition de la communauté (Legendre et Gallagher, 2001). Des approches basées sur des hypothèses *a priori* comme les modèles d'équations structurelles (SEMs) peuvent également s'avérer utiles, car elles permettent d'évaluer la vraisemblance d'un

réseau de relations causales reliant plusieurs variables en construisant un modèle basé sur des hypothèses spécifiées par l'utilisateur et en comparant ce modèle à la structure de variance-covariance d'un jeu de données (Grace *et al.*, 2012; Shipley, 2000). Les SEMs permettant entre autres d'estimer des relations indirectes entre prédicteurs et variables réponses, ce qui est difficile à faire avec des modèles linéaires généralisés (GLMs). Une question de recherche en écologie peut souvent se résumer à évaluer comment un ensemble de compartiments biotiques et abiotiques interagissent au sein d'un (éco)système: dans ce cas, les SEMs constituent des outils particulièrement adaptés pour évaluer la pertinence et la validité des hypothèses de départ sur le fonctionnement du système en question, et éventuellement proposer des mécanismes alternatifs si le modèle testé n'est pas conforme aux données mesurées sur le terrain. C'est cette approche que nous avons choisie pour analyser le jeu de données issu de l'expérience TIMEX et étudier l'effet de l'agrégation verticale sur la diversité d'une communauté nanophytoplanctonique (Chapitre I).

Les algorithmes d'apprentissage automatique (*machine learning*) peuvent aussi se révéler utiles pour comprendre quels facteurs environnementaux contrôlent l'assemblage des communautés planctoniques. De manière générale, les approches par apprentissage automatique sont employées pour produire des modèles de prédiction efficaces à partir de jeux de données en grande dimension (*big data*). En écologie, ces modèles sont notamment employés pour effectuer de la sélection de variables, c.a.d. pour identifier les meilleurs prédicteurs d'une mesure écosystémique d'intérêt parmi un grand nombre de variables environnementales. La sélection de variables est notamment indispensable pour analyser des données issues de campagnes d'échantillonnage de lacs à grandes échelles telles que NLA ou LakePulse qui incluent, pour des centaines de sites, des mesures pour un grand nombre de variables biotiques et abiotiques parfois très corrélées. Les analyses de type *Random Forests* sont une solution adaptée pour ce type de problème: ces modèles peuvent estimer l'importance relative des différents prédicteurs d'un modèle pour la précision de la prédiction d'une variable réponse, permettant ainsi d'identifier aisément les paramètres les plus importants pour déterminer pour la valeur de cette variable réponse. Cette approche a notamment été utilisée par Hansson *et al.* (2019) pour identifier les facteurs abiotiques qui contrôlent la prévalence du nanoplancton mixotrophe dans 55 lacs boréaux du Québec. Un autre avantage de cette méthode de sélection de variables est que l'algorithme peut identifier des relations non linéaires qui ne seraient pas forcément identifiables avec des approches plus

classiques de type GLM. Nous serons amenés à utiliser ces outils statistiques dans notre propre étude de la prévalence de la mixotrophie dans les lacs d'Amérique du Nord (Chapitre III).

0.6.2 Modèles mathématiques de la dynamique du nanoplancton

Les modèles mathématiques peuvent être utilisés pour traduire la dynamique d'un système écologique en un ensemble d'équations qui reflète notre compréhension théorique des interactions entre les différentes composantes de ce système. Les modèles permettent de simuler le comportement du système dans différentes conditions choisies, et ont historiquement été utilisés pour étudier la dynamique des communautés nanophytoplanctoniques. En effet, la relative simplicité physiologique du nanophytoplancton fait de ces organismes des candidats idéaux pour concevoir des modèles mécanistes de croissance et tester *in silico* des hypothèses sur les règles d'assemblages des communautés, en particulier dans le cadre de la compétition pour la ressource. Les modèles mécanistes classiques comprennent notamment les travaux pionniers de Jacques Monod (1950), qui proposa une équation décrivant l'absorption des ressources par les microalgues en fonction de la concentration externe en nutriments. Des études ultérieures se sont appuyées sur ce modèle pour proposer des ensembles d'équations différentielles ordinaires (ODE), prenant en compte des caractéristiques physiologiques plus complexes, comme les quotas cellulaires (Droop, 1968; Edwards *et al.*, 2013a) ou la dépendance de la croissance à la lumière pour les autotrophes (Geider *et al.*, 1998). Ces modèles peuvent décrire non seulement la dynamique des compartiments planctoniques, mais aussi celle des ressources, notamment les nutriments. La modélisation des apports des nutriments ou de la lumière dans le système permet ainsi de tester des hypothèses en lien avec l'effet de la disponibilité des ressources sur la dynamique du nanophytoplancton, hypothèses qu'il serait logistiquement difficile, voire impossible, de mettre en œuvre expérimentalement. Finalement, les modèles mathématiques permettent de répondre à des questions sur l'assemblage des communautés en autorisant l'ajout d'équations distinctes représentant différents compétiteurs (Grover, 1991). La paramétrisation des équations des différents compétiteurs permet d'intégrer dans le modèle les valeurs des traits fonctionnels, comme par exemple le taux de croissance maximal. La résolution mathématique, ou à défaut la simulation du système d'équations *in silico*, montre quels compétiteurs dominent la communauté, ou encore si la coexistence de multiples taxons dans le système est possible pour les valeurs de paramètres et de conditions initiales choisis.

Certaines catégories de modèles peuvent reproduire l'hétérogénéité spatiale de la dynamique du plancton en plus de simuler le comportement d'un système dans le temps. C'est notamment le cas des modèles en équations différentielles partielles (EDP) qui peuvent simuler dans le temps la diffusion des ressources et des compétiteurs dans la colonne d'eau (Weissing et Huisman, 1994; Yoshiyama *et al.*, 2009). Des mécanismes écosystémiques spatialisés importants pour la dynamique du nanophytoplancton peuvent aussi être pris en compte, comme la turbulence physique du système ou encore l'extinction lumineuse en fonction de la profondeur (Stefan *et al.*, 1983).

0.6.3 Modélisation de la mixotrophie

L'effet des traits fonctionnels sur l'assemblage des communautés peut être exploré par le biais de modèles mathématiques, et la mixotrophie ne fait pas exception. Les difficultés inhérentes à la mesure de la mixotrophie dans les milieux naturels font de la modélisation un outil particulièrement attractif pour l'étude de cette stratégie de nutrition alternative. En effet, bien que le potentiel pour la phago-mixotrophie d'un taxon nanophytoplanctonique soit généralement connu, la mesure réelle de taux d'ingestion *in situ* et l'estimation de la contribution de la bactérivorie à la croissance d'un mixotrophe est particulièrement difficile (Beisner *et al.*, 2019). Plus généralement pour l'étude des communautés planctoniques, il est logistiquement ardu de concevoir des expériences pour tester des hypothèses à l'échelle de l'environnement entier sans introduire des artefacts. Sachant que les modèles mathématiques peuvent reproduire assez fidèlement la dynamique du nanoplancton, ceux-ci semblent alors appropriés pour étudier des mécanismes régissant la composition d'une communauté en termes de stratégies d'acquisition des ressources. La difficulté est alors de choisir comment proprement transcrire la mixotrophie en équations.

La nécessité d'intégrer correctement la mixotrophie dans les études théoriques s'est imposée à la communauté des spécialistes du plancton, et il existe une diversité de modèles numériques de mixotrophie nanoplanctonique. Ces modèles numériques permettent de tester des hypothèses sur l'assemblage des stratégies de nutrition nanoplanctoniques en traduisant les processus physiologiques dans un cadre mathématique et en simulant la dynamique de la communauté, à condition qu'il existe une solide compréhension théorique des processus considérés. Certains de

ces modèles prennent la forme de systèmes d'équations différentielles qui détaillent précisément les mécanismes sous-tendant les processus de la photosynthèse et de la phagotrophie (Berge *et al.*, 2017; Flynn et Mitra, 2009; Kooijman *et al.*, 2002). Modéliser de façon exhaustive les voies physiologiques cellulaires liées à la photosynthèse ou à la phagotrophie dans une cadre mathématique flexible permet alors de tester la viabilité de diverses stratégies mixotrophiques entre la phototrophie pure et la phago-hétérotrophie (Flynn et Mitra, 2009). Il convient néanmoins de noter que ces modèles sont constitués de multiples équations, jusqu'à neuf équations pour un seul organisme phytoplanctonique dans le modèle proposé par Ghyoot *et al.* (2017), et nécessitent donc de trouver des valeurs pour un nombre important des variables difficiles à mesurer empiriquement. Ces modèles, bien que conceptuellement intéressants, sont difficiles à appliquer dans un contexte plus général de compétition entre plusieurs organismes planctoniques. Dans ce cas, d'autres approches sont possibles, comme définir le taux de croissance d'un mixotrophe comme une fonction additive d'apports osmo-phototrophes et phagotrophes qui dépendent directement de la quantité de lumière, des nutriments dissouts dans le milieu et de la quantité de proies. La contribution relative de chaque voie d'acquisition des ressources peut être alors être pondérée par une constante. Cette approche est notamment utilisée par Troost *et al.* (2005), ou encore par Crane et Grover (2010) dans un modèle de compétition entre plusieurs stratégies de nutrition dans un système spatialement homogène. Cette approche permet de représenter relativement simplement le caractère généraliste d'un compétiteur mixotrophe, ainsi que le compromis physiologique associé: investir dans un type de nutrition se fait aux dépens de l'autre mode d'acquisition des ressources. En ajoutant au système d'autres équations pour des organismes ne bénéficiant que d'une seule voie d'acquisition des ressources, le modèle permet de représenter une communauté abritant de multiples stratégies de nutrition. Il devient alors possible d'étudier les mécanismes régissant l'assemblage des stratégies de nutrition en modifiant de façon pertinente les paramètres de ce modèle.

Puisque la répartition des nutriments et de la lumière est généralement hétérogène dans les systèmes aquatiques, en particulier dans les lacs stratifiés, la prise en compte de cette dimension verticale dans les modèles de compétition est pertinente. Pourtant à ce jour, il n'existe pas de modèle de compétition entre plusieurs stratégies d'acquisition de ressources nanoplanctoniques dans un système spatialisé. C'est un vide à combler si l'on veut comprendre comment la viabilité

de la mixotrophie varie avec la profondeur, ou encore pour comparer les niches spatiales de compétiteurs ayant différentes stratégies de nutrition. Un modèle correspondant à ces spécifications est présenté dans le deuxième chapitre de cette dissertation.

CHAPITRE 1

Effects of vertical spatial overlap on phytoplankton functional diversity under experimentally altered lake stratification regimes

Philippe Le Noac'h, Vincent Ouellet Jobin and Beatrix E. Beisner

Department of Biological Sciences, University of Quebec at Montreal and Interuniversity Research Group in Limnology/Groupe de Recherche Interuniversitaire en Limnologie (GRIL), H2X 1Y4 Montreal, Quebec, Canada

1.1 Abstract

In phytoplankton communities, competitive exclusion might occur when functionally similar species are impeded from regulating their positions along light and nutrient gradients to reduce niche overlap. Greater spatial overlap (SO) between species due to water column mixing could thus promote competitive exclusion, reducing community taxonomic diversity. However, greater SO could also promote coexistence of functionally different taxa. Using data from a whole-lake experiment, we investigated the effects of SO and other relevant environmental factors on phytoplankton diversity across the water columns of lake basins with different thermocline manipulations. We estimated the SO using an in situ fluorometer, and overall community diversity microscopically. Using structured equation models, we estimated directional relationships between phytoplankton diversity, SO, the lake physical structure and the zooplankton community. No significant effect of SO on phytoplankton taxonomic or functional diversity was observed. However, change in lake physical structure and in the zooplankton community did affect diversity, with a negative response to increased top-down interactions. Overall, the alteration of water column stratification structure and top-down interactions were stronger drivers of phytoplankton diversity in our system than competitive interactions.

Keywords: diversity, composition, functional traits, competition, spatial ecology

1.2 Introduction

Spatial segregation along opposing resource gradients constitutes one of the mechanisms allowing multiple species to coexist on a finite number of resources (Connell, 1961; Hassell *et al.*, 1994). In thermally stratified lakes two important gradients for phytoplankton growth are represented by light and nutrient concentrations. Light decreases from a lake's surface, and nutrient concentrations increase at depth, thereby forming opposing gradients of essential resources. In this context, studies have theorized about the importance of phytoplankton segregation in the water column to mitigate interspecific competition (Borgnino *et al.*, 2019; Weissing et Huisman, 1994). Under stratified conditions, species can actively establish at different depths over these opposing gradients to maximise resource acquisition, while avoiding competitive exclusion (Elliott *et al.*, 2002; Jäger *et al.*, 2008; Olli and Seppälä, 2001). If species can differentiate their niches (light and nutrient requirements in particular) and spatially segregate

either through active motility or through differentiated growth rates over the vertical dimension, the amount of spatial overlap (*SO*) within the community should then decrease.

A handful of observational studies have linked species segregation (or its corollary, spatial overlap) to heterogeneous resource distributions (Clegg *et al.*, 2007; Olli and Seppälä, 2001). Combining field observation and predictive modelling, Clegg *et al.* (2007) observed an increase in flagellate diversity with stratification, which they linked to fine-scale species segregation over opposing resource gradients. In a study across multiple north-temperate lakes, more strongly stratified lakes had reduced *SO* amongst major phytoplankton groups than more mixed lakes and greater taxonomic evenness (Beisner and Longhi, 2013). Similarly, George and Heaney (1978) demonstrated that the physical environment can be one of the main drivers of phytoplankton spatial distribution. High levels of mixing homogenize nutrient concentrations within the water column thereby increasing *SO*, based on both the disruption of the nutrient gradient as well as of the active position regulation by phytoplankton.

If the vertical distribution of species in the water column affects competition, the levels of *SO* for a given phytoplankton community should affect its diversity, both taxonomically and functionally. Reduced *SO* should be associated with lower levels of interspecific competition, and consequently higher taxonomic diversity, as more species can coexist in the community (richness) and as spatial differentiation precludes dominance (more evenness). On the other hand, while taxonomic diversity should decline as *SO* increases (more competitive exclusion), the species that persist together should be more functionally diverse in their resource acquisition traits in order to permit some form of segregation along additional niche axes (e.g., resource acquisition rates, storage capacity, trophic strategies) instead of spatially. For example, Stomp *et al.* (2004) demonstrated experimentally that coexistence in a mixed system is possible between spatially overlapping cyanobacterial taxa with different photosynthetic pigment types, i.e., different light requirements. However, greater functional diversity could also be expected under low levels of *SO* when conditions are stratified, given that species growing at different depths face different local conditions that could select for a larger range of trait values. While they did not find any direct relationship between diversity and *SO*, Beisner and Longhi (2013) observed increases in phytoplankton taxonomic diversity and functional richness (in motility and resource acquisition traits) for deeper, stratified lakes with clear water columns, where phytoplankton

could reduce their *SO*, compared to shallow, polymictic lakes. It is also worth noting that the physical structure of the environment can itself directly influence community composition. For example, Reynolds *et al.* (1983) showed in a mesocosm experiment that altering the mixing depth affected the phytoplankton community composition, with shallower mixing depths favoring sinking diatoms. The composition of the zooplankton grazer community is also likely to affect the diversity of the phytoplankton community through top-down interactions. Currently, we lack a clear understanding of the effect of *SO* on taxonomic or functional trait diversity in natural communities under experimental conditions that control for extraneous factors such as lake morphometry, seasonality and grazer community.

To complement modeling and observational work done to date on the effect of spatial overlap and resource competition on phytoplankton diversity, we conducted an *in situ* experiment manipulating the water column stratification in a small lake with multiple basins. Our goal is to increase mechanistic understanding of (i) the effect thermal stratification disruptions of the water column on phytoplankton *SO*, (ii) the effect of *SO*, in conjunction with the physical structure of the water column and top-down interactions, on community taxonomic and functional diversity; all while controlling for lake morphometry, chemistry and global community composition. Data were from a whole-lake experimental thermal stratification manipulation of a temperate lake (Thermocline Induced Mixing Experiment; TIMEX) and used here to assess phytoplankton community diversity in conjunction with overlap (*SO*) between major phytoplankton groups. A previous study by Ouellet Jobin and Beisner (2014) showed that the TIMEX treatment application led to thermocline deepening as planned. This deepening of the warmer upper mixed layer (epilimnion) could impede species coexistence (reduced diversity predicted) owing to mixing across greater depth for the same wind. Experimentally-deepened thermoclines also resulted in the nutrient gradient being pushed deeper with the hypolimnetic waters, while the light gradient remained unchanged. Ouellet Jobin and Beisner (2014) also showed that the treatment application led to some metalimnetic thickening, at the expense of a deeper mixed layer, thereby increasing overall water column stability. This environmental shift should improve the ability of phytoplankton to segregate and avoid competitive exclusion across a more stable water column (increased diversity predicted).

By differentially altering the stratification structure of the different basins of the lake all possessing similar morphometries, we expect to have selectively altered the ability of phytoplankton species to spatially segregate. Within this experimental context, we examine how the spatial overlap (*SO*) of major phytoplankton groups relates to the overall community (taxonomic and functional) diversity, while accounting for other often time-varying changes in the background environmental (thermal stratification) and biotic (zooplankton grazing) variables. Previous results from the TIMEX experiment have shown important shifts in zooplankton composition with thermocline deepening from large-bodied cladocerans to smaller crustacean zooplankton composed of cyclopoid copepods and *Bosmina* spp. (Cantin *et al.*, 2011; Gauthier *et al.*, 2014). Less efficient feeding by these smaller zooplankton associated with deeper thermoclines, could also promote phytoplankton diversity. More generally, any change in the zooplankton community might affect phytoplankton diversity through altered top-down effects (Bergquist *et al.*, 1985).

Our focal experimental system thus consists of five main interacting compartments: *Thermocline depth, Metalimnion width, Grazer community,* and *SO*, all potentially influencing the *Phytoplankton diversity* response (Fig. 1.1). We further assume that changes in *Thermocline depth* and *Metalimnion width* through experimental thermocline deepening potentially affects every compartment in the system. We expect *Phytoplankton taxonomic diversity* to decline with greater *SO* because of greater competition between overlapping taxa. On the other hand, increased *SO* could favor greater *Phytoplankton functional diversity* through greater trait variation amongst co-existing taxa, although this effect might be mitigated if, under a lower *SO* regime, species established at different depth experience different environmental conditions, leading to trait differentiation. Finally, we expect changes in the *Zooplankton community* to affect *Phytoplankton diversity* through altered top-down effects and, in particular, negative effects on diversity of increasing Cladoceran biomass.

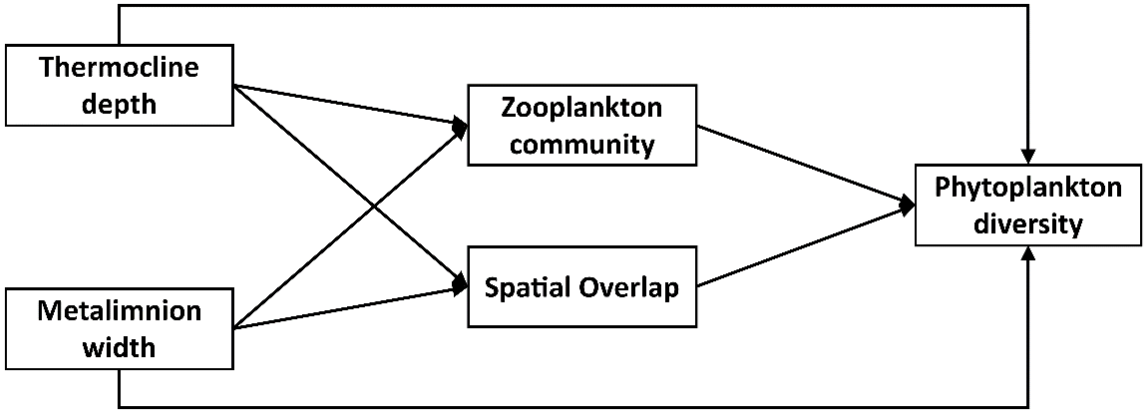

Figure 1.1. Initial Structural Equation Model. Each box represents a variable, and each arrow is a hypothesized relationship.

1.3 Materials and Methods

The Thermocline Induced Mixing EXperiment (TIMEX) was conducted from 2007 to 2012 (with 2007 and 2011 being non-experimental years when no treatment was applied) in Croche Lake (45.590 3500 N, 74.000 2800 W) at the Station de biologie des Laurentides, St-Hippolyte, Québec, Canada. Phytoplankton compositional data was only collected from 2009 to 2011. Samples were collected fortnightly during the day from ice-off to the end of September in each year at a sampling platform anchored at the deepest point of each basin. The main goal of the TIMEX experiment was to alter the depth of the thermocline of one of three lake basins. However, the treatment altered additional parameters related to the stratification structure as well, especially the width of the metalimnion, which was enlarged with thermocline deepening (Ouellet Jobin and Beisner, 2014).

1.3.1 Experimental setup

Croche Lake is meso-oligotrophic and naturally divided into three 10-11-m deep basins (Fig. 1.2). The eastern basin (B1) served as a control in all years. To lower the thermocline in the western-most basin (B3), a solar-powered lake mixer (SolarBee®, H_2O Logics Inc., Sherwood Park, Alberta, Canada) was run during the experimental years (2009-2010 in our dataset). Thermocline depth in the western B3 basin was successfully lowered from 4-m to around 8-m. This basin was isolated from the intermediately located basin (B2) by a narrow pass of 1-m deep water, an island and a 120-m wide and 6-m deep section where a black polyethylene curtain was

installed. In all treatment years, passive heat transfer occurred through the curtain, thereby also lowering the thermocline in B2 from 4-m to around 6-m (Fig. 1.3). For simplicity, the basins will be referred to as the control basin (B1), the passively deepened basin (B2) and the actively deepened basin (B3). This setup is described in other related publications (Cantin *et al.*, 2011; Ouellet Jobin et Beisner, 2014; Sastri *et al.*, 2014).

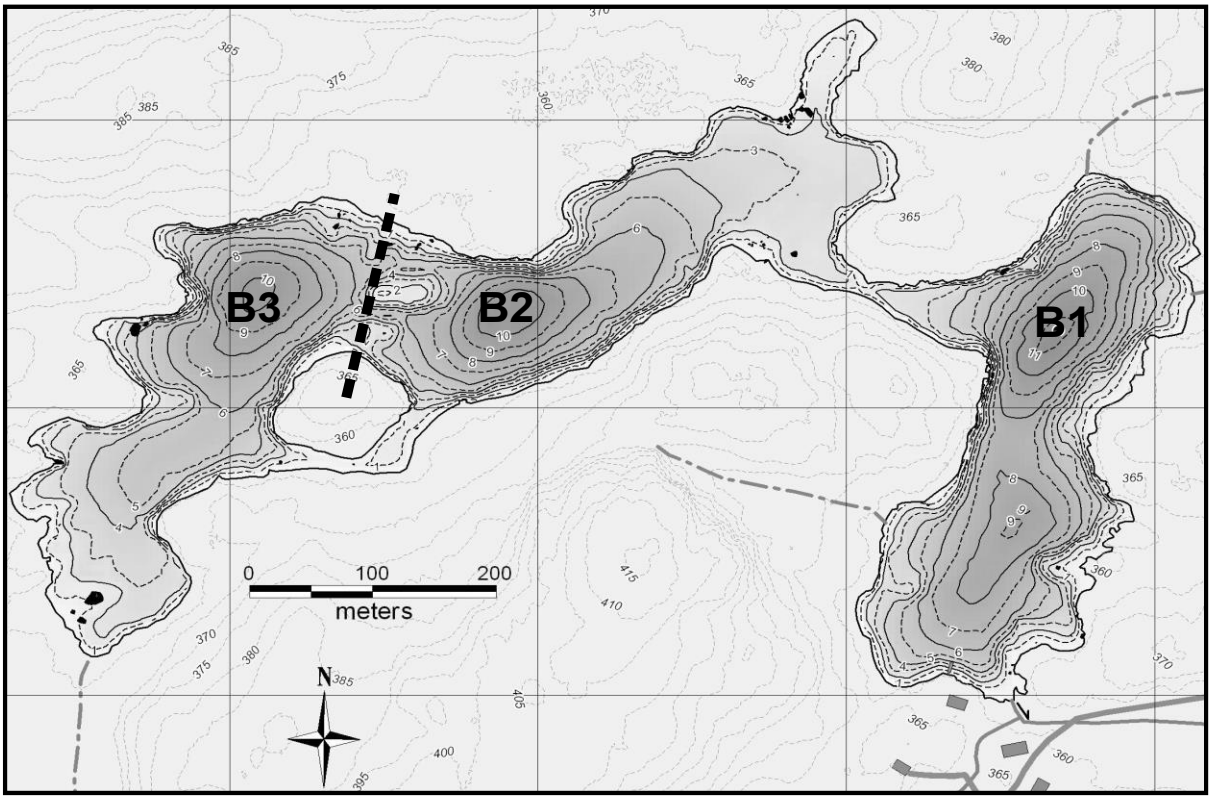

Figure 1.2. Bathymetric map of the lake (Courtesy of R. Carignan, Station de Biologie des Laurentians, University of Montreal, Montreal, Quebec). The dotted line represents the curtain and each basin is defined as follows: B1=control, B2=passively deepened, B3=actively deepened.

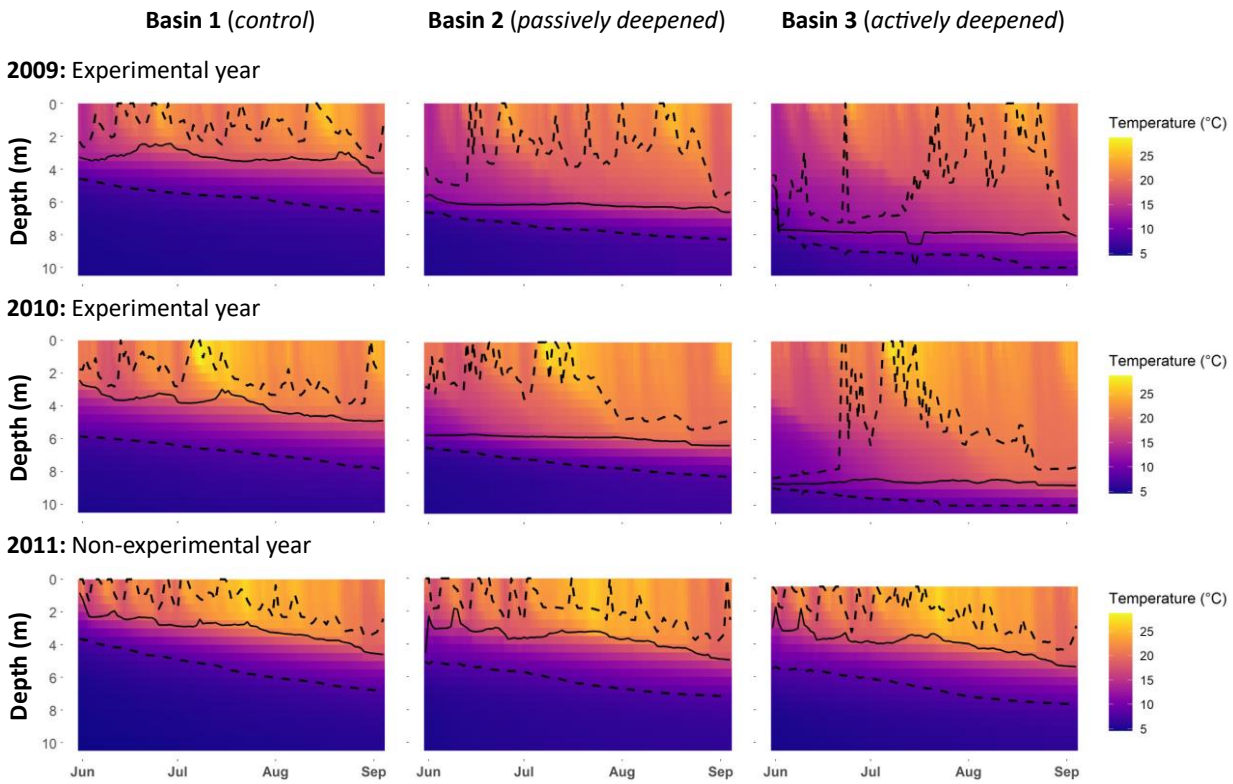

Figure 1.3. Contour plots of temperature at each depth in 2009, 2010 and 2011 in each of the three basins. The solid line represents the thermocline depth (computed daily) while the dotted lines represent the limits of the metalimnion.

1.3.2 Data collection

Total phosphorus (TP) concentrations were measured at the surface and at 2, 4, 6 and 8-m depth in each basin over the three years. A graphical investigation confirmed that the nutrient vertical gradient, present in the control basin B1, was disrupted in B3 during the experimental years (Annexe A).

Whole water column samples were taken for phytoplankton from each basin on each of 22 sampling occasions across the 3-years. An integrated 1.5-cm diameter PVC tube sampler was used to sample from the surface to 1-m above the sediments. Taxa composing the communities were identified and enumerated using the Ütermohl method on an inverted microscope (400x magnification). Biovolumes (in $mm^3.m^{-3}$) were determined based on measured cell dimensions and by applying geometric formulae for similarly shaped objects (Hillebrand *et al.*, 1999).

On each of sampling date, a FluoroProbe (FP; bbe-Moldaenke, Kiel, Germany) was used to measure the quantity of chlorophyll *a* (Chl *a*) associated with four major spectral groups

throughout the water column at the deepest point in each basin. The FP detects Chl *a* by fluorescence using excitation light sources at different wavelengths which enables grouping of phytoplankton according to their accessory pigments: BROWNS (diatoms, dinoflagellates and chrysophytes), GREENS (chlorophytes), CYANOS (phycocyanin-containing cyanophytes) and MIXED (cryptophytes in this lake). A UV-excitation source is used to subtract the fluorescence coming from chromophoric dissolved organic matter (CDOM). The FluoroProbe data have a vertical resolution of about 10 cm.

Also, at the deepest point in each basin, water temperature profiles were measured at 20-minute intervals using thermistor chains equipped with HOBO temperature loggers (±1^{o}C; Onset Computer Corporation, Cape Cod, MA, USA) at 0.5-m depth intervals and installed for the duration of the experiment. Owing to a defective sensor, temperature data were not available at the surface (0m) of B3 in 2011. However, this did not affect any subsequent estimations of thermal profile properties in the basin as it was always shallower than the upper limit of the metalimnion.

Finally, the zooplankton community was sampled by hauling a 54-µm-mesh net (150 cm in length; 30 cm in diameter) from the bottom of the lake (1-m above the sediments) to the surface at the deep station in each basin. Taxonomic identification was performed on sub-samples using an Olympus inverted microscope (x100 magnification), until a minimum of 200–300 total individuals had been enumerated. Biomasses (dry, in µg.L^{-1}) were estimated by applying length–mass relationships (Mccauley, 1984) to standard length measurements of 20 individuals per species.

1.3.3 Estimation of indices and metrics

Our dataset included 66 sampling events corresponding to unique combinations of sampling date and sites (basins). Overall, there were 21 observations in 2009 (7 time points per basin), 24 observations in 2010 (8 time points per basin) and 21 observations in 2011 (8 time points in B1; 7 in B2; 6 in B3). Index determination and statistical analyses were done in R version 4.1.0 (R Core Team, 2021). Indices related to physical structure of the water column (thermocline depth $Thermo_{Depth}$ and metalimnion width $Meta_{Width}$) were estimated for each sampling event from the

temperature profiles using the *rLakeAnalyzer* R package (Winslow *et al.*, 2019). *rLakeAnalyzer* estimates a density gradient over the water column (Read *et al.*, 2011). Thermocline depth is the depth at which this gradient is maximized. The upper and lower bounds of the metalimnion are defined as the depths at which the density gradient reaches a specified threshold value of 0.1 $kg.m^{-3}.m^{-1}$.

The FluoroProbe spectral profiles were used to calculate an index of spatial overlap (*SO*) between the spectral groups using a script for overlap in traits created by Mouillot *et al.* (2005) and modified in Beisner and Longhi (2013) for phytoplankton profiles. In summary, a kernel density function was applied to the vertical profile of each spectral group taken at a given sampling event. The proportion of the area under the overlapping curves shared between each pair of spectral groups was calculated with the mean of all these pairwise comparisons representing *SO*. The index ranges from 0 to 1, where 0 indicates no spatial overlap and 1 represents total overlap in the distribution curves of the spectral groups.

Phytoplankton taxonomic diversity was estimated using the Shannon diversity index (*H'*) based on biomass with the *vegan* R package (Oksanen *et al.*, 2020). The Shannon index takes into both the number of species and their relative biomass. A higher Shannon index value indicates a more diverse community, i.e., a community with more species and/or a set of species that contribute more evenly to the total community biomass (Sager and Hasler, 1969). Phytoplankton functional diversity was estimated from a functional trait matrix compiled by our research team for lake phytoplankton taxa across lakes in the region (Annexe C). This matrix included six functional traits related to morphology and resource acquisition as listed in Table 1.1. The traits used have been described in other publications and reflect important processes, in particular resource acquisition (Litchman and Klausmeier, 2008; Weithoff, 2003). All traits were categorical except for the continuous maximum linear dimension (MLD). The MLD is a measure of the size of a cell for a given taxon (in µm). Nitrogen fixation is the potential for some cyanobacteria taxa to fix atmospheric dinitrogen. Silica fixation refers to the production of external protective silica structures by diatoms and by some chrysophytes. Mixotrophy is the potential for a given taxon to acquire energy and nutrients through both phototrophy and phagotrophy via bacterivory. Coloniality refers to the tendency of some taxa to form chains or colonies of multiple cells. The Pigment trait comprises five categories corresponding to combinations of accessory pigments

found in one or several taxonomic groups: Brown (diatoms, dinoflagellates, chrysophyceae), Green (chlorophyceae, euglenophyceae), Blue-Green (cyanobacteria), Red (cryptophyceae) and Yellow-Green (xantophyceae). Traits related to nutrient consumption kinetics (e.g., half saturation constants, maximum absorption rates) could not be included in the trait matrix as they are not routinely available for freshwater taxa. However, several studies have noted that these traits correlate well with the body size of phytoplankton (Edwards *et al.*, 2012; Litchman *et al.*, 2009), making MLD a suitable proxy of life history strategy variation. We did not include a trait for motility structures like flagella or gas vacuoles, as motility is likely to directly affect spatial overlap, unlike the traits we chose to consider, that are also more direct proxies of resource competition. The trait values were assigned using microscopic observations and information available in the literature (Laplace-Treyture *et al.*, 2021; Rimet and Druart, 2018; Annexe M). Phytoplankton functional dispersion was (F_{Dis}) was estimated by applying our trait matrix with the genus biovolume matrix using the *FD* R package (Laliberté *et al.*, 2014; Laliberté and Legendre, 2010). F_{Dis} measures the dispersion of the taxa in the multidimensional space formed by the functional traits and the index increases with greater diversity. It corresponds to the mean distance of individual taxa, weighted by the relative abundances of the taxa, to the community centroid projected in trait space. This index can use both quantitative and qualitative traits.

A caveat of our study relates to the scale discrepancy in the data used to compute the *SO* and the diversity indices: *SO* was estimated using pigment measurements that combine broad phytoplankton taxonomic groups at fine spatial scales, while diversity was estimated at a finer taxonomic resolution using genus-level biomass, but across the water column. While, in theory, *SO* could be measured at a finer taxonomic scale by using phytoplankton counts in samples taken at many discrete depths, the sampling and counting effort required would be monumental and is simply not realistic in the context of measurements taken at multiple timepoints as in the TIMEX experiment. For the tools available to us during this unique whole-lake experiment, these discrepancies in scales were unavoidable, but our interpretation considers this context.

Table 1.1. List of the functional traits used in the study, their type and diversity index to which they are associated.

Functional traits	Values	Associated diversity index
Maximum Linear Dimension (MLD)	Quantitative	$CWvar_{MLD}$
Nitrogen fixation	Y/N	H_{Nfix}
Silicium fixation	Y/N	H_{Si}
Mixotrophy	Y/N	H_{Mix}
Coloniality	Y/N	H_{Col}

1.3.4 Statistical analyses

All 66 sampling events in our datasets were treated as independent observations. Causal relationships and links between variables were tested using structural equation modeling (SEM). This multivariate statistical framework allows evaluation of the network of causal relationships linking multiple variables based on user-specified hypotheses. The validity of the model is then assessed by confronting it with measured data (Grace *et al.*, 2012; Shipley, 2000). We first specified a general model that included the ecologically plausible pathways between five compartments: *Thermocline depth*, *Metalimnion width*, *Zooplankton community*, *Spatial overlap*, *Phytoplankton diversity* (Fig. 1.1). The relationships between these compartments reflect the hypotheses of our study. *Thermocline depth* ($Thermo_{Depth}$) and *Metalimnion width* ($Meta_{Width}$) directly relates to the treatment applied to our system, so we considered these compartments as exogenous variables, not affected by the other variables. All the other variables are endogenous, dependent on at least these two variables. Using this general model (Fig. 1.1) as a template, two distinct models were estimated for each type of community diversity, the first one using *H'* (taxonomic) and the second using F_{Dis} (functional) to represent the *Phytoplankton diversity* compartment. Variables representing the remaining compartments were identical across the two diversity models. The *Zooplankton community* compartment consisted of Cladoceran biomass ($Cladocera_{Biom}$) as these are the most efficient grazers constituting a reliable indicator of the intensity of top-down interactions shaping phytoplankton diversity. Furthermore, a previous analysis of the response of the zooplankton to the TIMEX experiment showed that cladocerans were particularly susceptible to the alteration of stratification structure (Gauthier *et al.*, 2014), justifying causal relationships between the compartments $Thermo_{Depth}$, $Meta_{Width}$ and

$Cladocera_{Biom}$ in the SEMs. Because SEMs do not support variables with very dissimilar observed variance, variables were transformed when necessary to stabilize variance. In particular, the variable $Cladocera_{Biom}$ was log-transformed. We checked for signs of temporal autocorrelation in the variables for each year and for each basin and found none.

Path significance and coefficients were determined through global estimation using the *lavaan* R package (Rosseel, 2012). This procedure determines path coefficients by minimizing the difference between the model-implied variance-covariance matrix and the observed data variance-covariance matrix; with the fit between the matrices being assessed by a chi-square test. A non-significant chi-square test indicates that the variance-covariance matrices do not differ and that the model structure thus fits the data adequatly. Owing to the non-normal distributions of several variables, we used a bootstrap procedure available in *lavaan* (10 000 bootstrapped samples) to estimate the p-values of the model paths. Additional metrics can be used to assess model fit, including the goodness-of-fit index (GFI). This index measures the relative proportion of variance and covariance in the data covariance matrix predicted by the model-implied covariance matrix. A p-value > 0.95 is indicative of a good fit (Schermelleh-Engel *et al.*, 2003). For each endogenous variable, an R^2 score can be calculated to quantify the amount of variation explained.

We further investigated the effects of environmental factors on individual functional traits. Multiple linear regression analyses were performed on indices of variability for each functional trait used to compute F_{Dis}, with $Thermo_{Depth}$, $Meta_{Width}$, $Cladocera_{Biom}$ and SO as predictors. For the quantitative trait, MLD, variability was estimated as the community weighted standard variance ($CWvar_{MLD}$), using a formula proposed by Peres-Neto *et al.* (2017). Applying the community weighted variance formula to a quantitative trait yields a weighted measure of the dispersion in trait values within the community. For the six other qualitative traits with two to five different modalities, we estimated the biomass of each trait modality in the community on each sampling date by summing biomasses across taxa presenting that modality. We then applied the formula of the Shannon index (H') on each trait, using the biomasses of the different modalities of a given trait rather than taxa as distinct statistical individuals. Applying the Shannon index formula to a given qualitative trait reflects both number of trait modalities represented in the community, as well as the evenness of the biomass distribution of those

modalities. These indices of variability were used as response variables in separate regression models: in total, six regression models were estimated (Table 1.2). The distributions of the response variables did not always meet the assumptions of frequentist Gaussian models, so we applied permutation tests (10 000 draws) to assess the significatively of the coefficients of the regression models, using the function *lmorigin* available in the R package *ape* (Paradis and Schliep, 2019).

1.4 Results

1.4.1 SEM for the taxonomic diversity

The SE model for taxonomic diversity H' was not significant ($\chi^2 = 0.404, df = 1,\ p = 0.525$) and the goodness-of-fit index was high ($GFI = 0.996$), together indicating a valid model adequately representing the observed data (Fig. 1.4a). The relationship of *H'* with *SO* was not significant and neither was the direct relationship with $Thermo_{Depth}$. However, taxonomic *Phytoplankton diversity* (*H'*) was significantly positively affected by $Meta_{Width}$. *H'* was also significantly negatively affected by $Cladocera_{Biom}$ (*Zooplankton community* compartment), which itself was negatively affected by $Thermo_{Depth}$ (but not by $Meta_{Width}$). A significant positive relationship was detected between $Thermo_{Depth}$ and *SO*, but not between $Meta_{Width}$ and *SO*. Although there was no direct significant relationship between $Thermo_{Depth}$ and *H'*, a larger epilimnion indirectly promoted the taxonomic *Phytoplankton diversity* compartment because $Thermo_{Depth}$ negatively affected $Cladocera_{Biom}$ which itself negatively affected *H'*. The model explained 18.1% of the variability in *SO*, 22.2% of the variability in $Cladocera_{Biom}$ and 35.4% of the variability in *H'*.

1.4.2 SEM for the functional diversity

The final SE model for F_{Dis} was very similar to the model for *H'* (Fig. 1.4b), as might be expected given that the predictors for the compartments were the same. This SEM did not reveal a significant effect of *SO* on F_{Dis}, indicating no influence of spatial overlap on functional *Phytoplankton diversity*. The model Chi-square test was not significant ($\chi^2 = 0.405, df = 1, p = 0.525$) and the goodness-of-fit index index was $GFI = 0.996$, indicating that the model provided an adequate fit to the data. This model explained 18.1%, 22.2% and 27.2 of the variability of *SO*, $Cladocera_{Biom}$ and F_{Dis} respectively.

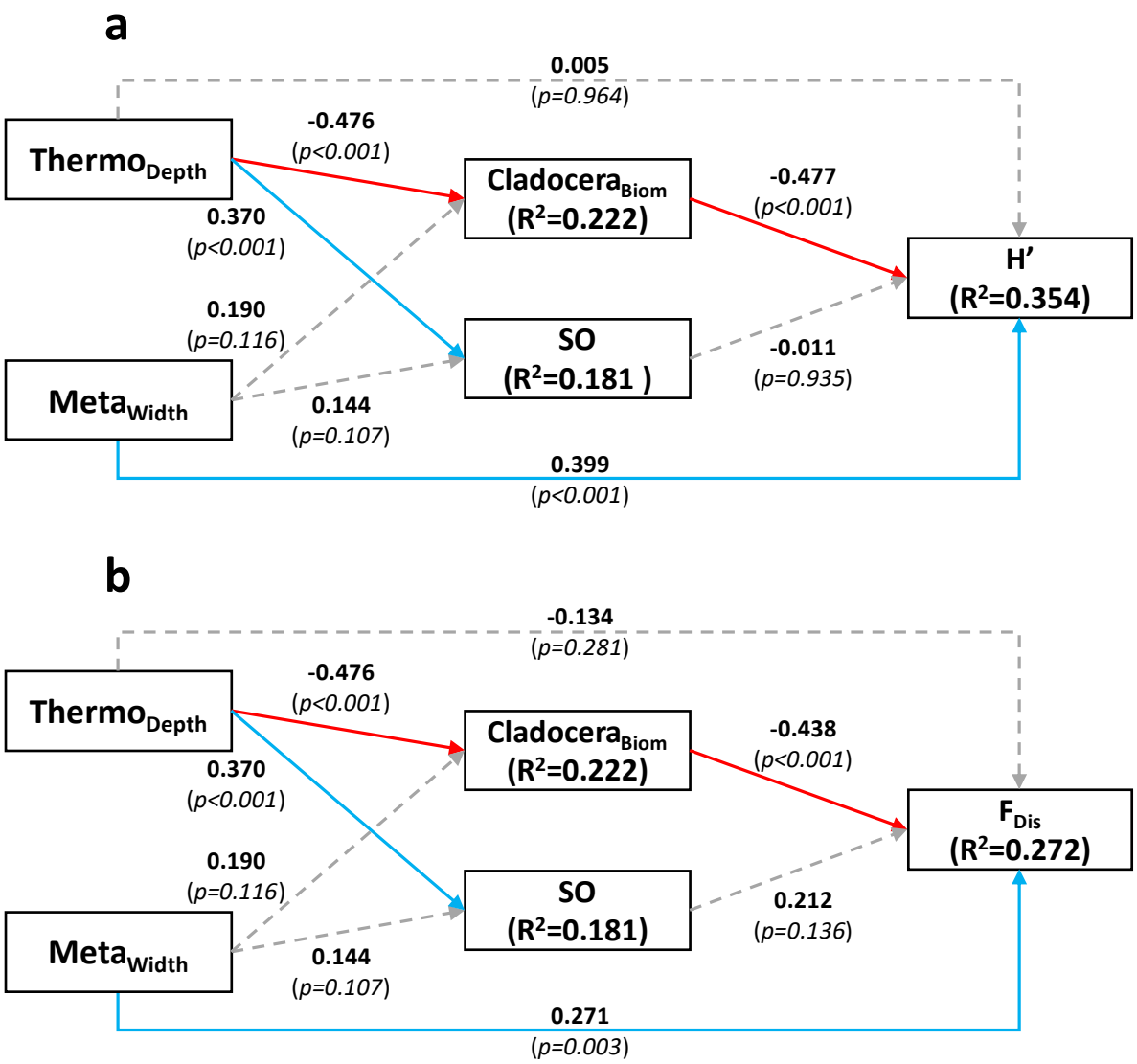

Figure 1.4. SE models for *H'* and F_{Dis} (a and b respectively). Dashed grey arrows represent non-significant relationships. Blue arrows represent significant positive relationship and red arrows represent significant negative relationship. Results shown are standardized coefficients and *p*-value (between parentheses), as well as R^2 scores for endogenous variables.

1.4.3 Effect of SEM predictors on the diversity of individual traits

We used $Thermo_{Depth}$, $Meta_{Width}$, $Cladocera_{Biom}$ and *SO* as predictors in the permutation multiple linear regression models on the individual trait variability indices (Table 1.2). $Thermo_{Depth}$ had a significant negative effect on the diversity of taxa cell sizes ($CWvar_{MLD}$) and a significant positive effect on the diversity of pigments (H_{Pig}). $Meta_{Width}$ significantly and positively affected the diversity of the nitrogen fixation and pigment traits (H_{Fix} and H_{Pig} respectively). $Cladocera_{Biom}$ had a significant negative effect on diversity of the pigment trait (H_{Pig}) and the coloniality trait

(H_{Col}). *SO* did not significantly affect any individual trait diversity indices, although the p-values for the diversity of silica fixation and mixotrophy traits were relatively close to the 0.05 threshold (with a positive trend for H_{Si} and a negative trend for H_{Mix}).

Table 1.2. Results of the permuted multiple linear regressions on the different trait diversity indices. For each regression, the coefficients for each potential explanatory factor (from left to right: *Thermocline depth*, *Metalimnion width*, *Zooplankton biomass* and *Spatial Overlap*) are indicated along with associated *p*-values in parentheses. Significant coefficients and *p-values* are indicated in bold.

	$Thermo_{Depth}$	$Meta_{Width}$	$Cladocera_{Biom}$	*SO*
$CWvar_{MLD}$	**157** **(1.00E-04)**	-15.3 (0.356)	3.05 (0.086)	69.7 (0.442)
H_{Nfix}	-9.05E-04 (0.401)	**8.34E-03** **(0.025)**	2.40E-04 (0.117)	0.01 (0.390)
H_{Si}	3.07E-03 (0.354)	3.15E-04 (0.498)	-5.14E-04 (0.161)	0.16 (0.073)
H_{Mix}	-9.340E-03 (0.111)	9.73E-03 (0.127)	-6.73E-04 (0.075)	-0.15 (0.069)
H_{Col}	-1.34E-03 (0.420)	0.0107 (0.092)	**-1.46E-03** **(0.001)**	0.09 (0.154)
H_{Pig}	**-0.033** **(0.030)**	**0.0613** **(0.001)**	**-2.55E-03** **(0.008)**	0.29 (0.100)

1.5 Discussion

We examined, in a whole-lake experimental context, whether altering the stratification structure of the water column would reveal an influence of spatial overlap on community diversity. We predicted that increased interspecific competition would reduce taxonomic diversity, but our analyses revealed no such effect of *SO* on the Shannon diversity index (*H'*) of the community. This absence of effect of community aggregation on H' could be explained if functional trait differentiation is effective at precluding taxonomic diversity decline through niche partitioning. However, while the slope coefficient of the linear relationship between of *SO* and F_{Dis} was positive in our SEM, this trend was not significant. While we anticipated that higher *SO* would be

associated with a generally greater diversity of resource acquisition and morphology traits, the expected positive effect of *SO* on functional diversity was not observed. Thus, a summary measure of functional diversity like F_{Dis} might be somewhat inadequate to capture potentially contrasting responses of individual traits to spatial overlap.

In our study, greater *SO* was associated with a deeper thermocline (Fig. 1.4a, 1.4b), and thus, by definition, a wider mixed (epilimnetic) layer. Overall, this implies a larger portion of the water column over which phytoplankton species cannot easily regulate their position and are thus potentially susceptible to greater competition. Therefore, we expected to see a negative effect of *SO* on *H'*. The absence of such signal indicates that the effect of spatial aggregation on diversity might not be as straightforward as we initially assumed, and that species can coexist even when spatial overlap is high – perhaps via coexistence of taxa utilizing different traits – although no effect on F_{Dis} was observed either. The absence of effect of *SO* on *H'* and F_{Dis} could also simply indicate that interspecific competition is not a strong driver of either taxonomic and functional diversity in our system. In the context of our experiment, the physical structure of the environment and top-down interactions appear to be more important drivers of diversity, as $Meta_{Width}$ and $Cladocera_{Biom}$ significantly affected *H'* and F_{Dis} in our SE models (Fig. 1.4a).

The SEMs featured a direct positive effect of metalimnetic width on both diversity types, but not a direct effect of thermocline depth itself. Focusing on functional diversity, further analyses revealed an effect of metalimnetic width on the diversity of pigments and diazotrophy strategy traits. A wider metalimnion implies a thicker stable layer covering a larger range of light intensities and colors. Species with different light requirement, hence with different pigment types, would be able to better coexist within a wider stratified layer by establishing at different depth (Pérez *et al.*, 2007). The positive effect of $Meta_{Width}$ on H_{Nfix} appears to mostly be the result of a taxonomic change in community contribution. Further investigation revealed that a larger metalimnion, implying a larger stratified portion of the water column, favors buoyant cyanobacteria that can use gas vacuoles to regulate their vertical positions (Annexe Ba) (Huisman *et al.*, 2004; Walsby *et al.*, 1997). Since some cyanobacterial taxa are able to fix dinitrogen, a larger metalimnion would then also contribute to a diversification (H_{Nfix}) of nitrogen fixation strategy (Paerl, 1990).

While thermocline depth did not have a similar direct significant effect on the overall functional diversity of the community, it did affect the diversity of several individual traits. In particular, a deeper thermocline positively affected the diversity of community cell sizes and negatively affected the diversity of pigments ($CWvar_{MLD}$ and H_{Pig} respectively). A larger mixed layer induced by thermocline deepening might allow larger sinking diatoms to be more prevalent where otherwise small non-sinking taxa would dominate. Indeed, Ptanick *et al.* (2003) demonstrated in a mesocosm experiment that large fast sinking diatoms benefit from higher mixing depths. Conversely, a deeper epilimnion could prevent some species from establishing at the optimal light absorption depth for their accessory pigment composition, leading to a loss of pigment diversity in the community; optimal adaptations being for varying light (more mixed taxa) or for reduced light (those that are able to remain near or in the hypolimnion). These effects of thermocline depth and metalimnetic width on phytoplankton diversity illustrate how the physical environment shapes community composition.

Returning to the relationship between *SO* and F_{Dis}, we expected higher levels of *SO* to be associated with higher levels of functional differentiation. As our SEM results indicates, this was not observed in our experiment, at least not a global index of trait diversity like F_{Dis}. A more detailed investigation of the effect of *SO* on individual trait diversity could nuance this result. For example, we expected to observe functional differentiation of traits related to resource acquisition at higher *SO* levels because when spatial niche overlap occurs within the actively mixed layer, species need to display different nutrient acquisition kinetics to avoid competitive exclusion (Sommer, 1984, 1985). However, we found no positive significant effect of *SO* on any individual trait diversities. We noted a near-significant trend ($p = 0.073$) indicating that *SO* might promote a better balance between silica-requiring taxa (i.e. diatoms and some chrysophyte genera) and non silica-requiring taxa (greater H_{Si}). In contrast, we observed a negative trend between *SO* and the diversity of resource acquisition strategies (H_{Mix}, $p = 0.068$). Further investigation revealed a trend to more dominance by autotrophy with greater *SO* (Annexe Bb). Our own theoretical study of competition between a phago-mixotrophic competitor and specialized competitors (a pure photo-autotroph and a pure heterotroph) indicates that generalist phago-mixotrophs are likely to be more competitive in a vertically structured community, as a they can grow at depths where the growth rate of a specialized photo-autotroph is not positive (see Chapter II). Thus reduced *SO*

levels (i.e., a more spatially structured nanophytoplankton community) could promote a better balance between phago-mixotrophs and photo-autotrophs, although here this effect is rather weak. Overall, our results indicate that *SO* does not act on the global functional diversity of the community and that while vertical aggregation might have contrasting effects on traits related to resource acquisition (promoting H_{Si} vs. lowering H_{Mix}), the effect of *SO* on individual traits is weak. Note that these results are conditioned by the selection of traits we could measure and chose to include in our analyses.

Grazing by zooplankton was also an important factor in regulating phytoplankton diversity in our SEM analyses. In particular, cladoceran biomass was one of the main factors affecting, negatively, phytoplankton both taxonomic and functional diversity. The $Cladocera_{Biom}$ effect on F_{Dis} was greater than *SO* in terms of the absolute values of the standardized relationship coefficients, indicating that the zooplankton community was a more important driver of *Functional diversity* than was *SO* in the context of our experiment. The negative grazing effect runs counter to theory that states that zooplankton grazing pressure should promote phytoplankton taxonomic diversity by reducing the amount of interspecific resource competition (McCauley and Briand, 1979; Menge and Sutherland, 1976), even experimentally for evenness (Sarnelle, 2005). However, detailed examination of phytoplankton communities under increasing levels of cladoceran grazing has demonstrated concomitant shifts to dominance by larger or colonial phytoplankton species (Sommer *et al.*, 2001), thereby reducing functional diversity, and thus potentially taxonomic diversity where such species are rare, as is the case in our study lake and as we observed. Indeed, individual trait diversity did demonstrate significantly reduced diversity within traits associated with coloniality (H_{Col}) and pigments (H_{Pig}), indicating that selective grazing by cladocerans can reduce the diversity of certain phytoplankton trait types as a result. Accompanying declines in taxonomic diversity would be expected in a relatively closed experimental system such as ours where selective feeding could remove entire taxa (based on traits) without replacement by other more resistant species from adjacent lakes (none upstream of our site) over the time scale of our experiment. Indeed, cladoceran feeding is known to be selective, as observed in experiments demonstrating that cladoceran gut pigment composition is significantly different from the pigment composition of the associated phytoplankton community (Wong *et al.*, 2006).

It is important to note that our spectral measurements of phytoplankton vertical structure can only approximate real values of *SO*, as they only inform on the pigment levels for four broad spectral groups, but at fine spatial scales. For example, we cannot quantify spatial overlap between chlorophyte taxa, as they all share the same green pigment detected spectrally. This leads to difficulty in fully assessing *SO* at very fine taxonomic scales, similar to those at which diversity was estimated. To utilize whole-lake experiments to their full potential, improved rapid tools to assess both spatial overlap at fine spatial scales and taxonomic resolution are needed.

1.6 Conclusions

Our study revealed that altering the thermal stratification structure of a lake, while controlling for lake morphometry, chemistry and global community composition, can affect spatial overlap amongst phytoplankton groups. Spatial overlap was not related to taxonomic diversity, indicating that forced coexistence does not necessarily translate into competitive exclusion. While we could have in turn expected vertical aggregation to favor functional diversity, as niche differentiation along trait axes could have alleviated interspecific competition and precluded an effect of spatial overlap on taxonomic diversity, we did not observe any effect of *SO* on global functional dispersion (F_{Dis}). Although *SO* does not affect the global functional diversity of the nanoplankton community in our system, vertical aggregation appeared to have some contrasting effects on individual trait diversity for resource acquisition. This highlights the importance of investigating the response of individual traits to the environment, as a global measure of functional diversity like functional dispersion would fail to capture potentially contrasting effects of an environmental driver on multiple traits. Globally our analyses revealed that the physical structure of the environment and cascading top-down interactions are the stronger drivers of phytoplankton diversity (both taxonomic and functional) in our system. To our knowledge, this study is the first to simultaneously assess the relative effects of not only spatial overlap, but also grazing and the physical environment on multiple dimensions of phytoplankton diversity.

CHAPITRE 2

Nanoplankton mixotrophy vs. specialist resource-acquisition strategies in a stratified water column: A spatial mechanistic modeling approach

Philippe Le Noac'h[1], Sebastian Diehl[2] and Beatrix E. Beisner[1]

[1]Department of Biological Sciences, University of Quebec at Montreal and Interuniversity Research Group in Limnology/Groupe de Recherche Interuniversitaire en Limnologie (GRIL), H2X 1Y4 Montreal, Quebec, Canada

[2]Department of Ecology and Environmental Science, Umea University, SE-90187 Umea, Sweden

2.1 Abstract

Along the opposing vertical gradients of light and nutrients usually present in stratified lakes, mixotrophy represents a generalist resource-acquisition strategy relative to photo-autotrophic or phago-heterotrophic specialist strategies. Yet it is still not entirely clear how mixotrophy, with its associated physiological costs can be viable against specialist strategies in a resource competition context. We developed a model that simulates the population dynamics of three competitors (pure photo-autotroph, mixotroph and pure phago-heterotroph) and bacterial prey over the vertical dimension of a stratified water column to investigate the prevalence of mixotrophy. In nature mixotrophs can be more or less photo-autotrophic, a flexibility that was incorporated into our model. Mixotrophy was viable under most resource availability conditions in our spatially heterogeneous system. Furthermore, the mixotroph could emerge as the dominant competitor if it displayed the right functional balance of photo-autotrophy and phago-heterotrophy, particularly when nutrient availability was low. One factor that potentially explained the success of the generalist competitor is that the mixotroph generally grew over a larger portion of the water column than the specialists. Finally, our model indicates that the spatial organization of nanophytoplankton communities in lakes could stem from the coexistence of multiple resource-acquisition strategies competing over vertical resource gradients.

Keywords: nanoplankton, phago-mixoplankton, resource competition, spatial gradient, mechanistic modeling

2.2 Introduction

Mixoplankton are aquatic microorganisms that display the necessary physiological structures to perform both phagotrophy and photosynthesis to acquire the energy and resources necessary for growth (Flynn *et al.*, 2019). This makes mixotrophy an alternative nutrition strategy to pure photo-autotrophy or pure phago-heterotrophy (Selosse *et al.*, 2017). Consequently, mixotrophs can be considered generalist competitors, in contrast to specialist photosynthetic phytoplankton and phagotrophic protists (Litchman and Klausmeier, 2008). However, the degree of mixotrophy expressed can vary greatly among mixotrophic taxa and plankton nutrition behaviour appears to form a gradient in terms of the relative roles of photo-autotrophy to phago-heterotrophy (Flynn *et al.*, 2013; Stoecker, 1998). Mixoplankton are ubiquitous in marine and freshwater environments, and plankton taxa previously assumed to be purely photo-autotrophic are now recognized as mixotrophs (Flynn *et al.*, 2013). Yet mixotrophy is often overlooked when investigating nanoplankton communities and has been long left out of conceptual ecosystem models (Mitra *et al.*, 2014) despite the significant part mixotrophy likely plays in ecosystem processes, including food web dynamics and aquatic carbon flux (Flynn *et al.*, 2013). While interest in mixotrophy has increased in recent years, there is still a gap between our theoretical understanding of mixotrophy and what we observe in nature. In particular, it is important to better understand what makes mixotrophy a viable strategy in a resource competition framework when mixoplankton compete with specialist competitors.

By investing in two distinct strategies of resource acquisition, mixotrophic nanoplankton taxa are generally considered less efficient at energy and nutrient acquisition for a given nutritional mode than taxa specialized in each corresponding resource-acquisition strategy (Dolan and Pérez, 2000; Raven, 1997). Yet mixoplankton are found in most aquatic ecosystems and can even dominate nanoplankton communities in many instances. It has been theorized that mixotrophy is most viable against specialists when nutrient availability is low, i.e., in oligotrophic systems (Crane and Grover, 2010), but mixotrophic taxa can also thrive under eutrophic conditions (Burkholder *et al.*, 2008). Other studies have proposed that mixotrophs should benefit from increased light availability (Edwards, 2019), although they can also dominate in colored lakes (Bergström *et al.*, 2000). One possible factor contributing to the apparent success of mixotrophy in many lakes is the heterogeneous distribution of resources. In stratified aquatic ecosystems, nanoplankton taxa

compete over two opposing resource gradients: light declining from the surface, and nutrients regenerated primarily towards the bottom of the water column. Under such opposing gradients, the efficiency of a given nutrition strategy should vary over depth, and each type of competitor, including mixotrophs, could potentially occupy its own spatial niche. Mixotrophs could potentially dominate at depths where pure phototrophs are light-limited, relying on phagotrophy to compensate for reduced photosynthetic energy acquisition. Indeed, distinct vertical patterns for different nutrition strategies have been observed in nature (Princiotta and Sanders, 2017; Romano *et al.*, 2021). Some theoretical studies have also stressed the importance of vertical spatial gradients for the coexistence of multiple competitors, although they have mostly focussed on pure photo-autotrophic strategists (Huisman *et al.*, 1999; Yoshiyama *et al.*, 2009). Another possible explanation to the pervasiveness of mixotrophy is the apparent plasticity of mixoplankton in their nutrition behaviour. Indeed, mixotrophy appears to be a highly flexible strategy: the reliance of a mixoplankton taxa on a given nutrition mode is dependent on the particular environmental resource availability conditions to which they are exposed (Lambert *et al.*, 2022; Li *et al.*, 2021).

One explanation for the delay in establishing the role of mixotrophy in lakes is the difficulty in properly assessing its occurrence, flexibility and prevalence under natural conditions. While it is often known that a given nanophytoplankton taxon has the potential to engage in mixotrophy, estimating rates of mixotrophy *in situ* is particularly difficult (Beisner *et al.*, 2019). Thus, we have limited knowledge on the relative prevalence of mixotrophy for energy and nutrient acquisition within a nanophytoplankton community. Similarly, we have little insight into variation in the success of a given resource-acquisition strategy with depth in stratified lakes. Consequently, our ability to understand of the role of mixotrophy from field data remains limited. One way to aid such eventual research is to develop model predictions using simulations over time and space of nanophytoplankton community dynamics including various resource-acquisition strategies. Numerical models allow testing of hypotheses in community ecology and simulations of population dynamics by translating physiological processes in a mathematical framework using differential equations, providing there is a solid theoretical understanding of the processes considered. Detailed sets of equations have been proposed to account for mixotrophy in a mechanistic framework (Berge *et al.*, 2017; Flynn and Mitra, 2009; Ghyoot *et al.*, 2017;

Kooijman *et al.*, 2002; Moeller *et al.*, 2019). While theoretical works that focus on resource competition between mixoplankton as well as specialist photo-autotrophic and phago-heterotrophic strategists exists for mixed systems (Crane and Grover, 2010; Thingstad *et al.*, 1996; Ward *et al.*, 2011), there is still a lack understanding of the role of resource competition between multiple trophic modes over the vertical dimension of a stratified water column.

Here we present a modelling approach to study resource competition between several plankton trophic strategies. Our model simulates over time and the vertical dimension of a stratified water column the dynamics of a photosynthetic autotroph, a phagotrophic heterotroph and a mixotroph competing over light, dissolved nutrients (phosphorus) and bacteria (Fig. 2.1). Our approach draws on previous modeling of plankton resource competition in a spatial lake setting (Klausmeier and Litchman, 2001; Yoshiyama *et al.*, 2009). The model is built upon classic functions of resource absorption kinetics and allows for a variable investment of the mixotroph into photo-autotrophy. This enables the inclusion of a mixotrophic competitors with a trophic strategy ranging from pure photo-autotrophy to pure phago-heterotrophy, allowing us to further test different scenarios of mixotrophy in our simplified community. We propose to use this model to simulate the dynamic of our nanoplankton community over a range of light and dissolved nutrient availability conditions to identify under which conditions the mixotroph can coexist with specialists or even potentially dominate the community. We will also compare the results to those from a modified version of the model that only include specialist competitors, to see how adding a generalist mixotroph affect the dynamic of a specialist system. Finally, we will investigate the spatial distribution of the competitors over the dual opposite vertical gradients of light and nutrient, as well as the relative spatial niche sizes of the competitors.

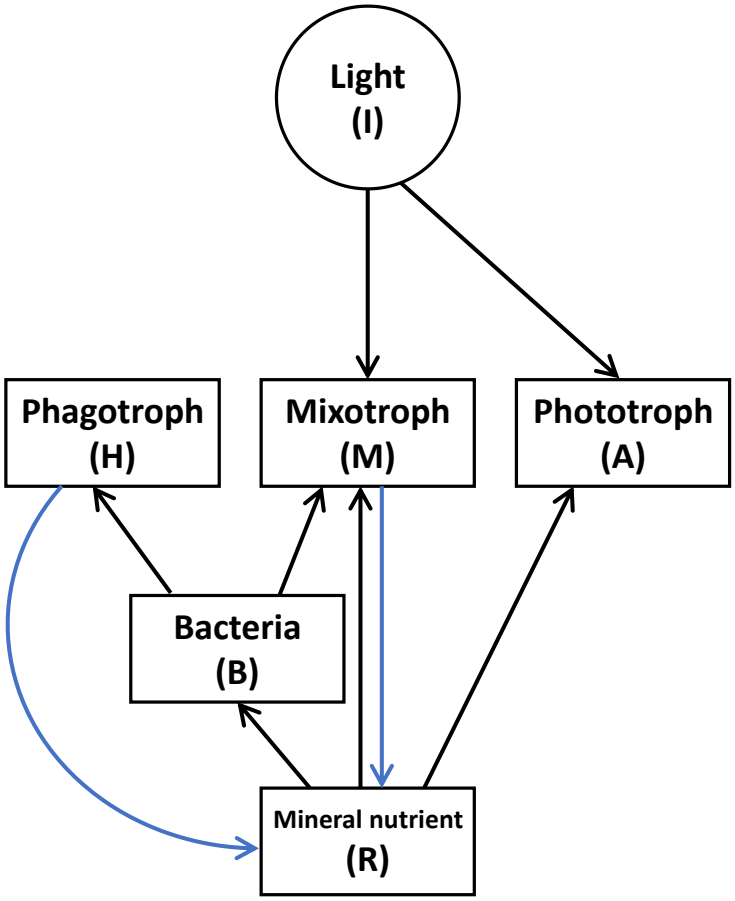

Figure 2.1. Food web representation of the study system. Each square box represents a state variable. Light, a forcing variable, is represented in a circle. Black arrows indicate the resources used by each competitor for growth; blue arrows indicate excretion of the mineral nutrient R by the competitors able to perform phago-heterotrophy (the mixotroph M and the pure phago-heterotroph H).

2.3 Methods

2.3.1 Model

The model takes the form of a set partial differential equations and in 1-D spatial modeling framework. This approach builds on that of Klausmeier and Litchman (2001) previously used to model the single phytoplankton species dynamics over opposite vertical gradients of light and mineral nutrient availability. Later studies expanded on this framework to include additional competitors and resources. For example, Yoshiyama *et al.* (2009) proposed a model that included multiple species with different trait (parameter) values related to resource acquisition. It should be noted populations and nutrients are assumed to move only through passive diffusion at a constant diffusion rate over the vertical spatial dimension in our model. Thus, any spatial structure that results does so purely based on competitive interactions along the resource gradients.

The model features three plankton competitor populations competing for three resources: mineral nutrients (R), light (I) and in some cases, bacteria (B). The model consists of a set of partial differential equations to describe over time (*t*) and space (*z*) the dynamics of the three competitor populations, B and R; while light availability over depth is evaluated using an algebraic equation. A partial list of the model parameters, definition and values is available in Table 2.1.

The growth of the photo-autotrophic specialist (A) requires I and R: its intrinsic growth rate determined at a given time and depth by applying Liebig's law of the minimum for limiting resources to a light-dependent growth rate $g_{AI}(I)$ and a nutrient-dependent growth rate $g_{AR}(R)$, such that:

$$g_A(t,z) = min\big(g_{AI}(I), g_{AR}(R)\big)$$

Liebig's law of the minimum is a common choice to model planktonic growth co-limitation by several key resources and was employed by Klaumeier and Litchman (2001) to model the response of phytoplankton to light and phosphorus availability in a spatialized system. The intrinsic growth rate of the mixotroph (M) at a given time and depth is also determined by Liebig's law of the minimum applied to light (carbon)-dependent and nutrient-dependent growth rates, although the function describing those growth rates depends not only on photo-autotrophy utilizing I and R, but also on phagotrophy for B, as follows:

$$g_M(t,z) = min\big(g_{MI}(I,B), g_{MR}(R,B)\big)$$

Both light and nutrient uptake by A and M are described by Michaelis-Menten type functions, as in the Monod model, while the consumption of B by M (i.e., phagotrophy) is a type III functional response. The intrinsic growth rate of the pure phago-heterotroph (H) is a type III functional response that depends exclusively on B, as H obtains all its necessary resources through bacterial predation (phagotrophy). Modelling bacterivory with a type III functional response is necessary to stabilize the predator-prey dynamic and avoid limit cases of preditor exclusion caused by the complete removal of the bacterial population from this closed system. This type of predation cinetic has been used to describe the feeding strategies of non-selective zooplankton taxa like *Daphnia* (Uszko *et al.*, 2015). The model allows for excretion of dissolved nutrients acquired

through phagotrophy: H is always a net excretor of R. Finally, the raw growth rate of B is a Michaelis-Menten type function that depends only on R: bacteria are exclusively nutrient-limited and carbon is never a limiting resource for B. Figure 2.1 outlines the trophic interactions between each compartments of the modelled community.

The modelled system is closed, such that we are assuming no-flux Neuman boundary conditions for any given state variable X at the surface and the bottom of our water column:

$$\left.\frac{\partial X}{\partial z}\right|_{z=0} = \left.\frac{\partial X}{\partial z}\right|_{z=z_{max}} = 0$$

The exception is for the mineral nutrient R at z_{max}, as nutrients enter the system from a theoretical sediment layer with a constant nutrient concentration. The boundary equation for R at z_{max} is then:

$$\left.\frac{\partial R}{\partial z}\right|_{z=z_{max}} = h(R_{in} - R(t, z_{max}))$$

With R_{in} the constant nutriment concentration at the sediment and h a permeability coefficient. This means that R enters the system exclusively from the bottom of the water column. Conversely, light comes exclusively from the surface z_0. Note that there is no temporal dynamic in light availability at the surface: the incoming light is constant (300 µmol photons m^{-2} s^{-1}). Light decreases with depth follows Beer-Lambert's law with as light extinction depending on the background attenuation coefficient k_{bg}, as well as on attenuation by the potentially photosynthetic competitors A and M, such that:

$$I(t,z) = I_{in} e^{-\int_0^z [k_A A(t,z) + \alpha k_M M(t,z) + k_{bg}] dz}$$

The trophic behaviour of the mixotroph M is determined by the value of the parameter α, the mixotrophic investment in photo-autotrophy. It specifies a physiological trade-off between photo-autotrophic and phago-heterotrophic growth and is featured in the equation for the growth rate of M, as well as in the fraction of light attenuation caused by M. Indeed, the carbon and nutrient

dependent specific growth rates of M can both be split into two components: an autotrophic component, i.e., a function of R or I, in which M invests a proportion α of its resources, and a heterotrophic (phagotrophic) component function of B in which M allocates a proportion $(1-\alpha)$ of its resource. The gross growth rate is the sum of these two parts. This is similar to the approach used by Crane and Grover (2010) in their model of competition between various nutritional strategies in a mixed system, and affinity functions of this type can be found in other models of mixotrophy (Troost *et al.*, 2005). This model component reflects the generalist character of mixotrophy, as well as the associated trade-off: investing physiological resources in one strategy is done at the expense of the other trophic mode. With $0 < \alpha < 1$, the gross photo-autotrophic and phago-heterotrophic growth rates of the generalist competitor M are, taken separately, always lower than the gross growth rates of either specialist competitors A and H. Indeed, the parameter values featured in the photo-autotrophic part of the growth rate of M are identical to those for A. Similarly, the parameter appearing in the phago-heterotrophic part of the growth rate of M have the same values to those for H. The trophic behaviour of M can then range from pure phago-heterotrophy ($\alpha = 0$) to pure photo-autotrophy ($\alpha = 1$). In those cases, the growth rate of M, and consequently its spatial and temporal dynamics, is indistinguishable from those of H and A respectively.

Note that phagotrophy can thus lead to a surplus acquisition of R, as bacteria have a higher nutrient to carbon stochiometric ratio than the three nanoplankton competitors in the model, and as carbon assimilation from bacteria is assumed to be incomplete (see Annexe H for the complete equation). H is thus a net excretor of R in the model. In contrast, the pure photo-autotroph A never excretes nutrients. M can be a net consumer or excretor of R depending on its photo-autotrophic investment α and on resource availability conditions. It is also important to note that B is better at acquiring R than both A or M when dissolved nutrient concentration is low. This is an important assumption in our model, but it is realistic to consider that bacteria are better competitors for nutrients than nanophytoplankton in freshwater systems if bacteria are not carbon-limited (Jansson, 1993; Joint *et al.*, 2002).

Table 2.1. Definition, units and values of the model parameters as outlined in the Methods section. The complete list of parameters is available as Supplementary Material (Annexe I).

Parameter	Definition	Unit	Value
t	Time	d	-
z	Depth	m	-
A	Biomass of photo-autotroph	g C . m^{-3}	-
M	Biomass of mixotroph	g C . m^{-3}	-
H	Biomass of phago-heterotroph	g C . m^{-3}	-
I	Photosynthetically active radiation	µmol photons . m^{-2} . s^{-1}	-
R	Mineral nutrient concentration	g P . m^{-3}	-
B	Biomass of bacteria	g C . m^{-3}	-
α	Effort spent by M on photosynthesis and mineral nutrient uptake	dimensionless	0 - 1
k_{bg}	Light attenuation coefficient of clear water	m^{-1}	0.1 – 0.6
R_{in}	Concentration of mineral nutrient in influx	mg P . m^{-3}	100 - 500
z_{max}	Maximal depth of the water column	m	10
k_A	Light attenuation coefficient of the photo-autotrophic biomass	m^2 . g C^{-1}	0.3
k_M	Light attenuation coefficient of the mixotrophic biomass (when $\alpha = 1$)	m^2 . g C^{-1}	0.3
I_{in}	Photosynthetically active radiation at the surface	µmol photons . m^{-2} . s^{-1}	300
h	Sediment-water column permeability	m^{-1}	0.05
D	Diffusion coefficient	cm^2 . s^{-1}	0.1

Complete model equations can be found in Annexe H. Parameter values were chosen to be representative of a temperate stratified system. In particular, parametrization for the dynamics of the nanoplankton competitors relies heavily on the work of Vasconcelos *et al.* (2019), a

theoretical study of a lake food web. A full list of the model parameters, including definition, values and relevant sources, is available as supplementary material (Annexe I).

2.3.2 Numerical simulations and indices computation

We simulated the system dynamics over time and space using the 1D partial differential equation solver *pdepe* available in Matlab (version R2022a). The *pdepe* algorithm is built around a finite-element method of spatial discretization to solve the system over a pre-specified spatial mesh (Skeel et Berzins, 1990). Furthermore, *pdepe* relies on the adaptive multistep *ode15s* Matlab solver to perform the time integration (Shampine et Reichelt, 1997).

Model simulations were run over an extended time period (4000 days) to ensure that the system reached equilibrium, either with stable coexistence of the three main plankton competitors, or with one or several competitors being excluded from the system. The spatial dimension of the system simulated a 10 meter-deep water column, from the surface ($z_0 = 0m$) to the sediment ($z_{max} = 10m$), with a 10 cm spatial resolution. We simulated the model over a range of conditions of resource availability and for different mixotrophic strategies. In practice, we performed multiple simulations by incrementally changing the values of relevant model parameters. We focused on three of the model parameters in particular: the sediment nutrient concentration R_{in}, the background light attenuation coefficient k_{bg} and the mixotrophic investment in photo-autotrophy α. R_{in} is part of the lower boundary condition equation for the mineral nutrient R and provides a constant nutrient supply to the water column from the sediment at $z = 10$-m. k_{bg} appears in the algebraic equation describing light extinction over depth. R_{in} and k_{bg} were selected as focal parameters because their values reflect resource availability in the system. R_{in} is directly related mineral nutrient supply and can be viewed as a proxy of the trophic state of the water column. k_{bg} is a measure of the opacity of the system, i.e., its color, independent of the photo-autotrophic and mixotrophic algal biomasses present in the water column: in a system with a high k_{bg} value, the depth of light extinction is located high in the water column.

From the biomass and nutrient vertical profiles at t_{max} resulting from the simulations, we computed various indices to characterize the overall prevalence, spatial position and spatial niche of the three plankton competitors. To this end, we computed the mean biomass across the entire

water column of each plankton competitor. Using those mean biomasses, we estimated the percent contribution of each competitor to the total plankton biomass. We also assessed the depths at which the biomasses of A, M and H were maximized. Finally, we calculated the size of the *Competitor Favorable range* (CFR), i.e., the size of the portion of the water column over which the net growth rate of a given competitor is positive (Ryabov and Blasius, 2011).

The contribution of each competitor to the total plankton biomass was computed after a series of simulations across the combined parameter space of R_{in} and k_{bg} and α values. R_{in} values ranged from 100 mg P m^{-3} to 500 mg P m^{-3}. k_{bg} ranged from 0.1 m^{-1} to 0.6 m^{-1}. The parameter ranges we explored are similar to those featured in other theoretical studies of lake nanoplankton dynamics (Klausmeier and Litchman, 2001; Yoshiyama *et al.*, 2009). Model outputs relevant to resource availability within the system across simulations, in particular estimated TP levels and light intensity at mid-depth, are available as Supplementary Materials (Annexe D). At first, three values of α were tested, essentially running the model with one of three types of mixotrophic competitors: a primarily photo-autotrophic mixotroph (α = 0.1), a balanced mixotroph (α = 0.5) and a primarily phago-heterotrophic mixotroph (α = 0.9). We also examined the response variables contribution of each competitor to the total plankton biomass, their depths of maximal biomass and the size of their CFRs over a gradient of α values ranging from 0 to 1 for fixed combinations of R_{in} and k_{bg} values. The simulation over the gradient of α values were performed with a 1 cm spatial resolution.

Results from an alternative model that only featured the specialist competitors A and H but not the phago-mixotroph M were also investigated over the $R_{in} \times k_{bg} \times \alpha$ parameter space previously described. For each set of parameter values, the relative difference between the two versions of the model in total biomass produced by the nanoplankton community integrated over the depth of the water column was computed as $\frac{Biom_{Full\ model} - Biom_{Specialist\ model}}{Biom_{Full\ model}}$, with $Biom_{Full\ model} = Biom_A + Biom_M + Biom_H$ in the full model and $Biom_{Specialist\ model} = Biom_A + Biom_H$ in the specialist model.

2.4 Results

2.4.1 Contribution of competitors to total plankton biomass

Each trophic strategy dominated the community under distinct conditions of resource availability corresponding to specific zones of the $R_{in} \times k_{bg}$ parameter space we explored (Fig. 2.2). As shown by the competitor contribution obtained from the specialist model, A was most dominant at high R_{in} values and low k_{bg} values, i.e. under conditions of high nutrient and light availability (Fig. 2.3a). Conversely, H dominated the community when both nutrient and light were scarce (low R_{in} and high k_{bg}). Having M in the system substantially affected the dominance pattern of the specialists (Fig. 2.2). M persisted over a wide range of conditions of nutrient and light availability although the pattern of its contribution to the total biomass was highly dependent on its investment α in photo-autotrophy. A primarily photo-autotrophic mixotroph ($\alpha = 0.9$) dominated the community, and even excluded the specialists, when light availability was high (low k_{bg} value), regardless of nutrient availability conditions. At intermediate ($\alpha = 0.5$) and low investment in photo-autotrophy ($\alpha = 0.1$), the mixotroph was less dominant over the parameter space explored, but resource conditions where M clearly outperformed the specialists could be identified and occurred mainly at lower nutrient availability levels. For the three mixotrophic strategies we tested, M was outcompeted by the specialists when light availability dropped (high k_{bg}), although the exact k_{bg} threshold for viability varied with α, as M could withstand higher k_{bg} values when α was low. Both A and M, regardless of its α value, were outcompeted by H and excluded from the community when both light and nutrient availability were very low (e.g. at R_{in} = 100 mg P m^{-3} and k_{bg} = 0.6 m^{-1}).

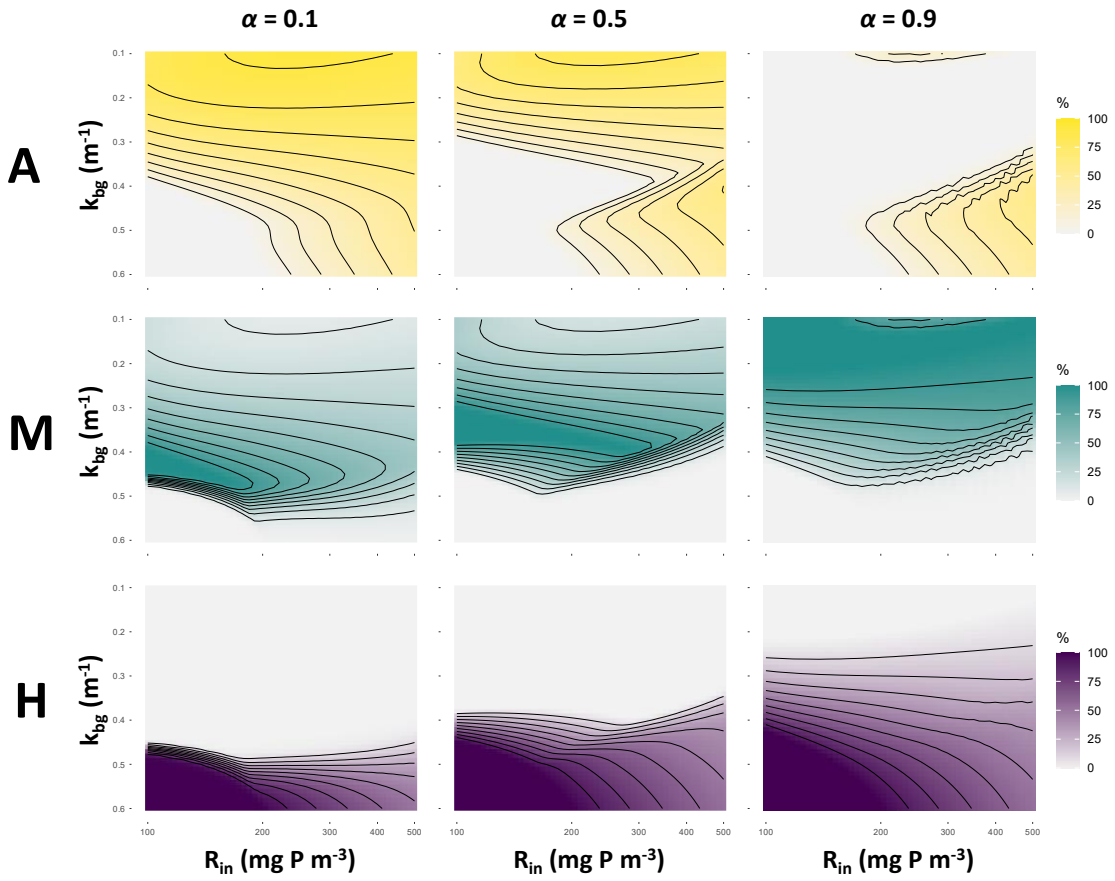

Figure 2.2. Contributions of the photo-autotrophic (A; yellow, first row), mixotrophic (M; green, second row) and phago-heterotrophic (H; purple, third row) competitors to the plankton community, as a percentage of the total biomass integrated over the entire depth of the water column. The y-axis (k_{bg}) is reversed, so that the zone of low resource availability (low R_{in} and high k_{bg}) in the parameter space corresponds to the bottom-left corner of each panel. Values on the x-axis (R_{in}) values are on a log-scale. Here we show results for three values of the mixotrophic investment in photo-autotrophy α: a low investment (α = 0.1; first column), a balanced investment (α = 0.5; second column) and a high investment (α = 0.9; third column). Each subplot represents the result of 2601 simulations (51 × 51 unique combinations of R_{in} and k_{bg} values). The black isolines delimitate the contribution results in intervals of 10%.

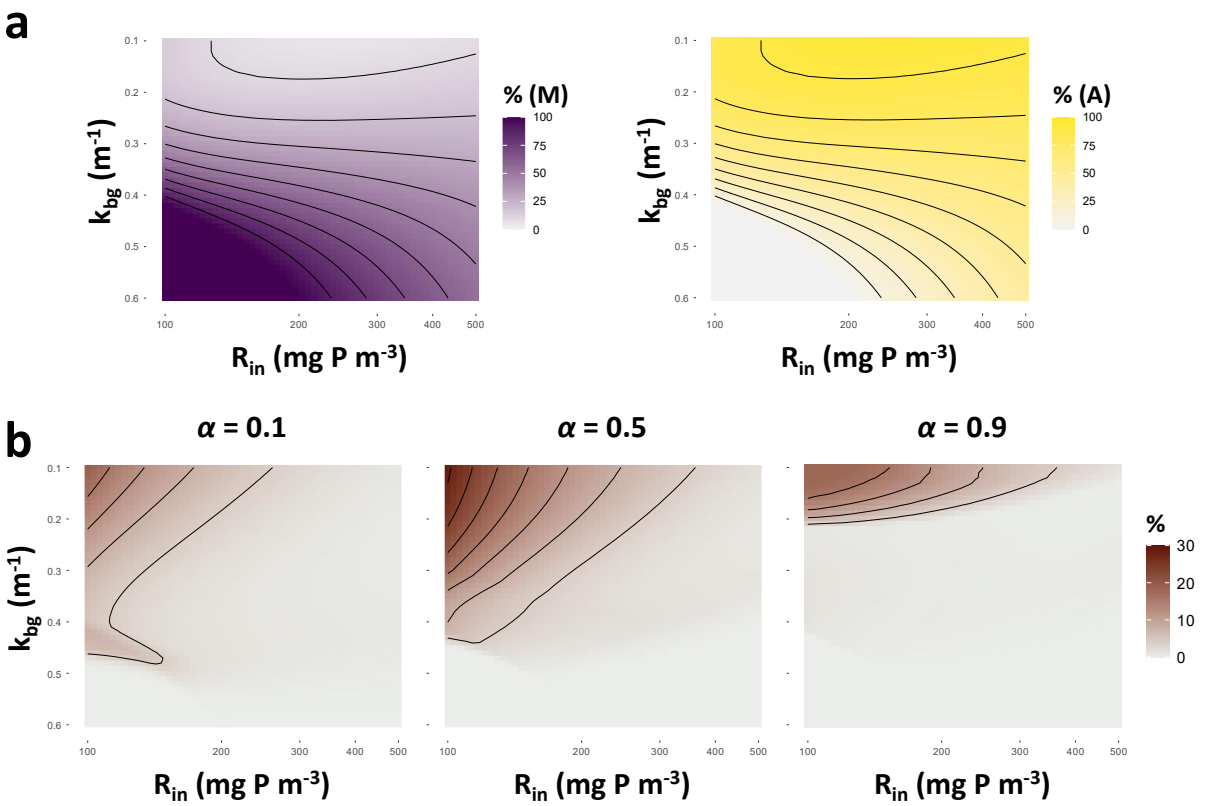

Figure 2.3. Contributions of the photo-autotrophic (A; yellow) and phago-heterotrophic (H; purple) competitors to the plankton community obtained from the specialist model (a) and community biomass differential between the full model and the specialist model integrated over the entire depth of the water column (expressed as a percentage of the community biomass of the specialist model) (b). The y-axes (k_{bg}) are reversed, so that the zone of low resource availability (low R_{in} and high k_{bg}) in the parameter space corresponds to the bottom-left corner of each panel. Values on the x-axis (R_{in}) values are on a log-scale. For the biomass differential results, higher values in the color gradient signal regions of the $R_{in} \times k_{bg}$ parameter space where the biomass of the community obtained from the full model (with a phago-mixotrophic competitor) exceed the biomass obtained from the specialist model (without a phago-mixotrophic competitor). Three values of the mixotrophic investment in photo-autotrophy α in the full model are shown: a low investment (α = 0.1; first plot), a balanced investment (α = 0.5; second plot) and a high investment (α = 0.9; third plot). The black isolines delimitate the results in intervals of 10% (a) and 4% (b).

Further simulations of the model over the range of α values clearly showed that, for a fixed set of R_{in} and k_{bg} values, the success of M (and consequently, the contributions of A and M to the community) was highly dependent on its physiological investment in photo-autotrophy α (Fig. 2.4). M thus dominated the community under various conditions of resource availability, providing the value of α was adequate. For example, mixotrophy was the best strategy when light availability was high and when M was mainly photo-autotrophic (i.e., when the value of α tended toward one). M completely excluded A and H at relatively high α when nutrient availability was low, providing light was available. M dominated less under low light and nutrients, but mixotrophy remained the best strategy even under these conditions when M was functionally

close to the pure phago-heterotroph (i.e., very low α). Generally, M tended to perform better than a given specialist competitor when the trophic strategy of M was close that of its competitor (i.e., when the value of α tends toward 0 or 1). As mentioned, when α was close to 1 (M mostly photo-autotrophic), M was very dominant under high light availability and could not only replace the specialist photo-autotroph A as the dominant trophic competitor, but outright excluded both specialists from the system. Note that M did not need to primarily invest in one strategy over the other to avoid exclusion, and that mixotrophy was still a viable strategy at intermediate α values. While a single competitor often dominated the community in a given region of parameter space, coexistence of all three competitors was possible (Fig. 2.4).

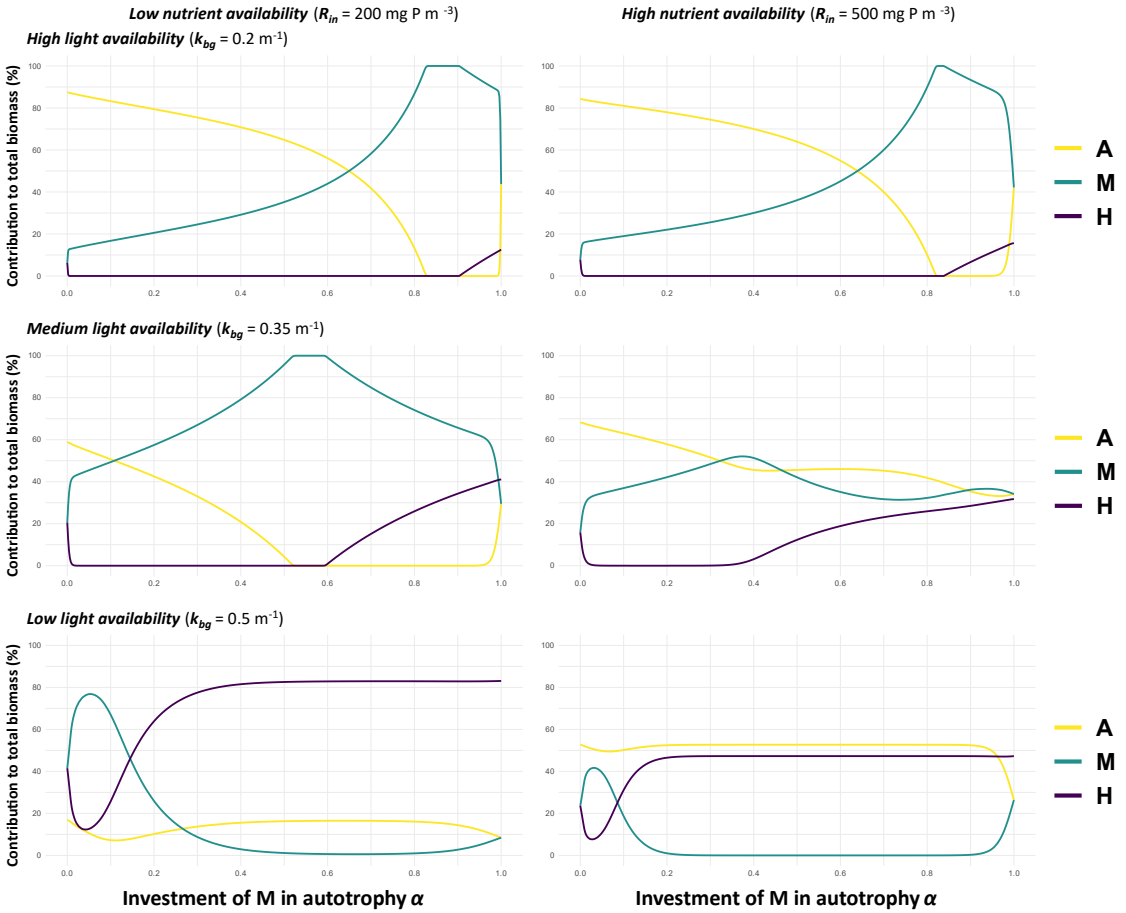

Figure 2.4. Contribution to the community (as a percentage of the total plankton biomass) of the photo-autotrophic (A, yellow lines), mixotrophic (M, green lines) and phago-heterotrophic (H, purple lines) competitors along a range of α values. The panels correspond to distinct conditions of nutrient and light availability (i.e., different combination of Rin and kbg values for the simulations). The three leftward panels correspond to conditions of relatively high nutrient availability (high Rin value) and the three rightward panels to relatively low nutrient availability (low Rin value). Light availability decreases from top to bottom (low to high kbg value). For each combination of Rin and kbg values, we simulated a range of α values (x axis) starting from α = 0, incrementally increasing the value of the parameter to the limit of α = 1.

Comparing the results from the full model to those obtained from a specialist model without mixotrophy (no M) model also revealed that the effect of M on nanoplankton community biomass production was most relevant when nutrients were scarce and light availability was high (low R_{in}, low k_{bg}) (Fig. 2.3b). In that corner of the R_{in}-k_{bg} parameter space, the specialist model (no M) yielded lower nanoplankton biomasses compared to the full model (with M) about 30% less at $\alpha = 0.5$, although this increase in biomass production was not as pronounced when α tended toward 0 or 1.

2.4.2 Spatial location of competitors within the water column

The depth at which competitors maximized their biomass depended on nutritional strategy and on conditions of resource availability (Fig. 2.5). H always maximized its biomass at z_{max}, regardless of nutrient and light availability. Under high nutrient supply (R_{in} = 500 mg P m^{-3}), A was most abundant at intermediate depth, reflecting its dependence on light coming from the surface z_0. The exact depth at which the biomass of A was maximal was dependent on the value of k_{bg}. Indeed, when light was readily available (low value for the background attenuation coefficient k_{bg}), A maximized its biomass closer to the sediments z_{max}, the point of entry of the mineral nutrient. The depth at which M maximised its biomass was driven by the value of α and tended toward z_{max} when α was close to 0 (when M was a pure phago-heterotroph). The depth of maximal biomass of M decreased with α, until it matched the depth of A at $\alpha = 1$ (when M was purely photo-autotrophic). At intermediate values of α, M maximized its biomass at a depth intermediate to that of the two specialist competitors. While the competitors each maximised biomass at different depths at moderate light levels when nutrient inputs were high (k_{bg} = 0.35 m^{-1}; R_{in} = 500 mg P m^{-3}), this was not the case when nutrient availability was relatively low (k_{bg} = 0.35 m^{-1}; R_{in} = 200 mg P m^{-3}), as both M and A were then systematically more prevalent at the bottom of the water column over the entire range of values α.

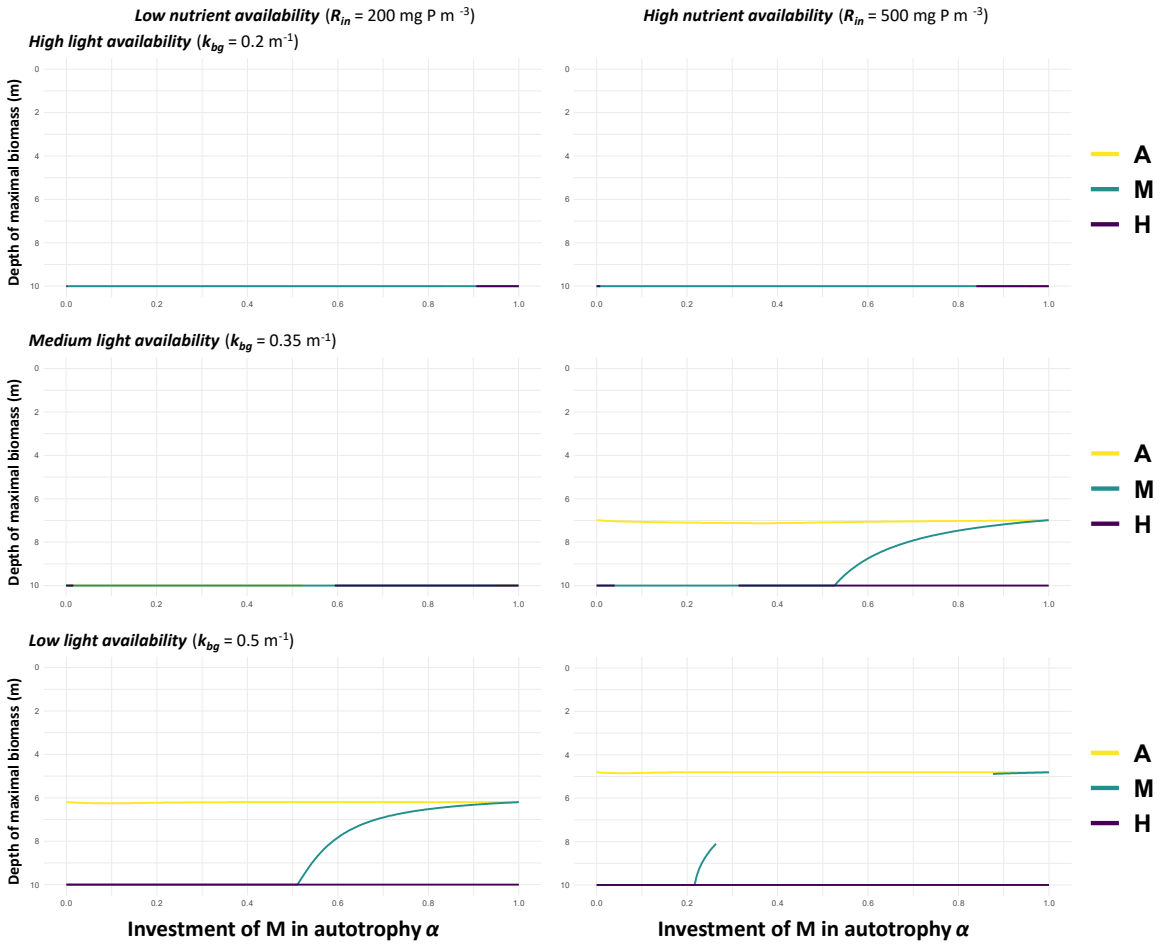

Figure 2.5. Depths at which the biomasses of the photo-autotrophic (A, yellow lines), mixotrophic (M, green lines) and phago-heterotrophic (H, purple lines) competitors are maximized. The panels correspond to distinct conditions of nutrients and light availability (i.e., different combination of Rin and kbg values for the simulations). The three leftward panels correspond to conditions of relatively high nutrient availability (high Rin value) and the three rightward panels to relatively low nutrient availability (low Rin value). Light availability decreases from top to bottom (low to high kbg value). For each combination of Rin and kbg values, we simulated over a range of α values (x axis) starting from α = 0, incrementally increasing the value of the parameter to the limit of α = 1. When a given competitor was excluded from the community at the end of the simulations, it had no biomass profile that could be processed, hence the fact that portions of the lines for the depths of maximal biomass are missing for some combinations of conditions of resource availability and *α* values.

2.4.3 Spatial niche of the competitors

The width of the depths over the water column at which populations of A, M and H had positive net growth rates (CFRs) were driven by resource availability (Fig. 2.6). High light availability yielded smaller CFRs, with the biomasses tending to be more abundant at the immediate vicinity of the lower boundary of the system at z_{max}, i.e., close to the sediment (an alternative version of Fig. 2.6 showing the depths of the limits of the competitors' CFR is available as Supplementary Material, Annexe E). It is worth noting that the niche size of H also depended on light

availability, and increased at low light (high k_{bg} value), although neither the growth rate of H, nor the growth rate of B, its sole resource, were directly dependent on I. The CFR of M was highly dependent on α and was generally larger than the CFRs of the specialists, especially when the value of α was close to one or the other specialists (0 or 1).

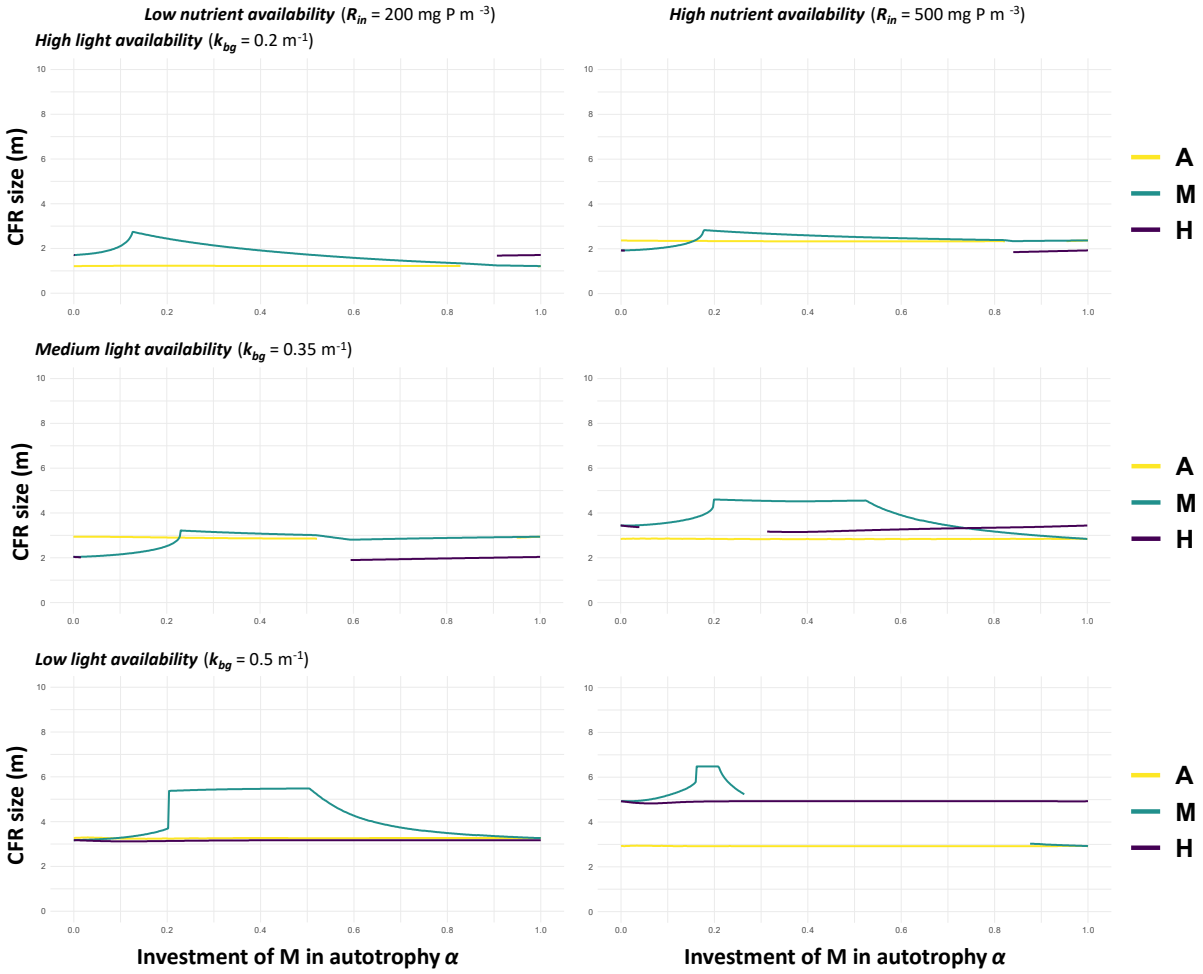

Figure 2.6. Size of the Competitor Favorable Range (CFR) of the photo-autotrophic (A, yellow lines), mixotrophic (M, green lines) and phago-heterotrophic (H, purple lines) competitors. The panels correspond to distinct conditions of nutrients and light availability (i.e., different combination of Rin and kbg values for the simulations). The three leftward panels correspond to conditions of relatively high nutrient availability (high Rin value) and the three rightward panels to relatively low nutrient availability (low Rin value). Light availability decreases from top to bottom (low to high kbg value). For each combination of Rin and kbg values, we simulated over a range of α values (x axis) starting from α = 0, incrementally increasing the value of the parameter to the limit of α = 1. When a given competitor was excluded from the community at the end of the simulations, it had no biomass profile that could be processed, hence the fact that portions of the lines for CFR sizes are missing for some combinations of conditions of resource availability and α values.

2.5 Discussion

2.5.1 Phago-mixotrophy is a viable strategy of resource acquisition against specialist competitors

Our model provides new insight into the viability of mixotrophy as a generalist trophic strategy against specialist competitors, as well as more general insight on competitive interactions between multiple plankton nutrition strategies in lake water columns. The generalist mixotroph could persist in the community under a wide range of resource availability conditions, providing it displayed a suitable balance between photo-autotrophy and phago-heterotrophy for the environmental conditions it faced. Generally, our model results indicate that the prevalence of phago-mixotrophy as a trait should increase within lake nanoplankton communities when nutrient availability declines. This broad pattern correspond to what is observed in the field, as the results reported by Saad *et al.* (2013) in a collection of lakes located in Tierra del Fuego show. Our own study of nanoplankton nutrition assemblages across North American lakes revealed that the prevalence of phago-mixotrophic nanoplankton taxa is higher in more oligotrophic sites (see Chapter III). This effect of nutrient availability on the prevalence of mixotrophy also corresponds to findings of other modelling studies on the coexistence of mixotrophy and specialist strategies (Crane and Grover, 2010; Ward *et al.*, 2011). In contrast, the success of mixotrophy over the gradient of light availability conditions is more dependent on the exact functional balance between phototrophy and phagotrophy displayed by the mixotrophic competitor. When nutrient availability was low and light availability was high to medium, mixotrophy was not just a viable strategy but actually the best overall strategy, as a mixotroph with the right investment in photo-autotrophy (i.e., via its α value) completely excluded the other competitors from our closed water column. Under such conditions, the best strategy for the mixotroph was to invest primarily in the photo-autotrophic nutrition mode (i.e., high α value), as a relatively small mixotrophic investment in bacterivory more than compensated the accompanying underinvestment in phototrophy. As light availability decreases, mixotrophy can remain the dominant nutrition strategies if the mixotroph invest more in phagotrophy (lower α). Providing it invests sufficiently in phagotrophy, our model shows that M can outcompete H under most conditions of light availability when nutrients were scarce, except when background light attenuation is very high (Fig. 2.4). When both light and nutrient are scarce, most of the nutrient stock is consumed by the bacteria at the bottom of the water column where A and M are light limited. Consequently, the mixotroph relies

solely on phago-heterotrophy for resource acquisition over much of the water column and is excluded by the specialist phago-heterotroph with a higher basal phagotrophic growth rate. Our assemblage results are compatible with findings from experimental studies. For example, Tittel *et al.* (2003) reported that mixotrophs were the dominant grazers throughout the water column of an oligotrophic lake and showed from batch culture experiments that pure phagotrophs could only out-compete mixotrophs in the dark, observed also in our own results. Similarly, Ptanick and al. (2016) showed that mixotrophy success was very dependent on light availability in batch culture experiments under oligotrophic conditions, and that mixotrophic eukaryotes outcompeted phago-heterotrophic flagellates under most conditions of light availability.

More generally, our results illustrate how complex competitive interactions can be, even in a relatively simple theoretical community, and how those interactions shape community composition. In our model, changes in the availability of any resource can indirectly affect the success of any of the three plankton competitors, leading to exclusion through competitive interactions. Under conditions of high light availability, H is excluded over most of the α values explored regardless of nutrient availability conditions, even though H (or its prey B) does not directly use light as a resource for its growth, as the mixotroph depletes the bacterial stock all-over the water column (Fig. 2.4). Furthermore, the prevalence and the characteristics of the spatial niche of the phago-heterotroph changed between simulations with different conditions of light availability (Fig. 2.6). It is also worth noting that grazing by the mixotroph and the phago-heterotroph prevented the photo-autotroph from being competitively excluded by the bacterial population in our system. Indeed, as shown by additional simulations where nanoplankton competitors were selectively removed from the model (Annexe F), A is excluded from the system in the absence of M and H under any conditions of resource availability, as bacteria are superior competitors for R.

2.5.2 Functional variability makes mixotrophy viable under a wide range of resource availability conditions

M tended to be more prevalent than H or A when α was close to 0 or 1 respectively. This means that, in our model, M is a more efficient competitor than the physiologically closest specialist and that divesting slightly from the main resource acquisition mechanism, whether it is photo-autotrophy or phago-heterotrophy, is beneficial and provides the mixotroph with a competitive

edge against the associated specialist competitor under most resource availability conditions. But crucially, M could also coexist with specialist (and even dominate the community) at intermediate values of α: investing significantly in both photo-autotrophy and phagotrophy was a viable strategy against specialist competitors, and M did not necessarily need to invest predominantly in one or the other resource acquisition mechanism to be competitive. It is thus conceivable that multiple mixotrophic taxa displaying different degrees of affinity for photo-autotrophy could coexist in a single plankton community. The fact that we could identify an optimal α value that varies with environmental conditions also fits the notion that plasticity in the balance between photo-autotrophy and phago-heterotrophy is an important factor explaining the success of mixotrophs in natural communities (Chan *et al.*, 2019; Lambert *et al.*, 2022; Li *et al.*, 2021). Studying the grazing ecology of the mixotrophic dinoflagellates *Florenciella sp.*, Li *et al.* (2021) determined from culture experiments that the bacterivory rates of this mixotroph were affected by nutrient availability and were substantially higher in nutrient-limited cultures, indicating a shift from a photo-autotrophic trophic mode to a mainly phago -heterotrophic nutrition mode. Using a machine-learning modeling approach based on metatranscriptomic profiles, Lambert *et al.* (2022) were also able to predict geographical patterns of predominant trophic modes for marine mixotrophic taxa in the open ocean that would signal shifts in resource acquisition strategies in response to environmental gradients, in particular nutrient and prey availability. If a mixotroph can regulate its investment in phago-heterotrophic and photo-autotrophic physiological structures in response to changing conditions of resource availability (be it prey, light or mineral nutrient), it would give this competitor another edge against specialists, as temporal heterogeneity in resource availability is a very common feature of aquatic environments. At a larger temporal scale, the balance between photo-autotrophy and phago-heterotrophy is almost certainly a trait subject to intense selective pressure.

2.5.3 A generalist mixotroph can supress generalist resources and favor system productivity

Our results hint at a potential key role of mixotrophy for ecosystem functioning, from bacterial and nutrient dynamics to system productivity as a whole. When M dominates the system, it does so by supressing resource concentration to levels unsustainable for specialist growth, as results from the specialist system show (Annexe G). Under those conditions of resource availability, despite the seemingly penalizing linear trade-off between the phototrophic and phagotrophic

mechanisms of resource acquisition, the combination of the two nutrition modes allows the mixotroph to support its population to level sufficient to in turn lower resource concentration under the minimal threshold required to yield a positive specialist growth rate. From an ecosystem functioning standpoint, the existence of mixotrophic nanoplankton feeding strategies should thus have substantial consequences for the bacterial population dynamic and inorganic nutrient concentrations in natural systems: at the very least, our results are in line with the findings from various studies that have found mixotrophs to be major contributors to bacterivory in natural system, in particular in oligotrophic conditions (Saad *et al.*, 2016; Unrein *et al.*, 2014; Zubkov and Tarran, 2008).

The generalist mixotroph not only competed successfully with specialists for resources, but it could exploit unused parts of the niche space under specific conditions of light and nutrient availability. As shown by comparing results from the three-competitor model with results from the modified specialist model, a community composed solely of specialist photo-autotrophs and phago-heterotrophs yields a lower biomass than a community that also includes a generalist phago-mixotroph under high light and low nutrient availability, about 30% less compared to a community with a balanced mixotroph ($\alpha = 0.5$). Elsewhere within the parameter space we observed no significant difference in productivity between the two systems, indicated that the mixotroph replaces and suppresses biomass production from one or both specialists where M is prevalent. Again, this has some interesting implications for ecosystem functioning in clear-oligotrophic lakes: our results would indicate that in those environments, mixotrophy is a crucial part of primary production and that the absence of a generalist nanoplankton competitor would profoundly decrease ecosystem productivity as a whole. In the broader theoretical framework of community ecology, this is another an example of the positive relationship between community productivity and functional diversity (Sonkoly *et al.*, 2019; Tilman *et al.*, 1997; Vallina *et al.*, 2017).

2.5.4 Diversity of nutrition strategies can induce vertical partitioning within the community

The modelled community was vertically structured over the dual opposing gradients of light and nutrients when light extinction in the system was high. The phago-heterotroph always maximized its growth at z_{max} where the abundance of bacteria was maximal, while the photo-autotroph was

positioned higher in the water column to optimally balance its light and nutrient requirements when light availability decrease. When the depths at which the two specialist competitors maximized their abundances were decoupled, the strategy of the mixotroph, i.e., its balance between photo-autotrophy and phago-heterotrophy, directly conditioned its depth of maximum growth, between the respective optimal depths of the corresponding specialists. Vertical partitioning of taxa is a common feature of phytoplankton communities in stratified system (Olli and Seppälä 2001; Gervais 2003) and our modelling results appear to match vertical distribution patterns of trophic modes observed in stratified aquatic environment. Studying the ciliate community of a lake, Princiotta and Sanders (2017) observed that during the period of stratification, phototrophic ciliates dominated the nanoplankton community in the epilimnion (close to the surface) and phago-heterotrophic ciliates were dominant in the hypolimnion (at the bottom), while mixotrophic ciliates were more evenly distributed throughout the water column. Note that the authors attributed the observed distribution pattern to a variety of environmental factors not considered in our model, like temperature and oxygen availability, in addition to resource gradients. In our system, vertical partitioning occurred when growth conditions were not suitable for autotrophic growth at the bottom of the water column, or in other words, when the lower limit of the CFR of A did not reach the bottom of the water column. Still, while a diversity of biotic and abiotic factors can shape the spatial distribution of taxa within a nanophytoplankton community (Beisner and Longhi, 2013), our results show that differences in trophic strategies within the community and competitive interaction alone are sufficient to induce vertical segregation of competitors when resource availability is heterogeneous.

2.5.5 The vertical niche of a competitor is shaped by its resource-acquisition strategy

A possible reason for the success of mixotrophs in spatially heterogeneous environment is their ability to maximize their vertical niche. Indeed, M generally had a larger spatial niche than did the specialist competitors in our system, highlighting the benefit of having multiple resource acquisition mechanisms when the environment is spatially heterogeneous. Phagotrophy allows M to compensate for low-light availability at depths where a pure photo-autotroph is light-limited and cannot grow, while photo-autotrophic resource acquisition pathways allow the mixotroph to grow higher in the water column where a pure phago-heterotroph is limited by low bacterial abundances. Although having a larger spatial niche is probably a contributing factor to the

viability of the generalist competitor, it is important to note that for a given set of resource availability conditions, the value at which M display its CFR size did not necessarily match the α value at which the contribution of M to the community was maximal (Fig. 2.4, Fig. 2.6). In any case, there was a high degree of overlap between the spatial niche of the specialists and of the generalist, meaning that M spatially co-occurred with specialist while maintaining a positive growth rate over much of the water column. While mixotrophs certainly benefit from well-defined resource gradients in stratified water columns and can thrive at depths where a physiologically close specialist competitor would be excluded, the spatial heterogeneity of resource availability and the vertical segregation of competitors does not appear to be necessary prerequisite for mixotrophy to be viable. Using a modelling approach, Våge *et al.* (2013) established that a mixotrophic competitor could coexist in a non-spatialized (i.e., mixed) system with pure phago-heterotrophic and osmo-heterotrophic competitors, although their modelling framework did not consider light as a limiting resource and did not feature a purely photo-autotrophic competitor. In a modelling approach similar to our own, but in a non-spatially explicit context, Crane and Grover (2010) showed that mixotrophy was favored under oligotrophic conditions (low mineral nutrient availability) and that multiple plankton nutrition strategies (pure photo-autotrophy, mixotrophy and pure phago-heterotrophy) could coexist with high nutrient availability. However, mixotrophy was viable over a more restricted range of α values under eutrophic conditions (high nutrient availability) in their model compared to ours. While those differences might stem from different parametrization or the fact that their model included variable resource internal quota for the competitors, our results indicate that well-defined resource gradients make mixotrophy viable over larger ranges of α values and resource availability conditions, compared to mixed water columns.

2.6 Perspectives

The system we have modelled is a relatively simple approximation of real aquatic environments. However, we believe it is an adequate tool to explore assemblage rules of nanoplankton resource-acquisition strategies. Yet it is worth acknowledging the limits of our study that could be built upon in future studies. We considered only three competitors, while real plankton communities are composed of dozens different taxa with many distinct traits. A single community could potentially harbor multiple mixotrophs with different trade-off modalities between photo-

autotrophy and phago-heterotrophy (different α). Furthermore, trophic interactions between the existing compartments of the model could be expanded: larger phago-heterotrophs and mixotrophs could potentially prey not only on bacteria, but also on smaller photo-autotrophs, thus potentially drastically changing the characteristics of their spatial niche and the overall prevalence of each competitor in the community. This would also imply that the community possesses an inherent size structure, further affecting parameters related to the growth rates of competitors (Leles *et al.*, 2018; Våge *et al.*, 2013). We also restricted the system to two limiting resources, light and nutrient (bacterial growth being dependent on nutrients): while those are generally considered to be the most important structuring resources for community composition, other resources could provide additional niche axes over which competitors with different relevant trait values could segregate. Future studies should consider applying a carbon limitation for bacteria, which we avoided at this early stage to avoid overly complexifying the system. While we believe that this is a reasonable assumption in the context of our study, that focuses primarily on the effect of light and nutrient availability on community assembly, it would be possible to feature additional compartments for carbon compounds assimilable by the bacteria (Thingstad and Lignell, 1997). The concentration of carbon compounds analogous to DOC could in turn affect light availability, resulting in the replacement of our current constant background attenuation coefficient k_{bg} by a more complex term, the value of which would depend on the system dynamics itself. Our model could be complexified to account for those additional limitation processes and investigate further how mixotrophy prevalence is affected by DOC concentration, identified as a possible driver of alternative nanophytoplankton trophic strategies in lakes (Hansson *et al.*, 2019). Finally, the model could be modified to take into account additional environmental forcing variables, in particular temperature. Temperature is known to affect the metabolism of nanoplankton organisms (Lepori-Bui *et al.*, 2022; Princiotta *et al.*, 2016), and it could realistically be made to vary with depth in our spatialized system. The effect of temperature could be featured by adding a multiplicative term to the growth functions of the competitors featured in the model (Geider *et al.*, 1998). In addition to refining the dynamic of the community in a spatially stratified system, a model taking into account temperature could be used to anticipate the response of nanoplankton nutrition strategy assemblages to rising water temperature in the context of global change.

We currently lack detailed field measurements of bacterivory by phago-heterotroph and mixotroph nanoplankton taxa across many types of lakes, and we can only compare our results to broad patterns of the prevalence of potentially mixotrophic taxa. The challenge of assessing *in situ* mixotrophy rates is in part why we chose a modeling approach to answer the research questions we pose here on the viability of mixotrophy. Still, we believe that observational or experimental studies of mixotrophy rates over the vertical dimension of an aquatic system, in mesocosms or in lake water columns, would provide an invaluable qualitative test of our model's predictions, to validate or insist on further refinement of our approach.

2.7 Conclusion

Our model conclusively shows that phago-mixotrophy is, in a pure resource competition framework, viable against specialized trophic nutritional modes and that a mixotroph can coexist with specialized photo-autotrophic and phago-heterotrophic competitors across a variety of resource availability conditions. By combining two trophic modes, the mixotroph can dominate the community when nutrients are scarce and light relatively abundant, particularly when it invests its resource mainly in photo-autotrophy. Mixotrophy appears generally less advantageous under more eutrophic conditions but remains a viable strategy. While our model predicts that the viability of mixotrophy is highly dependent on light availability and on the exact functional strategy of the mixotroph, a generalist mixotroph, regardless of its balance between phototrophy and phagotrophy, needs light to persist in the system and to avoid being excluded by a specialized phagotrophic competitor. When light and nutrient availability are respectively high and low, a higher diversity of resource acquisition strategies enhances the overall productivity of the nanoplankton community: this hints at the importance of mixotrophy for basic ecosystem functions, in particular primary productivity. While we could generally identify an optimal balance between photo-autotrophy and phagotrophy under any given conditions of resource availability, mixotrophy was viable or even the single best strategy over a large portion of the range of mixotrophic affinity for photo-autotrophy values we explored, indicating that a degree of plasticity in this functional trait would help explain the pervasiveness of mixotrophs in a variety of natural systems. The success of mixotrophs could also stem from their ability to grow over a large portion of the water column, hence maximizing the size of their spatial niche compared to specialized photo-autotrophs and phago-heterotrophs. Our modelling results also indicated that

the diversity of trophic strategies in natural systems could contribute to the vertical structuring of nanophytoplankton communities observed in stratified lakes, as our model predicts that different competitors with distinct trophic modes maximize their biomasses at different depths over the vertical light and nutrient gradients.

CHAPITRE 3

Nutrient availability is the main driver of nanophytoplankton mixotrophy in North American lake surface waters

Philippe Le Noac'h[1,2], Bruno Cremella[2,3], Jihyeon Kim[1,2], Yves Prairie[1,2], Yannick Huot[2,3] and Beatrix E. Beisner[1,2]

[1]Department of Biological Sciences, University of Quebec at Montreal, H2X 1Y4 Montreal, Quebec, Canada

[2]Interuniversity Research Group in Limnology/Groupe de Recherche Interuniversitaire en Limnologie (GRIL), H2X 1Y4 Montreal, Quebec, Canada

[3]Département de géomatique appliquée, Université de Sherbrooke, J1K 2R1 Sherbrooke, Quebec, Canada

3.1 Abstract

Nanophytoplankton mixotrophy is increasingly recognized as an important factor for community assembly and more generally as an important contributor to ecosystem function in lakes. Yet there has been limited research on the abiotic and biotic factors affecting the prevalence of phago-mixotrophy in freshwater ecosystems. In recent years, large-scale sampling campaigns like the EPA-National Lakes Assessment (NLA) survey across the continental United States and the NSERC LakePulse (LP) survey across Canada have generated surface water community composition data for hundreds of lakes across North America, covering large environmental gradients. We present results from our analyses of the nanophytoplankton community data from these two surveys, focusing on a taxonomic comparison of the mixotrophic communities across ecoregions and multivariate analyses of the environmental drivers of the prevalence of mixotrophy. We identified mixotrophic taxa in the overwhelming majority of sites and across all ecozones sampled. Lake trophic state was identified as the main predictor of nanophytoplankton resource-acquisition strategy assemblages, with lower prevalence of mixotrophy and less diverse mixotrophic communities in more eutrophic lakes. In contrast, the effect of light availability was minimal. Other relevant environmental predictors of the prevalence of mixotrophy included water chemistry and zooplankton abundances. Lake trophic state also controlled the composition of the mixotrophic community and increased total phosphorus levels were associated with a loss of taxonomic diversity in the mixotrophic portion of the nanophytoplankton community. This is the most comprehensive assessment of the prevalence of mixotrophy in lake nanophytoplankton communities to date spanning hundred of sites and a dozen ecozones.

Key words: nanophytoplankton, phago-mixotrophy, large scale surveys, community assembly, environmental gradients

3.2 Introduction

Nanophytoplanktonic protist communities constitute the primary producer base of trophic networks across most aquatic ecosystems, including lakes. Many nanophytoplankton taxa have flexible feeding behaviour. In particular, some taxa are mixotrophic, thereby able to acquire energy and nutrients necessary for their growth through both photosynthesis (autotrophy) and predation (phago-heterotrophy) (Flynn *et al.*, 2019). Mixotrophy is a widespread functional trait

within nanophytoplankton communities, and is found in all aquatic ecosystems (Faure *et al.*, 2019; Flynn *et al.*, 2013). It is a generalist trophic strategy that allows mixoplankton to thrive in environments that would be otherwise unfavourable to pure autotrophs, although the underlying investment trade-off between photosynthetic and phagotrophic physiological structures is thought to make mixotrophy less advantageous under conditions of high resource availability. Mixotrophy should thus play a major role in the assemblage of nanophytoplankton communities along environmental gradients. Overall, the relative prevalence of mixotrophy is likely to have important consequences for ecosystem functions, and correctly assessing the prevalence of alternative trophic strategies like mixotrophy is crucial to accurately estimate primary production and carbon transfer to higher echelons of the food chain (Leles *et al.*, 2018).

Nanophytoplankton resource-acquisition strategy assemblages (i.e., the composition of the assemblage in terms of trophic strategies) are potentially controlled by a variety of biotic and abiotic factors. First and foremost, mixotrophy can be define as an alternative strategy for resource acquisition, so nutrient and light availability can be expected to be important drivers of its prevalence in aquatic systems. Indeed, according to several observational studies, planktonic taxa able to perform mixotrophy tend to dominate under nutrient-poor conditions studies (Arenovski *et al.*, 1995; Saad *et al.*, 2013). In mesotrophic and oligotrophic environments, phagotrophy allows mixoplankton to complement their nutrient requirements and to outcompete purely autotrophic phytoplankton. The effect of light availability might not be as straightforward. Some mixotrophs can dominate the nanophytoplankton community under low-light conditions present in DOC-rich environments, as they can compensate the reduction in photosynthetic activity by grazing on bacteria (Bergström, 2009). Conversely, other studies have shown that some mixotrophic taxa need high levels of light to dominate the community, as they obtain the bulk of their carbon intake through photosynthesis and use phagotrophy mainly to complement their nutrient uptake (Calbet *et al.*, 2012). Indeed, mixotrophic biomass appears to be greater in high-irradiance marine environments (Edwards, 2019). The effect of light on resource-acquisition strategy assemblages in lakes might thus be dependent on the individual mixotrophic physiology, and consequently on the composition of mixotrophic communities. Nutrient and light availability are controlled by variety of environmental factors, including climate, lake watershed usage and site morphometry. Resource competition controls community composition in terms of the overall

availability of light and nutrients, but also in terms of where those resource are available in in the ecosystem, i.e., over the depth of the water column. Mixotrophs could potentially benefit from clearly defined resource gradients that create local conditions of light and nutrient availability favourable to taxa that can complement their growth through phagotrophy. The distribution of some mixotrophs has at the very least been shown to be vertically structured in stratified lakes (Bird and Kalff, 1987; Clegg *et al.*, 2007). The physical structure of the environment thus also appears to affect the success of mixotrophs, as the stratification status of the water column will determine how heterogeneous nutrient availability is over depth. Deeper stratified lakes with a high difference in temperature between the top and the bottom of the water column could potentially be more favourable environments for mixotrophs. Water temperature could by itself affect trophic resource-acquisition strategy assemblages and increased water temperature has been shown to promote phagotrophy within mixotroph (Lepori-Bui *et al.*, 2022). The prevalence of phago-mixotrophs over autotrophs could thus potentially increase with water temperature.

Top-down interactions can modulate the trophic composition of nanophytoplankton communities. Hansson *et al.* (2019) showed that high abundances of selective zooplankton feeders like copepods were associated with overall lower contribution of mixotrophs to nanophytoplankton communities in boreal lakes. They attributed this result to potential differences in stoichiometry between autotrophic and mixotrophic prey: autotrophic stochiometric ratios, in contrast to the elemental ratios of phago-mixotrophs, are dependent on conditions of light and nutrient availability and thus highly variable, making photo-autotrophs a sub-optimal source of food for zooplankton grazers in many instances. They also noted that the abundance of bacteria could be a potential biotic driver of the prevalence of mixotrophy.

One major impediment to the study of mixotrophy is the difficulty in assessing its occurrence in natural systems. Estimating *in situ* rates of mixotrophy is arduous and require dedicated experiments and procedures (Beisner *et al.*, 2019) making them difficult to implement in a lake survey design where each lake is visited only briefly. Even knowing whether a photosynthetic species is also potentially capable of bacterivory is difficult, and there is a clear lack of information on the trophic strategies of individual taxa available in the literature. Taxa previously traditionally considered purely autotrophic have been increasingly found recently to be able to graze on bacteria, even among groups traditionally considered purely autotrophic like green algae

(Bock *et al.*, 2021). Published trait databases that include the trophic strategy of taxa exist (Laplace-Treyture *et al.*, 2021; Rimet and Druart, 2018) but these are often inconsistent with one another and tend to attribute little, to no sources for the information they are reporting. Another point of contention is the semantic confusion between phago-mixotrophy, i.e., the ingestion of other organisms (most notably bacteria) and osmo-mixotrophy, i.e., the absorption of dissolved organic compounds present in the environment (as defined by Flynn *et al.*, 2019). Virtually all phytoplankton taxa are capable of performing osmo-mixotrophy, while phago-mixotrophy is less widespread as it implies a trade-off between autotrophy and heterotrophy.

Large scale biogeographical studies of mixotrophs have been conducted for the global ocean (Leles *et al.* 2017; Faure *et al.* 2019), but there has been to date, few equivalent effort for freshwater systems. Some studies have attempted to explore the biogeography of alternative trophic strategies in freshwater systems and to shed light on the environmental factors driving the prevalence of mixotrophy in lakes but those are often limited in scope, being restricted to limited geographical area or to a relatively small subset of lakes. Saad *et al.* (2016) highlighted to importance of trophic conditions for the success of mixotrophs in a study encompassing 24 oligotrophic to mesotrophic lakes in Patagonia combined with ingestion experiments. Hansson *et al.* (2019) showcased how prevalent mixotrophy can be in boreal lakes and how light conditions and top down-interaction drive the success of mixoplankton taxa, but their study were limited to 69 sites in eastern Canada. We currently lack a clear picture of the occurrence of plankton mixotrophy at larger geographical scales and over extended environmental gradients. The recent completion of large-scale lake surveys like the 2017 EPA-National Lake Assessment (NLA) survey in the US (EPA NLA, 2009) and the NERSC-Lake Pulse (LakePulse) survey in Canada (Huot *et al.*, 2019) offers a possibility to correct this knowledge gap. These surveys were designed to monitor the health status and water quality of lake across North America and involved the measurement of many biotic and abiotic variables, including microscopic identification of nanophytoplankton communities. Taken together, these two surveys cover more than 1700 sampling sites distributed over the entire continental US and over a sizable portion of Canada. The sampling methodology of the LakePulse survey was chosen to match those of the NLA surveys, thus combining the results into a unique dataset enabling the continental-scale study of nanophytoplankton assemblages of resource-acquisition strategies. Our main hypothesis

is that these assemblages will respond to resource availability conditions (light, nutrient and bacterial abundance). In particular, we expect to see an effect nutrient availability and a shift to higher prevalences of phago-mixotrophic taxa in more oligotrophic sites. More broadly, data from the combined LakePulse and NLA surveys should allow us to assess the response of lake nanoplankton nutritional assemblage types to a wide variety of biotic and abiotic predictors (e.g., zooplankton community, lake morphology, water physico-chemistry), and to identify the most important environmental predictors of the prevalence of the phago-mixotrophic trait in lentic freshwater ecosystems.

While it is crucial to better understand how the prevalence of mixotrophy varies over environmental gradients, it is also novel and interesting to investigate variation in the taxonomic composition of the mixotrophic community. Phago-mixotrophy is not performed uniformly among mixoplankton taxa, and studies have shown that the degree of mixotrophy can vary greatly between two mixotrophic taxa. Indeed, mixoplankton trophic behaviour is a gradient, with mainly autotrophic taxa on one end of the spectrum, and taxa that rely more heavily on phagotrophy for resource acquisition on the other hand (Flynn *et al.*, 2013; Jones, 1997; Stoecker, 1998). The physiological balance between phototrophy and phagotrophy of mixoplankton likely reflect their taxonomy and thus, taxonomic composition of the mixotrophic portion of the nanophytoplankton community could change with environmental conditions. For example, increased lake trophy likely favours primarily phototrophic mixoplankton taxa over more phago-mixotrophic taxa, as increased reliance on bacterivory is likely advantageous in a resource-poor environment. In their study of nanophytoplankton mixotrophy in Patagonia, Saad *et al.* (2016) identified a shift in the composition of the community as the trophic state of lakes increased, with higher contribution of mainly phago-heterotrophic cryptophytes in oligotrophic sites compare to communities in eutrophic systems that were dominated by phototrophic chrysophytes. While investigating precisely the ingestion dynamics of mixotrophic taxa is outside the scope of this study, the combined NLA and LakePulse surveys should prove useful to confirm similar patterns at larger geographical scale and potentially reveal community composition shifts over additional environmental gradients.

3.3 Methods

3.3.1 Harmonizing data from the NLA and LakePulse surveys

664 lakes were sampled once across Canada during the NSERC Canadian Lake Pulse survey (abbreviated as LakePulse) campaign during the mid summer (July-August) period in 2017, 2018 and 2019 (approximately 1/3 of lakes sampled per year). For the EPA-NLA survey, 1113 distinct lakes were sampled across the continental US (excluding Alaska). Some lakes (97 sites total) were sampled twice over the course of the NLA campaign: in those instances, both records were kept in the analyses when the time lag between them was superior or equal to thirty days (assumed to be long enough to permit several generations of community turnover). When the time lag was less than thirty days, only the sampling event closest to August 1st, i.e., the mid-point of the summer season in North America, was kept. Overall, the lakes included covered 12 ecoregions across North America (Fig. 3.1). Data measured at each site in both surveys included water-chemistry parameters, climate variables, site morphometric characteristics, nanophytoplankton and zooplankton composition and climate variables (Table 3.1). NLA data are publicly available online on the EPA website (https://www.epa.gov/national-aquatic-resource-surveys/data-national-aquatic-resource-surveys) and LakePulse data are set to be released publicly in 2023.

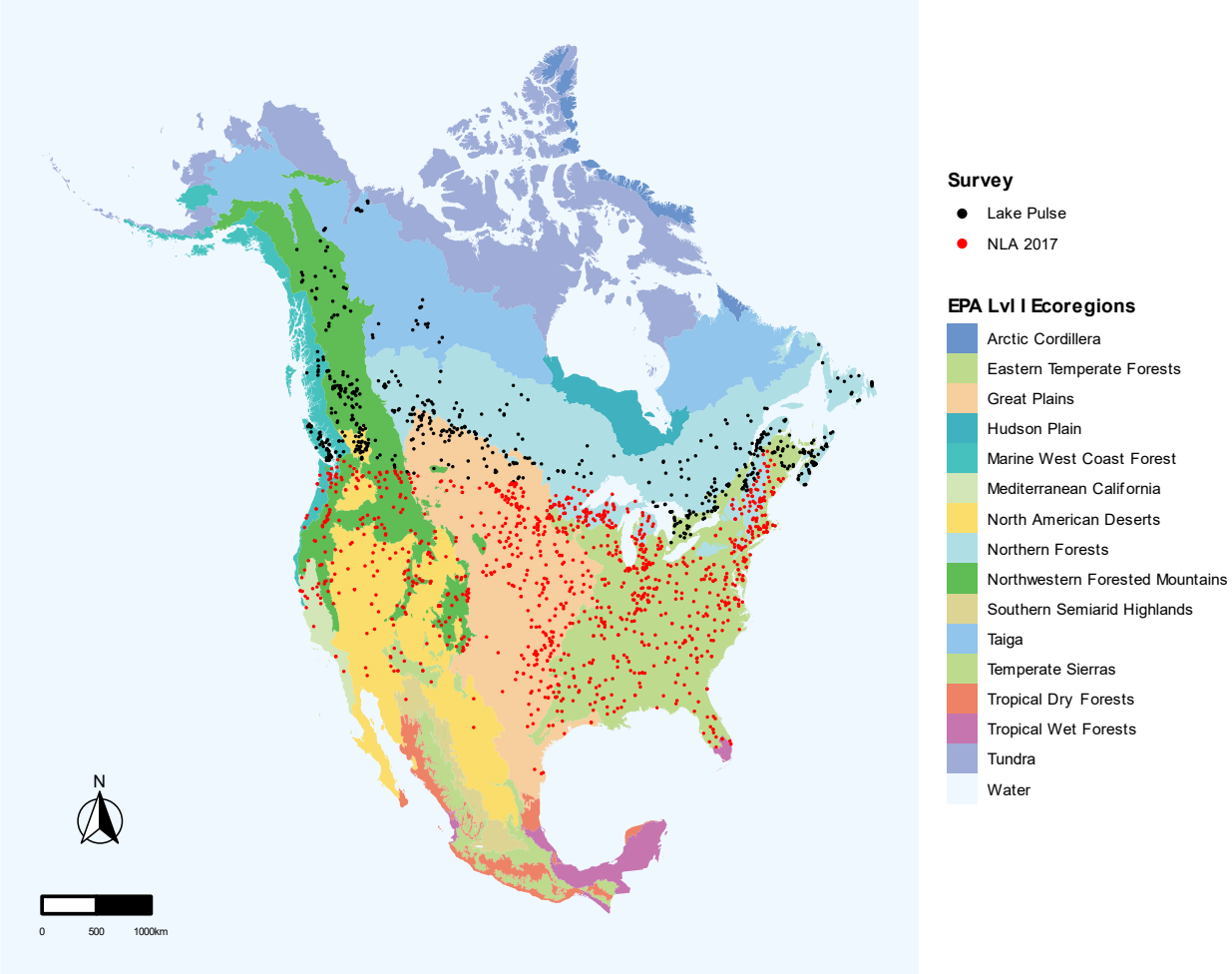

Figure 3.1. Map showing the geographical locations of the lakes that were sampled during the NLA survey (red dots) and LakePulse pan-Canadian lakes survey (black dots) and for which nanophytoplankton community composition data were available. This map was created using the NAD83 spatial reference system.

In addition to basic geographical information (latitude, longitude and altitude), information on site morphometry included lake perimeter and lake surface. Lake depth at the sampling point was also recorded. For LakePulse lakes sampling coincided with the deepest point of the lake, while for NLA lakes, the sampling point was chosen as a point close to the center of the lake but where the depth did not exceed 50 meters. *In situ* vertical depth profiles of key physico-chemical parameters were taken using a multiparameter probe in each survey. Those profiles were used to estimate the mean temperature, pH and dissolved oxygen concentration of the upper surface layer (surface to the minimum between 2m and the lower depth of the photic zone) and the bottom layer (max depth of the profile to one meter above this depth; for the mean temperature and pH but not the dissolved oxygen). Mean conductivity in the surface layer was also assessed from

those depth profiles for LakePulse lakes. For NLA sites, conductivity was measured in the lab from an integrated surface water sample. Using aggregated temperature estimates averaged at every meter of the depth profiles, a measure of the water mass stability, the mean Relative Temperature Resistance (*meanRTR*), was estimated by computing the salinity-corrected water densities differences of all adjacent layers of the profiles (Birge, 1910; Longhi and Beisner, 2009). Those density differences were then divided by the density difference of water at 4˚C and 5˚C and averaged, using the following formula:

$$meanRTR = \frac{1}{n}\sum_{i}^{n}\frac{\rho^{i}_{bottom} - \rho^{i}_{top}}{\rho_{4^{\circ}\mathrm{C}} - \rho_{5^{\circ}\mathrm{C}}}$$

where *n* is the number of temperature layer pairs, i.e., the maximum depth of the profile in meter minus one. Sites with higher values of *meanRTR* have relatively steep temperature gradients from the top to the bottom of the water column and are thus more thermally stable sites (in other words are less susceptible to mixing).

The depth of the photic zone was defined as the secchi depth (note that the secchi depth was not included in the analyses itself because of a large amount of missing values, especially for lakes that were clear over the entire water column). Additional surface water samples were collected and processed in the lab to estimate nutrient (TN, TP), DOC, DIC and ion concentrations. Water colour (in Platinium-Cobalt unit) was measured for NLA lakes from surface water samples. In LakePulse lakes water colour was instead estimated from light absorption coefficient values at 440nm (Cuthbert and del Giorgio, 1992).

Climate variables were obtained from the ERA-5 land hourly climate dataset (Muñoz-Sabater *et al.*, 2021). This is a dataset that combines physical modelling results with observation from across the world, and provides measurements for a variety of climate land variables over a latitude-longitude grid with a 0.1° x 0.1° horizontal resolution, all at an hourly time interval. The raw data were obtained through the dedicated API request system of the Copernicus web platform (https://cds.climate.copernicus.eu/cdsapp#!/home), and the climate attribute values for a given sites were extracted at the pixel of the grid containing the geographical coordinates of each lake. Variables available at all sites included the mean wind speed, the mean temperature 2-m

above ground, the net mean surface solar radiation and the total sum of precipitations. These variables were all averaged over the thirty days prior to the date of the sampling in each lake. The total number of degree days since the beginning of the sampling year (with a temperature threshold of 0°C) was also computed.

The composition of the nanophytoplankton community was assessed from integrated water samples taken in each lake, over the first two meters of the water column or down to the deepest limit of the photic zone (whichever was smaller) using an integrated sampling tube. In both surveys, nanophytoplankton taxa were identified by expert taxonomists and enumerated using the Ütermohl method on an inverted microscope (up to 1000× magnification). Taxa biovolumes (in $mm^3.m^{-3}$) were determined using geometric formulae corresponding to the shapes of the taxa applied to from cell dimensions measured in each sample (Hillebrand *et al.*, 1999). The composition of the crustacean zooplankton community was also assessed from vertical water samples collected from hauling meshed nets. Zooplankton taxa were then identified and enumerated by expert taxonomists, and the individual taxa biomasses were used to calculate the total biomass of several major taxonomic groups: calanoid copepods, cyclopoid copepods and cladocerans. The zooplankton community composition in NLA lakes was assessed from two vertical sample samples collected using a fine mesh net (50 µm) and a coarse mesh net (150 µm), with a vertical cumulative 5 m tow for each net. In contrast, a single 100 µm mesh net hauled over the water column depth from 1-m above the sediments was taken in the LakePulse survey.

All variables measured in both surveys were combined to create a unified dataset. Of the 1789 sites with nanophytoplankton community composition data, only 1162 sites had complete records for all of the environmental variables. To complete this latter dataset, a data imputation procedure was implemented using the *missForest* R package (Stekhoven et Bühlmann, 2012) after sites that were missing measurements for five or more environmental variables had been removed. At the end of the harmonizing process, 1652 sites (LakePulse, 570; NLA, 1082) had complete records for both environmental variables and phytoplankton taxonomic assessments.

3.3.2 Data specific to the LakePulse survey

The field and lab methods used during the LakePulse and NLA campaigns in 2017 were identical for most environmental measurements, as both those surveys based their methodology on that used in the NLA 2012 campaign (Huot *et al.*, 2019). The biggest obstacle in the harmonizing process was the fact that some potentially relevant environmental parameters to our study question were only available for the LakePulse survey (Table 3.1). This warranted additional analyses on LakePulse lakes exclusively. Lakes with missing measurements were removed before analyses, resulting in a dataset of 452 sites with complete records for predictors exclusive to LakePulse in addition to the variables common to the two surveys and estimates of the prevalence of mixotrophy.

Additional information on the morphometry of LakePulse lakes (lake volume, average depth, average discharge and shoreline development) were retrieved from the HydroLAKES database (Messager *et al.*, 2016). Because of the high level of collinearity between some of the morphological variables, a PCA was performed to summarize the shared variability in a reduced information space (Annexe J). The coordinates of the sites over the first two dimensions of this PCA plan were then used as predictors in subsequent statistical analyses instead of the raw HydroLAKES attributes. Information about the size of the watershed and the associated land-use types (i.e., the relative percentages of natural, agricultural and urbanized land within the watershed) were inferred using GIS (Huot *et al.*, 2019). Light availability variables were estimated as the daily mean photon flux density over the mixed layer (averaged over the two weeks prior to the sampling date) and as the mixed layer averaged spectral irradiance at 440nm and 665 nm. These were based on surface irradiance data obtained from the CERES *CER_SYN1deg-MHour_Terra-Aqua-MODIS_Edition4A* dataset (NASA/LARC/SD/ASDC, 2017) further processed in a semi-empirical model (Cremella 2022; pers.comm.) and corrected by field measurements obtained from a HydroScat-6P backscattering sensor (HOBI Labs, United States). Dissolved CO_2 and methane were estimated *in situ* using a field cavity ring down spectrometer (CRDS) equipped with a small sample isotopic module (SSIM, Picarro G2201-I, Picarro Inc., CA, USA). Finally, bacterial abundance at each site was estimated from flow cytometry analyses.

Table 3.1. Summary information on the environmental and biotic variables used as predictors in the statistical analyses.

Predictor	Abbreviation	Unit	Survey
Survey	-	-	NLA & LakePulse
Ecoregion	-	-	NLA & LakePulse
Elevation at lake coordinates.	*Altitude*	m	NLA & LakePulse
Surface area of the lake.	*Area*	km^2	NLA & LakePulse
Perimeter length of the lake.	*Perimeter*	m	NLA & LakePulse
Depth of the lake at the sampling site.	*Depth_site*	m	NLA & LakePulse
Water sodium concentration.	*Sodium*	$mg.L^{-1}$	NLA & LakePulse
Water calcium concentration.	*Calcium*	$mg.L^{-1}$	NLA & LakePulse
Water magnesium concentration.	*Magnesium*	$mg.L^{-1}$	NLA & LakePulse
Water chloride concentration.	*Chloride*	$mg.L^{-1}$	NLA & LakePulse
Water potassium concentration.	*Potassium*	$mg.L^{-1}$	NLA & LakePulse
Water sulfate concentration.	*Sulfate*	$mg.L^{-1}$	NLA & LakePulse
Mean temperature (sampling tube length)	*Temperature_up*	ºC	NLA & LakePulse
Mean temperature (bottom meter of the water column).	*Temperature_bottom*	ºC	NLA & LakePulse
Mean pH value (sampling tube length)	*pH_up*	pH unit	NLA & LakePulse
Mean pH value (bottom meter of the water column).	*pH_bottom*	pH unit	NLA & LakePulse
Mean concentration of dissolved oxygen (sampling tube length)	*DO_up*	$mg.L^{-1}$	NLA & LakePulse
Water conductivity.	*Conductivity*	$mS.cm^{-1}$	NLA & LakePulse
Total phosphorus concentration in surface water sample.	*TP*	$\mu g.L^{-1}$	NLA & LakePulse
Total nitrogen concentration in surface water sample.	*TN*	$mg.L^{-1}$	NLA & LakePulse
Dissolved Organic Carbon concentration.	*DOC*	$mg.L^{-1}$	NLA & LakePulse
Water colour.	*Colour*	APHA PT-CO / PCU scale unit	NLA & LakePulse
Mean wind speed over the 30 days prior to sampling.	*Wind_30d*	$m.s^{-1}$	NLA & LakePulse
Mean temperature over over the 30 days prior to sampling.	*T2m_30d*	°C	NLA & LakePulse
Net mean Surface Solar Radiation over the 30 days prior to sampling.	*SSR_30d*	$J.m^{-2}.day^{-1}$	NLA & LakePulse
Total sum of precipitation over the 30 days prior to sampling.	*TotPrec_30d*	m	NLA & LakePulse
Number of Degree days.	*DegreeDay*	°C	NLA & LakePulse
Cladoceran biomass.	*Biom_Cladocera*	$\mu g.L^{-1}$	NLA & LakePulse
Calanoid biomass.	*Biom_CopCal*	$\mu g.L^{-1}$	NLA & LakePulse
Cyclopoid biomass.	*Biom_CopCyc*	$\mu g.L^{-1}$	NLA & LakePulse
Zooplankton biomass (Cladocera + Copepoda).	*Biom_Zoo*	$\mu g.L^{-1}$	NLA & LakePulse
Mean Relative Thermal resistance	*meanRTR*	No unit (ratio)	NLA & LakePulse
CO2 surface water concentration.	*pCO2*	Parts per million (ppm)	LakePulse
CH4 surface water concentration.	*pCH4*	Parts per million (ppm)	LakePulse
Averaged photon flux density.	*PDP*	$\mu mol.photon.m^{-2}.s^{-1}$	LakePulse
Spectral irradiance at 440 nm.	*SI_440*	$\mu mol.photon.m^{-2}.s^{-1}.nm^{-1}$	LakePulse
Spectral irradiance at 665 nm.	*SI_665*	$\mu mol.photon.m^{-2}.s^{-1}.nm^{-1}$	LakePulse

Fraction of natural landscape within the watershed.	*NatLandscapes_frac*	No unit (percentage)	LakePulse
Fraction of agricultural landscape within the watershed.	*Agriculture_frac*	No unit (percentage)	LakePulse
Fraction of urbanized lands surface within the watershed.	*Urban_frac*	No unit (percentage)	LakePulse
Bacterial abundance	*Bacterial_ab*	cell.mL^{-1}	LakePulse
Shoreline development (ratio between shoreline length and the circumference of a circle with the same area).	*ShoreDev*	No unit (ratio)	LakePulse
Total lake volume.	*Vol_total*	Million of m^3	LakePulse
Average depth over the entire lake.	*Depth_avg*	m	LakePulse
Average long-term discharge.	*Dis_avg*	m^3.s^{-1}	LakePulse

3.3.3 Estimating the prevalence of mixotrophy

The first step to estimate the prevalence of mixotrophy in each lake was to assess the trophic strategies (pure phototroph, mixotroph or pure phagotroph) of all taxa identified in the two lake surveys. This assessment was based on our own taxonomic expertise, as well as on published database our study of nanophytoplankton trophic behavior. For example, all diatoms and cyanobacteria genera were considered autotrophic, as no taxa from these two groups is physiologically able to perform phagotrophy. Information available in published databases of phytoplankton traits was also used (Laplace-Treyture *et al.*, 2021; Olenina *et al.*, 2006; Rimet and Druart, 2018). However, such databases were sometimes inconsistent with one another, or simply did not include taxa from our surveys, as they covered different geographical areas or marine species. When the strategy of a given genus could not be established with certainty, a dedicated literature search was conducted for feeding behaviour descriptions. Publications reporting results from ingestion experiments were of particular interest. If no information was found for a particular genus, its strategy was inferred from those of closely taxonomically related taxa. Overall, a database of trophic strategies for over 270 genera present in North American lakes was produced (Annexe M).

Using the database of trophic strategies, the total biovolumes of the mixotrophic and autotrophic portion of the nanophytoplankton assemblage were computed at each site. The prevalence of mixotrophy at a given site ($prev_{Mixo}$) was then defined as the proportion of mixotrophic biomass within this overall nanophytoplankton community of this lake, i.e., the ratio between the total mixotrophic biomass and the sum of the total autotrophic and total mixotrophic biomasses. The biovolumes of purely phagotrophic (i.e., not mixotrophic or phototrophic) taxa were excluded

from the computations. The resulting index ranges from 0 (absence of mixotroph within the community) to 1 (all taxa in the community are mixotrophic).

3.3.4 Analyses of mixotrophic community composition and diversity

The effect of environmental variables on the composition of the mixotrophic portion of the community was investigated using redundancy analyses (RDA). RDAs are multivariate canonical analysis and constitute a useful tool to explain the variation in a dataset of continuous response variables like taxa abundances using a second dataset of explanatory variables, typically measurements of environmental variables (ter Braak et Prentice, 1988). RDAs can be seen as an extension of the multiple linear regression framework to a multivariate response dataset rather than a single response variable. The biological responses variables, the environmental predictors and the statistical sites (in this case, the different lakes) can be projected in a 2-dimensional figure whose axes are linear combinations of the predictors (Legendre *et al.*, 2011). The relative position of the taxa and environmental drivers can then be investigated to identify potential effects of environmental drivers on taxa abundance. RDA analysis were performed using the *vegan* R package (Oksanen *et al.*, 2020). Predictors were log-transformed and standardized prior to analysis and a Hellinger transformation was applied to the mixotroph biomasses to limit the weight of rare taxa, i.e., taxa found in a very limited number of sites, potentially giving them an undue influence in the analysis (Legendre et Gallagher, 2001). In addition, the list of predictors included in the analysis was refined by sequentially removing predictors with a VIF score superior to 10 to minimize collinearity in the analyses (Belsley *et al.*, 1980). The diversity of the nanophytoplankton communities were estimated as the Richness (*R*) and the Shannon diversity index (*H'*) at the genus level using the vegan R package (Oksanen *et al.*, 2020).

The environmental drivers of the prevalence of mixotrophy were identified using Random Forest (RF) analyses. In recent years, machine learning algorithms like RF have proven useful for understanding which environmental factors control the assembly of planktonic communities. RF algorithms seek to predict the values of a response variable by building multiple regression trees using several predictive variables (or predictors). Each tree is based on a unique bootstrapped sample of the original data and the final model is obtained by averaging the results of all the individual trees (Breiman, 2001). A permutation-based decrease in prediction accuracy score can

then be computed for each predictor by comparing the accuracy of a model built using a dataset where the values of the target predictor are permutated (thus breaking any existing relationship between the predictor and the response variable) to the accuracy of the model built using the original data (Strobl *et al.*, 2007). RF models can thus be used to perform variable selection: it is possible to estimate the relative importance of the different predictors in terms of their effect on the accuracy of the prediction of a response variable, thus allowing the user to identify the most important predictors of a response variable of interest. RF models and variable importance scores were estimated using the *party* R package (Hothorn *et al.*, 2006). Predictors were log-transformed and standardized prior to the analysis and a logit transformation was applied to the response variable $prev_{Mixo}$. To visualize how the environmental variables affect the prevalence of mixotrophy, the partial dependence effects of the most important predictors identified by the RF analyses were computed and used to produce partial dependence plots (PDPs). Predictor effects in RF analyses are not necessarily linear, meaning partial dependence effects PDPs can potentially reveal nonlinear trends.

3.4 Results

3.4.1 Distribution of mixotrophs across North American lakes

Across both surveys, 32 distinct mixotrophic genera were identified. Of the 1789 sites with community composition data, 46 contained no mixotrophs ($prev_{mixo} = 0$). The contribution of mixotrophic taxa to the total nanophytoplankton biomass was < 1% in 143 sites. The distribution of the prevalence of mixotrophy was heterogeneous across North America and varied by ecoregion (Fig. 3.2a) (non-parametric Kruskall-Wallis rank test, $p < 0.001$). A post-hoc Dunn's Kruskal-Wallis multiple comparison test further revealed that lakes in the *Great Plains* ecoregions had significantly lower prevalence of mixotrophy than the *Northern Forests*, *Marine West Coast Forest* and *Eastern Forests* ecoregions (Fig. 3.2a).

Three main mixotrophic taxonomic groups were found in most communities across the two surveys: chrysophytes, cryptophytes and dinophytes with the relative contribution of each varying across ecoregions (Fig. 3.2b). Cryptophytes dominated mixotrophic assemblages in the *Great Plains*, with relatively low contribution of chrysophytes in this ecoregion. In contrast, chrysophytes and dinophytes appeared to be more prevalent in the *Northern Forests* ecoregion.

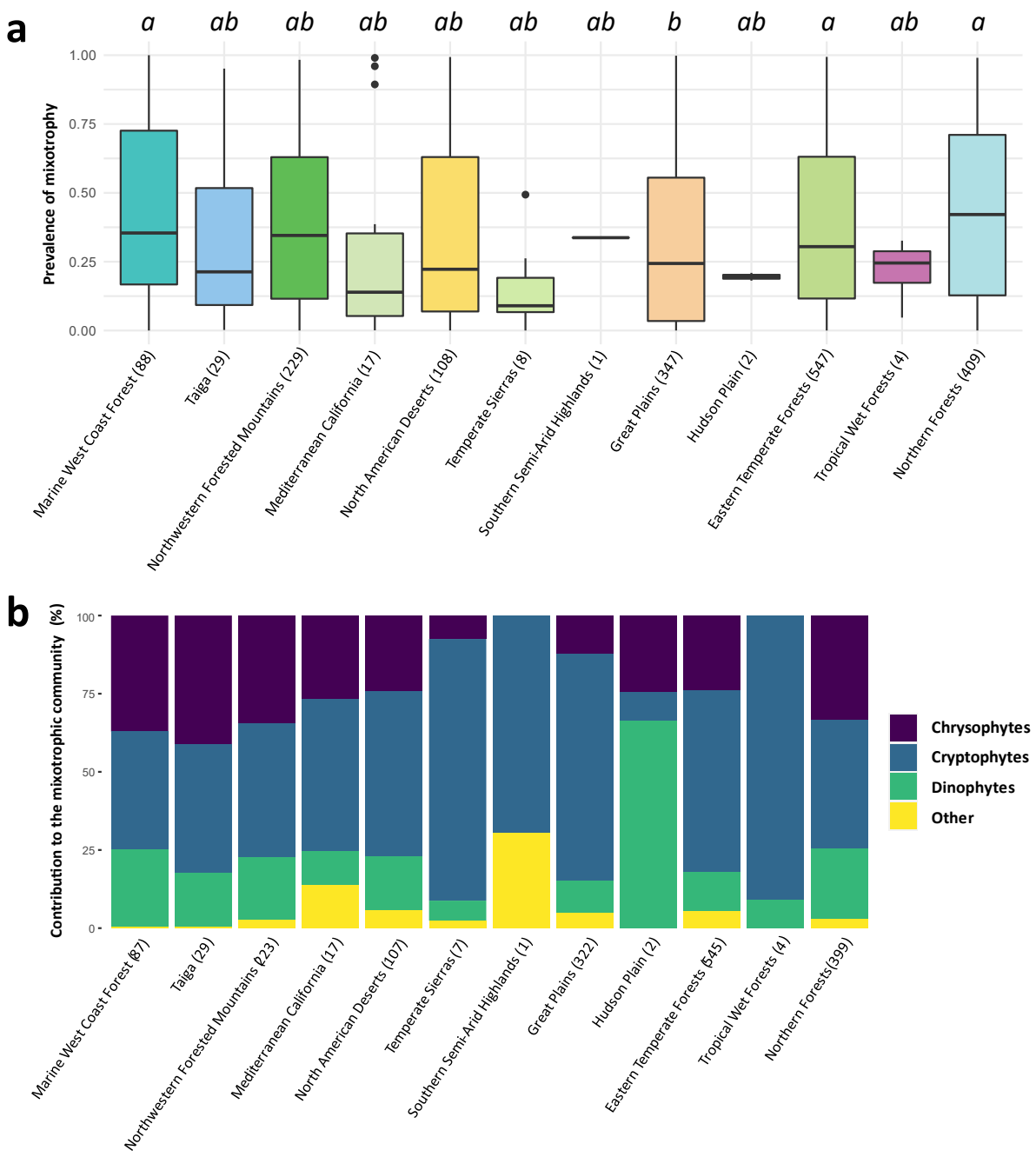

Figure 3.2. Boxplots of the prevalence of mixotrophy (a) and mean lake relative contributions of classic nanophytoplankton taxonomic groups to the mixotrophic community (b) across the ecoregions (EPA level I) covered by the combined NLA and LakePulse surveys. The number of sites sampled in each ecoregion is specified in the x-axis labels. The letters above the boxes in (a) indicate significant differences between ecoregions, according to the results of the post-hoc Dunn's Kruskal-Wallis multiple comparison test (at a $p < 0.05$ level).

3.4.2 Environmental drivers of mixotrophic community composition

The adjusted R^2 score of the RDA on the data from the combined surveys was relatively low ($R^2_{adj} = 0.105$), as was the variability explained by the first two axes (6.37% for the first axis and 2.35% for the second axis) (Fig. 3.3a). As the longest vector parallel to the first RDA axis, TP appears to be the most important factor for taxonomic composition. Most chrysophyte and dinophyte genera, and in particular the chrysophyte genera *Dinobryon* and *Ochromonas*, were placed in opposition to TP along the RDA1 axis, indicating greater contributions of these genera in deep oligotrophic lakes. In contrast, cryptophytes *Rhodomonas* and *Cryptomonas* were associated with somewhat higher TP concentrations, although modulated by other factors such as temperature (*T2m_30d*) and DOC-associated colour, respectively. A second discriminating dimension appeared to be the effect of light availability on community structure as determined by DOC levels and water colour in opposition to the mean surface solar radiation over 30 days (*SSR_30d*). *Cryptomonas* and C*eratium* (a dinophyte genus) separated from the rest of the community over this dimension, and both were more prevalent in coloured lakes with high DOC levels. In contrast, water chemistry predictors (*DO_up, pH_up, Conductivity*) and zooplankton abundance variables were not well represented in the RDA and appear to have relatively weak relations with community composition.

The RDA for the LakePulse survey alone (447 lakes) permitted inclusion of additional environmental predictors that were not collected at the NLA sites (Fig. 3.3b). The adjusted R^2 square was slightly lower than in the previous RDA ($R^2_{adj} = 0.090$), probably because of the larger number of predictors added to the model, and the first and second axis explained 6.54% and 2.84% of variation respectively. TP once again clearly constrained community assemblage and clearly aligned with the cryptophyte *Cryptomonas* (more prevalent in high TP sites) and in opposition to the chrysophyte *Ochromonas* (more prevalent in oligotrophic lakes). Predictors related to light availability again secondarily contributed to structuring the community, with water colour in opposition to photon flux density, spectral irradiance at 440 nm and lake depth (via the sites scores on the second PCA axis built from lake morphology). Compared to the results on the combined surveys, in Canadian lakes *Rhodomonas* was the mixotrophic taxa most prevalent in more coloured lakes with low light availability in the water column. Moreover, *Ceratium* prevalence was relatively higher in Canadian lakes having high zooplankton biomasses

and high ion concentrations, patterns that were not visible in the previous analysis. Finally, temperature-related variables were not well represented in the RDA of Canadian lakes.

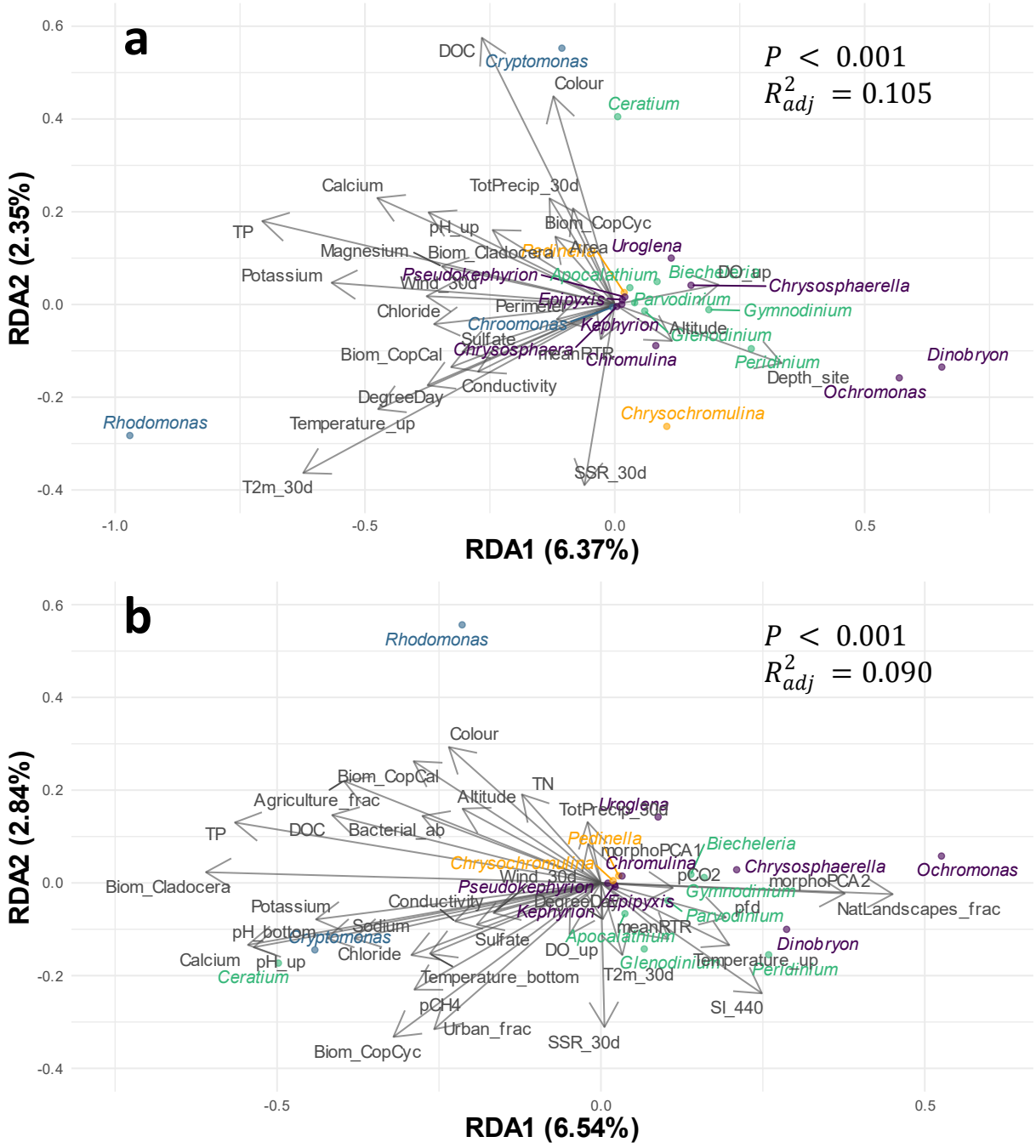

Figure 3.3. RDA triplot showing how environmental variables (grey arrows) constrained mixotrophic community composition in the combined NLA and LakePulse surveys (a) and LakePulse survey exclusively (b). To improve readability, individual site points were not plotted, and the taxon scores were plotted as dots rather than arrows. The taxon scores and names were coloured to reflect their broad taxonomic classification (purple: chrysophytes; blue: cryptophytes; green: dinophytes; orange: other).

Because TP was the strongest predictor in the RDAs, the effect of lake trophic state on the composition and the diversity of the mixotrophic portion of the community was further investigated. To facilitate visualization of potential community composition shift, sites were split into limnologically coherent categories of nutrient availability, i.e., each sites was grouped in one of four trophic state categories according to their *TP* values: oligotrophic ($TP < 12\ \mu g.L^{-1}$; 348 sites), mesotrophic ($12 \leq TP < 24\ \mu g.L^{-1}$; 421 sites), eutrophic ($24 \leq TP < 48\ \mu g.L^{-1}$; 312 sites) and hypereutrophic ($TP \geq 48\ \mu g.L^{-1}$; 528 sites) (Fig. 3.4). At the genus level mixotrophic assemblages changed with lake trophy: cryptophytes *Rhodomonas* and *Cryptomonas* contributed most biomass to the mixotrophic communities in eutrophic and hypereutrophic lakes, while *Dinobryon* (chrysophytes) clearly decreased with lake trophy (Fig. 3.4a). There was a clear shift from chrysophyte dominance in oligotrophic lakes to cryptophyte dominance in eutrophic and hypereutrophic sites (Fig. 3.4b). The prevalence of dinophytes also appeared to decrease in more eutrophic lakes. There was also a change in the relative prevalence of the most dominant taxa: mixotroph assemblages were dominated by relatively few genera in hypereutrophic sites compared to oligotrophic ones. This warranted additional analyses of the diversity response to lake trophic state: genus-level richness and Shannon diversity decreased from oligotrophic to hypereutrophic lakes (Fig. 3.4c, Fig. 3.4d). Group comparison tests (one-way Kruskal-Wallis analysis of variance for Richness and one-way ANOVA for Shannon diversity) revealed that the observed changes were very significant between the different categories of lake trophic state ($p < 0.001$ for both tests). Post-hoc multiple comparisons tests (Dunn's test for genera Richness and Bartlett test for Shannon diversity) further showed that these changes in diversity were significant between each pair of lake trophic state categories ($p < 0.05$).

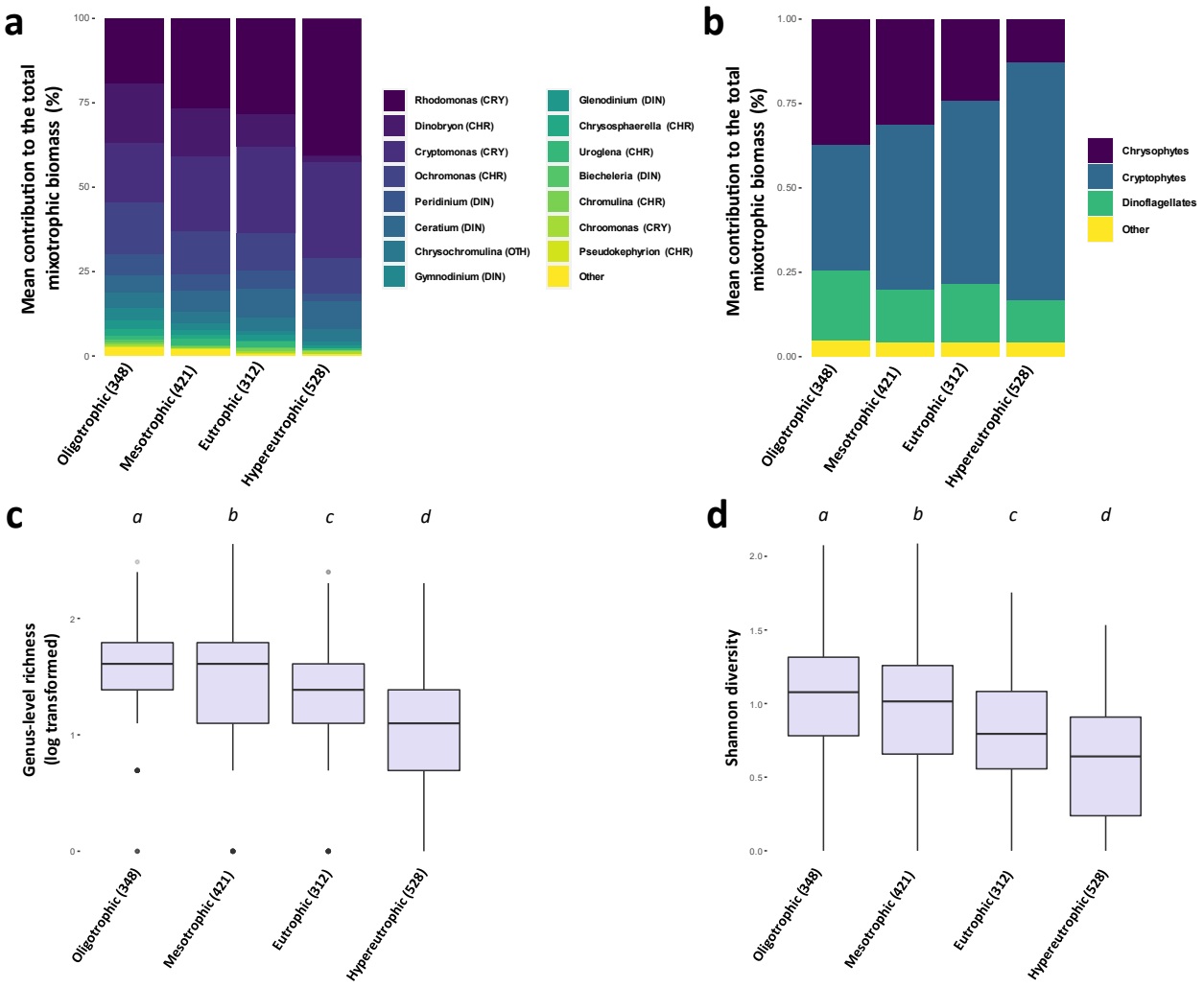

Figure 3.4. Mean contribution (percentage) of mixotrophic genera (a) and taxonomic groups (b) to the mixotrophic portion of the total nanophytoplankton biomass for different categories of lake trophic state. Boxplots of the log-transformed genus-level Richness (c) and Shannon diversity (d) across the four lake trophic state categories. The letters above each box indicate significant difference (at a $\boldsymbol{p < 0.05}$ level) between lake trophic categories according to relevant post-hoc multiple comparisons tests (Dunn's test for genera Richness and Bartlett test for Shannon diversity). In all panels, the number of sites in each category of trophic state is specified in the x-axis labels.

3.4.3 Environmental predictors of the prevalence of mixotrophy

The relative importance of each environmental predictor was estimated for sites from the combined surveys (Fig. 3.5a) and for the LakePulse survey exclusively (Fig. 3.5b) using RF models. The estimated R^2 computed from the Out-Of-Bag data for those RF models were 0.278 and 0.276 respectively. In each case, TP was by far the most important predictor of $prev_{Mixo}$.

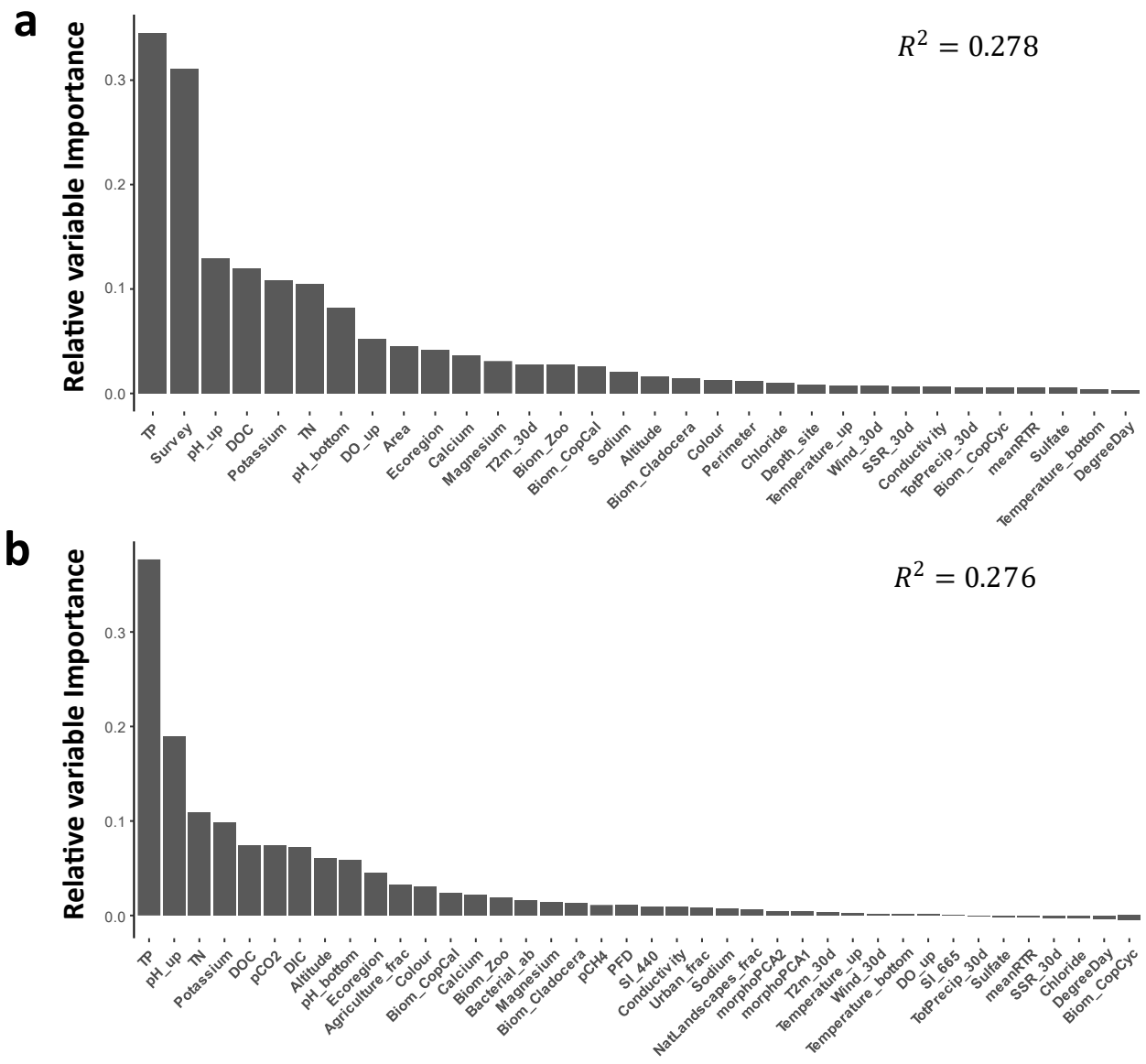

Figure 3.5. Variable Importance scores (computed as the mean decrease in model accuracy) obtained from the Random Forest analyses on the data from the combined surveys (a) and on LakePulse lakes exclusively (b).

For each model, partial dependency plots were produced for the ten most important quantitative predictors (Fig 3.6, 3.7). The partial dependence effects of other predictors that related to the initial hypotheses of this study were also assessed even if they were not in the top ten identified in the RF model. As outlined in the Introduction, these variables were: water colour (*Colour*), temperature of the upper layer of the water column (*Temperature_up*) and the index of thermal stability (*meanRTR*). The best zooplankton biomass predictors were also added (*Biom_CopCal* and *Biom_Zoo* for the combined surveys model and the LakePulse survey model respectively).

For the analyses on LakePulse sites alone, the partial dependent effect of the photon flux density, i.e., the quantity of light in the mixed layer (*PFD*) was also included (Fig. 3.7).

The model results did not differ greatly between the two analyses. TP (and to a lesser degree TN) was the most important predictor in both RF models, being negatively related to $prev_{Mixo}$. The effect of the qualitative predictors *Survey* and *Ecoregion* were also important for the combined survey analysis. Several variables related to water chemistry (*DO_up*, *pH_up* and *DOC*) were also selected and negatively affected mixotrophy prevalence. Ionic concentrations (Potassium and Magnesium mostly) were also associated to lower values of *prevMixo*. One variable pertaining to lake morphology, lake area, was negatively related to the prevalence of mixotrophy across North America (Fig. 3.6). Although their importance scores were low compared to that of TP and the magnitude of their partial effects was relatively limited, predictors relating to zooplankton biomass (*Biom_zoo*, *Biom_CopCal*) appear to be negatively related to $prev_{Mixo}$. Focussing on the analysis on LakePulse sites, and on the predictors exclusive to this survey, dissolved CO_2 and DIC concentrations had relatively elevated importance scores with positive and negative effects respectively on $prev_{Mixo}$ (Fig 3.7). The PDPs also revealed a mostly positive, though very low in magnitude effect of *PFD* on $prev_{Mixo}$.

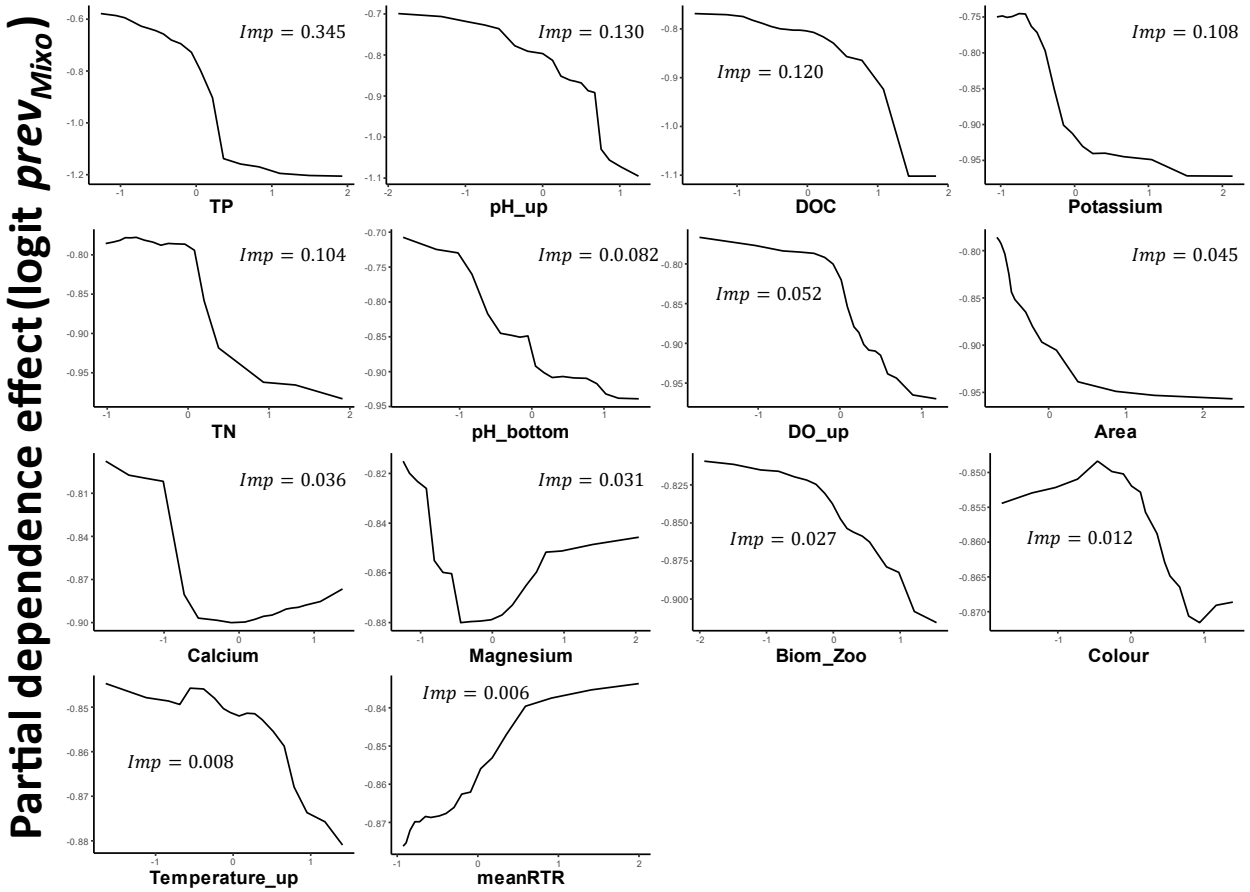

Figure 3.6. Partial dependency plots (PDPs) showing the marginal effects of quantitative Random Forest predictors on the logit transformed response variable mixotrophy prevalence ($prev_{Mixo}$) for the combined surveys. The importance scores of each predictor are indicated on the individual plots.

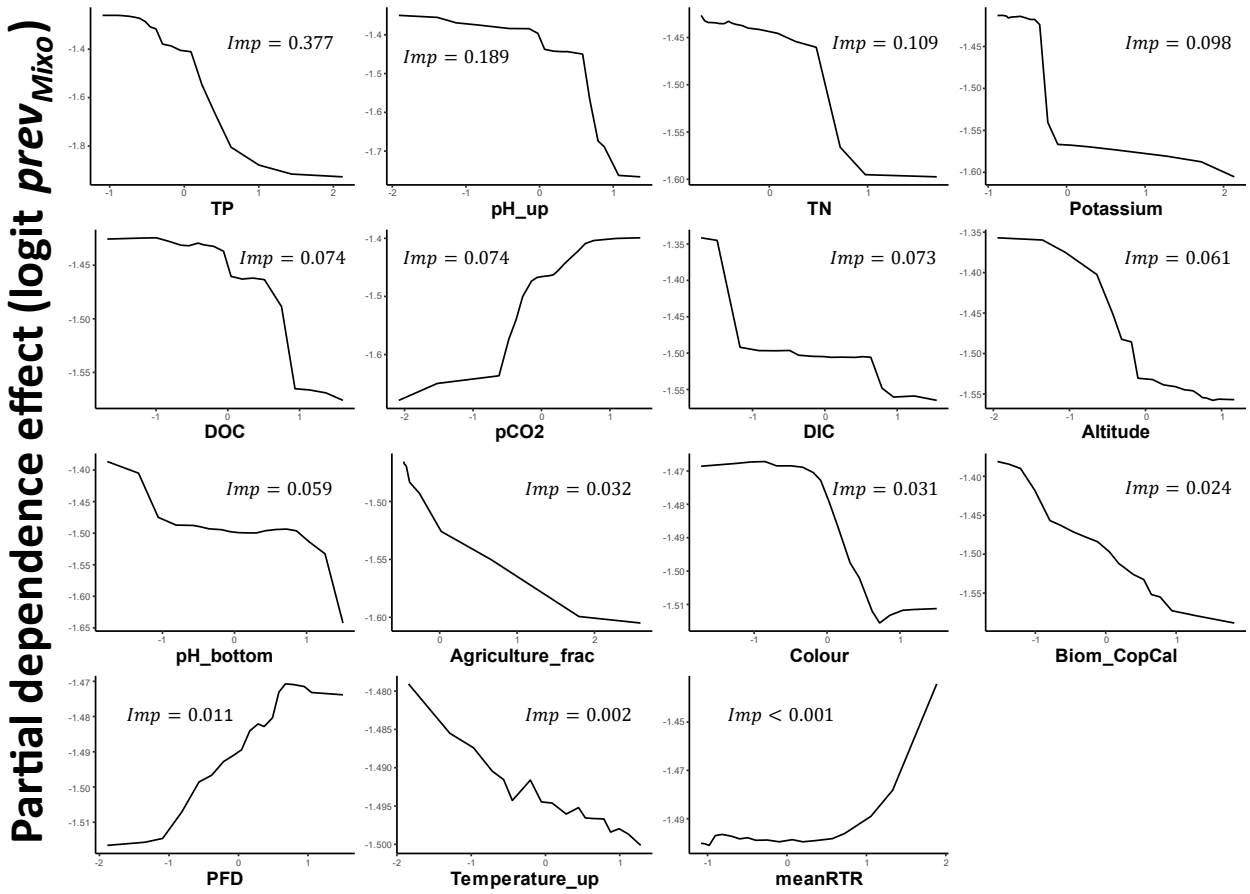

Figure 3.7. Partial dependency plots showing the marginal effects of quantitative Random Forest predictors on the logit transformed response variable mixotrophy prevalence ($prev_{Mixo}$) for the LakePulse survey. The importance scores of each predictor are indicated on the individual plots.

3.5 Discussion

3.5.1 Phago-mixotrophy is ubiquitous in North American lakes

Investigation of nanophytoplankton community records collected across the US and Canada revealed that the vast majority of North American lakes harbor phago-mixotrophic taxa. Of all the sites investigated, only a small portion of lakes featured no mixotrophic taxa (46 out of 1789 lakes). While mixotrophs were found in the overwhelming majority of lakes, the prevalence of mixotrophy was not evenly distributed across the continent and varied across ecoregions. Among the ecoregions with the most lakes sampled, the prevalence of mixotrophy was lowest in the *Great Plains*, and highest in more forested regions. These differences can most likely be attributed to alterations in land use and lake morphology that in turn control lake trophic state. Lakes in the *Great Plains* are notoriously more eutrophic than sites in less impacted ecoregions (Hollister *et al.*, 2016), mostly because these lakes are relatively shallow and because agricultural

activities are very prevalent in their watersheds. Analyses on LakePulse sites did not highlight watershed usage categories as particularly strong drivers of mixotrophy prevalence, but those same analyses revealed an outsized negative effect of TP on $prev_{Mixo}$, indicating that oligotrophic sites had a greater prevalence of mixotrophy than did eutrophic sites.

In addition to the overall prevalence of mixotrophy, the taxonomic composition of the mixotrophic community was not uniform across the continent. The most striking variation in mixotrophic community composition was the shift from cryptophyte-dominated mixotrophic communities in the *Great Plains* ecoregion to a dominance of chrysophytes and dinophytes in lakes situated in less agricultural and human-impacted ecoregions like the *Northern Forests* and the *Northwestern Forested Mountains*. As observed in the RDAs, these assemblage differences likely stem from environmental preferences, in particular lake trophic state, that are tied to differences in land use in the watershed.

3.5.2 Lake trophic state is the main driver of mixotrophy prevalence

Throughout the different analyses, lake trophic state appears to be the main driver of the prevalence of mixotrophy across North American lakes. TP was identified as the most important predictor in the RF models, and it had a strong, mostly linear negative partial dependant effect on $prev_{Mixo}$ with oligotrophic sites being more mixotrophic than eutrophic lakes. Another important driver of the prevalence of mixotrophy was DOC concentration. While we might expect $prev_{Mixo}$ to respond positively to DOC levels which favour bacterial production (Hessen, 1992), the negative effect of this variable on $prev_{Mixo}$ should probably be interpreted as another indication that more oligotrophic lakes favour mixotrophy: indeed there was a substantial positive correlation between TP and DOC in our dataset (Annexe K) and which did not distinguish coloured from non-coloured DOC. These results were in line with our initial hypotheses: mixotrophy is an alternative strategy for nutrient and carbon acquisition, the success of mixoplankton taxa in natural systems is thus primarily tied to conditions of resource availability. One possible mechanisms explaining the success of mixotrophs when nutrients are scarce is that bacterial growth is more efficient in oligotrophic lakes compared to more eutrophic sites (Smith et Prairie, 2004). Phago-heterotrophy is thus a viable strategy for resource acquisition when lake phosphorus availability is low.

Phosphorus availability also controlled the composition and the diversity of the mixotrophic community. The RDA results indicated that more eutrophic sites tend to have higher relative prevalence of cryptophyte like *Rhodomonas* and *Cryptomonas*. This pattern echoes the findings of a study of Patagonian lakes that also identified a shift in dominance from chrysophytes to cryptophytes over a lake trophic state gradient (Saad *et al.*, 2016). Using results from experiments on bacterivory activity, they attributed this shift to physiological differences between taxa that impact their fitness in different conditions of nutrient availability. Chrysophytes like *Ochromonas* were found to have higher grazing impact than cryptophytes like *Rhodomonas* or *Cryptomonas* and were thus more reliant on phagotrophy for nutrient acquisition (Saad *et al.*, 2016). Based on simulation models (Crane and Grover, 2010), this also appears to be a viable strategy in oligotrophic lakes, where dissolved nutrients are scarce and grazing on bacteria constitutes an alternative source of phosphorus. In more eutrophic environments, investment in the physiological structures needed to perform phagotrophy is not advantageous, as it renders primarily phagotrophic mixotrophs less competitive against more phototrophic mixotrophs and pure phototrophs who can consume dissolved nutrients at higher rates and consequently have higher growth rates.

Observed taxonomic shifts over the gradient of nutrient availability thus reflects the broad positions of mixotrophic taxa over the phototrophy-to-phagotrophy mixotrophic functional gradient. Our results shows that this assembly rule previously identified at a regional scale (Hansson *et al.*, 2019) is confirmed at a continental scale. Increased lake trophic state not only led to a shift in community composition, but also to a decrease in the taxonomic diversity of the mixotrophic community. Our analysis of the composition of the mixotrophic community shows that sites with high TP levels were overwhelmingly associated with high prevalence of a restricted number of cryptophyte taxa (*Rhodomonas* and *Cryptomonas*). This assembly shift and overall loss of diversity with lake trophy could be attributed to the presence of contrasting mixotrophic strategies within the community. As previously discussed, phagotrophy is probably a marginal means of resource acquisition for cryptophytes that rely more on photo-autotrophy. Cryptophytes are thus less likely to dominate the community under conditions of limited nutrient availability that favour phagotrophs. However, these cryptophytes can become more competitive against other mixotrophs when phosphorus availability is high as bacterivory supplements

autotrophy allowing them to increase their relative dominance and driving down taxonomic diversity. Additionally, the watersheds of eutrophic and hypereutrophic lakes tend to be more human-impacted by agriculture. Consequently, those lakes might also be subjected to herbicide pollution, which could potentially reduce the diversity of the nanophytoplankton community and lead to a loss of taxa, including within the mixotrophic portion of the community (Fugère *et al.*, 2020). A study of the entire protist community in LakePulse lakes, identified using metabarcoding, also showed a pattern of decreasing diversity with lake trophic state (Garner *et al.*, 2022).

3.5.3 Other factors related to mixotrophy

In contrast to the clear effect of nutrient availability, we did not detect any strong effect of light availability on the prevalence of mixotrophy. Our results indicate that highly coloured lakes supported a relatively lower prevalence of mixotrophy, but the importance of water colour in the RF analyses was very low across both surveys together. Interpreting the effect of water colour is further complicated by the fact that it is probably related to dissolved organic carbon concentration, which can not only affect light availability, but can also promote bacterial growth (Kroer, 1993), thus potentially affecting the processes carried out by mixotrophs (autotrophy and bacterivory) in different, and likely, opposite ways. Analyses that included more detailed measurements of light conditions in LakePulse sites alone indicated that greater light availability (*PFD*) was related to an increased prevalence of mixotrophy as also reported by Edwards (2019) in marine environments, although the amplitude of the partial dependence effect was low, as was the importance of this predictor. Many mixotrophic taxa are obligate phototrophs, for which bacterial ingestion is not sufficient to stave off carbon limitation when light availability is low (Jones, 2000). Experimental studies have shown that obligate mixotrophs favour high irradiance environments: for example, competition experiments in microcosms have shown that the prevalence of an obligate phototrophic mixotroph like *Ochromonas* (relative to the abundance of a pure phototroph) is higher under high irradiance growth conditions (Fischer *et al.*, 2017). Our own modelling results indicate that mixotrophs that are functionally more reliant on phototrophy increase their prevalence relative to pure autotrophs when light availability increase (see Chapter II of this dissertation). Thus the majority of the mixotrophic genera in lake surface waters of

North America may be operating primarily as phototrophs; although *in situ* growth experiments would be required to confirm this.

Despite this discussion of the relation between light availability and the success of mixotrophy, the importance scores of light-associated variables were exceedingly low in the RF analyses when compared to the importance of TP. This result could indicate that, at the scale of the entire community, nanophytoplankton phago-mixotrophy is more relevant for acquisition of phosphorus than for carbon. Another possible explanation for the lack of a strong effect of light conditions is that the nanophytoplankton community was sampled over the first 2-m of the water column, where light is less likely to be limiting. However, with respect to the mixotrophic assemblage composition, light conditions appear to have some effect (although still to a lesser degree than nutrient availability). Our RDA results indicate that *Cryptomonas* and *Ceratium* (as well as *Rhodomonas* in Canadian lakes) were more prevalent in coloured lakes where the amount of solar irradiance is low. Differences in prevalence across varying light availability conditions could reflect contrasting taxonomic strategies for carbon acquisition (photosynthesis vs. bacterivory) that would translate into different functional mixotrophic balances between phago-heterotrophy and photo-autotrophy for different species. Confirming whether these environmental patterns reflect actual physiological differences between taxa would require more detailed growth and bacterial ingestion experiments.

Other components of lake water chemistry were related to the prevalence of mixotrophy in addition to TP. Increased pH (and highly correlated DIC, Annexe K) and DO levels were associated with more autotrophic assemblages. In Canada, lakes with high dissolved CO_2 concentrations had a greater prevalence of mixotrophy. It is highly probable that CO_2 concentration, DO concentration and to an extent pH are reflective of photo-autotrophic primary productivity rather than actual drivers of phago-heterotrophy. Our analyses also revealed that the concentrations of several ionic species affect the prevalence of mixotrophy, in particular potassium. K is generally not considered to be a limiting resource for nanophytoplankton in freshwater system (Jaworski *et al.*, 2003), and there a little information available on how bacterivory relates to micronutrient acquisition or even how K availability would affect bacterial growth. Across North America, lakes with high ionic concentration tend to be eutrophic sites, as there is some correlation between TP and ionic species concentrations (in particular K) in our

dataset (Annexe K). In particular, sites in the Prairies ecoregion, which are generally eutrophic, also display the highest potassium concentration (Annexe L). The association between K and $prev_{Mixo}$ should thus probably be seen as another proxy effect of lake tropic state on nanophytoplankton assemblages of resource-acquisition strategies.

Top-down interactions can also shape nanophytoplankton assemblages and we observed negative (albeit weak) effects of zooplankton community biomass on mixotrophy prevalence. This could indicate a zooplankton preference for mixotrophic taxa, as copepods are selective feeders. This negative effect of zooplankton abundance on the prevalence of mixotrophy had previously been identified in a similar study of mostly oligotrophic boreal lakes (Hansson *et al.*, 2019). This relationship thus appears to hold at a continental scale, although it is worth noting that the marginal effects of zooplankton predictors were far lower than those of TP, indicating that top-down interactions are secondary drivers of the prevalence of mixotrophy in comparison to nutrient availability. While Hansson *et al.* (2019) attributed the large effect of zooplankton abundance on assemblages of resource-acquisition strategies to mixotrophs being more a generally more valuable prey source than pure photo-autotrophs for zooplankton, some mixotrophic taxa are apparently more preferred than others. For example, Vad *et al.* (2020) showed that for the cladoceran *Daphnia longispina* the nutritional value of *Dinobryon* was low compared to the nutritional value of *Cryptomonas*. Zooplankton abundances could thus be expected to be relevant drivers of the mixotrophic community composition, and our results show that this is apparently the case, at least in Canadian lakes. The various zooplankton predictors were not particularly relevant in the RDA on the combined surveys, although the cladoceran and copepod abundances were well represented in the LakePulse RDA. Higher abundances of these zooplankton groups appeared to be associated with greater prevalence of certain mixotrophs, in particular the cryptophytes *Cryptomonas* and *Rhodomonas* and the dinophytes *Ceratium*. It is tempting to attribute these patterns solely to zooplankton grazing preferences on other mixotrophs, reflecting the nutritional values of mixotrophic taxa with different mixotrophic strategies, but it is important to keep in mind that the effect of zooplankton grazing on community assembly could also reflect other trait differences within the community like cell size, toxin production or whether a given taxa form colonies (Colina *et al.*, 2016).

The effects of water temperature and lake stratification on resource-acquisition strategy assemblage were marginal at best, with very low importance scores in the RF models. The relative abundance of mixotrophic taxa appears to be generally lower in warmer lakes. It is likely that warmer water temperatures favour autotrophic cyanobacteria, thus pushing nanophytoplankton communities toward greater contributions of purely phototrophic taxa, especially cyanobacteria (Paerl et Huisman, 2009). While we anticipated that more stratified lakes might display higher prevalence of mixotrophy, we did not see such an effect in our results. This may reflect a methodological limitation inherent to the community assessment data, as the water samples used for nanophytoplankton taxonomic identification were taken over the first two meters of the photic zone rather than the entire water column. In stratified lakes, a significant portion of the nanophytoplankton community is concentrated within a Deep Chlorophyll Maximum (DCM) at the bottom of the euphotic zone, where taxa can optimally balance their light and nutrient requirements, oftentimes well below our survey sampling depths (Camacho, 2006; Leach *et al.*, 2018). This DCM component of the nanophytoplankton community was probably mostly excluded, especially in deeper lakes. While mixotrophs can be prevalent in epilimnetic waters because they can withstand nutrient scarcity through bacterivory (Tittel *et al.*, 2003), some mixotrophic taxa can also persist in conditions where photosynthesis is limited and could thus potentially be found below the photic zone (Skovgaard, 1996). If a strong stratification favours generalist trophic strategists by promoting a vertical gradient of nutrient availability conditions, detecting an effect of stratification on the prevalence of mixotrophy would probably require community assessments integrated over the entire water column, not just in surface waters.

In contrast, variables related to temperature were relatively well represented in the RDA from the combined survey dataset, indicated that temperature plays a role for mixotrophic assemblage composition. Studies have found that temperature affects phago-mixotrophic metabolic functions, and that warmer temperature favour taxa more reliant on phagotrophy for their growth (Lepori-Bui *et al.*, 2022), but it is unclear whether our results really support this idea. Indeed, the mixotrophic taxa that responded the most to temperature related variables was *Rhodomonas sp.* (sometime incorrectly referred to as *Plagioselmis nannoplanktica*), a cryptophyte genus whose relative biomass was greater in sites with warmer climate. The exact mixotrophic functional

balance of *Rhodomonas* is unknown, although other cryptophytes like *Cryptomonas* are generally considered to be mainly phototrophic (Jones, 1997). This result did not extend to the RDA results obtained from LakePulse sites exclusively, probably due to the reduced latitudinal range of this dataset that entailed a more restrained gradient of surface temperature values. Further research is needed to assess the exact physiology of freshwater mixotrophic taxa *in situ* and to see how mixotrophic community assembly change over a gradient of water temperatures when controlling for resource availability, especially in the context of a warming climate.

Finally, it is worth noting that our RDAs explained little overall variability in the taxonomic composition of the mixotrophic assemblage. This unexplained variability indicates that other assemblage rules are at play and might reflect the omission in the analyses of potentially important environmental drivers for the success of mixotrophs. It is also important to keep in mind that local environmental filtering is just one among a variety of processes that determine community assembly (Borics *et al.*, 2021).

3.6 Conclusions

We showed that phago-mixotrophy is ubiquitous across North American temperate and boreal lakes. Lakes without any mixotrophic nanophytoplankton taxa are the exception rather than the rule. However, the biogeography of mixotrophs is variable, with lakes in less human-impacted ecoregions displaying a higher prevalence of mixotrophy primarily via high contributions of chrysophytes and dinophytes. On the other hand, the more impacted Great Plains ecoregion harboured lakes that were generally more autotrophic and where cryptophytes were the dominant mixotrophic taxa. Indeed, we identified phosphorus availability (TP) as the main driver of phago-mixotrophy, with higher prevalence of mixotrophs in more oligotrophic sites. TP also constrained mixotrophic community assembly and taxonomic diversity. Other relevant environmental drivers of mixotrophy included water chemistry and zooplankton biomass. In contrast, light appears to have little effect on resource-acquisition strategy assemblages although it had to have some effect on the composition of the mixotrophic community. This absence of an effect of light highlights possible avenues of research for future studies of the drivers of nanophytoplankton mixotrophy. In addition to investigating the potential for mixotrophy within communities, measuring the actual contributions of phagotrophy to mixotrophic growth rates could reveal additional

differences between the main taxonomic groups across environmental gradients, in particular light availability. Overall, this study is the most extensive investigation of lake mixotrophy to date, covering almost 1800 of lakes and a dozen distinct ecozones, and demonstrates that large scale surveys like the NLA and LakePulse sampling campaigns are invaluable sources of empirical information and when well coordinated, useful to uncover community assembly rules at previously unstudied continental scales.

CONCLUSION

4.1 Objectifs généraux et résultats importants

Le but de ce travail de thèse était de mieux caractériser les mécanismes biotiques et abiotiques qui contrôlent la composition et la diversité des communautés nanoplanctonique lacustre. Ces résultats viennent d'abord renforcer les fondations de notre compréhension de l'effet de la compétition pour la ressource sur la diversité nanoplanctonique (Chapitre I) et sur les assemblages de stratégie d'acquisition des ressources nanoplanctoniques (Chapitre II). J'ai aussi pu brosser un portrait plus clair de la place des taxons phago-mixotrophes dans les lacs Nord-Américains et de la réponse de la prévalence de la mixotrophie aux gradients environnementaux (Chapitre III).

Les résultats présentés dans cette dissertation sont des contributions importantes pour l'étude des communautés nanoplanctoniques. Ils permettent aussi d'envisager de nouvelles directions de recherches pour de futures études sur ce compartiment biotique essentiel au fonctionnement écosystémique des lacs.

4.1.1 L'agrégation verticale des communautés nanoplanctoniques dépend de l'environnement physique; son effet sur la diversité de la communauté est marginal.

Dans le premier chapitre, j'ai montré que la répartition spatiale d'une communauté nanophytoplanctonique, et plus particulièrement la capacité des taxons à se différencier verticalement, peut être perturbée en changeant la structure physique du milieu (abaissement expérimental de la thermocline d'un lac stratifié). Mais contrairement à mes hypothèses initiales, je n'ai pas observé d'effet de l'altération de la structure verticale de cette communauté, et donc théoriquement de l'intensité de la compétition interspécifique, sur la diversité de cette communauté. Je n'ai pas détecté d'effet négatif du degré d'agrégation sur la diversité taxonomique (diversité de Shannon) de la communauté: entraver la capacité des taxons à se ségréger verticalement ne semble donc pas nécessairement entraîner une perte nette d'espèce dans la communauté par exclusion compétitive. Je n'ai pas non plus pu établir de lien entre le degré d'agrégation verticale et la diversité fonctionnelle (dispersion fonctionnelle) de la

communauté, alors que je m'attendais à ce que les taxons se séparent le long des axes de niche pour réduire l'intensité de la compétition et éviter l'exclusion lorsque l'agrégation augmente. Bien que l'agrégation spatiale n'affecte pas la diversité fonctionnelle globale de la communauté nanoplanctonique dans notre système, les résultats indiquent que l'agrégation verticale pourrait avoir des effets contrastés sur la diversité des traits individuels pour l'acquisition des ressources, notamment la capacité à fixer la silice et la stratégie d'acquisition des ressources (mixotrophie vs. autotrophie). L'expérience TIMEX a tout de même permis de comparer les effets relatifs de l'agrégation de la communauté, de la prédation zooplanctonique et de la manipulation de la structure de stratification du lac sur la diversité, révélant ainsi que, dans notre système d'étude, l'effet de la compétition interspécifique est un facteur de contrôle marginal de la diversité par rapport aux interactions de prédations et la structure thermique du milieu. De manière plus générale, l'expérience TIMEX s'est avérée être un cadre expérimental unique pour dresser un portrait des interactions entre l'environnement physique et la communauté nanophytoplanctonique à l'échelle d'un lac entier, à condition d'utiliser des modèles statistiques adaptés pour démêler les relations causales entre les différents compartiments de l'écosystème.

4.1.2 La phago-mixotrophie est une stratégie de nutrition viable face à des compétiteurs spécialisés pour une variété de conditions de disponibilité des ressources.

Comme le montrent les résultats du modèle mathématique proposé dans le Chapitre II, la phago-mixotrophie est une stratégie généraliste théoriquement viable face à des compétiteurs spécialisés dans un contexte de compétition pour la ressource dans un système spatialement hétérogène. Un mixotrophe peut dominer la communauté et même exclure des compétiteurs spécialisés lorsque la disponibilité des nutriments est faible et la lumière est relativement abondante. Le succès du généraliste est intimement lié à sa stratégie mixotrophique, c.a.d. son équilibre fonctionnel entre phototrophie et phagotrophie, et il est possible d'identifier une stratégie mixotrophique optimale pour la plupart des conditions environnementales de disponibilité des ressources testées. Le modèle indique aussi que dans un milieu oligotrophe clair, la productivité de notre communauté nanoplanctonique théorique est théoriquement supérieure à celle d'une communauté composée uniquement de compétiteurs spécialisés, indiquant que la diversité des stratégies trophiques pourrait être un paramètre clé du fonctionnement de ces écosystèmes. Un facteur expliquant le succès de la mixotrophie pourrait être la capacité des compétiteurs mixotrophes à croître sur une

plus grande portion de la colonne d'eau comparée aux spécialistes. Finalement, le modèle montre aussi que la structuration verticale d'une communauté nanoplanctonique, souvent observée dans les lacs stratifiés, peut être induite via les interactions de compétition entre différentes stratégies d'acquisition des ressources si les gradients de ressources (lumière et nutriments) verticaux sont définis et distincts. Cette approche de modélisation spatialisée de la compétition pour les ressources vient ainsi combler un vide dans le corpus des modèles théoriques de la mixotrophie nanoplanctonique.

4.1.3 La mixotrophie est omniprésente dans les lacs d'Amérique du Nord; sa prévalence dans les communautés nanophytoplanctonique varie avec la disponibilité des nutriments.

L'analyse des données combinées des campagnes d'échantillonnage NLA et LakePulse (Chapitre III) montre que l'on trouve des taxons mixotrophes dans la grande majorité des lacs d'Amérique du Nord. La biogéographie des mixotrophes est cependant contrastée: la contribution des phago-mixotrophes à la communauté nanophytoplanctonique, et plus spécifiquement la contribution des chrysophytes et des dinophytes, est généralement plus élevée dans des lacs situés dans les écorégions moins anthropisées. Au contraire, la prévalence de la mixotrophie est relativement faible dans les lacs situés dans l'écorégion des *Great Plains* où les bassins versants comportent généralement une activité agricole importante. Dans cette écorégion, les lacs sont plus autotrophes et les cryptophytes sont les taxons mixotrophes dominants. Je m'attendais à ce que la disponibilité des ressources (lumière et nutriments) dans le milieu soit la principale variable environnementale structurant les assemblages de stratégies de nutrition nanoplanctoniques lacustres. Cette hypothèse a pu être partiellement confirmée: les analyses ont révélé que dans les lacs d'Amérique du Nord, la concentration en phosphore totale (TP) est le principal prédicteur environnemental de la phago-mixotrophie: la prévalence de la mixotrophie diminue à mesure que la quantité de phosphore augmente. Le niveau trophique des lacs contrôle également l'assemblage des communautés mixotrophes et leur diversité taxonomique. En revanche, aucun effet de la disponibilité de la lumière sur les assemblages trophiques et la prévalence de la mixotrophie n'a été détecté, bien qu'elle exerce une influence sur la composition de la communauté mixotrophe. La chimie de l'eau et l'abondance du zooplancton sont aussi des paramètres environnementaux déterminant pour les assemblages de stratégies nanoplanctoniques, mais à un degré moindre que la disponibilité des nutriments.

4.2 Perspectives

4.2.1 Explorer la structure verticale des communautés nanoplanctoniques

L'expérience TIMEX (Chapitre I) n'a pas permis de montrer un effet de l'agrégation spatiale sur la diversité de la communauté nanoplanctonique, mais cette étude offre des perspectives intéressantes sur le lien entre la structure verticale et la composition fonctionnelle de la communauté, un champ d'études négligé car difficile à explorer. Il aurait par exemple été intéressant de voir si la distribution des traits individuels (comme la phago-mixotrophie) est spatialisée, i.e., si les différentes modalités d'un trait sont favorisées à des profondeurs différentes. Évidemment, cette perspective de recherche se heurte aux difficultés inhérentes à l'étude de la structure spatiale du nanoplancton, en particulier l'effort d'échantillonnage requis pour capturer cette caractéristique des communautés nanoplanctoniques. Dans le Chapitre I, les profils verticaux d'abondances des pigments obtenus grâce aux mesures du Fluoroprobe ont permis d'approximer les niveaux d'agrégation globale de la communauté, mais l'estimation de la composition de la communauté obtenue par cette méthode reste grossière en termes de résolution taxonomique. Comme je l'ai montré dans ce travail de doctorat, les approches de modélisation sont particulièrement adaptées pour étudier la structure verticale de la communauté nanoplanctonique. Le modèle présenté dans le Chapitre II de cette thèse offre des résultats sur l'organisation verticale des communautés nanoplanctoniques avec un degré de précision spatiale très fin: il serait difficilement envisageable d'obtenir des mesures à une telle résolution pour un vrai lac, du fait des contraintes logistiques pour la collecte et le traitement (identification microscopique) des échantillons. Pour des études biogéographiques à grande échelle comme celle conduite sur les données NLA et LakePulse, obtenir des données de composition de la communauté nanoplanctonique avec une résolution verticale fine n'est probablement pas envisageable, en tout cas pas avec les méthodes d'identification taxonomiques traditionnelles. À défaut de pouvoir capturer la structure verticale de la communauté dans le cadre de ces campagnes d'échantillonnage, il serait pertinent de reconsidérer les méthodes de collecte des données pour mieux capturer le compartiment nanoplanctonique dans ces systèmes. Bien que les enquêtes à grande échelle sur les lacs soient une source d'information inestimable pour étudier les assemblages trophiques des communautés sur de grands gradients environnementaux, les études futures sur la mixotrophie nanoplanctonique devraient adapter leur méthodologie pour capturer

cette dimension verticale de la communauté de manière plus adéquate. Il est impératif de collecter des échantillons d'eau intégrés sur l'ensemble de la colonne, en plus de ceux collectés dans la zone photique, pour évaluer plus précisément la prévalence de la mixotrophie dans les écosystèmes naturels.

4.2.2 Explorer la physiologie des mixotrophes

Comme discuté précédemment, les modèles théoriques permettent d'explorer des hypothèses difficiles ou impossibles à explorer avec des données de terrain ou acquises en laboratoire. Il est néanmoins important, quand cela est possible, de comparer et confirmer les résultats obtenus *in silico* avec des mesures prises sur le terrain. Par exemple, j'ai montré grâce au modèle présenté dans le Chapitre II que, théoriquement, les assemblages de stratégies de nutrition nanoplanctoniques sont très dépendants des conditions environnementales de disponibilité des ressources (lumière, nutriments et bactéries). En particulier, le modèle permet d'identifier une stratégie mixotrophe dominante par rapport aux spécialistes lorsque la disponibilité des nutriments est relativement faible (et si la disponibilité de la lumière ne descend pas en dessous d'un certain seuil). Cette règle d'assemblage est confirmée par les patrons d'assemblages des stratégies de nutrition nanophytoplanctoniques dans les lacs d'Amérique du Nord présentés dans le Chapitre III. J'ai identifié la disponibilité des nutriments comme étant le principal facteur environnemental qui contrôle la prévalence de la mixotrophie dans les eaux de surfaces des lacs: la contribution des mixotrophes à la communauté nanophytoplanctonique est plus élevée dans les lacs oligotrophes. En revanche, ces mêmes données n'ont pas permis de confirmer que les assemblages de stratégies de nutrition répondent aussi à la disponibilité de la lumière, comme le montre le modèle. Cette absence d'effet de la lumière dans nos résultats illustre les limites de l'approche utilisée dans le Chapitre III: seul le potentiel de mixotrophie a été considéré, plutôt que les taux réels de bactérivorie des différents taxons mixotrophes. Des mesures de la contribution de la phagotrophie aux taux de croissance mixotrophes auraient permis de nouvelles analyses et auraient pu potentiellement expliquer les variations observées dans la composition taxonomique de la communauté mixotrophe à travers les gradients environnementaux, en particulier la disponibilité de la lumière. Comme je l'ai relevé à plusieurs reprises, l'évaluation de la physiologie précise des taxons mixotrophes est difficile et aurait nécessité des expériences approfondies pour chaque communauté échantillonnée (Beisner *et al.*, 2019), un projet difficile à

concevoir pour l'ensemble des lacs échantillonnés à travers les campagnes NLA et LakePulse. La confirmation des patrons d'assemblage théoriques obtenus grâce au modèle n'est probablement pas envisageable avec des données de campagne d'échantillonnage classiques et ne serait possible que par la mise en œuvre d'expériences d'ingestion bactériennes poussées en milieu contrôlé (microcosme). Il serait cependant utile de réaliser une telle étude expérimentale pour compléter les résultats de modélisation et d'observation de terrain présentés ici, et notre modèle pourrait guider la mise en œuvre d'une telle étude. De manière générale, mieux caractériser la place des taxons phago-mixotrophiques le long du gradient de stratégies mixotrophes est nécessaire pour les futures études des communautés nanoplanctoniques (Jones, 2000).

4.2.3 Prise en compte du compartiment bactérien dans les approches théoriques et dans les mesures de terrain

Comme le montrent nos résultats de modélisation, les interactions de compétition entre les diverses stratégies de nutrition nanoplanctoniques et leurs ressources sont complexes. En particulier, les relations avec le compartiment bactérien valent la peine d'être considérées: dans le système théorique présenté dans le Chapitre II, le phototrophe spécialisé est en compétition avec les bactéries pour les nutriments, et peut être exclu du système en l'absence des compétiteurs phagotrophes. Le modèle pourrait être complexifié pour mieux prendre en compte cette dynamique du compartiment bactérien. En particulier, j'ai choisi de ne pas considérer de limitation en carbone pour les bactéries pour ne pas complexifier excessivement le système, une hypothèse raisonnable dans le contexte d'une étude qui se concentre sur la réponse de l'assemblage des trois stratégies nanoplanctoniques à la disponibilité en lumière et en nutriments. Il serait envisageable d'ajouter des variables d'état supplémentaires pour les composés carbonés assimilables par les bactéries (Thingstad et Lignell, 1997). Cela permettrait aussi de caractériser la disponibilité en lumière d'une manière plus dynamique: la concentration de composés carbonés analogues au COD pourrait être prise en compte dans le calcul de l'atténuation de la lumière dans la colonne d'eau, permettant ainsi de simuler le brunissement du système et son effet sur la dynamique de la communauté nanoplanctonique (Wilken *et al.*, 2018).

De même, il est crucial de faire le lien entre les assemblages nanoplanctoniques et le compartiment bactérien dans les études de terrains, ce que j'ai été partiellement en mesure de

faire ici. Dans leur étude de 69 lacs situés au Québec, Hansson *et al.* (2019) n'ont pas identifié l'abondance bactérienne comme un prédicteur de la prévalence de la mixotrophie mais il était important de tester cette relation à une échelle géographique plus large. Pour notre étude présentée dans le Chapitre III, de telles mesures n'étaient pas disponibles pour les lacs de la campagne NLA. Des mesures d'abondances bactériennes étaient disponibles pour les lacs LakePulse, et cette variable n'a pas été identifiée comme un prédicteur important de la mixotrophie dans les lacs canadiens. Ces données n'ont en revanche pas permis d'examiner un éventuel effet de la composition de la communauté bactérienne sur les assemblages de stratégies de nutrition nanophytoplanctoniques. Estimer l'abondance bactérienne et caractériser la composition de la communauté bactérienne à partir d'échantillons collectés sur le terrain nécessite des méthodes de laboratoire poussées (cytométrie de flux, génomique environnementale…), mais est un préalable nécessaire pour améliorer notre compréhension des facteurs environnementaux qui contrôle la prévalence de la phago-mixotrophie et la composition des assemblages nanoplanctoniques.

ANNEXE A

Vertical profiles of total phosphorus (TP) in the TIMEX experiment (CHAPITRE 1)

Annexe A. Vertical profiles of total phosphorus (TP) concentrations in 2009, 2010 and 2011 in each of the three basins. The solid line is the mean TP concentration over depth. The dotted lines are the limits of the 95% confidence interval around the value mean TP concentration over depth.

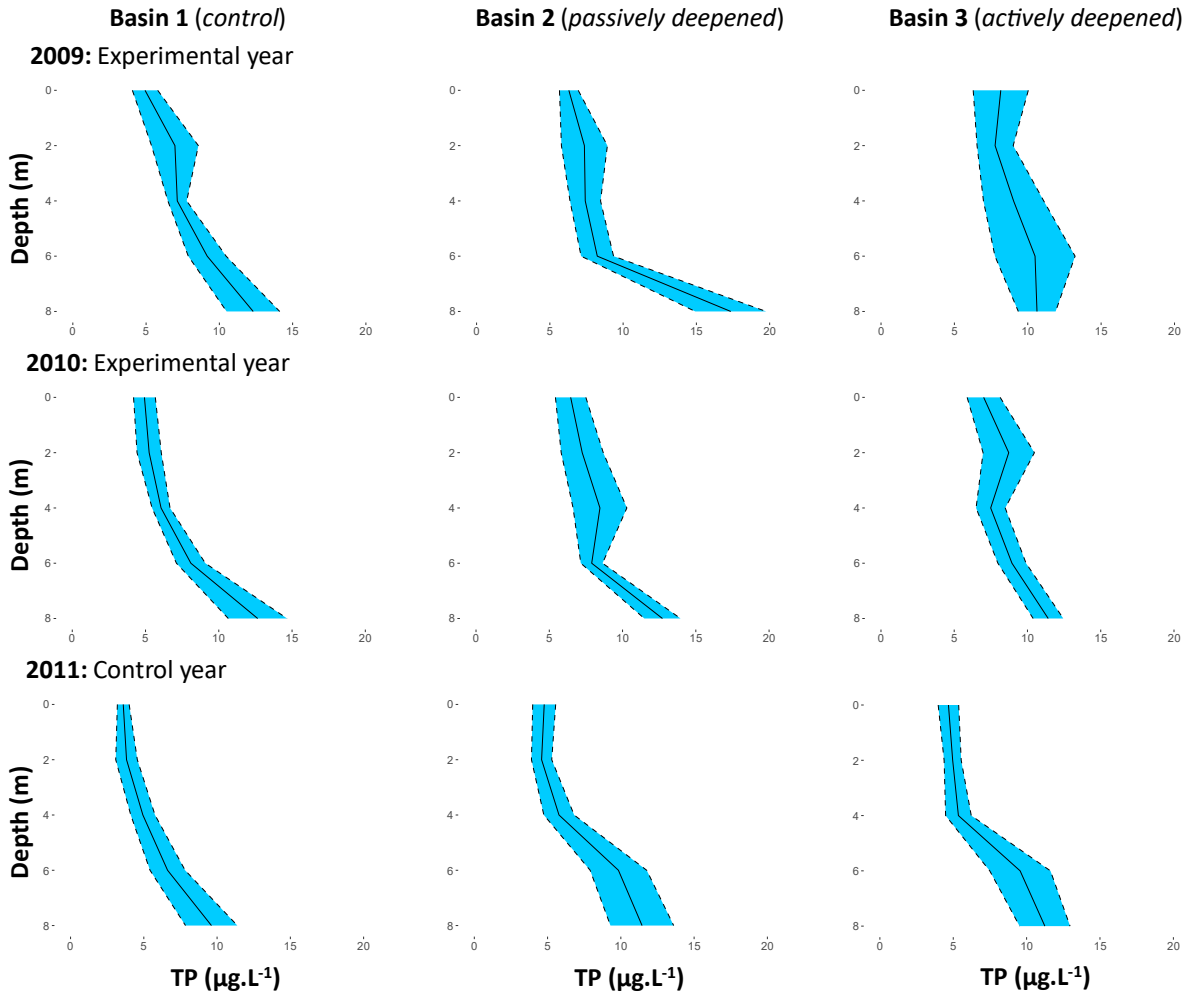

ANNEXE B

Bootstrapped linear regressions of the metalimnetic width and Spatial Overlap over the prevalence of cyanobacteria (a) and the prevalence mixotrophy (b) respectively (CHAPITRE 1)

Annexe B. Bootstrapped linear regressions (10000 iterations) of the metalimnetic width ($Meta_{Width}$) and Spatial Overlap (*SO*) over the prevalence of cyanobacteria (a) and the prevalence mixotrophy (b) respectively, with the 95% confidence interval around the slope in grey. We define the prevalence of cyanobacteria (and the prevalence of mixotrophy) as the percentage of the total community biomass belonging to cyanobacterial (and mixotrophic) taxa. The bootstrapped regressions were performed using functions from the R package *boot* (Canty et Ripley, 2021).

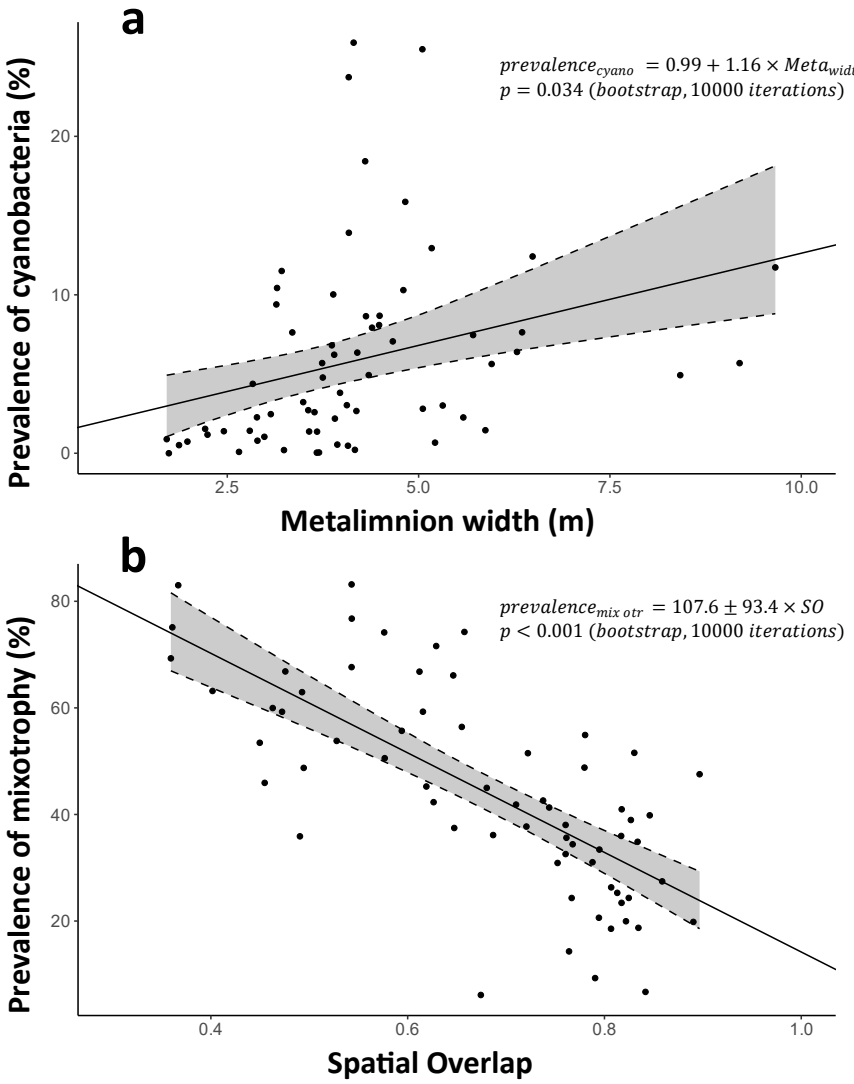

ANNEXE C

Functional trait matrix for the nanophytoplankton taxa identified in the TIMEX experiement (CHAPITRE 1)

Annexe C. Functional trait matrix used to compute the functional diversity of the nanophytoplankton community in the TIMEX experiment

Taxa	Groupe	Coloniality	Nitrogen fixation	Silicium fixation	Mixotrophy	Pigment	Maximum Linear Dimension (MLD)
Achnanthidium	DIATOM	n	n	y	n	Brown	9
Actinella	DIATOM	n	n	y	n	Brown	75
Aphanothece	CYANO	y	n	n	n	BlueGreen	2.625
Asterionella	DIATOM	y	n	y	n	Brown	82
Aulacoseira	DIATOM	y	n	y	n	Brown	123.1852
Bitrichia	CHRYSO	n	n	n	n	Brown	12
Botryococcus	GREENS	y	n	n	n	Green	21.06544
Chlamydomonas	GREENS	n	n	n	n	Green	9.166667
Chromulina	CHRYSO	n	n	n	y	Brown	6.666667
Chroococcus	CYANO	y	n	n	n	BlueGreen	7.3125
Chroomonas	CRYPTO	n	n	n	y	Red	10.25
Chrysidiastrum	CHRYSO	y	n	n	y	Brown	9.8
Chrysochromulina	CRYPTO	n	n	n	y	Brown	7.625
Chrysolykos	CHRYSO	n	n	n	y	Brown	3.875
Chrysophyte	CHRYSO	n	n	n	y	Brown	4.66627
Chrysosphaerella	CHRYSO	y	n	y	y	Brown	7
Chrysostephanosphaera	CHRYSO	y	n	n	y	Brown	9
Closterium	GREENS	n	n	n	n	Green	150
Coccomyxa	GREENS	y	n	n	n	Green	6
Coelastrum	GREENS	y	n	n	n	Green	8
Cosmarium	GREENS	n	n	n	n	Green	40.66667
Cryptaulax	CRYPTO	n	n	n	n	Red	5.886905
Cryptomonas	CRYPTO	n	n	n	y	Red	25.54545
Cyclotella	DIATOM	n	n	y	n	Brown	14.5
Cymbella	DIATOM	n	n	y	n	Brown	34.75
Dictyosphaerium	GREENS	y	n	n	n	Green	5.5
Dimorphococcus	GREENS	y	n	n	n	Green	14
Dinobryon	CHRYSO	y	n	n	y	Brown	10.66667
Dolichospermum	CYANO	y	y	n	n	BlueGreen	100

Elakatothrix	GREENS	y	n	n	n	Green	13
Ellipsoidion	TRIBOPHYCEAE	n	n	n	n	YellowG	11.5
Epipyxis	CHRYSO	n	n	n	y	Brown	6.692177
Euastrum	GREENS	n	n	n	n	Green	30.25
Euglena	EUGLENO	n	n	n	n	Green	29.71429
Eunotia	DIATOM	n	n	y	n	Brown	40
Fragilaria	DIATOM	y	n	y	n	Brown	14
Frustulia	DIATOM	y	n	y	n	Brown	52.48214
Gloeotila	GREENS	y	n	n	n	Green	10
Gomphonema	DIATOM	y	n	y	n	Brown	18
Gonatozygon	GREENS	y	n	n	n	Green	130.49
Gymnodinium	DINO	n	n	n	y	Brown	25.875
Gyromitus	GREENS	n	n	n	n	Green	10
Isthmochloron	TRIBOPHYCEAE	n	n	n	n	YellowG	7
Kephyrion	CHRYSO	n	n	n	y	Brown	7
Kirchneriella	GREENS	y	n	n	n	Green	5
Limnothrix	CYANO	y	n	n	n	BlueGreen	100
Mallomonas	CHRYSO	n	n	y	n	Brown	21.21429
Merismopedia	CYANO	y	n	n	n	BlueGreen	2.4
Monomastix	GREENS	n	n	n	n	Green	18
Monoraphidium	GREENS	n	n	n	n	Green	7.166667
Mougeotia	GREENS	y	n	n	n	Green	131.03
Navicula	DIATOM	n	n	y	n	Brown	20
Neidium	DIATOM	n	n	y	n	Brown	90
Nephrocytium	GREENS	y	n	n	n	Green	11
Nitzschia	DIATOM	n	n	y	n	Brown	62.7475
Oedogonium	GREENS	y	n	n	n	Green	10.5
Oocystis	GREENS	y	n	n	n	Green	12
Pediastrum	GREENS	y	n	n	n	Green	9.6
Pedinomonas	GREENS	n	n	n	n	Green	2.724206
Peridiniopsis	DINO	n	n	n	y	Brown	25.71429
Peridinium	DINO	n	n	n	y	Brown	35
Phacus	EUGLENO	n	n	n	n	Green	20
Pinnularia	DIATOM	n	n	y	n	Brown	92
Planctonema	GREENS	y	n	n	n	Green	6.666667
Planktolyngbya	CYANO	y	n	n	n	BlueGreen	92.7
Planktothrix	CYANO	y	n	n	n	BlueGreen	134.44
Pseudanabaena	CYANO	y	y	n	n	BlueGreen	100
Pseudokephyrion	CHRYSO	n	n	n	y	Brown	3.666667
Quadrigula	GREENS	y	n	n	n	Green	22
Radiocystis	CYANO	y	n	n	n	BlueGreen	2.5

Rhabdoderma	CYANO	y	n	n	n	BlueGreen	8.621032
Rhizochrysis	CHRYSO	n	n	n	y	Brown	5.319643
Rhodomonas	CRYPTO	n	n	n	y	Red	13.33333
Scenedesmus	GREENS	y	n	n	n	Green	8.142857
Scourfieldia	GREENS	n	n	n	n	Green	7
Sphaerocystis	GREENS	y	n	n	n	Green	3.659971
Spiniferomonas	CHRYSO	n	n	y	n	Brown	5.480556
Spondylosium	GREENS	y	n	n	n	Green	12
Staurastrum	GREENS	n	n	n	n	Green	23.38889
Staurodesmus	GREENS	n	n	n	n	Green	16.17222
Staurosirella	DIATOM	y	n	y	n	Brown	10
Stenopterobia	DIATOM	n	n	y	n	Brown	150.8
Surirella	DIATOM	n	n	y	n	Brown	18
Synedra	DIATOM	y	n	y	n	Brown	77.75
Synura	CHRYSO	y	n	y	n	Brown	15
Tabellaria	DIATOM	y	n	y	n	Brown	48
Tetrastrum	GREENS	y	n	n	n	Green	5
Trachelomonas	EUGLENO	n	n	n	n	Green	22.5
Uroglena	CHRYSO	y	n	n	y	Brown	9
Urosolenia	DIATOM	n	n	y	n	Brown	31.99229
Woronichinia	CYANO	y	n	n	n	BlueGreen	15.42857

ANNEXE D

Mean total over the water column and proportion of incident light intensity at mid-depth over the Rin × kbg parameter space (CHAPITRE 2)

Annexe D. Mean total phosphorus (q_AA + q_MM + q_HH + q_BB + R) over the water column (a) and proportion of incident light intensity at mid-depth $z = \frac{z_{max}}{2} = 5m$ (b) over the R_{in} × k_{bg} parameter space ($\alpha = 0.5$).

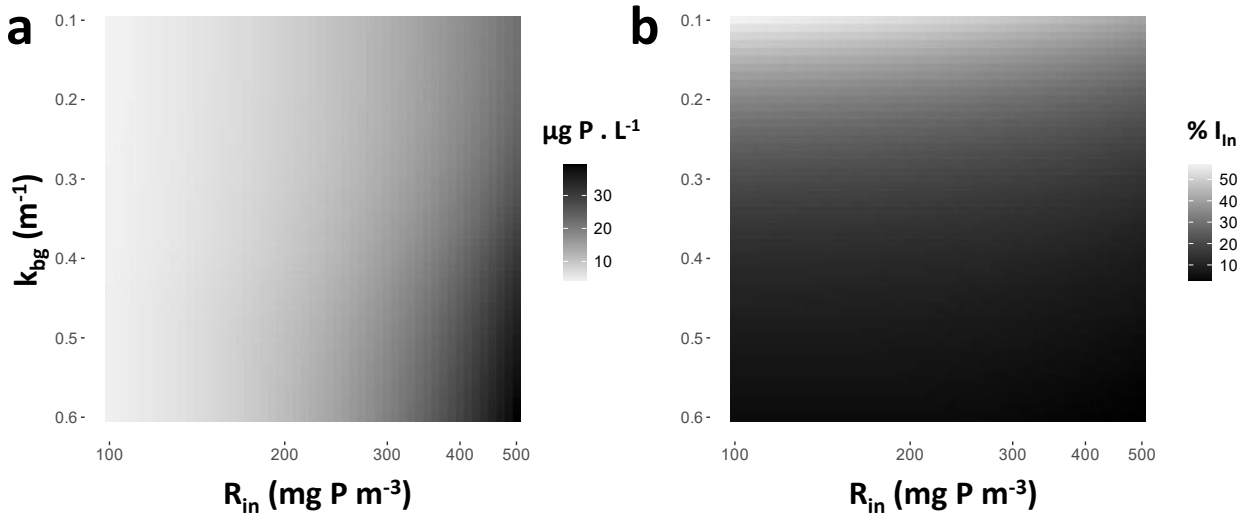

ANNEXE E

Depth of the upper and lower limits of the Competitor Favorable Range (CFR) of the three competitors (CHAPITRE 2)

Annexe E. Depth of the upper (solid lines) and lower (dashed lines) limits of the *Competitor Favorable Range* (CFR) of the photo-autotrophic (A, yellow), mixotrophic (M, green) and phago-heterotrophic (H, purple) competitors. The panels correspond to distinct conditions of nutrients and light availability (i.e., different combination of R_{in} and k_{bg} values for the simulations). The three leftward panels correspond to conditions of relatively high nutrient availability (high R_{in} value) and the three rightward panels to relatively low nutrient availability (low R_{in} value). Light availability decreases from top to bottom (low to high k_{bg} value). For each combination of R_{in} and k_{bg} values, we simulated over a range of α values (x axis) starting from $\alpha = 0$, incrementally increasing the value of the parameter to the limit of $\alpha = 1$. When a given competitor was excluded from the community at the end of the simulations, we did not compute its CFR size, hence the fact that portions of the lines for CFR spatial limits are missing for some combinations of conditions of resource availability and α values.

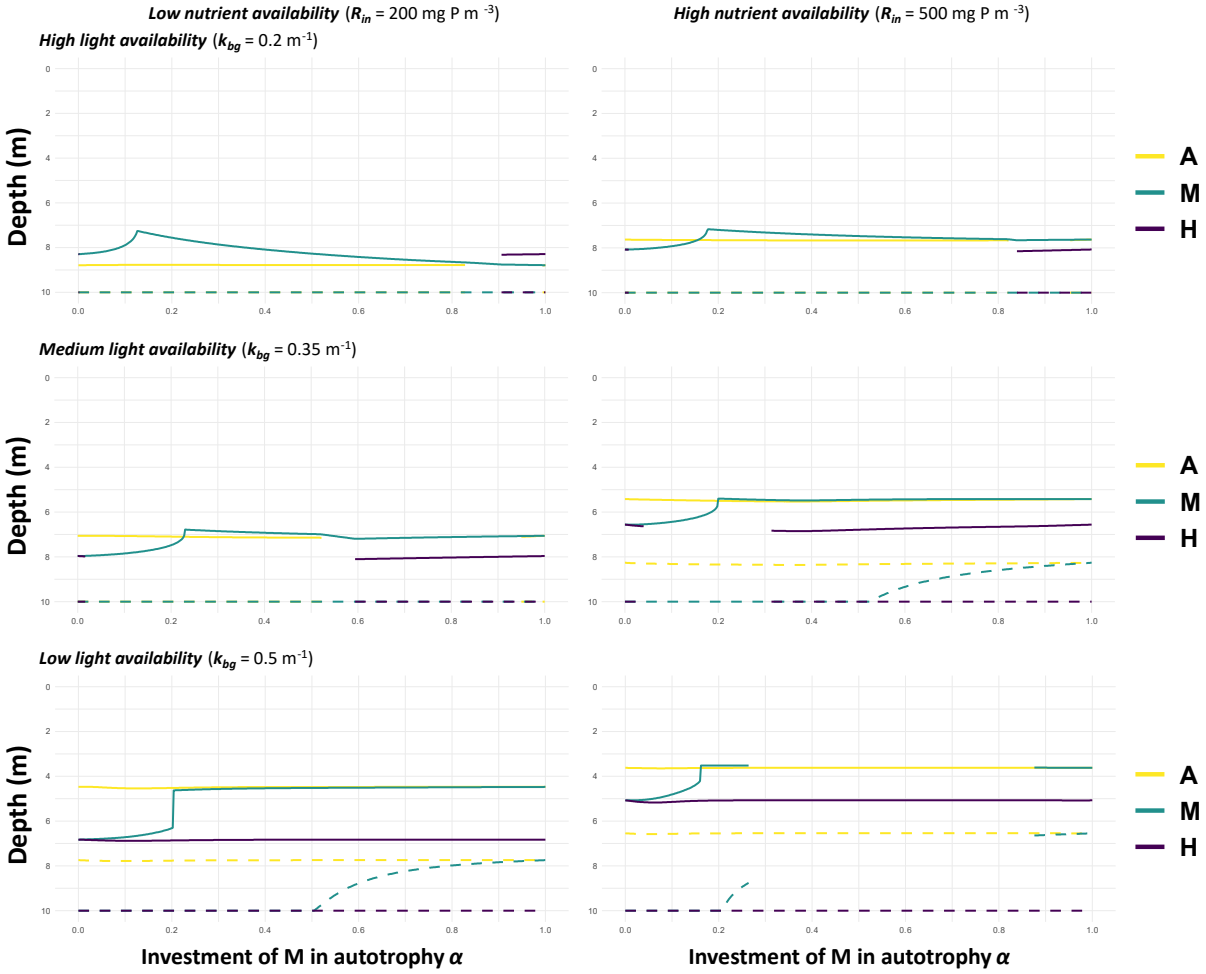

ANNEXE F

Contributions of the system variables to the total nutrient pool for different versions of the model (CHAPITRE 2)

Annexe F. Contributions of the photo-autotroph (A; yellow, first row), mixotroph (M; green, second row), phago-heterotroph (H; purple, third row), bacteria (B; red, fourth row) and dissolved nutrient (R; grey, fifth row) to the total phosphorus concentration in the system as a percentage of the total nutrient stock (q_AA + q_MM + q_HH + q_BB + R) integrated over the entire depth of the water column. The y-axes (k_{bg}) are reversed, so that the zone of low resource availability (low R_{in} and high k_{bg}) in the parameter space corresponds to the bottom-left corner of each panel. Values on the x-axis (R_{in}) values are on a log-scale. Each column corresponds to a different version of the model where one, two or three nanoplankton competitors were sequentially removed from the system, starting with the full model on the left progressing to a model with no nanoplanktonic competitor on the most right. Empty panels correspond to model variables that were removed. The investment of the mixotroph in phototrophy α was fixed at the intermediate value (α = 0.5). The black isolines delimitate the results in intervals of 10%.

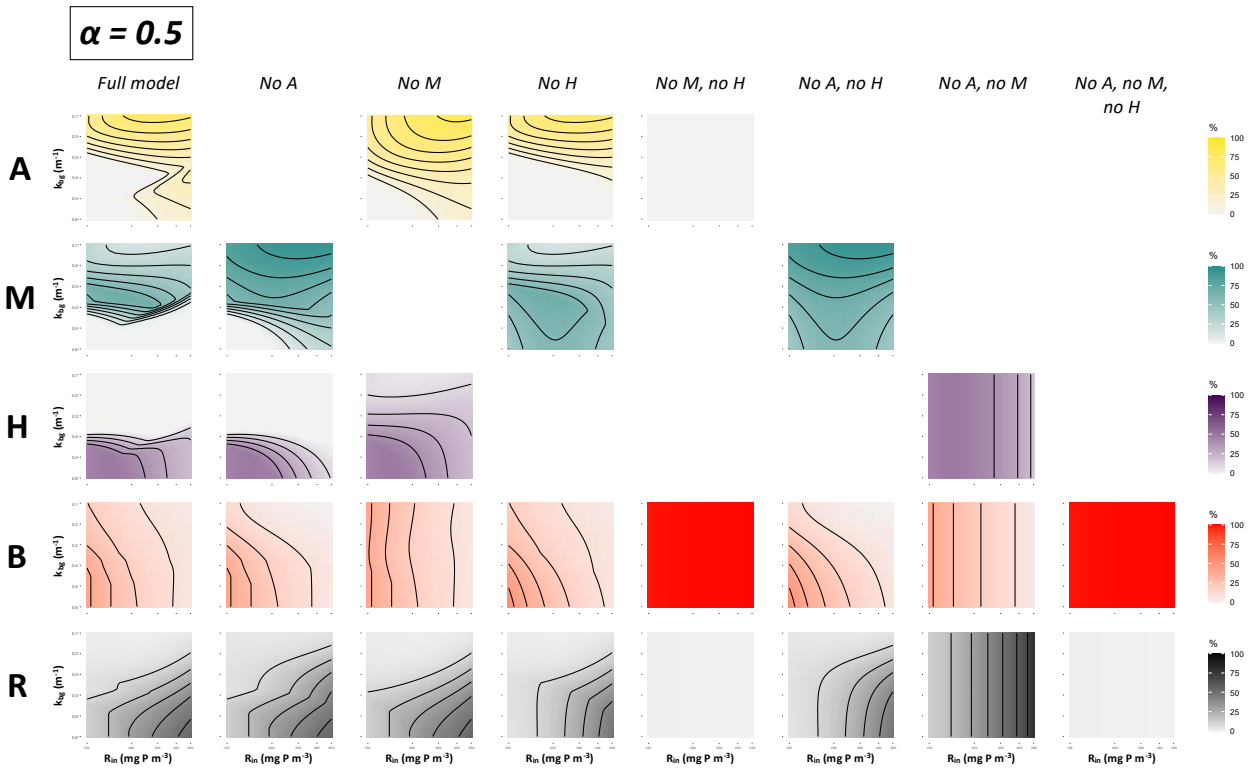

ANNEXE G

Effect of M on bacterial and nutrient availability (CHAPITRE 2)

Annexe G. Effect of M on bacterial (a) and nutrient (b) availability over the $R_{in} \times k_{bg}$ parameter space. The first two rows of each section are the contributions of the mixotroph biomass and that of its direct specialist competitors for the target resource to the combined biomass of these two competitors (M + H for section a; M + A for section b). The third row of each section is the raw abundances of the resource (B for section a, R for section b). The fourth row is the resource abundance differential (B for section a, R for section b) between the full and the specialist (no M) models relative to the abundance yielded in the specialist model. All effects are integrated over the entire depth of the water column. Results are shown for three values of the mixotrophic investment in photo-autotrophy α: a low investment ($\alpha = 0.1$; first column), a balanced investment ($\alpha = 0.5$; second column) and a high investment ($\alpha = 0.9$; third column). The black isolines delimitate the results in intervals of 10% of the maximal value of the response variable.

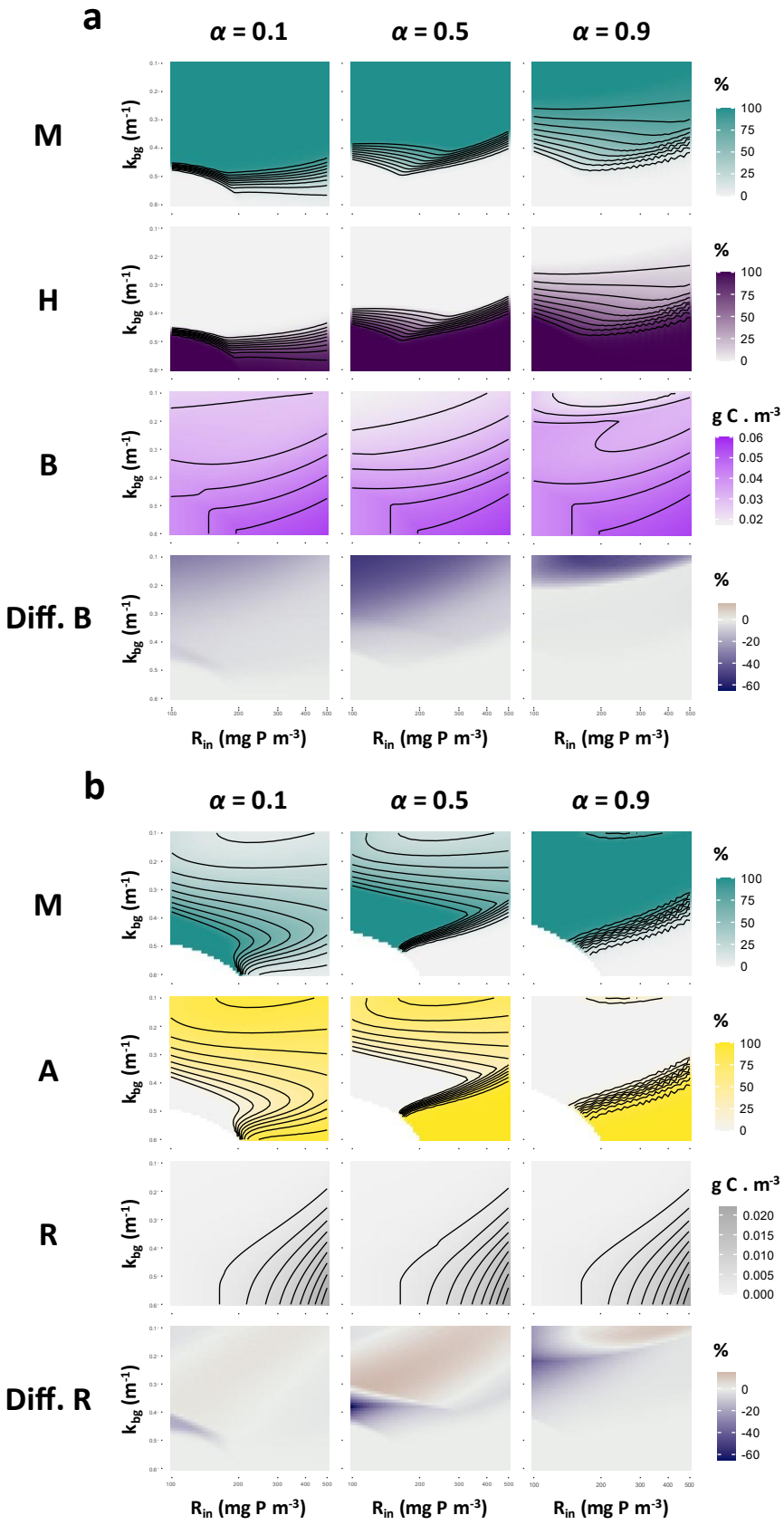
a
α = 0.1
α = 0.5
α = 0.9
M
H
B
Diff. B
k_bg (m^-1)
R_in (mg P m^-3)
%
100
75
50
25
0
g C . m^-3
0.06
0.05
0.04
0.03
0.02
-20
-40
-60
b
A
R
0.020
0.015
0.010
0.005
0.000
Diff. R

ANNEXE H

Full equations for the competition model (CHAPITRE 2)

Annexe H. Complete equations for the different state variables featured in the model.

Pure autotroph A:

$$\frac{\partial A}{\partial t} = min\left[p_A \frac{I_z}{I_z + H_A};\ p_A \frac{R}{R + S_{RA}}\right] A - l_A A + D_A \frac{\partial^2 A}{\partial z^2}$$

Mixotroph M:

$$\frac{\partial M}{\partial t} = min\left[\alpha p_M \frac{I_z}{I_z + H_M} + c_{BM}(1-\alpha) J_{BM} \frac{B^2}{B^2 + S_{BM}^2};\ \alpha p_M \frac{R}{R + S_{RM}} + \frac{q_B}{q_M}(1-\alpha) J_{BM} \frac{B^2}{B^2 + S_{BM}^2}\right] M - l_M M + D \frac{\partial^2 M}{\partial z^2}$$

Pure heterotroph H:

$$\frac{\partial H}{\partial t} = \left(c_{BH} J_{BH} \frac{B^2}{B^2 + S_{BH}^2}\right) H - l_H H + D \frac{\partial^2 H}{\partial z^2}$$

Bacteria B:

$$\frac{\partial B}{\partial t} = \left(\frac{J_{RB}}{q_B} \frac{R}{R + S_{RB}}\right) B - l_B B - (1-\alpha) J_{BM} \frac{B^2}{B^2 + S_{BM}^2} M - J_{BH} \frac{B^2}{B^2 + S_{BH}^2} H + D \frac{\partial^2 B}{\partial z^2}$$

Mineral nutrient R:

$$\frac{\partial R}{\partial t} = -min\left[p_A \frac{I_z}{I_z + S_{IA}};\ p_A \frac{R}{R + S_{RA}}\right] q_A A$$
$$- min\left[\alpha p_M \frac{I_z}{I_z + S_{IM}} + (1-\alpha)(c_{BM} - \frac{q_B}{q_M}) J_{BM} \frac{B^2}{B^2 + S_{BM}^2};\ \alpha p_M \frac{R}{R + S_{RM}}\right] q_M M$$
$$- \left((c_{BH} - \frac{q_B}{q_H}) J_{BH} \frac{B^2}{B^2 + S_{BH}^2}\right) q_H H - \left(J_{RB} \frac{R}{R + S_{RB}}\right) B + D \frac{\partial^2 R}{\partial z^2}$$

Light I:

$$I(t,z) = I_{in} e^{-\int_0^z [k_A A(t,z) + \alpha k_M M(t,z) + k_{bg}] dz}$$

No-flux boundary conditions for any given state variable X:

$$\left.\frac{\partial X}{\partial z}\right|_{z=0} = \left.\frac{\partial X}{\partial z}\right|_{z=z_{max}} = 0$$

The exception is the lower boundary conditions for R at the sediment depth z_{max} (i.e., the point of entry of the mineral nutrient in the system):

$$\left.\frac{\partial R}{\partial z}\right|_{z=z_{max}} = h(R_{in} - R(t, z_{max}))$$

Since $c_{BH} - \frac{q_B}{q_H} < 0$, H is always a net excretor of R at a rate $\left((c_{BH} - \frac{q_B}{q_H}) J_{BH} \frac{B^2}{B^2 + S_{BH}^2}\right) q_H H$.

R uptake by M is equal to:

$$min\left[\alpha p_M \frac{I_z}{I_z + S_{IM}} + (1-\alpha)(c_{BM} - \frac{q_B}{q_M}) J_{BM} \frac{B^2}{B^2 + S_{BM}^2};\ \alpha p_M \frac{R}{R + S_{RM}}\right] q_M M$$

R uptake by M can thus take a negative value depending on resource availability conditions and the strategy of M (i.e., the value of α), especially when the nutrition mode of M tends toward pure heterotrophy (i.e., when α tends toward 0). In that case, M is a net excretor of R.

ANNEXE I

Full parameter table for the competition model (CHAPITRE 2)

Annexe I. Definition, units, values and references for the model parameters.

Parameter	Definition	Units	Value	Reference
t	Time	d		
z	Depth	m		
A	Biomass of the autotroph	g C . m^{-3}		
M	Biomass of the mixotroph	g C . m^{-3}		
H	Biomass of the heterotroph	g C . m^{-3}		
I	Photosynthetically active radiation	µmol photons m^{-2} s^{-1}		
R	Mineral nutrient concentration	g P . m^{-3}		
B	Biomass of bacteria	g C . m^{-3}		
R_{in}	Concentration of mineral nutrient in influx	mg P . m^{-3}	100-500	
k_{bg}	Light attenuation coefficient of clear water	m^2 g . C^{-1}	0.1-0.6	
α	Mixotrophic investment in autotrophy (i.e., effort spent by M on photosynthesis and mineral nutrient uptake)	dimensionless	0-1	
z_{max}	Depth of the water column	m	10	
k_A	Light attenuation coefficient of autotroph	m^2 g . C^{-1}	0.3	Vasconcelos *et al.* 2019
k_M	Light attenuation coefficient of mixotroph	m^2 g . C^{-1}	0.3	Vasconcelos *et al.* 2019 (same as the autotroph)

p_A	Maximum light- and mineral nutrient-dependent growth rate of A	d^{-1}	1.5	Vasconcelos *et al.* 2019
p_M	Maximum light- and mineral nutrient-dependent growth rate of M	d^{-1}	1.5	Vasconcelos *et al.* 2019 (same as the autotroph)
J_{BM}	Maximum ingestion rate of B by M	d^{-1}	3	Same as for the heterotroph
J_{BH}	Maximum ingestion rate of B by H	d^{-1}	3	Menon *et al.* 1996
J_{RB}	Maximum uptake rate of R by B	g P . g C^{-1} . d^{-1}	0.085	Yields a net maximal bacterial growth rate $\left(\frac{J_{RB}}{q_B} - l_B\right)$ is equal to 1.6 (Jansson *et al.*, 2006; Šimek *et al.*, 2006)
H_A	Half-saturation constant of light-dependent growth of A	µmol photons . m^{-2} . s^{-1}	80	Vasconcelos *et al.* 2019
H_M	Half-saturation constant of light-dependent growth of M	µmol photons . m^{-2} . s^{-1}	80	Vasconcelos *et al.* 2019 (same as the autotroph)
S_{RA}	Half-saturation constant of nutrient-dependent growth of A	g P . m^{-3}	0.003	Vasconcelos *et al.* 2019
S_{RM}	Half-saturation constant of nutrient-dependent growth of M	g P . m^{-3}	0.003	Vasconcelos *et al.* 2019 (same as the autotroph)
S_{RB}	Half-saturation constant of nutrient uptake by B	g P . m^{-3}	0.0018	Šimek *et al.* 2006
S_{BM}	Half-saturation constant of bacterial consumption by M	g C . m^{-3}	0.25	Menon *et al.* 1996

				(same as the heterotroph)
S_{BH}	Half-saturation constant of bacterial consumption by H	g C . m^{-3}	0.25	Menon *et al.* 1996
q_A	Nutrient to carbon quota of A	g P . g C^{-1}	0.025	Vasconcelos *et al.* 2019 (same for the three plankton competitors)
q_M	Nutrient to carbon quota of M	g P . g C^{-1}	0.025	Vasconcelos *et al.* 2019 (same for the three plankton competitors)
q_H	Nutrient to carbon quota of H	g P . g C^{-1}	0.025	Vasconcelos *et al.* 2019 (same for the three plankton competitors)
q_B	Nutrient to carbon quota of B	g P . g C^{-1}	0.05	Vrede 1998
c_{BM}	Carbon conversion efficiency of M (feeding on B)	dimensionless	0.5	Same as the heterotroph.
c_{BH}	Carbon conversion efficiency of H (feeding on B)	dimensionless	0.5	Yields a gross maximal growth for H ($c_{BH}J_{BH}$) equal to $p_A = 1.5$
l_A	Metabolic and mortality loss rate of A	d^{-1}	0.1	Vasconcelos *et al.* 2019 (same for the three plankton competitors and bacteria)
l_M	Metabolic and mortality loss rate of M	d^{-1}	0.1	Vasconcelos *et al.* 2019

				(same for the three plankton competitors and bacteria)
l_H	Metabolic and mortality loss rate of H	d^{-1}	0.1	Vasconcelos *et al.* 2019 (same for the three plankton competitors and bacteria)
l_B	Metabolic and mortality loss rate of B	d^{-1}	0.1	Vasconcelos *et al.* 2019 (same for the three plankton competitors and bacteria)
D	Eddy diffusion coefficient	$m^2 . d^{-1}$ ($cm^2 . s^{-1}$)	0.864 (0.1)	Huisman *et al.* 2004
I_{in}	Photosynthetically active radiation at lake surface	µmol photons $. m^{-2} . s^{-1}$	300	Vasconcelos *et al.* 2019
h	Sediment-water column permeability	m^{-1}	0.05	(Yoshiyama *et al.*, 2009)

ANNEXE J

Projection of the HydroLakes attributes on the first two dimensions of a PCA (a) and correlation plot showing how the variables relates to those dimensions (b) (CHAPITRE 3)

Annexe J. PCA results showing the correlation of morphological attributes for LakePulse lakes. Projection of the variables on the plane formed by the first two PCA dimensions (a) and correlation plot showing how the variables relates to the PCA dimensions (b). For the correlation plot, the size and the colour shade of the dots indicate the direction and the magnitude of the correlation (green dot: positive correlation; purple dot: negative correlation).

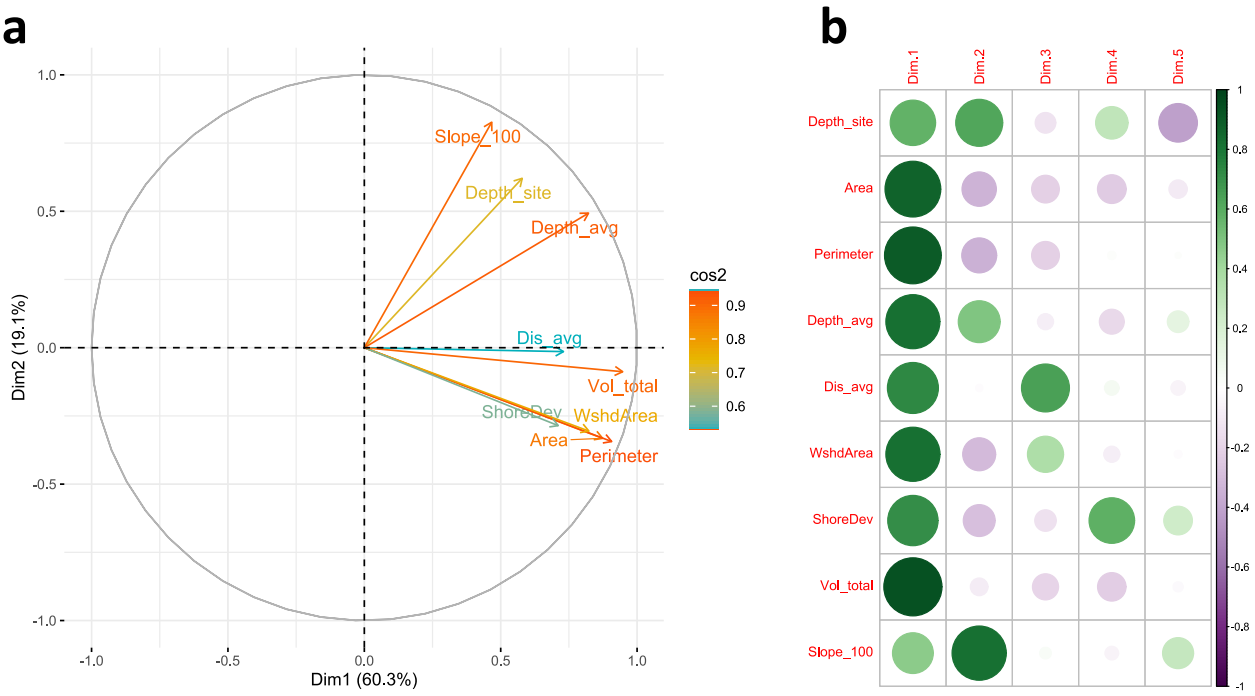

ANNEXE K

Correlation matrices of the environmental predictors for lakes from the combined surveys (a) and for LakePulse sites exclusively (b) (CHAPITRE 3)

Annexe K. Correlation matrices of the quantitative environmental variables (scaled and log-transformed) used as predictors in the Random Forest analyses on lakes form the combined surveys (a) and on LakePulse sites exclusively (b). For the correlation matrices, the size and the colour shade of the dots indicate the direction and the magnitude of the correlation (green dot: positive correlation; purple dot: negative correlation).

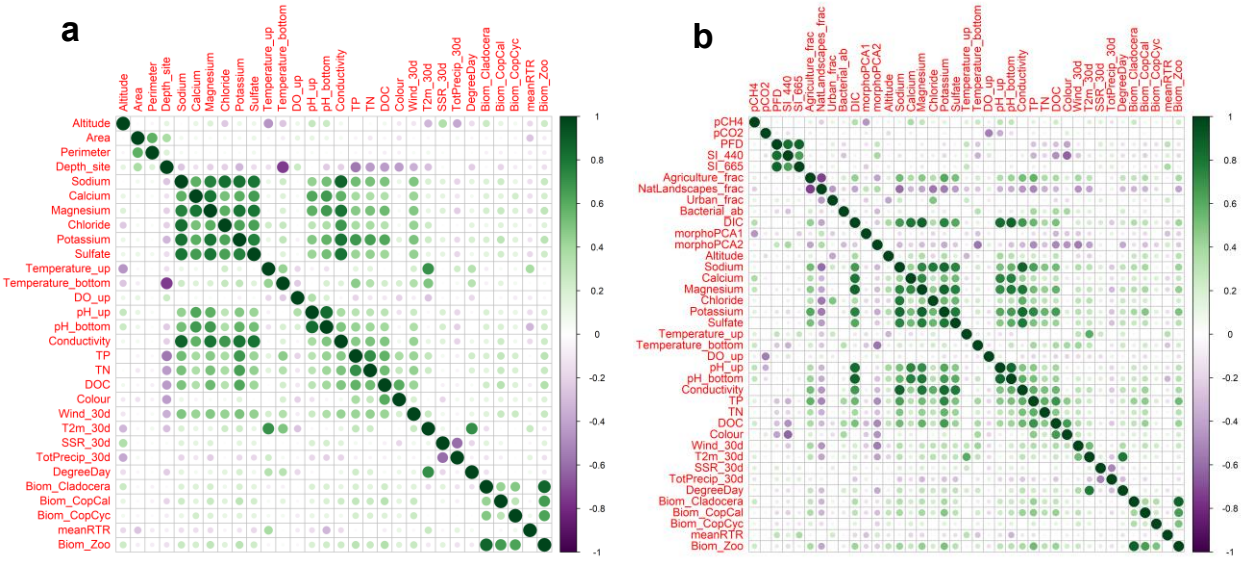

ANNEXE L

Surface water concentrations of potassium (a) and TP (b) across the ecoregions (EPA level I) covered by the combined NLA and LakePulse surveys (CHAPITRE 3)

Annexe L. Boxplots of the $\log_{10}$ transformed surface water concentrations of potassium (a) and TP (b) across the ecoregions (EPA level I) covered by the combined NLA and LakePulse surveys. The number of sites sampled in each ecoregion is specified in the x-axis labels.

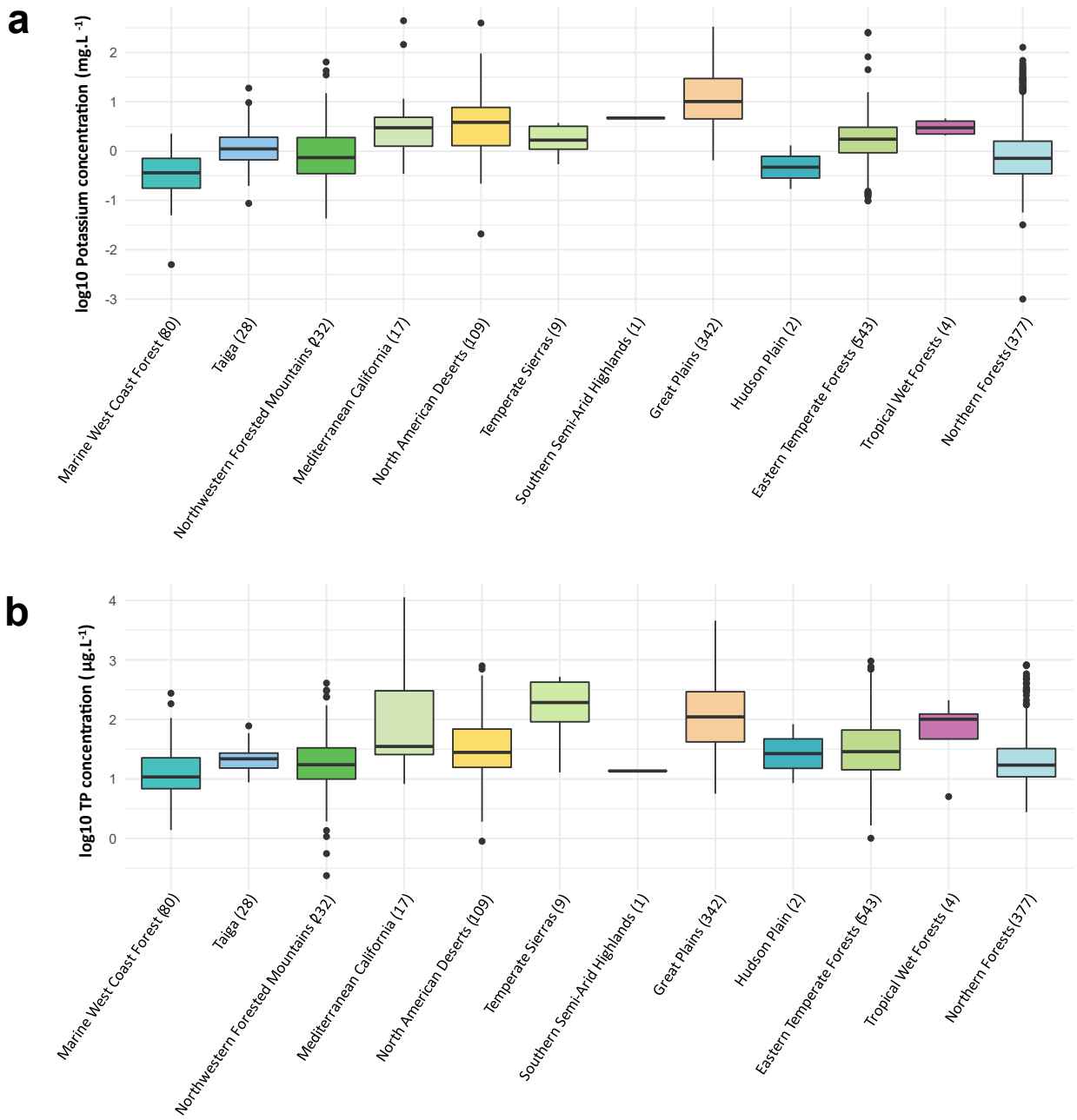

ANNEXE M

Database of resource aquisiton strategies hor the nanophytoplankton taxa identified in the LakePulse and NLA suveys (CHAPITRE 3)

Annexe M. Database of resource aquisiton strategies for the nanophytoplankton taxa identified in the LakePulse and NLA suveys. The strategy of each taxon is given in the column *Resource acquisition strategy*. The final decision on the resource acquisition strategy (column *Method used to reach final decision*) was reach either by acknowlelging whether the taxa was a cyanobacteria or diatom (*Cyano/Diatom*), by using information from exixting trait databases (*DB Scrap.*), through taxonomic proximity to taxa with known strategies (*Tax. Eval.*) or by a dedicating literature search (*Litt. Rev.*). See the Methods section of Chapter III for more details.

Genus	Classic group	Class	Order	Family	Method used to reach final decision	Resource acquisition strategy
Bacillaria	DIATOMS	Bacillariophyceae	Bacillariales	Bacillariaceae	Cyano/Diatom	**Autotroph**
Cylindrotheca	DIATOMS	Bacillariophyceae	Bacillariales	Bacillariaceae	Cyano/Diatom	**Autotroph**
Denticula	DIATOMS	Bacillariophyceae	Bacillariales	Bacillariaceae	Cyano/Diatom	**Autotroph**
Nitzschia	DIATOMS	Bacillariophyceae	Bacillariales	Bacillariaceae	Cyano/Diatom	**Autotroph**
Achnanthidium	DIATOMS	Bacillariophyceae	Cocconeidales	Achnanthidiaceae	Cyano/Diatom	**Autotroph**
Cocconeis	DIATOMS	Bacillariophyceae	Cocconeidales	Cocconeidaceae	Cyano/Diatom	**Autotroph**
Cymbella	DIATOMS	Bacillariophyceae	Cymbellales	Cymbellaceae	Cyano/Diatom	**Autotroph**
Encyonopsis	DIATOMS	Bacillariophyceae	Cymbellales	Cymbellaceae	Cyano/Diatom	**Autotroph**
Delicatophycus	DIATOMS	Bacillariophyceae	Cymbellales	Gomphonemataceae	Cyano/Diatom	**Autotroph**
Encyonema	DIATOMS	Bacillariophyceae	Cymbellales	Gomphonemataceae	Cyano/Diatom	**Autotroph**
Gomphonema	DIATOMS	Bacillariophyceae	Cymbellales	Gomphonemataceae	Cyano/Diatom	**Autotroph**
Rhoicosphenia	DIATOMS	Bacillariophyceae	Cymbellales	Rhoicospheniaceae	Cyano/Diatom	**Autotroph**
Actinella	DIATOMS	Bacillariophyceae	Eunotiales	Eunotiaceae	Cyano/Diatom	**Autotroph**
Eunotia	DIATOMS	Bacillariophyceae	Eunotiales	Eunotiaceae	Cyano/Diatom	**Autotroph**
Fragilaria	DIATOMS	Bacillariophyceae	Fragilariales	Fragilariaceae	Cyano/Diatom	**Autotroph**
Odontidium	DIATOMS	Bacillariophyceae	Fragilariales	Fragilariaceae	Cyano/Diatom	**Autotroph**
Synedra	DIATOMS	Bacillariophyceae	Fragilariales	Fragilariaceae	Cyano/Diatom	**Autotroph**
Pseudostaurosira	DIATOMS	Bacillariophyceae	Fragilariales	Staurosiraceae	Cyano/Diatom	**Autotroph**
Staurosira	DIATOMS	Bacillariophyceae	Fragilariales	Staurosiraceae	Cyano/Diatom	**Autotroph**
Staurosirella	DIATOMS	Bacillariophyceae	Fragilariales	Staurosiraceae	Cyano/Diatom	**Autotroph**
Ctenophora	DIATOMS	Bacillariophyceae	Licmophorales	Ulnariaceae	Cyano/Diatom	**Autotroph**
Pennales	DIATOMS	Bacillariophyceae	Licmophorales	Ulnariaceae	Cyano/Diatom	**Autotroph**
Ulnaria	DIATOMS	Bacillariophyceae	Licmophorales	Ulnariaceae	Cyano/Diatom	**Autotroph**
Mastogloia	DIATOMS	Bacillariophyceae	Mastogloiales	Mastogloiaceae	Cyano/Diatom	**Autotroph**
Amphipleura	DIATOMS	Bacillariophyceae	Naviculales	Amphipleuraceae	Cyano/Diatom	**Autotroph**

Frustulia	DIATOMS	Bacillariophyceae	Naviculales	Amphipleuraceae	Cyano/Diatom	**Autotroph**
Brachysira	DIATOMS	Bacillariophyceae	Naviculales	Brachysiraceae	Cyano/Diatom	**Autotroph**
Capartogramma	DIATOMS	Bacillariophyceae	Naviculales	Naviculaceae	Cyano/Diatom	**Autotroph**
Gyrosigma	DIATOMS	Bacillariophyceae	Naviculales	Naviculaceae	Cyano/Diatom	**Autotroph**
Hippodonta	DIATOMS	Bacillariophyceae	Naviculales	Naviculaceae	Cyano/Diatom	**Autotroph**
Navicula	DIATOMS	Bacillariophyceae	Naviculales	Naviculaceae	Cyano/Diatom	**Autotroph**
Pinnularia	DIATOMS	Bacillariophyceae	Naviculales	Pinnulariaceae	Cyano/Diatom	**Autotroph**
Fallacia	DIATOMS	Bacillariophyceae	Naviculales	Sellaphoraceae	Cyano/Diatom	**Autotroph**
Sellaphora	DIATOMS	Bacillariophyceae	Naviculales	Sellaphoraceae	Cyano/Diatom	**Autotroph**
Craticula	DIATOMS	Bacillariophyceae	Naviculales	Stauroneidaceae	Cyano/Diatom	**Autotroph**
Stauroneis	DIATOMS	Bacillariophyceae	Naviculales	Stauroneidaceae	Cyano/Diatom	**Autotroph**
Hantzschia	DIATOMS	Bacillariophyceae	Pennales	Bacillariaceae	Cyano/Diatom	**Autotroph**
Epithemia	DIATOMS	Bacillariophyceae	Rhopalodiales	Rhopalodiaceae	Cyano/Diatom	**Autotroph**
Rhopalodia	DIATOMS	Bacillariophyceae	Rhopalodiales	Rhopalodiaceae	Cyano/Diatom	**Autotroph**
Entomoneis	DIATOMS	Bacillariophyceae	Surirellales	Entomoneidaceae	Cyano/Diatom	**Autotroph**
Surirella	DIATOMS	Bacillariophyceae	Surirellales	Surirellaceae	Cyano/Diatom	**Autotroph**
Asterionella	DIATOMS	Bacillariophyceae	Tabellariales	Tabellariaceae	Cyano/Diatom	**Autotroph**
Diatoma	DIATOMS	Bacillariophyceae	Tabellariales	Tabellariaceae	Cyano/Diatom	**Autotroph**
Tabellaria	DIATOMS	Bacillariophyceae	Tabellariales	Tabellariaceae	Cyano/Diatom	**Autotroph**
Amphora	DIATOMS	Bacillariophyceae	Thalassiophysales	Catenulaceae	Cyano/Diatom	**Autotroph**
Aulacoseira	DIATOMS	Coscinodiscophyceae	Aulacoseirales	Aulacoseiraceae	Cyano/Diatom	**Autotroph**
Centrales	DIATOMS	Coscinodiscophyceae	Coscinodiscales	Coscinodiscaceae	Cyano/Diatom	**Autotroph**
Coscinodiscus	DIATOMS	Coscinodiscophyceae	Coscinodiscales	Coscinodiscaceae	Cyano/Diatom	**Autotroph**
Melosira	DIATOMS	Coscinodiscophyceae	Melosirales	Melosiraceae	Cyano/Diatom	**Autotroph**
Rhizosolenia	DIATOMS	Coscinodiscophyceae	Rhizosoleniales	Rhizosoleniaceae	Cyano/Diatom	**Autotroph**
Urosolenia	DIATOMS	Coscinodiscophyceae	Rhizosoleniales	Rhizosoleniaceae	Cyano/Diatom	**Autotroph**
Acanthoceras	DIATOMS	Mediophyceae	Chaetocerotales	Chaetocerotaceae	Cyano/Diatom	**Autotroph**
Chaetoceros	DIATOMS	Mediophyceae	Chaetocerotales	Chaetocerotaceae	Cyano/Diatom	**Autotroph**
Cyclotella	DIATOMS	Mediophyceae	Stephanodiscales	Stephanodiscaceae	Cyano/Diatom	**Autotroph**
Discostella	DIATOMS	Mediophyceae	Stephanodiscales	Stephanodiscaceae	Cyano/Diatom	**Autotroph**
Lindavia	DIATOMS	Mediophyceae	Stephanodiscales	Stephanodiscaceae	Cyano/Diatom	**Autotroph**
Pantocsekiella	DIATOMS	Mediophyceae	Stephanodiscales	Stephanodiscaceae	Cyano/Diatom	**Autotroph**
Stephanodiscus	DIATOMS	Mediophyceae	Stephanodiscales	Stephanodiscaceae	Cyano/Diatom	**Autotroph**
Skeletonema	DIATOMS	Mediophyceae	Thalassiosirales	Skeletonemataceae	Cyano/Diatom	**Autotroph**
Elakatothrix	GREEN ALGAE	Klebsormidiophyceae	Klebsormidiales	Elakatotrichaceae	DB Scrap.	**Autotroph**
Closterium	GREEN ALGAE	Zygnematophyceae	Desmidiales	Closteriaceae	DB Scrap.	**Autotroph**
Arthrodesmus	GREEN ALGAE	Zygnematophyceae	Desmidiales	Desmidiaceae	Litt. Rev.	**Autotroph**
Cosmarium	GREEN ALGAE	Zygnematophyceae	Desmidiales	Desmidiaceae	DB Scrap.	**Autotroph**
Desmidium	GREEN ALGAE	Zygnematophyceae	Desmidiales	Desmidiaceae	Litt. Rev.	**Autotroph**
Euastrum	GREEN ALGAE	Zygnematophyceae	Desmidiales	Desmidiaceae	DB Scrap.	**Autotroph**
Spondylosium	GREEN ALGAE	Zygnematophyceae	Desmidiales	Desmidiaceae	DB Scrap.	**Autotroph**

Staurastrum	GREEN ALGAE	Zygnematophyceae	Desmidiales	Desmidiaceae	DB Scrap.	**Autotroph**
Staurodesmus	GREEN ALGAE	Zygnematophyceae	Desmidiales	Desmidiaceae	DB Scrap.	**Autotroph**
Teilingia	GREEN ALGAE	Zygnematophyceae	Desmidiales	Desmidiaceae	DB Scrap.	**Autotroph**
Gonatozygon	GREEN ALGAE	Zygnematophyceae	Desmidiales	Gonatozygaceae	Litt. Rev.	**Autotroph**
Netrium	GREEN ALGAE	Zygnematophyceae	Zygnematales	Mesotaeniaceae	Litt. Rev.	**Autotroph**
Mougeotia	GREEN ALGAE	Zygnematophyceae	Zygnematales	Zygnemataceae	DB Scrap.	**Autotroph**
Spirogyra	GREEN ALGAE	Zygnematophyceae	Zygnematales	Zygnemataceae	Litt. Rev.	**Autotroph**
Tetraselmis	GREEN ALGAE	Chlorodendrophyceae	Chlorodendrales	Chlorodendraceae	DB Scrap.	**Autotroph**
Carteria	GREEN ALGAE	Chlorophyceae	Chlamydomonadales	Chlamydomonadaceae	DB Scrap.	**Autotroph**
Chlamydomonas	GREEN ALGAE	Chlorophyceae	Chlamydomonadales	Chlamydomonadaceae	Litt. Rev.	**Autotroph**
Chloromonas	GREEN ALGAE	Chlorophyceae	Chlamydomonadales	Chlamydomonadaceae	Litt. Rev.	**Autotroph**
Lobomonas	GREEN ALGAE	Chlorophyceae	Chlamydomonadales	Chlamydomonadaceae	Tax. Eval.	**Autotroph**
Vitreochlamys	GREEN ALGAE	Chlorophyceae	Chlamydomonadales	Chlamydomonadaceae	Tax. Eval.	**Autotroph**
Hafniomonas	GREEN ALGAE	Chlorophyceae	Chlamydomonadales	Dunaliellaceae	Tax. Eval.	**Autotroph**
Spermatozopsis	GREEN ALGAE	Chlorophyceae	Chlamydomonadales	Dunaliellaceae	DB Scrap.	**Autotroph**
Gonium	GREEN ALGAE	Chlorophyceae	Chlamydomonadales	Goniaceae	DB Scrap.	**Autotroph**
Chlorogonium	GREEN ALGAE	Chlorophyceae	Chlamydomonadales	Haematococcaceae	DB Scrap.	**Autotroph**
Chlamydocapsa	GREEN ALGAE	Chlorophyceae	Chlamydomonadales	Palmellopsidaceae	DB Scrap.	**Autotroph**
Pteromonas	GREEN ALGAE	Chlorophyceae	Chlamydomonadales	Phacotaceae	DB Scrap.	**Autotroph**
Sphaerocystis	GREEN ALGAE	Chlorophyceae	Chlamydomonadales	Sphaerocystidaceae	DB Scrap.	**Autotroph**
Tetrabaena	GREEN ALGAE	Chlorophyceae	Chlamydomonadales	Tetrabaenaceae	Litt. Rev.	**Autotroph**
Tetraspora	GREEN ALGAE	Chlorophyceae	Chlamydomonadales	Tetrasporaceae	Tax. Eval.	**Autotroph**
Eudorina	GREEN ALGAE	Chlorophyceae	Chlamydomonadales	Volvocaceae	DB Scrap.	**Autotroph**
Pandorina	GREEN ALGAE	Chlorophyceae	Chlamydomonadales	Volvocaceae	Litt. Rev.	**Autotroph**
Volvox	GREEN ALGAE	Chlorophyceae	Chlamydomonadales	Volvocaceae	Litt. Rev.	**Autotroph**
Golenkiniopsis	GREEN ALGAE	Chlorophyceae	Chlorellales	Chlorellacae	DB Scrap.	**Autotroph**
Diplochloris	GREEN ALGAE	Chlorophyceae	Chlorophyceae incertae sedis	Chlorophyceae familia incertae sedis	Litt. Rev.	**Autotroph**
Oedogonium	GREEN ALGAE	Chlorophyceae	Oedogoniales	Oedogoniaceae	DB Scrap.	**Autotroph**
Ankyra	GREEN ALGAE	Chlorophyceae	Sphaeropleales	Characiaceae	DB Scrap.	**Autotroph**
Characium	GREEN ALGAE	Chlorophyceae	Sphaeropleales	Characiaceae	Litt. Rev.	**Autotroph**
Korshikoviella	GREEN ALGAE	Chlorophyceae	Sphaeropleales	Characiaceae	DB Scrap.	**Autotroph**
Lanceola	GREEN ALGAE	Chlorophyceae	Sphaeropleales	Characiaceae	DB Scrap.	**Autotroph**
Pseudoschroederia	GREEN ALGAE	Chlorophyceae	Sphaeropleales	Characiaceae	Litt. Rev.	**Autotroph**
Fusola	GREEN ALGAE	Chlorophyceae	Sphaeropleales	Cylindrocapsaceae	Litt. Rev.	**Autotroph**
Monactinus	GREEN ALGAE	Chlorophyceae	Sphaeropleales	Hydrodictyaceae	DB Scrap.	**Autotroph**
Pediastrum	GREEN ALGAE	Chlorophyceae	Sphaeropleales	Hydrodictyaceae	DB Scrap.	**Autotroph**
Pseudopediastrum	GREEN ALGAE	Chlorophyceae	Sphaeropleales	Hydrodictyaceae	DB Scrap.	**Autotroph**
Stauridium	GREEN ALGAE	Chlorophyceae	Sphaeropleales	Hydrodictyaceae	DB Scrap.	**Autotroph**
Tetraedron	GREEN ALGAE	Chlorophyceae	Sphaeropleales	Hydrodictyaceae	DB Scrap.	**Autotroph**
Chlorotetraedron	GREEN ALGAE	Chlorophyceae	Sphaeropleales	Neochloridaceae	Tax. Eval.	**Autotroph**
Coenochloris	GREEN ALGAE	Chlorophyceae	Sphaeropleales	Radiococcaceae	DB Scrap.	**Autotroph**

Coenocystis	GREEN ALGAE	Chlorophyceae	Sphaeropleales	Radiococcaceae	DB Scrap.	**Autotroph**
Gloeocystis	GREEN ALGAE	Chlorophyceae	Sphaeropleales	Radiococcaceae	DB Scrap.	**Autotroph**
Radiococcus	GREEN ALGAE	Chlorophyceae	Sphaeropleales	Radiococcaceae	Litt. Rev.	**Autotroph**
Acutodesmus	GREEN ALGAE	Chlorophyceae	Sphaeropleales	Scenedesmaceae	Litt. Rev.	**Autotroph**
Coelastrum	GREEN ALGAE	Chlorophyceae	Sphaeropleales	Scenedesmaceae	DB Scrap.	**Autotroph**
Comasiella	GREEN ALGAE	Chlorophyceae	Sphaeropleales	Scenedesmaceae	Litt. Rev.	**Autotroph**
Crucigeniella	GREEN ALGAE	Chlorophyceae	Sphaeropleales	Scenedesmaceae	DB Scrap.	**Autotroph**
Desmodesmus	GREEN ALGAE	Chlorophyceae	Sphaeropleales	Scenedesmaceae	DB Scrap.	**Autotroph**
Scenedesmus	GREEN ALGAE	Chlorophyceae	Sphaeropleales	Scenedesmaceae	DB Scrap.	**Autotroph**
Tetradesmus	GREEN ALGAE	Chlorophyceae	Sphaeropleales	Scenedesmaceae	DB Scrap.	**Autotroph**
Tetrastrum	GREEN ALGAE	Chlorophyceae	Sphaeropleales	Scenedesmaceae	DB Scrap.	**Autotroph**
Planktosphaeria	GREEN ALGAE	Chlorophyceae	Sphaeropleales	Schizochlamydaceae	Litt. Rev.	**Autotroph**
Schroederia	GREEN ALGAE	Chlorophyceae	Sphaeropleales	Schroederiaceae	DB Scrap.	**Autotroph**
Ankistrodesmus	GREEN ALGAE	Chlorophyceae	Sphaeropleales	Selenastraceae	DB Scrap.	**Autotroph**
Chlorolobion	GREEN ALGAE	Chlorophyceae	Sphaeropleales	Selenastraceae	DB Scrap.	**Autotroph**
Drepanochloris	GREEN ALGAE	Chlorophyceae	Sphaeropleales	Selenastraceae	Tax. Eval.	**Autotroph**
Gregiochloris	GREEN ALGAE	Chlorophyceae	Sphaeropleales	Selenastraceae	Litt. Rev.	**Autotroph**
Kirchneriella	GREEN ALGAE	Chlorophyceae	Sphaeropleales	Selenastraceae	DB Scrap.	**Autotroph**
Messastrum	GREEN ALGAE	Chlorophyceae	Sphaeropleales	Selenastraceae	DB Scrap.	**Autotroph**
Monoraphidium	GREEN ALGAE	Chlorophyceae	Sphaeropleales	Selenastraceae	DB Scrap.	**Autotroph**
Quadrigula	GREEN ALGAE	Chlorophyceae	Sphaeropleales	Selenastraceae	DB Scrap.	**Autotroph**
Raphidocelis	GREEN ALGAE	Chlorophyceae	Sphaeropleales	Selenastraceae	DB Scrap.	**Autotroph**
Selenastrum	GREEN ALGAE	Chlorophyceae	Sphaeropleales	Selenastraceae	DB Scrap.	**Autotroph**
Treubaria	GREEN ALGAE	Chlorophyceae	Sphaeropleales	Treubariaceae	DB Scrap.	**Autotroph**
Pedinomonas	GREEN ALGAE	Pedinophyceae	Pedinomonadales	Pedinomonadaceae	Litt. Rev.	**Autotroph**
Scourfieldia	GREEN ALGAE	Pedinophyceae	Scourfieldiales	Scourfieldiaceae	Litt. Rev.	**Autotroph**
Actinastrum	GREEN ALGAE	Trebouxiophyceae	Chlorellales	Chlorellaceae	DB Scrap.	**Autotroph**
Chlorella	GREEN ALGAE	Trebouxiophyceae	Chlorellales	Chlorellaceae	DB Scrap.	**Autotroph**
Closteriopsis	GREEN ALGAE	Trebouxiophyceae	Chlorellales	Chlorellaceae	DB Scrap.	**Autotroph**
Dictyosphaerium	GREEN ALGAE	Trebouxiophyceae	Chlorellales	Chlorellaceae	DB Scrap.	**Autotroph**
Gloeotila	GREEN ALGAE	Trebouxiophyceae	Chlorellales	Chlorellaceae	Litt. Rev.	**Autotroph**
Golenkinia	GREEN ALGAE	Trebouxiophyceae	Chlorellales	Chlorellaceae	DB Scrap.	**Autotroph**
Keratococcus	GREEN ALGAE	Trebouxiophyceae	Chlorellales	Chlorellaceae	Litt. Rev.	**Autotroph**
Micractinium	GREEN ALGAE	Trebouxiophyceae	Chlorellales	Chlorellaceae	DB Scrap.	**Autotroph**
Mucidosphaerium	GREEN ALGAE	Trebouxiophyceae	Chlorellales	Chlorellaceae	DB Scrap.	**Autotroph**
Neglectella	GREEN ALGAE	Trebouxiophyceae	Chlorellales	Eremosphaeraceae	Litt. Rev.	**Autotroph**
Eremosphaera	GREEN ALGAE	Trebouxiophyceae	Chlorellales	Oocystaceae	Litt. Rev.	**Autotroph**
Franceia	GREEN ALGAE	Trebouxiophyceae	Chlorellales	Oocystaceae	Litt. Rev.	**Autotroph**
Lagerheimia	GREEN ALGAE	Trebouxiophyceae	Chlorellales	Oocystaceae	DB Scrap.	**Autotroph**
Nephrocytium	GREEN ALGAE	Trebouxiophyceae	Chlorellales	Oocystaceae	DB Scrap.	**Autotroph**
Oocystis	GREEN ALGAE	Trebouxiophyceae	Chlorellales	Oocystaceae	DB Scrap.	**Autotroph**

Willea	GREEN ALGAE	Trebouxiophyceae	Chlorellales	Oocystaceae	Litt. Rev.	**Autotroph**
Koliella	GREEN ALGAE	Trebouxiophyceae	Prasiolales	Koliellaceae	DB Scrap.	**Autotroph**
Botryococcus	GREEN ALGAE	Trebouxiophyceae	Trebouxiales	Botryococcaceae	DB Scrap.	**Autotroph**
Dichotomococcus	GREEN ALGAE	Trebouxiophyceae	Trebouxiales	Botryococcaceae	Litt. Rev.	**Autotroph**
Chloroidium	GREEN ALGAE	Trebouxiophyceae	Trebouxiophyceae ordo incertae sedis	Trebouxiophyceae incertae sedis	Litt. Rev.	**Autotroph**
Crucigenia	GREEN ALGAE	Trebouxiophyceae	Trebouxiophyceae ordo incertae sedis	Trebouxiophyceae incertae sedis	DB Scrap.	**Autotroph**
Lemmermannia	GREEN ALGAE	Trebouxiophyceae	Trebouxiophyceae ordo incertae sedis	Trebouxiophyceae incertae sedis	Litt. Rev.	**Autotroph**
Cladophora	GREEN ALGAE	Ulvophyceae	Cladophorales	Cladophoraceae	Litt. Rev.	**Autotroph**
Binuclearia	GREEN ALGAE	Ulvophyceae	Ulotrichales	Binucleariaceae	Litt. Rev.	**Autotroph**
Ulothrix	GREEN ALGAE	Ulvophyceae	Ulotrichales	Ulotrichaceae	Litt. Rev.	**Autotroph**
Pseudendoclonium	GREEN ALGAE	Ulvophyceae	Ulvales	Ulvales incertae sedis	Litt. Rev.	**Autotroph**
Cryptomonas	CRYPTOPHYTES	Cryptophyceae	Cryptomonadales	Cryptomonadaceae	Litt. Rev.	**Mixotroph**
Chroomonas	CRYPTOPHYTES	Cryptophyceae	Cryptomonadales	Hemiselmidaceae	Litt. Rev.	**Mixotroph**
Komma	CRYPTOPHYTES	Cryptophyceae	Cryptomonadales	Hemiselmidaceae	Litt. Rev.	**Mixotroph**
Rhodomonas	CRYPTOPHYTES	Cryptophyceae	Pyrenomonadales	Pyrenomonadaceae	Litt. Rev.	**Mixotroph**
Aphanothece	CYANOBACTERIA	Cyanophyceae	Chroococcales	Aphanothecaceae	Cyano/Diatom	**Autotroph**
Gloeothece	CYANOBACTERIA	Cyanophyceae	Chroococcales	Aphanothecaceae	Cyano/Diatom	**Autotroph**
Myxobaktron	CYANOBACTERIA	Cyanophyceae	Chroococcales	Aphanothecaceae	Cyano/Diatom	**Autotroph**
Chroococcus	CYANOBACTERIA	Cyanophyceae	Chroococcales	Chroococcaceae	Cyano/Diatom	**Autotroph**
Dactylococcopsis	CYANOBACTERIA	Cyanophyceae	Chroococcales	Chroococcaceae	Cyano/Diatom	**Autotroph**
Siphononema	CYANOBACTERIA	Cyanophyceae	Chroococcales	Entophysalidaceae	Cyano/Diatom	**Autotroph**
Gomphosphaeria	CYANOBACTERIA	Cyanophyceae	Chroococcales	Gomphosphaeriaceae	Cyano/Diatom	**Autotroph**
Gloeocapsa	CYANOBACTERIA	Cyanophyceae	Chroococcales	Microcystaceae	Cyano/Diatom	**Autotroph**
Microcystis	CYANOBACTERIA	Cyanophyceae	Chroococcales	Microcystaceae	Cyano/Diatom	**Autotroph**
Radiocystis	CYANOBACTERIA	Cyanophyceae	Chroococcales	Microcystaceae	Cyano/Diatom	**Autotroph**
Anabaenopsis	CYANOBACTERIA	Cyanophyceae	Nostocales	Aphanizomenonaceae	Cyano/Diatom	**Autotroph**
Aphanizomenon	CYANOBACTERIA	Cyanophyceae	Nostocales	Aphanizomenonaceae	Cyano/Diatom	**Autotroph**
Chrysosporum	CYANOBACTERIA	Cyanophyceae	Nostocales	Aphanizomenonaceae	Cyano/Diatom	**Autotroph**
Cuspidothrix	CYANOBACTERIA	Cyanophyceae	Nostocales	Aphanizomenonaceae	Cyano/Diatom	**Autotroph**
Cylindrospermopsis	CYANOBACTERIA	Cyanophyceae	Nostocales	Aphanizomenonaceae	Cyano/Diatom	**Autotroph**
Dolichospermum	CYANOBACTERIA	Cyanophyceae	Nostocales	Aphanizomenonaceae	Cyano/Diatom	**Autotroph**
Nodularia	CYANOBACTERIA	Cyanophyceae	Nostocales	Aphanizomenonaceae	Cyano/Diatom	**Autotroph**
Raphidiopsis	CYANOBACTERIA	Cyanophyceae	Nostocales	Aphanizomenonaceae	Cyano/Diatom	**Autotroph**
Gloeotrichia	CYANOBACTERIA	Cyanophyceae	Nostocales	Gloeotrichiaceae	Cyano/Diatom	**Autotroph**
Anabaena	CYANOBACTERIA	Cyanophyceae	Nostocales	Nostocaceae	Cyano/Diatom	**Autotroph**
Macrospermum	CYANOBACTERIA	Cyanophyceae	Nostocales	Nostocaceae	Cyano/Diatom	**Autotroph**
Nostoc	CYANOBACTERIA	Cyanophyceae	Nostocales	Nostocaceae	Cyano/Diatom	**Autotroph**
Rivularia	CYANOBACTERIA	Cyanophyceae	Nostocales	Rivulariaceae	Cyano/Diatom	**Autotroph**
Anagnostidinema	CYANOBACTERIA	Cyanophyceae	Oscillatoriales	Coleofasciculaceae	Cyano/Diatom	**Autotroph**
Geitlerinema	CYANOBACTERIA	Cyanophyceae	Oscillatoriales	Coleofasciculaceae	Cyano/Diatom	**Autotroph**

Komvophoron	CYANOBACTERIA	Cyanophyceae	Oscillatoriales	Gomontiellaceae	Cyano/Diatom	**Autotroph**
Arthrospira	CYANOBACTERIA	Cyanophyceae	Oscillatoriales	Microcoleaceae	Cyano/Diatom	**Autotroph**
Microcoleus	CYANOBACTERIA	Cyanophyceae	Oscillatoriales	Microcoleaceae	Cyano/Diatom	**Autotroph**
Planktothrix	CYANOBACTERIA	Cyanophyceae	Oscillatoriales	Microcoleaceae	Cyano/Diatom	**Autotroph**
Limnoraphis	CYANOBACTERIA	Cyanophyceae	Oscillatoriales	Oscillatoriaceae	Cyano/Diatom	**Autotroph**
Lyngbya	CYANOBACTERIA	Cyanophyceae	Oscillatoriales	Oscillatoriaceae	Cyano/Diatom	**Autotroph**
Oscillatoria	CYANOBACTERIA	Cyanophyceae	Oscillatoriales	Oscillatoriaceae	Cyano/Diatom	**Autotroph**
Phormidium	CYANOBACTERIA	Cyanophyceae	Oscillatoriales	Oscillatoriaceae	Cyano/Diatom	**Autotroph**
Glaucospira	CYANOBACTERIA	Cyanophyceae	Spirulinales	Spirulinaceae	Cyano/Diatom	**Autotroph**
Spirulina	CYANOBACTERIA	Cyanophyceae	Spirulinales	Spirulinaceae	Cyano/Diatom	**Autotroph**
Coelomoron	CYANOBACTERIA	Cyanophyceae	Synechococcales	Coelosphaeriaceae	Cyano/Diatom	**Autotroph**
Coelosphaerium	CYANOBACTERIA	Cyanophyceae	Synechococcales	Coelosphaeriaceae	Cyano/Diatom	**Autotroph**
Snowella	CYANOBACTERIA	Cyanophyceae	Synechococcales	Coelosphaeriaceae	Cyano/Diatom	**Autotroph**
Woronichinia	CYANOBACTERIA	Cyanophyceae	Synechococcales	Coelosphaeriaceae	Cyano/Diatom	**Autotroph**
Leibleinia	CYANOBACTERIA	Cyanophyceae	Synechococcales	Leptolyngbyaceae	Cyano/Diatom	**Autotroph**
Leptolyngbya	CYANOBACTERIA	Cyanophyceae	Synechococcales	Leptolyngbyaceae	Cyano/Diatom	**Autotroph**
Limnolyngbya	CYANOBACTERIA	Cyanophyceae	Synechococcales	Leptolyngbyaceae	Cyano/Diatom	**Autotroph**
Planktolyngbya	CYANOBACTERIA	Cyanophyceae	Synechococcales	Leptolyngbyaceae	Cyano/Diatom	**Autotroph**
Romeria	CYANOBACTERIA	Cyanophyceae	Synechococcales	Leptolyngbyaceae	Cyano/Diatom	**Autotroph**
Aphanocapsa	CYANOBACTERIA	Cyanophyceae	Synechococcales	Merismopediaceae	Cyano/Diatom	**Autotroph**
Eucapsis	CYANOBACTERIA	Cyanophyceae	Synechococcales	Merismopediaceae	Cyano/Diatom	**Autotroph**
Limnococcus	CYANOBACTERIA	Cyanophyceae	Synechococcales	Merismopediaceae	Cyano/Diatom	**Autotroph**
Merismopedia	CYANOBACTERIA	Cyanophyceae	Synechococcales	Merismopediaceae	Cyano/Diatom	**Autotroph**
Pannus	CYANOBACTERIA	Cyanophyceae	Synechococcales	Merismopediaceae	Cyano/Diatom	**Autotroph**
Limnothrix	CYANOBACTERIA	Cyanophyceae	Synechococcales	Pseudanabaenaceae	Cyano/Diatom	**Autotroph**
Pseudanabaena	CYANOBACTERIA	Cyanophyceae	Synechococcales	Pseudanabaenaceae	Cyano/Diatom	**Autotroph**
Anathece	CYANOBACTERIA	Cyanophyceae	Synechococcales	Synechococcaceae	Cyano/Diatom	**Autotroph**
Cyanobium	CYANOBACTERIA	Cyanophyceae	Synechococcales	Synechococcaceae	Cyano/Diatom	**Autotroph**
Cyanodictyon	CYANOBACTERIA	Cyanophyceae	Synechococcales	Synechococcaceae	Cyano/Diatom	**Autotroph**
Cyanonephron	CYANOBACTERIA	Cyanophyceae	Synechococcales	Synechococcaceae	Cyano/Diatom	**Autotroph**
Rhabdoderma	CYANOBACTERIA	Cyanophyceae	Synechococcales	Synechococcaceae	Cyano/Diatom	**Autotroph**
Rhabdogloea	CYANOBACTERIA	Cyanophyceae	Synechococcales	Synechococcaceae	Cyano/Diatom	**Autotroph**
Synechococcus	CYANOBACTERIA	Cyanophyceae	Synechococcales	Synechococcaceae	Cyano/Diatom	**Autotroph**
Heteroleibleinia	CYANOBACTERIA	Cyanophyceae	Synechococcales	Synechococcales familia incertae sedis	Cyano/Diatom	**Autotroph**
Colacium	EUGLENOIDS	Euglenophyceae	Euglenida	Euglenidae	Litt. Rev.	**Autotroph**
Euglena	EUGLENOIDS	Euglenophyceae	Euglenida	Euglenidae	Litt. Rev.	**Autotroph**
Strombomonas	EUGLENOIDS	Euglenophyceae	Euglenida	Euglenidae	Litt. Rev.	**Autotroph**
Trachelomonas	EUGLENOIDS	Euglenophyceae	Euglenida	Euglenidae	Litt. Rev.	**Autotroph**
Lepocinclis	EUGLENOIDS	Euglenophyceae	Euglenida	Phacidae	Litt. Rev.	**Autotroph**
Phacus	EUGLENOIDS	Euglenophyceae	Euglenida	Phacidae	Litt. Rev.	**Autotroph**
Chrysochromulina	OTHER	Coccolithophyceae	Prymnesiales	Chrysochromulinaceae	DB Scrap.	**Mixotroph**

Prymnesium	OTHER	Coccolithophyceae	Prymnesiales	Prymnesiaceae	Litt. Rev.	**Mixotroph**
Amphidinium	DINOFLAGELLATES	Dinophyceae	Amphidiniales	Amphidiniaceae	Litt. Rev.	**Mixotroph**
Ceratium	DINOFLAGELLATES	Dinophyceae	Gonyaulacales	Ceratiaceae	Litt. Rev.	**Mixotroph**
Gymnodinium	DINOFLAGELLATES	Dinophyceae	Gymnodiniales	Gymnodiniaceae	Litt. Rev.	**Mixotroph**
Nusuttodinium	DINOFLAGELLATES	Dinophyceae	Gymnodiniales	Gymnodiniaceae	Litt. Rev.	**Mixotroph**
Gyrodinium	DINOFLAGELLATES	Dinophyceae	Gymnodiniales	Gyrodiniaceae	Litt. Rev.	**Mixotroph**
Glochidinium	DINOFLAGELLATES	Dinophyceae	Peridiniales	Peridiniaceae	Litt. Rev.	**Mixotroph**
Parvodinium	DINOFLAGELLATES	Dinophyceae	Peridiniales	Peridiniaceae	Litt. Rev.	**Mixotroph**
Peridinium	DINOFLAGELLATES	Dinophyceae	Peridiniales	Peridiniaceae	DB Scrap.	**Mixotroph**
Glenodinium	DINOFLAGELLATES	Dinophyceae	Peridiniales	Peridiniales incertae sedis	Litt. Rev.	**Mixotroph**
Biecheleria	DINOFLAGELLATES	Dinophyceae	Suessiales	Suessiaceae	Litt. Rev.	**Mixotroph**
Apocalathium	DINOFLAGELLATES	Dinophyceae	Thoracosphaerales	Thoracosphaeraceae	Litt. Rev.	**Mixotroph**
Fusiperidinium	DINOFLAGELLATES	Dinophyceae	Thoracosphaerales	Thoracosphaeraceae	Litt. Rev.	**Mixotroph**
Chromulina	CHRYSOPHYTES	Chrysophyceae	Chromulinales	Chromulinaceae	DB Scrap.	**Mixotroph**
Ochromonas	CHRYSOPHYTES	Chrysophyceae	Chromulinales	Chromulinaceae	DB Scrap.	**Mixotroph**
Uroglena	CHRYSOPHYTES	Chrysophyceae	Chromulinales	Chromulinaceae	Litt. Rev.	**Mixotroph**
Chrysamoeba	CHRYSOPHYTES	Chrysophyceae	Chromulinales	Chrysamoebaceae	Litt. Rev.	**Mixotroph**
Chrysosphaera	CHRYSOPHYTES	Chrysophyceae	Chromulinales	Chrysosphaeraceae	Litt. Rev.	**Mixotroph**
Chrysococcus	CHRYSOPHYTES	Chrysophyceae	Chromulinales	Dinobryaceae	Litt. Rev.	**Mixotroph**
Chrysoikos	CHRYSOPHYTES	Chrysophyceae	Chromulinales	Dinobryaceae	Litt. Rev.	**Mixotroph**
Chrysolykos	CHRYSOPHYTES	Chrysophyceae	Chromulinales	Dinobryaceae	DB Scrap.	**Mixotroph**
Dinobryon	CHRYSOPHYTES	Chrysophyceae	Chromulinales	Dinobryaceae	DB Scrap.	**Mixotroph**
Epipyxis	CHRYSOPHYTES	Chrysophyceae	Chromulinales	Dinobryaceae	DB Scrap.	**Mixotroph**
Kephyrion	CHRYSOPHYTES	Chrysophyceae	Chromulinales	Dinobryaceae	DB Scrap.	**Mixotroph**
Pseudokephyrion	CHRYSOPHYTES	Chrysophyceae	Chromulinales	Dinobryaceae	Litt. Rev.	**Mixotroph**
Bitrichia	CHRYSOPHYTES	Chrysophyceae	Hibberdiales	Stylococcaceae	Litt. Rev.	**Autotroph**
Lagynion	CHRYSOPHYTES	Chrysophyceae	Hibberdiales	Stylococcaceae	Litt. Rev.	**Autotroph**
Stephanoporos	CHRYSOPHYTES	Chrysophyceae	Hibberdiales	Stylococcaceae	Litt. Rev.	**Autotroph**
Chrysosphaerella	CHRYSOPHYTES	Chrysophyceae	Paraphysomonadales	Chrysosphaerellaceae	Litt. Rev.	**Mixotroph**
Pedinella	OTHER	Dictyochophyceae	Pedinellales	Pedinellaceae	Litt. Rev.	**Mixotroph**
Pseudocharaciopsis	EUSTIGMATOPHYTES	Eustigmatophyceae	Eustigmatales	Pseudocharaciopsidaceae	Litt. Rev.	**Autotroph**
Goniochloris	EUSTIGMATOPHYTES	Eustigmatophyceae	Goniochloridales	Goniochloridaceae	DB Scrap.	**Autotroph**
Tetraedriella	EUSTIGMATOPHYTES	Eustigmatophyceae	Goniochloridales	Goniochloridaceae	Litt. Rev.	**Autotroph**
Stichogloea	OTHER	Phaeothamniophyceae	Phaeothamniales	Phaeothamniaceae	Litt. Rev.	**Autotroph**
Gonyostomum	OTHER	Raphidophyceae	Chattonellales	Vacuolariaceae	Litt. Rev.	**Autotroph**
Mallomonas	CHRYSOPHYTES	Synurophyceae	Synurales	Mallomonadaceae	Litt. Rev.	**Autotroph**
Spiniferomonas	CHRYSOPHYTES	Synurophyceae	Synurales	Synuraceae	DB Scrap.	**Autotroph**
Synura	CHRYSOPHYTES	Synurophyceae	Synurales	Synuraceae	Litt. Rev.	**Autotroph**
Centritractus	YELLOW-GREEN ALGAE	Xanthophyceae	Mischococcales	Centritractaceae	DB Scrap.	**Autotroph**
Characiopsis	YELLOW-GREEN ALGAE	Xanthophyceae	Mischococcales	Characiopsidaceae	Litt. Rev.	**Autotroph**

Peroniella	YELLOW-GREEN ALGAE	Xanthophyceae	Mischococcales	Characiopsidaceae	Litt. Rev.	**Autotroph**
Ophiocytium	YELLOW-GREEN ALGAE	Xanthophyceae	Mischococcales	Ophiocytiaceae	DB Scrap.	**Autotroph**

RÉFÉRENCES

Anderies, J. M. et Beisner, B. E. (2000). Fluctuating Environments and Phytoplankton Community Structure: A Stochastic Model. *The American Naturalist*, *155*(4), 556-569. https://doi.org/10.1086/303336

Arenovski, A. L., Lim, E. L. et Caron, D. A. (1995). Mixotrophic nanoplankton in oligotrophic surface waters of the Sargasso Sea may employ phagotrophy to obtain major nutrients. *Journal of Plankton Research*, *17*(4), 801-820. https://doi.org/10.1093/plankt/17.4.801

Beisner, B. E., Grossart, H.-P. et Gasol, J. M. (2019). A guide to methods for estimating phago-mixotrophy in nanophytoplankton. *Journal of Plankton Research*, *41*(2), 77-89. https://doi.org/10.1093/plankt/fbz008

Beisner, B. E. et Longhi, M. L. (2013). Spatial overlap in lake phytoplankton: Relations with environmental factors and consequences for diversity. *Limnology and Oceanography*, *58*(4), 1419-1430. https://doi.org/10.4319/lo.2013.58.4.1419

Bella, D. A. (1970). Simulating the Effect of Sinking and Vertical Mixing on Algal Population Dynamics. *Journal (Water Pollution Control Federation)*, *42*(5), R140-R152.

Belsley, D. A., Kuh, E. et Welsch, R. E. (1980). *Regression Diagnostics: Identifying Influential Data and Sources of Collinearity*. John Wiley & Sons.

Berge, T., Chakraborty, S., Hansen, P. J. et Andersen, K. H. (2017). Modeling succession of key resource-harvesting traits of mixotrophic plankton. *The ISME Journal*, *11*(1), 212-223. https://doi.org/10.1038/ismej.2016.92

Bergquist, A. M., Carpenter, S. R. et Latino, J. C. (1985). Shifts in phytoplankton size structure and community composition during grazing by contrasting zooplankton assemblages1: Phytoplankton size structure. *Limnology and Oceanography*, *30*(5), 1037-1045. https://doi.org/10.4319/lo.1985.30.5.1037

Bergström, A.-K. (2009). Seasonal dynamics of bacteria and mixotrophic flagellates as related to input of allochthonous dissolved organic carbon. *SIL Proceedings, 1922-2010*, *30*(6), 923-928. https://doi.org/10.1080/03680770.2009.11902273

Bergström, A.-K., Jansson, M., Blomqvist, P. et Drakare, S. (2000). The influence of water colour and effective light climate on mixotrophic phytoflagellates in three small Swedish dystrophic lakes. *SIL Proceedings, 1922-2010*, *27*(4), 1861-1865. https://doi.org/10.1080/03680770.1998.11901562

Bird, D. F. et Kalff, J. (1987). Algal phagotrophy: Regulating factors and importance relative to photosynthesis in Dinobryon (Chrysophyceae)1. *Limnology and Oceanography*, *32*(2), 277-284. https://doi.org/10.4319/lo.1987.32.2.0277

Birge, E. A. (1910). An unregarded factor in lakes temperatures. *Transactions of the Wisconsin Academy of Sciences, Arts and Letters*, *16*, 989-1004.

Bock, N. A., Charvet, S., Burns, J., Gyaltshen, Y., Rozenberg, A., Duhamel, S. et Kim, E. (2021). Experimental identification and in silico prediction of bacterivory in green algae. *The ISME Journal*, *15*(7), 1987-2000. https://doi.org/10.1038/s41396-021-00899-w

Bonachela, J. A., Klausmeier, C. A., Edwards, K. F., Litchman, E. et Levin, S. A. (2016). The role of phytoplankton diversity in the emergent oceanic stoichiometry. *Journal of Plankton Research*, *38*(4), 1021-1035. https://doi.org/10.1093/plankt/fbv087

Borgnino, M., Arrieta, J., Boffetta, G., De Lillo, F. et Tuval, I. (2019). Turbulence induces clustering and segregation of non-motile, buoyancy-regulating phytoplankton. *Journal of The Royal Society Interface*, *16*(159), 20190324. https://doi.org/10.1098/rsif.2019.0324

Borics, G., Abonyi, A., Salmaso, N. et Ptacnik, R. (2021). Freshwater phytoplankton diversity: models, drivers and implications for ecosystem properties. *Hydrobiologia*, *848*(1), 53-75. https://doi.org/10.1007/s10750-020-04332-9

Bracco, A., Provenzale, A. et Scheuring, I. (2000). Mesoscale vortices and the paradox of the plankton. *Proceedings of the Royal Society of London. Series B: Biological Sciences*, *267*(1454), 1795-1800. https://doi.org/10.1098/rspb.2000.1212

Breiman, L. (2001). Random Forests. *Machine Learning*, *45*(1), 5-32. https://doi.org/10.1023/A:1010933404324

Bulling, M. T., Hicks, N., Murray, L., Paterson, D. M., Raffaelli, D., White, P. C. L. et Solan, M. (2010). Marine biodiversity–ecosystem functions under uncertain environmental futures. *Philosophical Transactions of the Royal Society B: Biological Sciences*, *365*(1549), 2107-2116. https://doi.org/10.1098/rstb.2010.0022

Burkholder, J. M., Glibert, P. M. et Skelton, H. M. (2008). Mixotrophy, a major mode of nutrition for harmful algal species in eutrophic waters. *Harmful Algae*, *8*(1), 77-93. https://doi.org/10.1016/j.hal.2008.08.010

Burson, A., Stomp, M., Greenwell, E., Grosse, J. et Huisman, J. (2018). Competition for nutrients and light: testing advances in resource competition with a natural phytoplankton community. *Ecology*, *99*(5), 1108-1118. https://doi.org/10.1002/ecy.2187

Calbet, A., Martínez, R. A., Isari, S., Zervoudaki, S., Nejstgaard, J. C., Pitta, P., Sazhin, A. F., Sousoni, D., Gomes, A., Berger, S. A., Tsagaraki, T. M. et Ptacnik, R. (2012). Effects of light availability on mixotrophy and microzooplankton grazing in an oligotrophic plankton food web: Evidences from a mesocosm study in Eastern Mediterranean waters. *Journal of Experimental Marine Biology and Ecology*, *424-425*, 66-77. https://doi.org/10.1016/j.jembe.2012.05.005

Camacho, A. (2006). On the occurrence and ecological features of deep chlorophyll maxima (DCM) in Spanish stratified lakes. *Limnetica*, *25*(1-2), 453-478.

Cantin, A., Beisner, B. E., Gunn, J. M., Prairie, Y. T. et Winter, J. G. (2011). Effects of thermocline deepening on lake plankton communities. *Canadian Journal of Fisheries and Aquatic Sciences*, *68*(2), 260-276. https://doi.org/10.1139/F10-138

Canty, A. et Ripley, B. (2021). *boot: Bootstrap R (S-Plus) Functions (version 1.3.28)*. https://CRAN.R-project.org/package=boot

Chan, Y.-F., Chiang, K.-P., Ku, Y. et Gong, G.-C. (2019). Abiotic and Biotic Factors Affecting the Ingestion Rates of Mixotrophic Nanoflagellates (Haptophyta). *Microbial Ecology*, *77*(3), 607-615. https://doi.org/10.1007/s00248-018-1249-2

Clegg, M. R., Maberly, S. C. et Jones, R. I. (2007). Behavioral response as a predictor of seasonal depth distribution and vertical niche separation in freshwater phytoplanktonic flagellates. *Limnology and Oceanography*, *52*(1), 441-455. https://doi.org/10.4319/lo.2007.52.1.0441

Colina, M., Calliari, D., Carballo, C. et Kruk, C. (2016). A trait-based approach to summarize zooplankton–phytoplankton interactions in freshwaters. *Hydrobiologia*, *767*(1), 221-233. https://doi.org/10.1007/s10750-015-2503-y

Connell, J. H. (1961). The Influence of Interspecific Competition and Other Factors on the Distribution of the Barnacle Chthamalus Stellatus. *Ecology*, *42*(4), 710-723. https://doi.org/10.2307/1933500

Connell, J. H. (1978). Diversity in Tropical Rain Forests and Coral Reefs. *Science*, *199*(4335), 1302-1310. https://doi.org/10.1126/science.199.4335.1302

Crane, K. W. et Grover, J. P. (2010). Coexistence of mixotrophs, autotrophs, and heterotrophs in planktonic microbial communities. *Journal of Theoretical Biology*, *262*(3), 517-527. https://doi.org/10.1016/j.jtbi.2009.10.027

Cremella, B. (2022, mars). *Optimization of Phytoplankton Pigments in Response to Water Column Irradiance in Canadian Lakes* [Poster]. GRIL Symposium 2022, Montréal.

Cuthbert, I. D. et del Giorgio, P. (1992). Toward a standard method of measuring color in freshwater. *Limnology and Oceanography*, *37*(6), 1319-1326. https://doi.org/10.4319/lo.1992.37.6.1319

Daly, A. J., Baetens, J. M. et De Baets, B. (2018). Ecological Diversity: Measuring the Unmeasurable. *Mathematics*, *6*(7), 119. https://doi.org/10.3390/math6070119

Dolan, J. R. et Pérez, M. T. (2000). Costs, benefits and characteristics of mixotrophy in marine oligotrichs. *Freshwater Biology*, *45*(2), 227-238. https://doi.org/10.1046/j.1365-2427.2000.00659.x

Droop, M. R. (1968). Vitamin B12 and Marine Ecology. IV. The Kinetics of Uptake, Growth and Inhibition in Monochrysis Lutheri. *Journal of the Marine Biological Association of the United Kingdom*, *48*(3), 689-733. https://doi.org/10.1017/S0025315400019238

Edwards, K. F. (2019). Mixotrophy in nanoflagellates across environmental gradients in the ocean. *Proceedings of the National Academy of Sciences*, *116*(13), 6211-6220. https://doi.org/10.1073/pnas.1814860116

Edwards, K. F., Litchman, E. et Klausmeier, C. A. (2013a). Functional traits explain phytoplankton community structure and seasonal dynamics in a marine ecosystem. *Ecology Letters*, *16*(1), 56-63. https://doi.org/10.1111/ele.12012

Edwards, K. F., Litchman, E. et Klausmeier, C. A. (2013b). Functional traits explain phytoplankton responses to environmental gradients across lakes of the United States. *Ecology*, *94*(7), 1626-1635. https://doi.org/10.1890/12-1459.1

Edwards, K. F., Thomas, M. K., Klausmeier, C. A. et Litchman, E. (2012). Allometric scaling and taxonomic variation in nutrient utilization traits and maximum growth rate of phytoplankton. *Limnology and Oceanography*, *57*(2), 554-566. https://doi.org/10.4319/lo.2012.57.2.0554

Elliott, J. A., Irish, A. E. et Reynolds, C. S. (2002). Predicting the spatial dominance of phytoplankton in a light limited and incompletely mixed eutrophic water column using the PROTECH model. *Freshwater Biology*, *47*(3), 433-440. https://doi.org/10.1046/j.1365-2427.2002.00813.x

EPA NLA. (2009). *National Lakes Assessment: A Collaborative Survey of the Nation's Lakes* (EPA 841-R-09-001). Office of Water and Office of Research and Development, US Environmental Protection Agency. https://www.epa.gov/sites/default/files/2013-11/documents/nla_newlowres_fullrpt.pdf#page=26

Faure, E., Not, F., Benoiston, A.-S., Labadie, K., Bittner, L. et Ayata, S.-D. (2019). Mixotrophic protists display contrasted biogeographies in the global ocean. *The ISME Journal*, *13*(4), 1072-1083. https://doi.org/10.1038/s41396-018-0340-5

Fischer, R., Giebel, H.-A., Hillebrand, H. et Ptacnik, R. (2017). Importance of mixotrophic bacterivory can be predicted by light and loss rates. *Oikos*, *126*(5), 713-722. https://doi.org/10.1111/oik.03539

Flynn, K. J. et Mitra, A. (2009). Building the « perfect beast »: modelling mixotrophic plankton. *Journal of Plankton Research*, *31*(9), 965-992. https://doi.org/10.1093/plankt/fbp044

Flynn, K. J., Mitra, A., Anestis, K., Anschütz, A. A., Calbet, A., Ferreira, G. D., Gypens, N., Hansen, P. J., John, U., Martin, J. L., Mansour, J. S., Maselli, M., Medić, N., Norlin, A., Not, F., Pitta, P., Romano, F., Saiz, E., Schneider, L. K., … Traboni, C. (2019). Mixotrophic protists and a new paradigm for marine ecology: where does plankton research go now? *Journal of Plankton Research*, *41*(4), 375-391. https://doi.org/10.1093/plankt/fbz026

Flynn, K. J., Stoecker, D. K., Mitra, A., Raven, J. A., Glibert, P. M., Hansen, P. J., Granéli, E. et Burkholder, J. M. (2013). Misuse of the phytoplankton–zooplankton dichotomy: the need

to assign organisms as mixotrophs within plankton functional types. *Journal of Plankton Research*, *35*(1), 3-11. https://doi.org/10.1093/plankt/fbs062

Fugère, V., Hébert, M.-P., da Costa, N. B., Xu, C. C. Y., Barrett, R. D. H., Beisner, B. E., Bell, G., Fussmann, G. F., Shapiro, B. J., Yargeau, V. et Gonzalez, A. (2020). Community rescue in experimental phytoplankton communities facing severe herbicide pollution. *Nature Ecology & Evolution*, *4*(4), 578-588. https://doi.org/10.1038/s41559-020-1134-5

Garner, R. E., Kraemer, S. A., Onana, V. E., Huot, Y., Gregory-Eaves, I. et Walsh, D. A. (2022). Protist Diversity and Metabolic Strategy in Freshwater Lakes Are Shaped by Trophic State and Watershed Land Use on a Continental Scale. *mSystems*, *0*(0), e00316-22. https://doi.org/10.1128/msystems.00316-22

Gasol, J. M., Simons, A. M. et Kalff, J. (1995). Patterns in the top-down versus bottom-up regulation of heterotrophic nanoflagellates in temperate lakes. *Journal of Plankton Research*, *17*(10), 1879-1903. https://doi.org/10.1093/plankt/17.10.1879

Gause, G. F. (1934). Experimental Analysis of Vito Volterra's Mathematical Theory of the Struggle for Existence. *Science, New Series*, *79*(2036), 16-17.

Gauthier, J., Prairie, Y. T. et Beisner, B. E. (2014). Thermocline deepening and mixing alter zooplankton phenology, biomass and body size in a whole-lake experiment. *Freshwater Biology*, *59*(5), 998-1011. https://doi.org/10.1111/fwb.12322

Geider, R. J., Maclntyre, H. L. et Kana, T. M. (1998). A dynamic regulatory model of phytoplanktonic acclimation to light, nutrients, and temperature. *Limnology and Oceanography*, *43*(4), 679-694. https://doi.org/10.4319/lo.1998.43.4.0679

George, D. G. et Heaney, S. I. (1978). Factors Influencing the Spatial Distribution of Phytoplankton in a Small Productive Lake. *Journal of Ecology*, *66*(1), 133-155. https://doi.org/10.2307/2259185

Gervais, F. (2003). Small-scale vertical distribution of phytoplankton, nutrients and sulphide below the oxycline of a mesotrophic lake. *Journal of Plankton Research*, *25*(3), 273-278. https://doi.org/10.1093/plankt/25.3.273

Ghyoot, C., Flynn, K. J., Mitra, A., Lancelot, C. et Gypens, N. (2017). Modeling Plankton Mixotrophy: A Mechanistic Model Consistent with the Shuter-Type Biochemical Approach. *Frontiers in Ecology and Evolution*, *5*, art78. https://doi.org/10.3389/fevo.2017.00078

Glibert, P. M. (2016). Margalef revisited: A new phytoplankton mandala incorporating twelve dimensions, including nutritional physiology. *Harmful Algae*, *55*, 25-30. https://doi.org/10.1016/j.hal.2016.01.008

Grace, J. B., Schoolmaster, D. R., Guntenspergen, G. R., Little, A. M., Mitchell, B. R., Miller, K. M. et Schweiger, E. W. (2012). Guidelines for a graph-theoretic implementation of

structural equation modeling. *Ecosphere, 3*(8), art73. https://doi.org/10.1890/ES12-00048.1

Grover, J. P. (1991). Resource Competition in a Variable Environment: Phytoplankton Growing According to the Variable-Internal-Stores Model. *The American Naturalist*, *138*(4), 811-835.

Hansson, T. H., Grossart, H.-P., Giorgio, P. A. del, St-Gelais, N. F. et Beisner, B. E. (2019). Environmental drivers of mixotrophs in boreal lakes. *Limnology and Oceanography*, *64*(4), 1688-1705. https://doi.org/10.1002/lno.11144

Hardin, G. (1960). The Competitive Exclusion Principle. *Science*, *131*(3409), 1292-1297.

Hassell, M. P., Comins, H. N. et May, R. M. (1994). Species coexistence and self-organizing spatial dynamics. *Nature*, *370*(6487), 290-292. https://doi.org/10.1038/370290a0

Hébert, M.-P., Beisner, B. E. et Maranger, R. (2017). Linking zooplankton communities to ecosystem functioning: toward an effect-trait framework. *Journal of Plankton Research*, *39*(1), 3-12. https://doi.org/10.1093/plankt/fbw068

Hessen, D. O. (1992). Dissolved organic carbon in a humic lake: effects on bacterial production and respiration. *Hydrobiologia*, *229*(1), 115-123. https://doi.org/10.1007/BF00006995

Hillebrand, H., Dürselen, C.-D., Kirschtel, D., Pollingher, U. et Zohary, T. (1999). Biovolume Calculation for Pelagic and Benthic Microalgae. *Journal of Phycology*, *35*(2), 403-424. https://doi.org/10.1046/j.1529-8817.1999.3520403.x

Hollister, J. W., Milstead, W. B. et Kreakie, B. J. (2016). Modeling lake trophic state: a random forest approach. *Ecosphere*, *7*(3), e01321. https://doi.org/10.1002/ecs2.1321

Hothorn, T., Hornik, K. et Zeileis, A. (2006). Unbiased Recursive Partitioning: A Conditional Inference Framework. *Journal of Computational and Graphical Statistics*, *15*(3), 651-674. https://doi.org/10.1198/106186006X133933

Huisman, J., Sharples, J., Stroom, J. M., Visser, P. M., Kardinaal, W. E. A., Verspagen, J. M. H. et Sommeijer, B. (2004). Changes in turbulent mixing shift competition for light between phytoplankton species. *Ecology*, *85*(11), 2960-2970. https://doi.org/10.1890/03-0763

Huisman, J., van Oostveen, P. et Weissing, F. J. (1999). Species Dynamics in Phytoplankton Blooms: Incomplete Mixing and Competition for Light. *The American Naturalist*, *154*(1), 46-68. https://doi.org/10.1086/303220

Huisman, J. et Weissing, F. J. (1995). Competition for Nutrients and Light in a Mixed Water Column: A Theoretical Analysis. *The American Naturalist*, *146*(4), 536-564. https://doi.org/10.1086/285814

Huot, Y., Brown, C. A., Potvin, G., Antoniades, D., Baulch, H. M., Beisner, B. E., Bélanger, S., Brazeau, S., Cabana, H., Cardille, J. A., del Giorgio, P. A., Gregory-Eaves, I., Fortin, M.-

J., Lang, A. S., Laurion, I., Maranger, R., Prairie, Y. T., Rusak, J. A., Segura, P. A., … Walsh, D. A. (2019). The NSERC Canadian Lake Pulse Network: A national assessment of lake health providing science for water management in a changing climate. *Science of The Total Environment, 695,* 133668. https://doi.org/10.1016/j.scitotenv.2019.133668

Hutchinson, G. E. (1961). The Paradox of the Plankton. *The American Naturalist*, *95*(882), 137-145. https://doi.org/10.1086/282171

Interlandi, S. J. et Kilham, S. S. (2001). Limiting Resources and the Regulation of Diversity in Phytoplankton Communities. *Ecology*, *82*(5), 1270-1282. https://doi.org/10.1890/0012-9658(2001)082[1270:LRATRO]2.0.CO;2

Jäger, C. G., Diehl, S. et Schmidt, G. M. (2008). Influence of water-column depth and mixing on phytoplankton biomass, community composition, and nutrients. *Limnology and Oceanography*, *53*(6), 2361-2373. https://doi.org/10.4319/lo.2008.53.6.2361

Jansson, M. (1993). Uptake, exchange and excretion of orthophosphate in phosphate-starved Scenedesmus quadricauda and Pseudomonas K7. *Limnology and Oceanography*, *38*(6), 1162-1178. https://doi.org/10.4319/lo.1993.38.6.1162

Jansson, M., Bergström, A.-K., Lymer, D., Vrede, K. et Karlsson, J. (2006). Bacterioplankton Growth and Nutrient Use Efficiencies Under Variable Organic Carbon and Inorganic Phosphorus Ratios. *Microbial Ecology*, *52*(2), 358-364. https://doi.org/10.1007/s00248-006-9013-4

Jaworski, G. H. M., Talling, J. F. et Heaney, S. I. (2003). Potassium dependence and phytoplankton ecology: an experimental study. *Freshwater Biology*, *48*(5), 833-840. https://doi.org/10.1046/j.1365-2427.2003.01051.x

Joint, I., Henriksen, P., Fonnes, G. A., Bourne, D., Thingstad, T. F. et Riemann, B. (2002). Competition for inorganic nutrients between phytoplankton and bacterioplankton in nutrient manipulated mesocosms. *Aquatic Microbial Ecology*, *29*(2), 145-159. https://doi.org/10.3354/ame029145

Jones, H. (1997). A classification of mixotrophic protists based on their behaviour. *Freshwater Biology*, *37*(1), 35-43. https://doi.org/10.1046/j.1365-2427.1997.00138.x

Jones, R. I. (2000). Mixotrophy in planktonic protists: an overview. *Freshwater Biology*, *45*(2), 219-226. https://doi.org/10.1046/j.1365-2427.2000.00672.x

Klausmeier, C. A. et Litchman, E. (2001). Algal games: The vertical distribution of phytoplankton in poorly mixed water columns. *Limnology and Oceanography*, *46*(8), 1998-2007. https://doi.org/10.4319/lo.2001.46.8.1998

Kooijman, S. A. L. M., Dijkstra, H. A. et Kooi, B. W. (2002). Light-induced Mass Turnover in a Mono-species Community of Mixotrophs. *Journal of Theoretical Biology*, *214*(2), 233-254. https://doi.org/10.1006/jtbi.2001.2458

Kroer, N. (1993). Bacterial growth efficiency on natural dissolved organic matter. *Limnology and Oceanography*, *38*(6), 1282-1290. https://doi.org/10.4319/lo.1993.38.6.1282

Laliberté, E. et Legendre, P. (2010). A distance-based framework for measuring functional diversity from multiple traits. *Ecology*, *91*(1), 299-305. https://doi.org/10.1890/08-2244.1

Laliberté, E., Legendre, P. et Shipley, B. (2014). *FD: Measuring functional diversity (FD) from multiple traits, and other tools for functional ecology (R package version 1.0-12)*. https://CRAN.R-project.org/package=FD

Lambert, B. S., Groussman, R. D., Schatz, M. J., Coesel, S. N., Durham, B. P., Alverson, A. J., White, A. E. et Armbrust, E. V. (2022). The dynamic trophic architecture of open-ocean protist communities revealed through machine-guided metatranscriptomics. *Proceedings of the National Academy of Sciences*, *119*(7), e2100916119. https://doi.org/10.1073/pnas.2100916119

Laplace-Treyture, C., Derot, J., Prévost, E., Le Mat, A. et Jamoneau, A. (2021). Phytoplankton morpho-functional trait dataset from French water-bodies. *Scientific Data*, *8*(1), 40. https://doi.org/10.1038/s41597-021-00814-0

Leach, T. H., Beisner, B. E., Carey, C. C., Pernica, P., Rose, K. C., Huot, Y., Brentrup, J. A., Domaizon, I., Grossart, H.-P., Ibelings, B. W., Jacquet, S., Kelly, P. T., Rusak, J. A., Stockwell, J. D., Straile, D. et Verburg, P. (2018). Patterns and drivers of deep chlorophyll maxima structure in 100 lakes: The relative importance of light and thermal stratification: Patterns and drivers of DCM structure across lakes. *Limnology and Oceanography*, *63*(2), 628-646. https://doi.org/10.1002/lno.10656

Legendre, P. et Gallagher, E. D. (2001). Ecologically meaningful transformations for ordination of species data. *Oecologia*, *129*(2), 271-280. https://doi.org/10.1007/s004420100716

Legendre, P., Oksanen, J. et ter Braak, C. J. F. (2011). Testing the significance of canonical axes in redundancy analysis. *Methods in Ecology and Evolution*, *2*(3), 269-277. https://doi.org/10.1111/j.2041-210X.2010.00078.x

Leles, S. G., Mitra, A., Flynn, K. J., Stoecker, D. K., Hansen, P. J., Calbet, A., McManus, G. B., Sanders, R. W., Caron, D. A., Not, F., Hallegraeff, G. M., Pitta, P., Raven, J. A., Johnson, M. D., Glibert, P. M. et Våge, S. (2017). Oceanic protists with different forms of acquired phototrophy display contrasting biogeographies and abundance. *Proceedings of the Royal Society B: Biological Sciences*, *284*(1860), 20170664. https://doi.org/10.1098/rspb.2017.0664

Leles, S. G., Mitra, A., Flynn, K. J., Tillmann, U., Stoecker, D., Jeong, H. J., Burkholder, J., Hansen, P. J., Caron, D. A., Glibert, P. M., Hallegraeff, G., Raven, J. A., Sanders, R. W. et Zubkov, M. (2019). Sampling bias misrepresents the biogeographical significance of constitutive mixotrophs across global oceans. *Global Ecology and Biogeography*, *28*(4), 418-428. https://doi.org/10.1111/geb.12853

Leles, S. G., Polimene, L., Bruggeman, J., Blackford, J., Ciavatta, S., Mitra, A. et Flynn, K. J. (2018). Modelling mixotrophic functional diversity and implications for ecosystem function. *Journal of Plankton Research*, *40*(6), 627-642. https://doi.org/10.1093/plankt/fby044

Lepori-Bui, M., Paight, C., Eberhard, E., Mertz, C. M. et Moeller, H. V. (2022). Evidence for evolutionary adaptation of mixotrophic nanoflagellates to warmer temperatures. *Global Change Biology*, *28*(23), 7094-7107. https://doi.org/10.1111/gcb.16431

Li, L. et Chesson, P. (2016). The Effects of Dynamical Rates on Species Coexistence in a Variable Environment: The Paradox of the Plankton Revisited. *The American Naturalist*, *188*(2), E46-E58. https://doi.org/10.1086/687111

Li, Q., Edwards, K. F., Schvarcz, C. R., Selph, K. E. et Steward, G. F. (2021). Plasticity in the grazing ecophysiology of Florenciella (Dichtyochophyceae), a mixotrophic nanoflagellate that consumes Prochlorococcus and other bacteria. *Limnology and Oceanography*, *66*(1), 47-60. https://doi.org/10.1002/lno.11585

Litchman, E., de Tezanos Pinto, P., Edwards, K. F., Klausmeier, C. A., Kremer, C. T. et Thomas, M. K. (2015). Global biogeochemical impacts of phytoplankton: a trait-based perspective. *Journal of Ecology*, *103*(6), 1384-1396. https://doi.org/10.1111/1365-2745.12438

Litchman, E., de Tezanos Pinto, P., Klausmeier, C. A., Thomas, M. K. et Yoshiyama, K. (2010). Linking traits to species diversity and community structure in phytoplankton. *Hydrobiologia*, *653*(1), 15-28. https://doi.org/10.1007/s10750-010-0341-5

Litchman, E. et Klausmeier, C. A. (2008). Trait-Based Community Ecology of Phytoplankton. *Annual Review of Ecology, Evolution, and Systematics*, *39*(1), 615-639. https://doi.org/10.1146/annurev.ecolsys.39.110707.173549

Litchman, E., Klausmeier, C. A., Schofield, O. M. et Falkowski, P. G. (2007). The role of functional traits and trade-offs in structuring phytoplankton communities: scaling from cellular to ecosystem level. *Ecology Letters*, *10*(12), 1170-1181. https://doi.org/10.1111/j.1461-0248.2007.01117.x

Litchman, E., Klausmeier, C. A. et Yoshiyama, K. (2009). Contrasting size evolution in marine and freshwater diatoms. *Proceedings of the National Academy of Sciences*, *106*(8), 2665-2670. https://doi.org/10.1073/pnas.0810891106

Longhi, M. L. et Beisner, B. E. (2009). Environmental factors controlling the vertical distribution of phytoplankton in lakes. *Journal of Plankton Research*, *31*(10), 1195-1207. https://doi.org/10.1093/plankt/fbp065

Margalef, R. (1978). Life-forms of phytoplankton as survival alternatives in an unstable environment. *Oceanologica acta*, *134*, 493-509.

Mccauley, E. (1984). The Estimation of the Abundance and Biomass of Zooplankton in Samples. Dans *Manual on Methods for the Assessment of Secondary Productivity in Fresh Waters* (Downing J.A. & Rigler F.H., p. 228-265). Blackwell Scientific Publications.

McCauley, E. et Briand, F. (1979). Zooplankton grazing and phytoplankton species richness: Field tests of the predation hypothesis. *Limnology and Oceanography*, *24*(2), 243-252. https://doi.org/10.4319/lo.1979.24.2.0243

McGill, B., Enquist, B., Weiher, E. et Westoby, M. (2006). Rebuilding community ecology from functional traits. *Trends in Ecology & Evolution*, *21*(4), 178-185. https://doi.org/10.1016/j.tree.2006.02.002

Menge, B. A. et Sutherland, J. P. (1976). Species Diversity Gradients: Synthesis of the Roles of Predation, Competition, and Temporal Heterogeneity. *The American Naturalist*, *110*(973), 351-369. https://doi.org/10.1086/283073

Menon, P., Becquevort, S., Billen, G. et Servais, P. (1996). Kinetics of flagellate grazing in the presence of two types of bacterial prey. *Microbial Ecology*, *31*(1), 89-101. https://doi.org/10.1007/BF00175078

Messager, M. L., Lehner, B., Grill, G., Nedeva, I. et Schmitt, O. (2016). Estimating the volume and age of water stored in global lakes using a geo-statistical approach. *Nature Communications*, *7*(1), 1-11. https://doi.org/10.1038/ncomms13603

Mitra, A. et Flynn, K. J. (2010). Modelling mixotrophy in harmful algal blooms: More or less the sum of the parts? *Journal of Marine Systems*, *83*(3-4), 158-169. https://doi.org/10.1016/j.jmarsys.2010.04.006

Mitra, A., Flynn, K. J., Burkholder, J. M., Berge, T., Calbet, A., Raven, J. A., Granéli, E., Glibert, P. M., Hansen, P. J., Stoecker, D. K., Thingstad, F., Tillmann, U., Våge, S., Wilken, S. et Zubkov, M. V. (2014). The role of mixotrophic protists in the biological carbon pump. *Biogeosciences*, *11*(4), 995-1005. https://doi.org/10.5194/bg-11-995-2014

Mitra, A., Flynn, K. J., Tillmann, U., Raven, J. A., Caron, D., Stoecker, D. K., Not, F., Hansen, P. J., Hallegraeff, G., Sanders, R., Wilken, S., McManus, G., Johnson, M., Pitta, P., Våge, S., Berge, T., Calbet, A., Thingstad, F., Jeong, H. J., … Lundgren, V. (2016). Defining Planktonic Protist Functional Groups on Mechanisms for Energy and Nutrient Acquisition: Incorporation of Diverse Mixotrophic Strategies. *Protist*, *167*(2), 106-120. https://doi.org/10.1016/j.protis.2016.01.003

Moeller, H. V., Neubert, M. G. et Johnson, M. D. (2019). Intraguild predation enables coexistence of competing phytoplankton in a well-mixed water column. *Ecology*, *100*(12). https://doi.org/10.1002/ecy.2874

Monod, J. (1950). Technique, Theory and Applications of Continuous Culture. *Ann. Inst. Pasteur*, *79*(4), 390-410.

Mouillot, D., Stubbs, W., Faure, M., Dumay, O., Tomasini, J. A., Wilson, J. B. et Chi, T. D. (2005). Niche overlap estimates based on quantitative functional traits: a new family of non-parametric indices. *Oecologia*, *145*(3), 345-353. https://doi.org/10.1007/s00442-005-0151-z

Muñoz-Sabater, J., Dutra, E., Agustí-Panareda, A., Albergel, C., Arduini, G., Balsamo, G., Boussetta, S., Choulga, M., Harrigan, S., Hersbach, H., Martens, B., Miralles, D. G., Piles, M., Rodríguez-Fernández, N. J., Zsoter, E., Buontempo, C. et Thépaut, J.-N. (2021). ERA5-Land: a state-of-the-art global reanalysis dataset for land applications. *Earth System Science Data*, *13*(9), 4349-4383. https://doi.org/10.5194/essd-13-4349-2021

NASA/LARC/SD/ASDC. (2017). CERES and GEO-Enhanced TOA, Within-Atmosphere and Surface Fluxes, Clouds and Aerosols Monthly-Averaged 1-Hourly Terra-Aqua Edition4A [Data set]. *NASA Langley Atmospheric Science Data Center DAAC*. https://doi.org/10.5067/Terra+Aqua/CERES/SYN1deg-MHour_L3.004A

Oksanen, J., Blanchet, F. G., Friendly, M., Kindt, R., Legendre, P., McGlinn, D., Minchin, P. R., O'Hara, R. B., Simpson, G. L., Solymos, P., Stevens, M. H. H., Szoecs, E. et Wagner, H. (2020). *vegan: Community Ecology Package (R package version 2.5-7)*. https://CRAN.R-project.org/package=vegan

Olenina, I., Hajdu, S., Edler, L., Andersson, A., Wasmund, N., Busch, S., Göbel, J., Gromisz, S., Huseby, S., Huttunen, M., Jaanus, A., Kokkonen, P., Ledaine, I. et Niemkiewicz, E. (2006). Biovolumes and size-classes of phytoplankton in the Baltic Sea. *HELCOM, Balt. Sea Environ. Proc*, *106*, 1-144.

Olli, K. et Seppälä, J. (2001). Vertical niche separation of phytoplankton: large-scale mesocosm experiments. *Marine Ecology Progress Series*, *217*, 219-233. https://doi.org/10.3354/meps217219

Ouellet Jobin, V. et Beisner, B. E. (2014). Deep chlorophyll maxima, spatial overlap and diversity in phytoplankton exposed to experimentally altered thermal stratification. *Journal of Plankton Research*, *36*(4), 933-942. https://doi.org/10.1093/plankt/fbu036

Paerl, H. W. (1990). Physiological Ecology and Regulation of N2 Fixation in Natural Waters. Dans K. C. Marshall (dir.), *Advances in Microbial Ecology* (p. 305-344). Springer US. https://doi.org/10.1007/978-1-4684-7612-5_8

Paerl, H. W. et Huisman, J. (2009). Climate change: a catalyst for global expansion of harmful cyanobacterial blooms. *Environmental Microbiology Reports*, *1*(1), 27-37. https://doi.org/10.1111/j.1758-2229.2008.00004.x

Paradis, E. et Schliep, K. (2019). ape 5.0: an environment for modern phylogenetics and evolutionary analyses in R. *Bioinformatics (Oxford, England)*, *35*(3), 526-528. https://doi.org/10.1093/bioinformatics/bty633

Peres-Neto, P. R., Dray, S. et Braak, C. J. F. ter. (2017). Linking trait variation to the environment: critical issues with community-weighted mean correlation resolved by the fourth-corner approach. *Ecography*, *40*(7), 806-816. https://doi.org/10.1111/ecog.02302

Pérez, G., Queimaliños, C., Balseiro, E. et Modenutti, B. (2007). Phytoplankton absorption spectra along the water column in deep North Patagonian Andean lakes (Argentina). *Limnologica*, *37*(1), 3-16. https://doi.org/10.1016/j.limno.2006.08.005

Pielou, E. C. (1975). Ecological Diversity. Wiley.

Princiotta, S. D. et Sanders, R. W. (2017). Heterotrophic and mixotrophic nanoflagellates in a mesotrophic lake: Abundance and grazing impacts across season and depth. *Limnology and Oceanography*, *62*(2), 632-644. https://doi.org/10.1002/lno.10450

Princiotta, S. D., Smith, B. T. et Sanders, R. W. (2016). Temperature-dependent phagotrophy and phototrophy in a mixotrophic chrysophyte. *Journal of Phycology*, *52*(3), 432-440. https://doi.org/10.1111/jpy.12405

Ptacnik, R., Diehl, S. et Berger, S. (2003). Performance of sinking and nonsinking phytoplankton taxa in a gradient of mixing depths. *Limnology and Oceanography*, *48*(5), 1903-1912. https://doi.org/10.4319/lo.2003.48.5.1903

R Core Team. (2021). *R: A Language and Environment for Statistical Computing*. R Foundation for Statistical Computing. https://www.R-project.org/

Raven, J. A. (1997). Phagotrophy in phototrophs. *Limnology and Oceanography*, *42*(1), 198-205. https://doi.org/10.4319/lo.1997.42.1.0198

Read, J. S., Hamilton, D. P., Jones, I. D., Muraoka, K., Winslow, L. A., Kroiss, R., Wu, C. H. et Gaiser, E. (2011). Derivation of lake mixing and stratification indices from high-resolution lake buoy data. *Environmental Modelling & Software*, *26*(11), 1325-1336. https://doi.org/10.1016/j.envsoft.2011.05.006

Reynolds, C. S., Huszar, V., Kruk, C., Naselli-Flores, L. et Melo, S. (2002). Towards a functional classification of the freshwater phytoplankton. *Journal of Plankton Research*, *24*(5), 417-428. https://doi.org/10.1093/plankt/24.5.417

Reynolds, C. S., Wiseman, S. W., Godfrey, B. M. et Butterwick, C. (1983). Some effects of artificial mixing on the dynamics of phytoplankton populations in large limnetic enclosures. *Journal of Plankton Research*, *5*(2), 203-234. https://doi.org/10.1093/plankt/5.2.203

Rimet, F. et Druart, J.-C. (2018). A trait database for Phytoplankton of temperate lakes. *Annales de Limnologie - International Journal of Limnology*, *54*, 18. https://doi.org/10.1051/limn/2018009

Romano, F., Symiakaki, K. et Pitta, P. (2021). Temporal Variability of Planktonic Ciliates in a Coastal Oligotrophic Environment: Mixotrophy, Size Classes and Vertical Distribution. *Frontiers in Marine Science, 8*. https://doi.org/10.3389/fmars.2021.641589

Rosseel, Y. (2012). lavaan: An R Package for Structural Equation Modeling. *Journal of Statistical Software, 48*(2), 1-36. https://doi.org/10.18637/jss.v048.i02

Rothhaupt, K. O. (1996). Utilization of Substitutable Carbon and Phosphorus Sources by the Mixotrophic Chrysophyte Ochromonas Sp. *Ecology, 77*(3), 706-715. https://doi.org/10.2307/2265495

Roy, S. et Chattopadhyay, J. (2007). Towards a resolution of 'the paradox of the plankton': A brief overview of the proposed mechanisms. *Ecological Complexity, 4*(1-2), 26-33. https://doi.org/10.1016/j.ecocom.2007.02.016

Ryabov, A. B. et Blasius, B. (2011). A graphical theory of competition on spatial resource gradients. *Ecology Letters, 14*(3), 220-228. https://doi.org/10.1111/j.1461-0248.2010.01574.x

Saad, J. F., Schiaffino, M. R., Vinocur, A., O'Farrell, I., Tell, G. et Izaguirre, I. (2013). Microbial planktonic communities of freshwater environments from Tierra del Fuego: dominant trophic strategies in lakes with contrasting features. *Journal of Plankton Research, 35*(6), 1220-1233. https://doi.org/10.1093/plankt/fbt075

Saad, J. F., Unrein, F., Tribelli, P. M., López, N. et Izaguirre, I. (2016). Influence of lake trophic conditions on the dominant mixotrophic algal assemblages. *Journal of Plankton Research, 38*(4), 818-829. https://doi.org/10.1093/plankt/fbw029

Sager, P. E. et Hasler, A. D. (1969). Species Diversity in Lacustrine Phytoplankton. I. The Components of the Index of Diversity from Shannon's Formula. *The American Naturalist, 103*(929), 51-59, world. https://doi.org/10.1086/282581

Sanders, R. W., Porter, K. G. et Bennett, S. J. (1990). Heterotrophic, autotrophic, and mixotrophic nanoflagellates: Seasonal abundances and bacterivory in a eutrophic lake. *Limnology and Oceanography, 35*(8), 1821-1832. https://doi.org/10.4319/lo.1990.35.8.1821

Sarnelle, O. (2005). Daphnia as keystone predators: effects on phytoplankton diversity and grazing resistance. *Journal of Plankton Research, 27*(12), 1229-1238. https://doi.org/10.1093/plankt/fbi086

Sastri, A. R., Gauthier, J., Juneau, P. et Beisner, B. E. (2014). Biomass and productivity responses of zooplankton communities to experimental thermocline deepening. *Limnology and Oceanography, 59*(1), 1-16. https://doi.org/10.4319/lo.2014.59.1.0001

Schermelleh-Engel, K., Moosbrugger, H. et Müller, H. (2003). Evaluating the Fit of Structural Equation Models: Tests of Significance and Descriptive Goodness-of-Fit Measures. *Methods of Psychological Research, 8*(2), 23-74.

Selosse, M.-A., Charpin, M. et Not, F. (2017). Mixotrophy everywhere on land and in water: the grand écart hypothesis. *Ecology Letters, 20*(2), 246-263. https://doi.org/10.1111/ele.12714

Shampine, L. F. et Reichelt, M. W. (1997). The MATLAB ODE Suite. *SIAM Journal on Scientific Computing, 18*(1), 1-22. https://doi.org/10.1137/S1064827594276424

Shannon, C. E. (1948). A Mathematical Theory of Communication. *Bell System Technical Journal, 27*(3), 379-423. https://doi.org/10.1002/j.1538-7305.1948.tb01338.x

Shipley, B. (2000). *Cause and correlation in biology: a user's guide to path analysis, structural equations, and causal inference*. Cambridge University Press.

Šimek, K., Horňák, K., Jezbera, J., Nedoma, J., Vrba, J., Straškrábová, V., Macek, M., Dolan, J. R. et Hahn, M. W. (2006). Maximum growth rates and possible life strategies of different bacterioplankton groups in relation to phosphorus availability in a freshwater reservoir. *Environmental Microbiology, 8*(9), 1613-1624. https://doi.org/10.1111/j.1462-2920.2006.01053.x

Skeel, R. et Berzins, M. (1990). A Method for the Spatial Discretization of Parabolic Equations in One Space Variable. *SIAM J. Sci. Comput.* https://doi.org/10.1137/0911001

Skovgaard, A. (1996). Mixotrophy in Fragilidium subglobosum (Dinophyceae): growth and grazing responses as functions of light intensity. *Marine Ecology Progress Series, 143*, 247-253. https://doi.org/10.3354/meps143247

Smith, E. M. et Prairie, Y. T. (2004). Bacterial metabolism and growth efficiency in lakes: The importance of phosphorus availability. *Limnology and Oceanography, 49*(1), 137-147. https://doi.org/10.4319/lo.2004.49.1.0137

Sommer, U. (1984). The paradox of the plankton: Fluctuations of phosphorus availability maintain diversity of phytoplankton in flow-through cultures1. *Limnology and Oceanography, 29*(3), 633-636. https://doi.org/10.4319/lo.1984.29.3.0633

Sommer, U. (1985). Comparison between steady state and non-steady state competition: Experiments with natural phytoplankton: Phytoplankton competition. *Limnology and Oceanography, 30*(2), 335-346. https://doi.org/10.4319/lo.1985.30.2.0335

Sommer, U., Sommer, F., Santer, B., Jamieson, C., Boersma, M., Becker, C. et Hansen, T. (2001). Complementary impact of copepods and cladocerans on phytoplankton. *Ecology Letters, 4*(6), 545-550. https://doi.org/10.1046/j.1461-0248.2001.00263.x

Sonkoly, J., Kelemen, A., Valkó, O., Deák, B., Kiss, R., Tóth, K., Miglécz, T., Tóthmérész, B. et Török, P. (2019). Both mass ratio effects and community diversity drive biomass production in a grassland experiment. *Scientific Reports, 9*(1), 1848. https://doi.org/10.1038/s41598-018-37190-6

Stefan, H. G., Cardoni, J. J., Schiebe, F. R. et Cooper, C. M. (1983). Model of light penetration in a turbid lake. *Water Resources Research*, *19*(1), 109-120. https://doi.org/10.1029/WR019i001p00109

Stekhoven, D. J. et Bühlmann, P. (2012). MissForest—non-parametric missing value imputation for mixed-type data. *Bioinformatics*, *28*(1), 112-118. https://doi.org/10.1093/bioinformatics/btr597

Stoecker, D. K. (1998). Conceptual models of mixotrophy in planktonic protists and some ecological and evolutionary implications. *European Journal of Protistology*, *34*(3), 281-290. https://doi.org/10.1016/S0932-4739(98)80055-2

Stomp, M., Huisman, J., de Jongh, F., Veraart, A. J., Gerla, D., Rijkeboer, M., Ibelings, B. W., Wollenzien, U. I. A. et Stal, L. J. (2004). Adaptive divergence in pigment composition promotes phytoplankton biodiversity. *Nature*, *432*(7013), 104-107. https://doi.org/10.1038/nature03044

Striebel, M., Singer, G., Stibor, H. et Andersen, T. (2012). "Trophic overyielding": Phytoplankton diversity promotes zooplankton productivity. *Ecology*, *93*(12), 2719-2727. https://doi.org/10.1890/12-0003.1

Strobl, C., Boulesteix, A.-L., Zeileis, A. et Hothorn, T. (2007). Bias in random forest variable importance measures: Illustrations, sources and a solution. *BMC Bioinformatics*, *8*(1), 25. https://doi.org/10.1186/1471-2105-8-25

ter Braak, C. J. F. et Prentice, I. C. (1988). A Theory of Gradient Analysis. Dans M. Begon, A. H. Fitter, E. D. Ford et A. Macfadyen (dir.), *Advances in Ecological Research* (vol. 18, p. 271-317). Academic Press. https://doi.org/10.1016/S0065-2504(08)60183-X

Thingstad et Lignell, R. (1997). Theoretical models for the control of bacterial growth rate, abundance, diversity and carbon demand. *Aquatic Microbial Ecology*, *13*(1), 19-27. https://doi.org/10.3354/ame013019

Thingstad, T. F., Havskum, H., Garde, K. et Riemann, B. (1996). On the Strategy of « Eating Your Competitor »: A Mathematical Analysis of Algal Mixotrophy. *Ecology*, *77*(7), 2108-2118. https://doi.org/10.2307/2265705

Tilman, D. (1981). Tests of Resource Competition Theory Using Four Species of Lake Michigan Algae. *Ecology*, *62*(3), 802-815. https://doi.org/10.2307/1937747

Tilman, D., Isbell, F. et Cowles, J. M. (2014). Biodiversity and Ecosystem Functioning. *Annual Review of Ecology, Evolution, and Systematics*, *45*(1), 471-493. https://doi.org/10.1146/annurev-ecolsys-120213-091917

Tilman, D., Lehman, C. L. et Thomson, K. T. (1997). Plant diversity and ecosystem productivity: Theoretical considerations. *Proceedings of the National Academy of Sciences*, *94*(5), 1857-1861. https://doi.org/10.1073/pnas.94.5.1857

Tilman, D., Reich, P. B. et Knops, J. M. H. (2006). Biodiversity and ecosystem stability in a decade-long grassland experiment. *Nature*, *441*(7093), 629-632. https://doi.org/10.1038/nature04742

Tittel, J., Bissinger, V., Zippel, B., Gaedke, U., Bell, E., Lorke, A. et Kamjunke, N. (2003). Mixotrophs combine resource use to outcompete specialists: Implications for aquatic food webs. *Proceedings of the National Academy of Sciences*, *100*(22), 12776-12781. https://doi.org/10.1073/pnas.2130696100

Troost, T. A., Kooi, B. W. et Kooijman, S. A. L. M. (2005). Ecological Specialization of Mixotrophic Plankton in a Mixed Water Column. *The American Naturalist*, *166*(3), E45-E61. https://doi.org/10.1086/432038

Unrein, F., Gasol, J. M., Not, F., Forn, I. et Massana, R. (2014). Mixotrophic haptophytes are key bacterial grazers in oligotrophic coastal waters. *The ISME Journal*, *8*(1), 164-176. https://doi.org/10.1038/ismej.2013.132

Uszko, W., Diehl, S., Pitsch, N., Lengfellner, K. et Müller, T. (2015). When is a type III functional response stabilizing? Theory and practice of predicting plankton dynamics under enrichment. *Ecology*, *96*(12), 3243-3256. https://doi.org/10.1890/15-0055.1

Vad, C. F., Schneider, C., Lukić, D., Horváth, Z., Kainz, M. J., Stibor, H. et Ptacnik, R. (2020). Grazing resistance and poor food quality of a widespread mixotroph impair zooplankton secondary production. *Oecologia*, *193*(2), 489-502. https://doi.org/10.1007/s00442-020-04677-x

Våge, S., Castellani, M., Giske, J. et Thingstad, T. F. (2013). Successful strategies in size structured mixotrophic food webs. *Aquatic Ecology*, *47*(3), 329-347. https://doi.org/10.1007/s10452-013-9447-y

Vallina, S. M., Cermeno, P., Dutkiewicz, S., Loreau, M. et Montoya, J. M. (2017). Phytoplankton functional diversity increases ecosystem productivity and stability. *Ecological Modelling*, *361*, 184-196. https://doi.org/10.1016/j.ecolmodel.2017.06.020

Vasconcelos, F. R., Diehl, S., Rodríguez, P., Hedström, P., Karlsson, J. et Byström, P. (2019). Bottom-up and top-down effects of browning and warming on shallow lake food webs. *Global Change Biology*, *25*(2), 504-521. https://doi.org/10.1111/gcb.14521

Violle, C., Navas, M.-L., Vile, D., Kazakou, E., Fortunel, C., Hummel, I. et Garnier, E. (2007). Let the concept of trait be functional! *Oikos*, *116*(5), 882-892. https://doi.org/10.1111/j.0030-1299.2007.15559.x

Vrede, T. (1998). Elemental composition (C:N:P) and growth rates of bacteria and Rhodomonas grazed by Daphnia. *Journal of Plankton Research*, *20*(3), 455-470. https://doi.org/10.1093/plankt/20.3.455

Wall, D. et Briand, F. (1980). Spatial and temporal overlap in lake phytoplankton communities. *Archiv für Hydrobiologie*, *88*, 45-57.

Walsby, A. E., Hayes, P. K., Boje, R. et Stal, L. J. (1997). The selective advantage of buoyancy provided by gas vesicles for planktonic cyanobacteria in the Baltic Sea. *The New Phytologist*, *136*(3), 407-417. https://doi.org/10.1046/j.1469-8137.1997.00754.x

Ward, B. A., Dutkiewicz, S., Barton, A. D. et Follows, M. J. (2011). Biophysical Aspects of Resource Acquisition and Competition in Algal Mixotrophs. *The American Naturalist*, *178*(1), 98-112. https://doi.org/10.1086/660284

Weissing, F. J. et Huisman, J. (1994). Growth and Competition in a Light Gradient. *Journal of Theoretical Biology*, *168*(3), 323-336. https://doi.org/10.1006/jtbi.1994.1113

Weithoff, G. (2003a). The concepts of 'plant functional types' and 'functional diversity' in lake phytoplankton – a new understanding of phytoplankton ecology? *Freshwater Biology*, *48*(9), 1669-1675. https://doi.org/10.1046/j.1365-2427.2003.01116.x

Weithoff, G. (2003b). The concepts of 'plant functional types' and 'functional diversity' in lake phytoplankton – a new understanding of phytoplankton ecology? *Freshwater Biology*, *48*(9), 1669-1675. https://doi.org/10.1046/j.1365-2427.2003.01116.x

Wilken, S., Soares, M., Urrutia-Cordero, P., Ratcovich, J., Ekvall, M. K., Van Donk, E. et Hansson, L.-A. (2018). Primary producers or consumers? Increasing phytoplankton bacterivory along a gradient of lake warming and browning. *Limnology and Oceanography*, *63*(S1), S142-S155. https://doi.org/10.1002/lno.10728

Winslow, L., Read, J., Woolway, R., Brentrup, J., Leach, T., Zwart, J., Albers, S. et Collinge, D. (2019). *rLakeAnalyzer: Lake Physics Tools (version 1.11.4.1)*. https://CRAN.R-project.org/package=rLakeAnalyzer

Wong, C. K., Liu, X.-J., Siu, Y. Y. et Hwang, J.-S. (2006). Study of selective feeding in the marine cladoceran Penilia avirostris by HPLC pigment analysis. *Journal of Experimental Marine Biology and Ecology*, *331*(1), 21-32. https://doi.org/10.1016/j.jembe.2005.09.019

Yoshiyama, K., Mellard, J. P., Litchman, E. et Klausmeier, C. A. (2009). Phytoplankton Competition for Nutrients and Light in a Stratified Water Column. *The American Naturalist*, *174*(2), 190-203. https://doi.org/10.1086/600113

Zubkov, M. V. et Tarran, G. A. (2008). High bacterivory by the smallest phytoplankton in the North Atlantic Ocean. *Nature*, *455*(7210), 224-226. https://doi.org/10.1038/nature07236